

**MicroRNA-132 is a physiological regulator
of hematopoietic stem cell function and B-
cell development**

Thesis by
Arnav Mehta

In Partial Fulfillment of the Requirements for the
degree of
Doctor of Philosophy



CALIFORNIA INSTITUTE OF TECHNOLOGY
Pasadena, California
2015
Defended 3/24/15

Acknowledgements

I have had a wonderful time in graduate school and words alone cannot do justice to how appreciative I am of those around me who have guided me through this adventure and made it so enjoyable. I end this part of my journey completely inspired by the people I have encountered both at Caltech and elsewhere during conferences and other travel.

Importantly, my time here has only strengthened my burning desire to pursue mysterious scientific questions, as I feel equipped with new tools to study biological complexity, and I am more eager than ever to delve into the interface of computer science, mathematics, and basic biology. My experience in grad school has also had its downs, including two knee surgeries that took me away from lab for months at a time. I have many people to thank for helping me through all this and for my being where I am today, but it must start with my parents, who have been the backbone for my pursuits throughout my whole life. My father was a marine engineer, who later pursued work as a management consultant, and several times throughout his life pursued further education and successfully redefined his interests and career. He has been an inspiration and role model to me and now, as he starts his own company, I continue to draw energy from his experiences and support in pursuing my own independent goals. My mother has always been there to support me at each corner of my life, and has come to my aid in an instant whenever I've needed it. She came to support me at the drop of a hat during both my surgeries and has always been unselfish in caring for both my brother and myself. I can't explain how grateful I am to her. Both my parents have also given me the freedom and opportunity to pursue all my interests, for which I am also extremely grateful.

My brother likewise has been a huge source of inspiration over the last several years, and has turned into an amazing young adult and a role model to me. Even being 5 years younger he has been the voice of reason and maturity during critical stages of my graduate education. Importantly, as a future physician scientist himself he has been a wonderful sounding board for new ideas, while constantly challenging me on these ideas. For this and many other reasons I don't have time to explain, I cannot have asked for a more caring and supportive younger brother.

I would be remiss not to thank David Baltimore, my advisor, for making my graduate school experience absolutely wonderful and educational. David has been more than just a mentor and inspiration to me, but a friend whom I always trust to provide guidance with my best interests at heart. He has given me the freedom to pursue new ideas freely, and leverage my background in mathematics and chemistry to tackle interesting problems in biology in unconventional ways. His mentorship has meant that I feel comfortable identifying important problems in biology and delving deeply into their solution, while also being unafraid to utilize new technologies at the cutting edge of bioengineering. He has made me fearless in this regard by affording me the opportunity to travel to learn about new techniques, including a visit to the Broad Institute to learn how to do RNA-seq. David, thank you so much for being a wonderful mentor and guide, and, importantly, for always encouraging an open and collaborative approach to tackling scientific problems.

Critical to my development as a scientist has also been my thesis committee. I have to thank Sarkis Mazmanian for his unwavering support over the past few years. Sarkis, you have been a wonderful mentor and friend, and I am extremely lucky to have had your support. Thank you for always challenging me to be a better scientist and for being available to help whenever I've needed it. Importantly, thank you for pushing me to be focused and rigorous with how I did experiments. I also have to thank Ellen Rothenberg for her wonderful mentorship and for reshaping the way I think about hematopoiesis, and Mitch Guttman, for teaching me so much about computational biology.

I also have to thank many in the Baltimore lab who have been instrumental in making my graduate school experience fun and enjoyable. I thank Mati Mann, for always being there for me, whether when I fall off my bike or when I need help with an experiment, and pushing me to be a better scientist and athlete. Importantly, I thank you, Mati, for joining me in this new adventure into single-cell RNA-seq; I am looking forward to completing this promising new project! I also have to thank Michael Bethune, my baymate, with whom I spend pretty much all my time at work chatting with and discussing science, music, and everything you can imagine. Thank you, Michael, for always being available as a sounding board for my ideas, and for exemplifying to me how to be a rigorous experimentalist, a

clever problem solver, and most importantly, a creative scientist. In addition, I thank Jimmy Zhao for being a wonderful mentor and showing me the ropes on how to study HSC and microRNA biology. Thank you for always looking out for me, Jimmy, and for guiding me through the physician-scientist career path. I thank Devdoot Majumdar for many wonderful explorations into B cell biology and long noncoding RNAs, and for always being the first one to offer academic support when I've needed it. Finally, I thank the rest of the Baltimore lab for making my experience as wonderful as it has been!

Last but not least, I have to thank Avery House for all the wonderful experiences and relationships I've built over the last four years there, and my soccer team, Ernies, for an amazing few years playing in local leagues in Glendale, Pasadena, and in the Caltech GSC league! Together, they have made my experience so wonderfully balanced and have given me plenty of opportunity to take my mind off work when I've wanted it.

Abstract

MicroRNAs are a class of small non-coding RNAs that negatively regulate gene expression. Several microRNAs have been implicated in altering hematopoietic cell fate decisions. Importantly, deregulation of many microRNAs can lead to deleterious consequences in the hematopoietic system, including the onset of cancer, autoimmunity, or a failure to respond effectively to infection. As such, microRNAs fine-tune the balance between normal hematopoietic output and pathologic consequences. In this work, we explore the role of two microRNAs, miR-132 and miR-125b, in regulating hematopoietic stem cell (HSC) function and B cell development. In particular, we uncover the role of miR-132 in maintaining the appropriate balance between self-renewal, differentiation, and survival in aging HSCs by buffering the expression of a critical transcription factor, FOXO3. By maintain this balance, miR-132 may play a critical role in preventing aging-associated hematopoietic conditions such as autoimmune disease and cancer. We also find that miR-132 plays a critical role in B cell development by targeting a key transcription factor, Sox4, that is responsible for the differentiation of pro-B cells into pre-B cells. We find that miR-132 regulates B cell apoptosis, and by delivering miR-132 to mice that are predisposed to developing B cell cancers, we can inhibit the formation of these cancers and improve the survival of these mice. In addition to miR-132, we uncovered the role of another critical microRNA, miR-125b, that potentiates hematopoietic stem cell function. We found that enforced expression of miR-125b causes an aggressive myeloid leukemia by downregulation of its target Lin28a. Importantly, miR-125b also plays a critical role in inhibiting the formation of pro-B cells. Thus, we have discovered two microRNAs with important roles in regulating normal hematopoiesis, and whose dregulation can lead to deleterious consequences such as cancer in the aging hematopoietic system. Both miR-132 and miR-125b may therefore be targeted for therapeutics to inhibit age-related immune diseases associated with the loss of HSC function and cancer progression.

TABLE OF CONTENTS

Acknowledgements	iii
Abstract.....	vi
Table of Contents	vii
Chapter 1: Introduction to immune system development and microRNAs	1
Overview of thesis.....	2
Overview of hematopoiesis.....	4
Normal function of the hematopoietic system.....	5
The aging hematopoietic system.....	8
Hematopoietic malignancies.....	9
Overview of microRNAs	10
MicroRNA biogenesis.....	10
MicroRNAs involved in hematopoietic stem cell function.....	10
MicroRNAs involved in B cell development	11
The microRNA-212/132 cluster	12
MicroRNA-125b and Lin28a.....	13
References	15
Chapter 2: The microRNA-212/132 cluster buffers hematopoietic stem cell function with age	23
Abstract.....	24
Introduction	25
Results	26
Discussion	40
Experimental Procedures	45
Figure Legends.....	50
References	56
Supplemental Figure Legends.....	61
Supplemental Experimental Procedures	67
Supplemental Tables	73
Table S1: Sequences for FOXO3 shRNA constructs.....	73
Table S2: Primer sequences used for qPCR	74
Supplemental References.....	75
Figures	76
Figure 1: microRNA-132 is expressed in hematopoietic stem cells (HSCs) and over-expression alters hematopoiesis	76
Figure 2: Genetic deletion of the microRNA-212/132 cluster in mice alters hematopoietic output with age	77
Figure 3: Genetic deletion of the microRNA-212/132 cluster in mice alters hematopoietic output and cycling in response to LPS stimulation	78
Figure 4: The microRNA-212/132 cluster regulates long-term	

reconstitution potential of HSCs with age	79
Figure 5: FOXO3 is a direct target of microRNA-132 in bone marrow cells	80
Figure 6: Co-expression of FOXO3 with miR-132 rescues the hematopoietic defects observed with expression of miR-132 alone	81
Figure 7: Genetic deletion of the miR-212/132 ^{-/-} cluster results in a FOXO3 dependent alteration in autophagy and survival of HSCs ..	82
Figure S1: Validation of miR-132 over-expression in bone marrow cells expressing control or a miR-132 over-expressing vector	83
Figure S2: Ectopic expression of miR-132 leads to deregulated hematopoiesis	84
Figure S3: Ectopic expression of miR-132 leads to deficits in several early and late hematopoietic progenitor populations	85
Figure S4: Genetic deletion of the microRNA-212/132 cluster has no observable effect on hematopoiesis in young mice	86
Figure S5: Genetic deletion of the microRNA-212/132 cluster in mice leads to deregulated hematopoiesis with age	87
Figure S6: Summary of RNA-sequencing analysis on WT and miR-212/132 ^{-/-} HSCs from 16-week old mice.....	88
Figure S7: Validation of microRNA-132 and FOXO3 over-expression in FOXO3 rescue experiment.....	89
Chapter 3: The microRNA-212/132 cluster regulates B cell development and apoptosis by targeting Sox4	90
Abstract.....	91
Introduction	92
Results	92
Discussion	100
Experimental Procedures	103
Figure Legends.....	108
References	113
Supplemental Figure Legends.....	118
Supplemental Tables	122
Table S1: Sequences for SOX4 shRNA constructs.....	122
Table S2: Primer sequences used for qPCR	123
Figures	124
Figure 1: miR-132 is induced in B cells and over-expression of miR-132 in mice alters B cell development	124
Figure 2: miR-132 causes a block in early B cell development.....	125
Figure 3: miR-212/132 regulates B cell apoptosis	126
Figure 4: Loss of miR-212/132 alters B cell development under non-homeostatic conditions	127
Figure 5: SOX4 is a direct target of miR-132 and is a key regulator of B cell development	128
Figure 6: Co-expression of SOX4 rescues the defect in B cell	

Development with expression of miR-132 alone	129
Figure 7: Enforced expression of miR-132 inhibits the Development of spontaneous B cell cancers in cells with the E μ -myc transgene.....	130
Figure S1: miR-212/132 is induced in B cells by activation of the B cell receptor (BCR).....	131
Figure S2: Enforced expression of miR-132 alters B cell output in mice up to 9 months post-reconstitution.....	132
Figure S3: Enforced expression of miR-212 has a marginal effect on B cell output	133
Figure S4: Simulation of B cells through the B cell receptor (BCR) results in dramatic gene expression changes	134
Figure S5: miR-212/132 regulates B cell apoptosis	135
Figure S6: miR-212/132 ^{-/-} mice demonstrate no observable defect in B cell output under steady state conditions	136
Figure S7: miR-212/132 targets SOX4 in B cells	137
Chapter 4: MicroRNA-125b regulates hematopoiesis by targeting Lin28a...	138
Abstract.....	139
Introduction	140
Results	140
Discussion	146
Experimental Procedures	150
Figure Legends.....	154
References	157
Supplemental Figure Legends.....	160
Figures	164
Figure 1: MiR-125b over-expression causes an aggressive invasive myeloid leukemia	164
Figure 2: MiR-125b over-expression causes a skewing of the hematopoietic system at seven weeks post-bone marrow reconstitution	165
Figure 3: Inhibiting miR-125b function decrease hematopoietic output.....	166
Figure 4: MiR-125b represses Lin28A expression in mouse and human hematopoietic cells.....	167
Figure 5: Lin28A over-expression inhibits hematopoiesis.....	168
Figure 6: Inhibition of Lin28A increases the number of myeloid cells but decreases B cells	169
Figure S1: MiR-125b overexpressing animals exhibit myeloid Infiltration into peripheral organs five months post- reconstitution	170
Figure S2: MiR-125a overexpression causes an aggressive leukemia six months post-reconstitution	171
Figure S3: MiR-125b overexpression increases leukocyte count five months post-reconstitution	172

Figure S4: Bone marrow and peripheral blood from MG-125b animals early post-reconstitution display hematopoietic reconfiguration	173
Figure S5: Inhibiting miR-125b function decreases hematopoietic output	174
Figure S6: MiR-125b represses Lin28 expression in mouse and human hematopoietic cells	175
Figure S7: Lin28A and Lin28B expression in miR-125b over-expressing leukemic samples	176
Figure S8: Lin28 over-expression inhibits hematopoiesis	177
Chapter 5: Conclusions and Future Directions	178
A putative role of microRNAs in maintaining HSC function with age ...	179
Uncovering potential roles of miR-132 in normal and malignant B cell development	179
A proposal to better understand HSC aging with age at single-cell resolution	180
Significance	180
Innovation	181
Approach	182
References	195
APPENDIX: Conversion of Danger Signals by Hematopoietic Progenitors	197

Chapter 1: Introduction to immune system development and microRNAs

Overview of thesis

In this thesis we explore the role of a class of noncoding RNAs, called microRNAs, in fine-tuning hematopoietic cell fate decisions and function. MicroRNAs are key post-transcriptional regulators of gene-expression and we seek to understand how these microRNAs control the balance between normal and pathological hematopoiesis with age. Aging of the hematopoietic system leads to an increased incidence of several hematopoietic diseases, including cancer, autoimmune function, and a general failure to combat infections. We uncover the role of two microRNAs that, when altered, severely affect stem cell and B cell development, function, and survival in the immune system.

The first chapter will present background information on the normal function of hematopoietic stem cells and B cells. We then delve into how aging may lead to pathological hematopoiesis and the development of immune cell cancers. Next, we explore microRNA biogenesis and the contribution of microRNAs to hematopoietic cell fate decisions. In chapter 2, we describe the role of a previously unappreciated microRNA cluster, miR-212/132, in hematopoietic stem cells. We find that miR-212/132 buffers the expression of its target Foxo3 with age, and in doing so allows these stem cells to maintain a critical balance between self-renewal, differentiation, and survival. When altered, miR-212/132 can lead to poor stem cell function with age, and possibly to the onset of pathological consequences such as anemia and cancer. In chapter 3, we continue the exploration of miR-212/132 in the aging hematopoietic system by elucidating its role in B cell development and the treatment of B cell cancers. We find a novel target for miR-

212/132, the transcription factor Sox4, and demonstrate that when altered this microRNA cluster severely inhibits B cell development and survival. We next take advantage of this role of miR-212/132 in B cell development to alter the progression of B cell cancer, thus revealing a potential therapeutic application of this microRNA. In chapter 4, we continue to explore the role of microRNAs with potential therapeutic applications in blood cancers by uncovering a mechanism by which miR-125b, another regulator of HSC function, causes myeloid leukemia and inhibits B cell development by targeting the pluripotency factor Lin28a. We consider the future directions and potential implications of this work in chapter 5, and discuss ongoing work to investigate the heterogeneous nature of young and aged HSCs in order to understand the mechanisms underlying age-associated hematopoietic diseases.

Overview of hematopoiesis

Normal functions of the hematopoietic system

We begin this introduction with an overview of normal hematopoietic function. The hematopoietic system is remarkable in its ability to produce millions of cells every second (Orkin and Zon, 2008). Each cell originates from a single hematopoietic stem cell (HSC) that has the unique ability to self-renew (create identical copies of itself) and to differentiate into more committed progenitors that lose their ability to self-renew but eventually lead to all other cell types in the immune system (Figure 1) (Orkin and Zon, 2008). The goal of the hematopoietic system is to produce a balanced output of functional

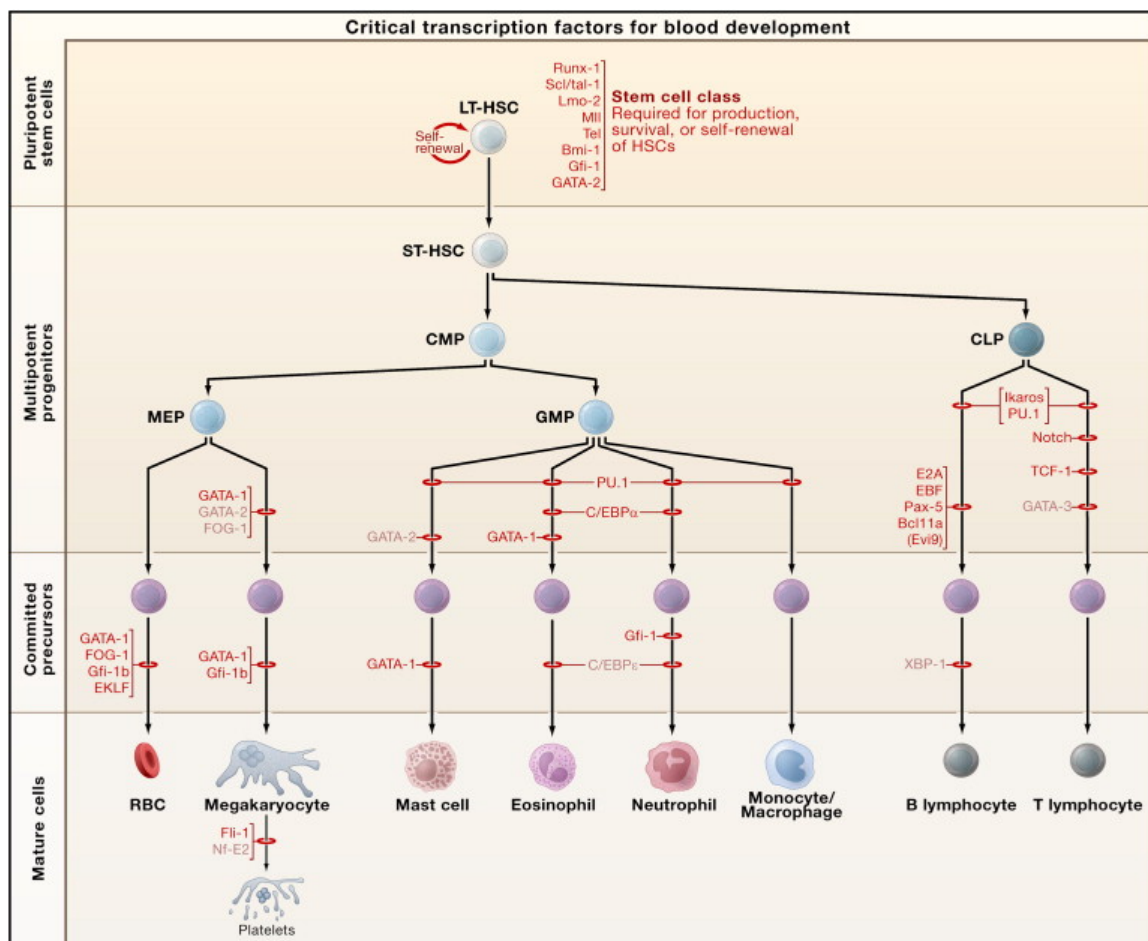


Figure 1. The hematopoietic tree. Adapted from (Orkin and Zon, 2008).

red blood cells, myeloid cells (such as macrophages and granulocytes, which largely govern innate immune function) and lymphoid cells such as B cells and T cells, which are primarily responsible for adaptive immune function (Orkin and Zon, 2008). As such, lineage commitment and cell fate in this system is governed by a complex set of gene regulatory pathways, epigenetic changes, and post-transcriptional modifications (Cabezas-Wallscheid et al., 2014; Laurenti et al., 2013; O'Connell et al., 2010b; Sun et al., 2014). The developmental intermediates, or hematopoietic progenitors, that lead to each of these cell types are being actively explored. While several lineage-committed progenitors such as the common myeloid progenitor (CMP) and common lymphoid progenitor (CLP) have been identified, it is becoming extremely clear that the hematopoietic tree is intricate and complex, with several overlapping intermediates that maintain some potential to produce more diverse cell types than originally anticipated (Orkin and Zon, 2008). We focus this review on two particular cells in the hematopoietic stem cell relevant to the work discussed later. These are the hematopoietic stem cell and the B cell.

Hematopoietic stem cells

The origin of all blood cells in the body is the hematopoietic stem cell (HSC) (Orkin and Zon, 2008). HSCs must maintain an intricate balance between self-renewal and differentiation throughout the course of our life (Morrison and Weissman, 1994; Rossi et al., 2012). As such, many different genes, epigenetic modifications, and other intrinsic factors regulate them (Cabezas-Wallscheid et al., 2014; Sun et al., 2014). Importantly, HSCs reside in the bone marrow niche and are also strongly influenced by extrinsic signals, such as cytokines and growth factors (Orkin and Zon, 2008). It is also becoming

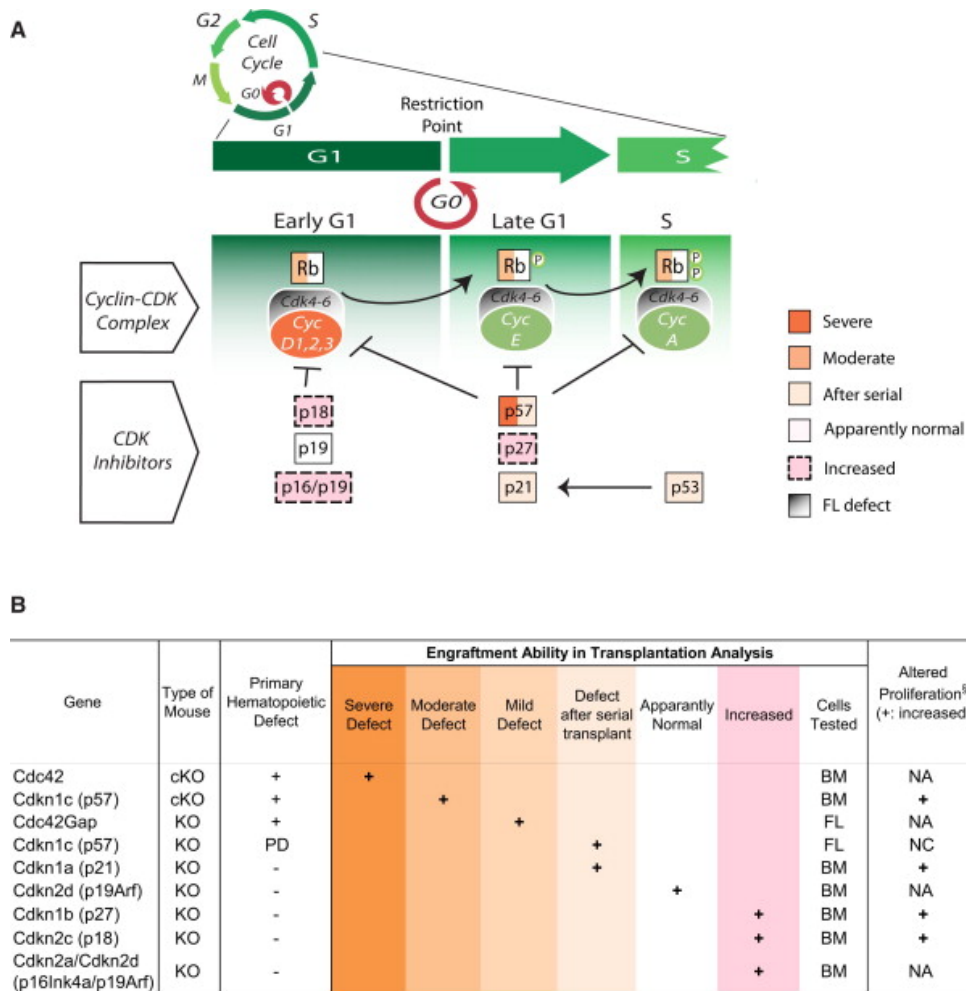


Figure 2. Cell cycle regulation of hematopoietic stem cells. Adapted from (Rossi et al., 2012).

increasingly apparent that HSCs might respond directly to foreign material, such as pathogens, that enter the body (Nagai et al., 2006; Zhao et al., 2014).

At the peak of the cellular hierarchy is what is known as the long-term HSC (LT-HSCs). These LT-HSCs are essential for maintaining a life-long supply of blood. Immediately downstream of these cells are slightly more committed progenitors, known as short-term HSCs (ST-HSCs) and multipotent progenitors (MPPs). ST-HSCs and MPPs have lost the

ability to self-renew; however, they maintain the ability to differentiate into all cell types. Downstream of the MPPs are several lineage-restricted progenitors, which then give rise to mature cells (Figure 1) (Orkin and Zon, 2008).

The majority of HSCs reside in the bone marrow in a quiescent state. It is believed that it is these HSCs that have the best long-term reconstitution potential upon bone marrow transplant (Morrison and Weissman, 1994; Orkin and Zon, 2008; Rossi et al., 2012). HSCs that become activated cycle more rapidly, and this active proliferation is closely related to differentiation (Morrison and Weissman, 1994; Rossi et al., 2012). Furthermore, many HSCs periodically circulate in the peripheral blood and hone back to the bone marrow eventually. Several genes regulate HSC cycling, including genes that control cell cycle check-points such as p21, p27, and p57, as well as several other factors (Figure 2) (Morrison and Weissman, 1994; Rossi et al., 2012). Other factors that alter HSC function include those that regulate the ability of HSCs to stay in the bone marrow niche, such as Mmp9, those that affect survival, such as Foxo3, and others that alter signaling in HSCs, such as the Wnt pathway (Rossi et al., 2012).

B cells

B cells are the primary producers of immunoglobulin and play a critical role in adaptive immunity (Mauri and Bosma, 2012). The maintenance of proper B cell output from early hematopoietic progenitors, along with the production of an appropriate antibody repertoire, is critical in maintaining the balance between normal immune function and diseases such as autoimmunity and cancer. Therefore, B lymphopoiesis requires the intricate interplay of

many different transcription factors in a complex gene regulatory network that controls lineage specification and commitment (Mandel and Grosschedl, 2010; Matthias and Rolink, 2005; Nutt and Kee, 2007).

Antigen-independent B cell development begins with the differentiation of lymphoid primed multipotent progenitors (LMPPs) to common lymphoid progenitors (CLPs), a process driven by the expression of PU.1 and Ikaros (Matthias and Rolink, 2005; Nutt and Kee, 2007), both of which may play a role in regulating Flt3 and IL-7R expression (DeKoter et al., 2002; Yoshida et al., 2006). These early progenitors also express Rag1 and Rag2, and thus begin the process of rearrangement of the immunoglobulin heavy chain (IgH) locus (Igarashi et al., 2002). Lineage specification to the next stages of B cell development, the pre-pro-B cell and pro-B cell, involves the upregulation of several genes controlled by E2A and Ebf1 (O'Riordan and Grosschedl, 1999), including Pax5 (Cobaleda et al., 2007). Pax5 is essential for B cell lineage commitment, as it represses genes that are inappropriate for B cell development (Souabni et al., 2002). The transition to pre-B cells, the stage at which immunoglobulin light chain (IgL) rearrangement begins, and immature B cells, involves many factors including Sox4 (Sun et al., 2013), which has also been implicated in regulating the expression of the Rag genes (Mallampati et al., 2014).

The aging hematopoietic system

Aged HSCs are characterized by increased self-renewal potential, loss of long-term reconstitution capability, myeloid-biased differentiation, and a change in niche localization. As a consequence, aged mice demonstrate an accumulation of phenotypically defined

HSCs with a poor ability to hone to the bone marrow niche (Geiger et al., 2013). These aged HSCs also develop a requirement for basal autophagy for survival, because replication stress and the accumulation of reactive oxygen species have harmful consequences on HSC numbers and function with age (Flach et al., 2014; Tothova et al., 2007). The loss of critical autophagic factors is often associated with altered cell cycling of HSCs, and leads to apoptosis and a rapid loss of HSC numbers in aged mice (Miyamoto et al., 2007; Rubinsztein et al., 2011; Warr et al., 2013). A critical balance between cell cycling and differentiation, and survival of aged HSCs must therefore be established to maintain normal hematopoietic output.

Hematopoietic malignancies

Deregulation of hematopoietic stem cell function or immune developmental processes can have deleterious consequences, including the development of leukemias and lymphomas (O'Connell et al., 2010b). MiR-125b is up-regulated in a range of human leukemias, including acute myeloid leukemia (AML) (Bousquet et al., 2008; Enomoto et al., 2011), chronic myeloid leukemia (CML) (Enomoto et al., 2011), acute megakaryocytic leukemia (AMKL) (Klusmann et al., 2010), childhood acute lymphoblastic leukemia (ALL) with the ETV6/Runx1 fusion protein (Gefen et al., 2010), and Philadelphia-chromosome positive B-cell precursor ALL (Enomoto et al., 2011). Indeed, over-expression of miR-125b alone in the bone marrow of mice is sufficient to induce leukemia (Bousquet et al., 2010; Enomoto et al., 2011; O'Connell et al., 2010a). Recent *in vitro* work has also uncovered a role for miR-125b in the development of plasma cells (Gururajan et al., 2010) and effector T cells (Rossi et al., 2011), suggesting that miR-125b regulates immune cell development in

addition to promoting leukemia.

Overview of microRNAs

MicroRNA biogenesis

miRs are ~18-22 nucleotide non-coding RNAs that negatively regulate gene expression through translational inhibition and mRNA degradation (Friedman et al., 2009; Guo et al., 2010a). They are transcribed by PolIII and sequentially cleaved by the enzymes Drosha and Dicer before being incorporated into the RNA-induced silencing complex (RISC) in their mature form (He and Hannon, 2004). Current evidence suggests that miRs base-pair with the 3' untranslated region (UTR) of their mRNA targets, and this interaction is mediated by a 6-8 nucleotide “seed sequence” at the 5' end of the miR (Friedman et al., 2009). miRs serve as “fine-tuners” of gene expression, and when deregulated they can drastically alter the balance of dynamic biological processes, such as hematopoietic cell fate decisions (O'Connell et al., 2010a; O'Connell et al., 2008; O'Connell et al., 2011).

MicroRNAs that regulate hematopoietic stem cell function

A number of microRNAs regulate the function of HSCs in a cell-intrinsic fashion. Our lab has demonstrated that miR-125b potentiates the function of HSCs by increasing their ability to home to the bone marrow niche, engraft the bone marrow, and fully reconstitute a mouse immune system (O'Connell et al., 2010a). It has also been demonstrated that miR-125b may lead to an expansion of the number of HSCs in the bone marrow by targeting the pro-apoptotic genes *Bmf* and *Klf13* (Ooi et al., 2010). Enforced expression of the miR-

125b family member, miR-125a, analogously leads to an accumulation of HSCs in the bone marrow by targeting the apoptosis gene Bak1 (Guo et al., 2010b).

Other microRNAs regulate HSC function and longevity through different mechanisms. Loss of miR-126 has been shown to lead to an accumulation of HSCs, and over-expression to a loss of HSCs through alteration of cycling (Lechman et al., 2012). It is believed that miR-126 does this by targeting several different mRNAs that are implicated in the PI3-kinase/AKT axis (Lechman et al., 2012). Two other microRNAs, miR-146a, a tumor suppressor, and miR-22, an oncomir, have also been shown to regulate cell cycling of HSCs (Song et al., 2013; Zhao et al., 2013). The inhibition of miR-22 leads to decreased HSC proliferation through upregulation of its target TET2 (Song et al., 2013). Conversely, the loss of miR-146a leads to hyperproliferation and exhaustion of HSCs with age. This hyperproliferation is linked to a defect in bone marrow reconstitution capability of HSCs (Zhao et al., 2013).

MicroRNAs that regulate B cell development

Several microRNAs regulate key checkpoints in B cell development and the loss of a microRNA processing protein, Dicer, results in a block in the pro-B to pre-B cell transition (Koralov et al., 2008). In particular, both miR-150 and miR-34a regulate this transition by targeting c-Myb and Foxp1, respectively (Rao et al., 2010; Xiao et al., 2007; Zhou et al., 2007). Another example is miR-148a, which regulates plasma cell differentiation by targeting Bach2 (Jordan et al., 2015). In addition, miR-181 and miR-155 play an important role in B cell immune function by targeting AID to regulate class-switching and somatic

hypermethylation (de Yebenes et al., 2008; Teng et al., 2008; Thai et al., 2007).

Importantly, deregulation of the expression of many microRNAs important in B cell development and function results in autoimmunity (Xiao et al., 2008) and the onset of B cell cancers (Calin et al., 2008; Costinean et al., 2006; Eis et al., 2005; Puissegur et al., 2012; Xiao et al., 2008).

The microRNA-212/132 cluster

MiR-132 is highly conserved among vertebrates and is expressed in a cluster with miR-212, with which it shares an identical seed sequence (Ucar et al., 2010; Wanet et al., 2012). In mice, miR-132 is transcribed from the first intron of a non-coding transcript on chromosome 11; however, a recent report has demonstrated that it is also expressed on the second exon of an alternatively spliced transcript variant, which is prevalent in immune cells (Ucar et al., 2010). Since the discovery of miR-132, most studies have focused on its role in neuronal development and in angiogenesis (Anand et al., 2010; Smith et al., 2011; Wanet et al., 2012). Our lab first identified the potential importance of miR-132 in immune function after observing that it was induced in response to toll-like receptor 4 (TLR4) signaling in a human acute monocytic leukemia cell line (THP-1) (Taganov et al., 2006). Recent reports have confirmed this finding, showing miR-132 is induced five-fold in human macrophages in response to lipopolysaccharide (LPS) and CpG stimulation, and approximately three-fold in the spleen and bone marrow of mice injected with LPS (Shaked et al., 2009). Importantly, miR-132 negatively regulates acetylcholinesterase expression in this context, and has thus been implicated in the inhibition of peripheral inflammation (Shaked et al., 2009).

MiR-132 has also been implicated in a broad range of other immunological processes. The induction of miR-132 by immunoglobulin E (IgE) activation in mast cells leads to negative regulation of heparin-binding epidermal growth factor (HB-EGF), which is important in cell proliferation, migration, and wound healing (Molnar et al., 2012). Similarly, induction of miR-132 by IL-12 in natural killer cells is responsible for tolerance to long-term IL-12 signaling through repression of STAT4 (Huang et al., 2011). A recent report also suggests that miR-132 is induced in THP-1 cells in response to infection with herpes virus family members, and that it plays a role in suppressing the host inflammatory response by targeting the transcriptional co-activator p300 (Lagos et al., 2010). These results highlight the importance of this miR as a breaking mechanism for uncontrolled activation of various immune functions. To this end, miR-132 is also deregulated in human samples of acute myeloid leukemia and B-cell chronic lymphocytic leukemia (Calin et al., 2004).

MicroRNA-125b and Lin28a

Our lab started studying miR-125b after noticing that it was enriched in hematopoietic stem cells (HSCs) and conferred on them a competitive advantage for bone marrow engraftment (O'Connell et al., 2010a). miR-125b is the mammalian homologue of the first discovered miR, lin-4, found in *C. elegans*. Lin-4 has been shown to regulate the transition from the early L1 stage of larval development to later stages, and does so by repressing its target genes, the transcription factor Lin14 and the RNA-binding protein Lin28 (Feinbaum and Ambros, 1999; Ha et al., 1996; Lee et al., 1993; Moss et al., 1997; Wightman et al., 1993). Lin28 in turn regulates expression of another miR, let-7, by binding a motif in the terminal

loop of the let-7 precursor (pre-let-7) (Heo et al., 2008; Loughlin et al., 2012; Newman et al., 2008; Viswanathan and Daley, 2010; Viswanathan et al., 2008). In mammals, Lin28 has two homologs, Lin28 and Lin28B. Lin28 recruits a terminal uridylyl transferase and marks pre-let-7 for degradation, preventing Dicer from processing pre-let-7 into its mature form, whereas Lin28B prevents processing of primary let-7 transcripts by Drosha (Heo et al., 2008; Newman et al., 2008; Piskounova et al., 2011; Van Wynsberghe et al., 2011; Viswanathan and Daley, 2010). Importantly, the lin-4:Lin28:let-7 axis is conserved in mammals (Viswanathan et al., 2008; Wu and Belasco, 2005).

References

Anand, S., Majeti, B.K., Acevedo, L.M., Murphy, E.A., Mukthavaram, R., Schepke, L., Huang, M., Shields, D.J., Lindquist, J.N., Lapinski, P.E., *et al.* (2010). MicroRNA-132-mediated loss of p120RasGAP activates the endothelium to facilitate pathological angiogenesis. *Nature medicine* *16*, 909-914.

Bousquet, M., Harris, M.H., Zhou, B., and Lodish, H.F. (2010). MicroRNA miR-125b causes leukemia. *Proceedings of the National Academy of Sciences of the United States of America* *107*, 21558-21563.

Bousquet, M., Quelen, C., Rosati, R., Mansat-De Mas, V., La Starza, R., Bastard, C., Lippert, E., Talmant, P., Lafage-Pochitaloff, M., Leroux, D., *et al.* (2008). Myeloid cell differentiation arrest by miR-125b-1 in myelodysplastic syndrome and acute myeloid leukemia with the t(2;11)(p21;q23) translocation. *The Journal of experimental medicine* *205*, 2499-2506.

Cabezas-Wallscheid, N., Klimmeck, D., Hansson, J., Lipka, D.B., Reyes, A., Wang, Q., Weichenhan, D., Lier, A., von Paleske, L., Renders, S., *et al.* (2014). Identification of regulatory networks in HSCs and their immediate progeny via integrated proteome, transcriptome, and DNA Methylation analysis. *Cell stem cell* *15*, 507-522.

Calin, G.A., Cimmino, A., Fabbri, M., Ferracin, M., Wojcik, S.E., Shimizu, M., Taccioli, C., Zanesi, N., Garzon, R., Aqeilan, R.I., *et al.* (2008). MiR-15a and miR-16-1 cluster functions in human leukemia. *Proceedings of the National Academy of Sciences of the United States of America* *105*, 5166-5171.

Calin, G.A., Liu, C.G., Sevignani, C., Ferracin, M., Felli, N., Dumitru, C.D., Shimizu, M., Cimmino, A., Zupo, S., Dono, M., *et al.* (2004). MicroRNA profiling reveals distinct signatures in B cell chronic lymphocytic leukemias. *Proc Natl Acad Sci U S A* *101*, 11755-11760.

Cobaleda, C., Schebesta, A., Delogu, A., and Busslinger, M. (2007). Pax5: the guardian of B cell identity and function. *Nature immunology* *8*, 463-470.

Costinean, S., Zanesi, N., Pekarsky, Y., Tili, E., Volinia, S., Heerema, N., and Croce, C.M. (2006). Pre-B cell proliferation and lymphoblastic leukemia/high-grade lymphoma in E(mu)-miR155 transgenic mice. *Proceedings of the National Academy of Sciences of the United States of America* *103*, 7024-7029.

de Yebenes, V.G., Belver, L., Pisano, D.G., Gonzalez, S., Villasante, A., Croce, C., He, L., and Ramiro, A.R. (2008). miR-181b negatively regulates activation-induced cytidine deaminase in B cells. *The Journal of experimental medicine* *205*, 2199-2206.

- DeKoter, R.P., Lee, H.J., and Singh, H. (2002). PU.1 regulates expression of the interleukin-7 receptor in lymphoid progenitors. *Immunity* *16*, 297-309.
- Eis, P.S., Tam, W., Sun, L., Chadburn, A., Li, Z., Gomez, M.F., Lund, E., and Dahlberg, J.E. (2005). Accumulation of miR-155 and BIC RNA in human B cell lymphomas. *Proceedings of the National Academy of Sciences of the United States of America* *102*, 3627-3632.
- Enomoto, Y., Kitaura, J., Hatakeyama, K., Watanuki, J., Akasaka, T., Kato, N., Shimanuki, M., Nishimura, K., Takahashi, M., Taniwaki, M., *et al.* (2011). Emu/miR-125b transgenic mice develop lethal B-cell malignancies. *Leukemia* *25*, 1849-1856.
- Feinbaum, R., and Ambros, V. (1999). The timing of lin-4 RNA accumulation controls the timing of postembryonic developmental events in *Caenorhabditis elegans*. *Dev Biol* *210*, 87-95.
- Flach, J., Bakker, S.T., Mohrin, M., Conroy, P.C., Pietras, E.M., Reynaud, D., Alvarez, S., Diolaiti, M.E., Ugarte, F., Forsberg, E.C., *et al.* (2014). Replication stress is a potent driver of functional decline in ageing haematopoietic stem cells. *Nature* *512*, 198-202.
- Friedman, R.C., Farh, K.K., Burge, C.B., and Bartel, D.P. (2009). Most mammalian mRNAs are conserved targets of microRNAs. *Genome research* *19*, 92-105.
- Gefen, N., Binder, V., Zaliouva, M., Linka, Y., Morrow, M., Novosel, A., Edry, L., Hertzberg, L., Shomron, N., Williams, O., *et al.* (2010). Hsa-mir-125b-2 is highly expressed in childhood ETV6/RUNX1 (TEL/AML1) leukemias and confers survival advantage to growth inhibitory signals independent of p53. *Leukemia* *24*, 89-96.
- Geiger, H., de Haan, G., and Florian, M.C. (2013). The ageing haematopoietic stem cell compartment. *Nature reviews. Immunology* *13*, 376-389.
- Guo, H., Ingolia, N.T., Weissman, J.S., and Bartel, D.P. (2010a). Mammalian microRNAs predominantly act to decrease target mRNA levels. *Nature* *466*, 835-840.
- Guo, S., Lu, J., Schlanger, R., Zhang, H., Wang, J.Y., Fox, M.C., Purton, L.E., Fleming, H.H., Cobb, B., Merkenschlager, M., *et al.* (2010b). MicroRNA miR-125a controls hematopoietic stem cell number. *Proceedings of the National Academy of Sciences of the United States of America* *107*, 14229-14234.
- Gururajan, M., Haga, C.L., Das, S., Leu, C.M., Hodson, D., Josson, S., Turner, M., and Cooper, M.D. (2010). MicroRNA 125b inhibition of B cell differentiation in germinal centers. *International immunology* *22*, 583-592.

- Ha, I., Wightman, B., and Ruvkun, G. (1996). A bulged lin-4/lin-14 RNA duplex is sufficient for *Caenorhabditis elegans* lin-14 temporal gradient formation. *Genes Dev* *10*, 3041-3050.
- He, L., and Hannon, G.J. (2004). MicroRNAs: small RNAs with a big role in gene regulation. *Nat Rev Genet* *5*, 522-531.
- Heo, I., Joo, C., Cho, J., Ha, M., Han, J., and Kim, V.N. (2008). Lin28 mediates the terminal uridylation of let-7 precursor MicroRNA. *Mol Cell* *32*, 276-284.
- Huang, Y., Lei, Y., Zhang, H., Hou, L., Zhang, M., and Dayton, A.I. (2011). MicroRNA regulation of STAT4 protein expression: rapid and sensitive modulation of IL-12 signaling in human natural killer cells. *Blood* *118*, 6793-6802.
- Igarashi, H., Gregory, S.C., Yokota, T., Sakaguchi, N., and Kincade, P.W. (2002). Transcription from the RAG1 locus marks the earliest lymphocyte progenitors in bone marrow. *Immunity* *17*, 117-130.
- Jordan, M.A., Zhao, J.L., Casellas, R., Athanasopoulos, V., Vinuesa, C.G., Porstner, M., Winkelmann, R., Daum, P., Schmid, J., Pracht, K., *et al.* (2015). miR-148a promotes plasma cell differentiation and targets the germinal center transcription factors Mitf and Bach2. *Nature communications*.
- Klusmann, J.H., Li, Z., Bohmer, K., Maroz, A., Koch, M.L., Emmrich, S., Godinho, F.J., Orkin, S.H., and Reinhardt, D. (2010). miR-125b-2 is a potential oncomiR on human chromosome 21 in megakaryoblastic leukemia. *Genes & development* *24*, 478-490.
- Koralov, S.B., Muljo, S.A., Galler, G.R., Krek, A., Chakraborty, T., Kanellopoulou, C., Jensen, K., Cobb, B.S., Merckenschlager, M., Rajewsky, N., and Rajewsky, K. (2008). Dicer ablation affects antibody diversity and cell survival in the B lymphocyte lineage. *Cell* *132*, 860-874.
- Lagos, D., Pollara, G., Henderson, S., Gratrix, F., Fabani, M., Milne, R.S., Gotch, F., and Boshoff, C. (2010). miR-132 regulates antiviral innate immunity through suppression of the p300 transcriptional co-activator. *Nature cell biology* *12*, 513-519.
- Laurenti, E., Doulatov, S., Zandi, S., Plumb, I., Chen, J., April, C., Fan, J.B., and Dick, J.E. (2013). The transcriptional architecture of early human hematopoiesis identifies multilevel control of lymphoid commitment. *Nature immunology* *14*, 756-763.
- Lechman, E.R., Gentner, B., van Galen, P., Giustacchini, A., Saini, M., Boccalatte, F.E., Hiramatsu, H., Restuccia, U., Bachi, A., Voisin, V., *et al.* (2012). Attenuation of miR-126 activity expands HSC in vivo without exhaustion. *Cell stem cell* *11*, 799-811.

- Lee, R.C., Feinbaum, R.L., and Ambros, V. (1993). The *C. elegans* heterochronic gene *lin-4* encodes small RNAs with antisense complementarity to *lin-14*. *Cell* *75*, 843-854.
- Loughlin, F.E., Gebert, L.F., Towbin, H., Brunschweiler, A., Hall, J., and Allain, F.H. (2012). Structural basis of pre-let-7 miRNA recognition by the zinc knuckles of pluripotency factor Lin28. *Nat Struct Mol Biol* *19*, 84-89.
- Mallampati, S., Sun, B., Lu, Y., Ma, H., Gong, Y., Wang, D., Lee, J.S., Lin, K., and Sun, X. (2014). Integrated genetic approaches identify the molecular mechanisms of Sox4 in early B-cell development: intricate roles for RAG1/2 and CK1epsilon. *Blood* *123*, 4064-4076.
- Mandel, E.M., and Grosschedl, R. (2010). Transcription control of early B cell differentiation. *Current opinion in immunology* *22*, 161-167.
- Matthias, P., and Rolink, A.G. (2005). Transcriptional networks in developing and mature B cells. *Nature reviews. Immunology* *5*, 497-508.
- Mauri, C., and Bosma, A. (2012). Immune regulatory function of B cells. *Annual review of immunology* *30*, 221-241.
- Miyamoto, K., Araki, K.Y., Naka, K., Arai, F., Takubo, K., Yamazaki, S., Matsuoka, S., Miyamoto, T., Ito, K., Ohmura, M., *et al.* (2007). Foxo3a is essential for maintenance of the hematopoietic stem cell pool. *Cell stem cell* *1*, 101-112.
- Molnar, V., Ersek, B., Wiener, Z., Tombol, Z., Szabo, P.M., Igaz, P., and Falus, A. (2012). MicroRNA-132 targets HB-EGF upon IgE-mediated activation in murine and human mast cells. *Cell Mol Life Sci* *69*, 793-808.
- Morrison, S.J., and Weissman, I.L. (1994). The long-term repopulating subset of hematopoietic stem cells is deterministic and isolatable by phenotype. *Immunity* *1*, 661-673.
- Moss, E.G., Lee, R.C., and Ambros, V. (1997). The cold shock domain protein LIN-28 controls developmental timing in *C. elegans* and is regulated by the *lin-4* RNA. *Cell* *88*, 637-646.
- Nagai, Y., Garrett, K.P., Ohta, S., Bahrun, U., Kouro, T., Akira, S., Takatsu, K., and Kincade, P.W. (2006). Toll-like receptors on hematopoietic progenitor cells stimulate innate immune system replenishment. *Immunity* *24*, 801-812.
- Newman, M.A., Thomson, J.M., and Hammond, S.M. (2008). Lin-28 interaction with the Let-7 precursor loop mediates regulated microRNA processing. *RNA* *14*, 1539-1549.
- Nutt, S.L., and Kee, B.L. (2007). The transcriptional regulation of B cell lineage commitment. *Immunity* *26*, 715-725.

O'Connell, R.M., Chaudhuri, A.A., Rao, D.S., Gibson, W.S., Balazs, A.B., and Baltimore, D. (2010a). MicroRNAs enriched in hematopoietic stem cells differentially regulate long-term hematopoietic output. *Proceedings of the National Academy of Sciences of the United States of America* *107*, 14235-14240.

O'Connell, R.M., Rao, D.S., Chaudhuri, A.A., and Baltimore, D. (2010b). Physiological and pathological roles for microRNAs in the immune system. *Nature reviews. Immunology* *10*, 111-122.

O'Connell, R.M., Rao, D.S., Chaudhuri, A.A., Boldin, M.P., Taganov, K.D., Nicoll, J., Paquette, R.L., and Baltimore, D. (2008). Sustained expression of microRNA-155 in hematopoietic stem cells causes a myeloproliferative disorder. *J Exp Med* *205*, 585-594.

O'Connell, R.M., Zhao, J.L., and Rao, D.S. (2011). MicroRNA function in myeloid biology. *Blood* *118*, 2960-2969.

O'Riordan, M., and Grosschedl, R. (1999). Coordinate regulation of B cell differentiation by the transcription factors EBF and E2A. *Immunity* *11*, 21-31.

Ooi, A.G., Sahoo, D., Adorno, M., Wang, Y., Weissman, I.L., and Park, C.Y. (2010). MicroRNA-125b expands hematopoietic stem cells and enriches for the lymphoid-balanced and lymphoid-biased subsets. *Proceedings of the National Academy of Sciences of the United States of America* *107*, 21505-21510.

Orkin, S.H., and Zon, L.I. (2008). Hematopoiesis: an evolving paradigm for stem cell biology. *Cell* *132*, 631-644.

Piskounova, E., Polytarchou, C., Thornton, J.E., LaPierre, R.J., Pothoulakis, C., Hagan, J.P., Iliopoulos, D., and Gregory, R.I. (2011). Lin28A and Lin28B inhibit let-7 microRNA biogenesis by distinct mechanisms. *Cell* *147*, 1066-1079.

Puissegur, M.P., Eichner, R., Quelen, C., Coyaud, E., Mari, B., Lebrigand, K., Broccardo, C., Nguyen-Khac, F., Bousquet, M., and Brousset, P. (2012). B-cell regulator of immunoglobulin heavy-chain transcription (Bright)/ARID3a is a direct target of the oncomir microRNA-125b in progenitor B-cells. *Leukemia* *26*, 2224-2232.

Rao, D.S., O'Connell, R.M., Chaudhuri, A.A., Garcia-Flores, Y., Geiger, T.L., and Baltimore, D. (2010). MicroRNA-34a perturbs B lymphocyte development by repressing the forkhead box transcription factor Foxp1. *Immunity* *33*, 48-59.

Rossi, L., Lin, K.K., Boles, N.C., Yang, L., King, K.Y., Jeong, M., Mayle, A., and Goodell, M.A. (2012). Less is more: unveiling the functional core of hematopoietic stem cells through knockout mice. *Cell stem cell* *11*, 302-317.

- Rossi, R.L., Rossetti, G., Wenandy, L., Curti, S., Ripamonti, A., Bonnal, R.J., Birolo, R.S., Moro, M., Crosti, M.C., Gruarin, P., *et al.* (2011). Distinct microRNA signatures in human lymphocyte subsets and enforcement of the naive state in CD4⁺ T cells by the microRNA miR-125b. *Nature immunology* *12*, 796-803.
- Rubinsztein, D.C., Marino, G., and Kroemer, G. (2011). Autophagy and aging. *Cell* *146*, 682-695.
- Shaked, I., Meerson, A., Wolf, Y., Avni, R., Greenberg, D., Gilboa-Geffen, A., and Soreq, H. (2009). MicroRNA-132 potentiates cholinergic anti-inflammatory signaling by targeting acetylcholinesterase. *Immunity* *31*, 965-973.
- Smith, P.Y., Delay, C., Girard, J., Papon, M.A., Planel, E., Sergeant, N., Buee, L., and Hebert, S.S. (2011). MicroRNA-132 loss is associated with tau exon 10 inclusion in progressive supranuclear palsy. *Hum Mol Genet* *20*, 4016-4024.
- Song, S.J., Ito, K., Ala, U., Kats, L., Webster, K., Sun, S.M., Jongen-Lavrencic, M., Manova-Todorova, K., Teruya-Feldstein, J., Avigan, D.E., *et al.* (2013). The oncogenic microRNA miR-22 targets the TET2 tumor suppressor to promote hematopoietic stem cell self-renewal and transformation. *Cell stem cell* *13*, 87-101.
- Souabni, A., Cobaleda, C., Schebesta, M., and Busslinger, M. (2002). Pax5 promotes B lymphopoiesis and blocks T cell development by repressing Notch1. *Immunity* *17*, 781-793.
- Sun, B., Mallampati, S., Gong, Y., Wang, D., Lefebvre, V., and Sun, X. (2013). Sox4 is required for the survival of pro-B cells. *Journal of immunology (Baltimore, Md. : 1950)* *190*, 2080-2089.
- Sun, D., Luo, M., Jeong, M., Rodriguez, B., Xia, Z., Hannah, R., Wang, H., Le, T., Faull, K.F., Chen, R., *et al.* (2014). Epigenomic profiling of young and aged HSCs reveals concerted changes during aging that reinforce self-renewal. *Cell stem cell* *14*, 673-688.
- Taganov, K.D., Boldin, M.P., Chang, K.J., and Baltimore, D. (2006). NF-kappaB-dependent induction of microRNA miR-146, an inhibitor targeted to signaling proteins of innate immune responses. *Proceedings of the National Academy of Sciences of the United States of America* *103*, 12481-12486.
- Teng, G., Hakimpour, P., Landgraf, P., Rice, A., Tuschl, T., Casellas, R., and Papavasiliou, F.N. (2008). MicroRNA-155 is a negative regulator of activation-induced cytidine deaminase. *Immunity* *28*, 621-629.
- Thai, T.H., Calado, D.P., Casola, S., Ansel, K.M., Xiao, C., Xue, Y., Murphy, A., Frendewey, D., Valenzuela, D., Kutok, J.L., *et al.* (2007). Regulation of the germinal center response by microRNA-155. *Science (New York, N.Y.)* *316*, 604-608.

- Tothova, Z., Kollipara, R., Huntly, B.J., Lee, B.H., Castrillon, D.H., Cullen, D.E., McDowell, E.P., Lazo-Kallanian, S., Williams, I.R., Sears, C., *et al.* (2007). FoxOs are critical mediators of hematopoietic stem cell resistance to physiologic oxidative stress. *Cell* *128*, 325-339.
- Ucar, A., Vafaizadeh, V., Jarry, H., Fiedler, J., Klemmt, P.A., Thum, T., Groner, B., and Chowdhury, K. (2010). miR-212 and miR-132 are required for epithelial stromal interactions necessary for mouse mammary gland development. *Nat Genet* *42*, 1101-1108.
- Van Wynsberghe, P.M., Kai, Z.S., Massirer, K.B., Burton, V.H., Yeo, G.W., and Pasquinelli, A.E. (2011). LIN-28 co-transcriptionally binds primary let-7 to regulate miRNA maturation in *Caenorhabditis elegans*. *Nat Struct Mol Biol* *18*, 302-308.
- Viswanathan, S.R., and Daley, G.Q. (2010). Lin28: A microRNA regulator with a macro role. *Cell* *140*, 445-449.
- Viswanathan, S.R., Daley, G.Q., and Gregory, R.I. (2008). Selective blockade of microRNA processing by Lin28. *Science* *320*, 97-100.
- Wanet, A., Tacheny, A., Arnould, T., and Renard, P. (2012). miR-212/132 expression and functions: within and beyond the neuronal compartment. *Nucleic Acids Res.*
- Warr, M.R., Binnewies, M., Flach, J., Reynaud, D., Garg, T., Malhotra, R., Debnath, J., and Passegue, E. (2013). FOXO3A directs a protective autophagy program in haematopoietic stem cells. *Nature* *494*, 323-327.
- Wightman, B., Ha, I., and Ruvkun, G. (1993). Posttranscriptional regulation of the heterochronic gene *lin-14* by *lin-4* mediates temporal pattern formation in *C. elegans*. *Cell* *75*, 855-862.
- Wu, L., and Belasco, J.G. (2005). Micro-RNA regulation of the mammalian *lin-28* gene during neuronal differentiation of embryonal carcinoma cells. *Mol Cell Biol* *25*, 9198-9208.
- Xiao, C., Calado, D.P., Galler, G., Thai, T.H., Patterson, H.C., Wang, J., Rajewsky, N., Bender, T.P., and Rajewsky, K. (2007). MiR-150 controls B cell differentiation by targeting the transcription factor *c-Myb*. *Cell* *131*, 146-159.
- Xiao, C., Srinivasan, L., Calado, D.P., Patterson, H.C., Zhang, B., Wang, J., Henderson, J.M., Kutok, J.L., and Rajewsky, K. (2008). Lymphoproliferative disease and autoimmunity in mice with increased miR-17-92 expression in lymphocytes. *Nature immunology* *9*, 405-414.

Yoshida, T., Ng, S.Y., Zuniga-Pflucker, J.C., and Georgopoulos, K. (2006). Early hematopoietic lineage restrictions directed by Ikaros. *Nature immunology* 7, 382-391.

Zhao, J.L., Ma, C., O'Connell, R.M., Mehta, A., DiLoreto, R., Heath, J.R., and Baltimore, D. (2014). Conversion of danger signals into cytokine signals by hematopoietic stem and progenitor cells for regulation of stress-induced hematopoiesis. *Cell stem cell* 14, 445-459.

Zhao, J.L., Rao, D.S., O'Connell, R.M., Garcia-Flores, Y., and Baltimore, D. (2013). MicroRNA-146a acts as a guardian of the quality and longevity of hematopoietic stem cells in mice. *eLife* 2, e00537.

Zhou, B., Wang, S., Mayr, C., Bartel, D.P., and Lodish, H.F. (2007). miR-150, a microRNA expressed in mature B and T cells, blocks early B cell development when expressed prematurely. *Proceedings of the National Academy of Sciences of the United States of America* 104, 7080-7085.

Chapter 2: The microRNA-212/132 cluster buffers hematopoietic stem cell function with age

Published as: A Mehta, JL Zhao, N Sinha, GK Marinov, M Mann, MS Kowalczyk, RP Galimidi, X Du, E Erikci, A Regev, K Chowdhury, D Baltimore (2015). The microRNA-212/132 cluster regulates hematopoietic stem cell maintenance and survival with age by buffering FOXO3 expression. *In review*.

Abstract

MicroRNAs are critical post-transcriptional regulators of hematopoietic cell-fate decisions, though little remains known about their role in aging hematopoietic stem cells (HSCs). The microRNA-212/132 cluster (miR-212/132) is enriched in HSCs and is up-regulated during hematopoietic aging. Both over-expression and deletion of microRNAs in this cluster leads to inappropriate hematopoiesis with age. Enforced expression of miR-132 in the bone marrow compartment of mice led to rapid HSC cycling followed by HSC depletion. A genetic deletion of the miR-212/132 cluster in mice resulted in HSCs that had altered cycling, function, and survival in response to growth factor starvation. We found that miR-212/132 exerts its effect on aging HSCs by targeting the transcription factor FOXO3, a known aging associated gene. Our data demonstrates that miR-212/132 plays a role in maintaining balanced hematopoietic output by buffering FOXO3 expression. We have thus identified a novel target that may play a role in age-related hematopoietic defects.

Introduction

Hematopoietic stem cells (HSCs) are the source of most all the immune cells in our body (Orkin and Zon, 2008). A complex gene regulatory network tightly regulates the function and survival of HSCs to ensure balanced and appropriate hematopoietic output (Novershtern et al., 2011). Alteration of the HSC niche and deregulation in cell-intrinsic properties such as HSC self-renewal and cycling, metabolism, and survival can have drastic consequences on hematopoietic output (Passegue et al., 2005; Suda et al., 2011; Takubo et al., 2010). As an organism ages, the balance between HSC self-renewal, function, and survival is drastically altered (Geiger et al., 2013), and this may lead to deleterious consequences such as the inability to effectively combat infection, and the onset of autoimmune disease or hematologic cancers (Frasca and Blomberg, 2011; Henry et al., 2011).

Several genetic and epigenetic factors have been identified as important regulators of hematopoietic stem cell aging (Geiger et al., 2013; Rossi et al., 2012; Sun et al., 2014). To date, however, little is known about the role of noncoding RNAs in the regulation of hematopoietic stem cells with age. MicroRNAs, a class of small-noncoding RNA molecules, are important post-transcriptional regulators of hematopoietic cell-fate decisions (Baltimore et al., 2008; Chen et al., 2004; Gangaraju and Lin, 2009). They alter cell fate by negatively regulating gene expression through direct binding to the 3'untranslated regions of target mRNAs (Filipowicz et al., 2008). Importantly, as post-transcriptional regulators they function to buffer the protein expression of their targets and confer robustness to

biological processes such as lineage commitment (Ebert and Sharp, 2012; Mukherji et al., 2011; Strovas et al., 2014).

Several microRNAs have been found to regulate normal function of HSCs, including cell cycling and engraftment potential (Guo et al., 2010; Lechman et al., 2012; Ooi et al., 2010; Song et al., 2013; Zhao et al., 2013). However, it is unclear what role microRNAs might play in regulating stem cell function in the aging hematopoietic system. In this work, we study a previously unappreciated microRNA cluster, miR-212/132, that is enriched in HSCs and up-regulated with age. These two microRNAs share a seed sequence and therefore target many of the same genes. Several groups have demonstrated that the miR-212/132 is an important regulator of immune function (Lagos et al., 2010; Nakahama et al., 2013; Ni et al., 2014; Shaked et al., 2009). We now show that the miR-212/132 cluster plays a critical role in maintaining the balance between function and survival of aged HSCs. It does this by buffering the expression of its target FOXO3, one of only a few known genes associated with human longevity (Willcox et al., 2008).

Results

Enforced expression of miR-132 leads to depletion of HSCs and extramedullary hematopoiesis

To understand the role of the microRNA-212/132 cluster (miR-212/132) in hematopoiesis, we first examined the expression of both microRNAs during hematopoietic differentiation. We determined that miR-132 is enriched in early hematopoietic progenitors (Lineage-

Sca1⁺ cKit⁺; LSK cells) and in long-term hematopoietic stem cells in particular (HSCs: LSK CD150⁺ CD48⁻; Figure 1A). We initially focused on miR-132 since it was the more enriched of the two microRNAs (Supplemental Figure 1A). To investigate the function of miR-132 in these progenitors, we used a retroviral vector to ectopically express miR-132 in hematopoietic stem and progenitor cells (HSPCs) and transferred these miR-132 over-expressing cells into lethally irradiated wild-type (WT) C57BL/6 recipient mice (Supplemental Figure 1B-D). We then monitored mature cell output in the peripheral blood of these mice using flow-cytometry to detect the cell-surface markers that identify each cell type. Mice over-expressing miR-132 in the bone marrow compartment (herein referred to as WT^{miR-132}) when compared to empty vector controls (WT^{MG}) demonstrated a rapid accumulation of CD45⁺ peripheral blood leukocytes at 2 months post-reconstitution, followed by a progressive decline in the number of these cells by 4 months (Figure 1B). A closer inspection of the bone marrow compartment at 2 months post-reconstitution revealed that WT^{miR-132} mice displayed an expansion in the total number of LSK cells and HSCs (Figure 1C and Supplemental Figure 2A-C). These cells were additionally more proliferative, as measured by the proportion of cells expressing the proliferation marker Ki67, compared to LSK cells and HSCs from age-matched WT^{MG} controls (Figure 1D and Supplemental Figure 2D). WT^{miR-132} HSPCs further demonstrated a down-regulation in protein and RNA expression of several negative cell cycle regulators, including p27 and p57, although no change in p21 transcript levels was observed (Figure 1E and Supplemental Figure 2E). The mRNA expression of p27 remained down-regulated in WT^{miR-132} HSPCs compared to WT^{MG} HSPCs at 4-months post-reconstitution (Supplemental Figure 2F).

We next sought to characterize the cellular basis by which WT^{miR-132} mice undergo depletion in peripheral blood leukocytes at 4 months post-reconstitution. Almost two-thirds (29/44) of the WT^{miR-132} mice presented with gross pathology characteristic of extramedullary hematopoiesis, including enlarged spleens and pale, fibrotic bone marrow (Figure 1F and Supplemental Figure 2G). Strikingly, none of the age-matched WT^{MG} mice presented such a phenotype. Consistent with the onset of extramedullary hematopoiesis, spleens from WT^{miR-132} mice had a significant elevation of erythroid cells (Ter11+) and a slight elevation, albeit not statistically significant, of myeloid cells (CD11b+, Gr-1+) when compared to WT^{MG} mice (Supplemental Figure 2H). No elevation of myeloid cells was found in the peripheral blood of WT^{miR-132} mice compared to controls (Supplemental Figure 2I). Examination of the bone marrow, however, revealed that WT^{miR-132} mice had a severe (approximately 3-fold) depletion in the frequency and total number of LSK cells and HSCs compared to WT^{MG} controls (Figure 1G and Supplementary Figure 2J,K). A similar, though more dramatic, phenotype was observed at 9 months post-reconstitution in WT^{miR-132} mice (Supplemental Figure 3A). This phenotype of rapid proliferation followed by depletion of HSCs in the bone marrow compartment is an example of HSC exhaustion.

The depletion of HSCs in WT^{miR-132} mice had the expected dramatic effect on the numbers of more mature progenitor cells, including multi-potent progenitors (MPPs; LSK CD150-CD48+), lymphoid-primed MPPs (LMPPs; LSK Flt3+), and megakaryocyte/erythroid progenitors (MEPs; Lineage- Sca1- cKit+ CD34- FcRg-). However, no depletion in common myeloid progenitors (CMPs; Lineage- Sca1- cKit+ CD34+ FcRg-) or

granulocyte-myeloid progenitors (GMPs; Lineage- Sca1- cKit+ CD34+ FcRg+) was observed (Supplemental Figure 3B-F). Importantly, the observed alteration in WT^{miR-132} HSCs was intrinsic to the expression of the miR-132 over-expression vector, because no depletion in the proportion of HSCs was evident among the GFP- cells of WT^{miR-132} and WT^{MG} mice (Supplemental Figure 3H). Furthermore, we found that the observed phenotype was specific to the expression of authentic miR-132 because over-expression of a miR-132 mutant lacking the correct miR-132 seed sequence resulted in no observable phenotype at 9 months post-reconstitution when compared to WT^{MG} controls (Supplemental Figure 3H).

We next sought to investigate the role of miR-212 in HSC maintenance. We found that enforced expression of miR-212 in the bone marrow compartment of mice didn't result in a significant change in the total number of bone marrow CD45+ cells or LSK cells compared to controls (Supplemental Figure 3I,J). However, we found that there was a significant depletion of HSCs at 4-months post-reconstitution in these mice (Supplemental Figure 3K), thus suggesting a less severe phenotype than enforced miR-132 expression, which is consistent with the lower levels of enrichment of miR-212 in HSCs.

The microRNA-212/132 cluster has a physiological role of protecting the aging hematopoietic system

To determine if miR-132 has a physiological role in regulating hematopoietic stem cell function, we obtained mice that had a genetic deletion in the entire miR-212/132 cluster (herein referred to as miR-212/132^{-/-} mice) (Ucar et al., 2012). We observed no apparent

defect in the output of mature hematopoietic cells in the peripheral blood, spleen, and bone marrow of 12-week old miR-212/132^{-/-} mice when compared to age-matched wild-type (WT) controls (Supplemental Figure 4). We noticed, however, an up-regulation of miR-132 expression in the bone marrow and LSK compartment of aged (2-year old) WT mice compared to young (12-week old) WT mice (Figure 2A), and posited a more important role of miR-132 in maintaining the fidelity of aging HSCs. Consistent with this, we found that unlike in 12-week old mice (Supplemental Figure 4D), aged (60-week old) miR-212/132^{-/-} mice had an elevation in the total number of HSCs (LSK CD150⁺ CD48⁻ and LSK EPCR⁺) in the bone marrow compartment compared to WT controls (Figure 2B). Surprisingly, this was accompanied by a decrease in the total number of bone marrow LSK cells, which are mostly downstream products of HSCs (Figure 2B). Aged miR-212/132^{-/-} mice further presented with enlarged spleens (Supplemental Figure 5A) and a global depletion of all major mature cell types in the bone marrow compartment (Supplemental Figure 5B), indicative of a failure of HSCs to maintain normal hematopoietic output and the onset of extramedullary hematopoiesis.

To investigate the molecular basis for the role of the miR-212/132 cluster in HSCs, we performed gene expression analysis by bulk population RNA-sequencing on WT and miR-212/132^{-/-} long-term HSCs (LSK CD150⁺ CD48⁻), short term HSCs (LSK CD150⁻ CD48⁻), and multipotent progenitors (LSK CD150⁻ CD48⁺). Approximately 14,000 genes were expressed in each sample (Supplemental Figure 6A), and clustering based on the number differentially expressed genes revealed close similarity between WT short-term and long-term HSC subsets and miR-212/132^{-/-} short-term and long-term HSC subsets, with both

these groups differing significantly from the MPP populations (Figure 2C). Differentially expressed genes between the WT and miR-212/132^{-/-} HSC populations were enriched for several functional annotations relevant to HSC biology, including regulation of cell-cycle, cell differentiation, response to stress, and cell death (Figure 2D).

To investigate if the observed phenotype in miR-212/132^{-/-} mice is intrinsic to the hematopoietic system, we transferred bone marrow cells from 12-week old WT or miR-212/132^{-/-} mice into irradiated WT recipients. After one year, we found that the phenotypes in transplanted mice closely resembled that of aged WT and miR-212/132^{-/-} mice, respectively, consistent with a defect intrinsic to the hematopoietic system (Supplemental Figure 5C). We next employed an inflammatory model for hematopoietic aging (Esplin et al., 2011) to determine if this is sufficient to recreate the observed alteration in hematopoiesis. We delivered LPS eight times over one month to 16-week old miR-212/132^{-/-} and WT mice. We found that, consistent with the altered hematopoietic output we observed in aged mice, miR-212/132^{-/-} mice presented with severely enlarged spleens containing an enrichment of splenic HSCs compared to WT mice also injected with LPS (Figure 3A and Supplemental Figure 5D). Similar to aged miR-212/132^{-/-} mice, LPS treated miR-212/132^{-/-} mice also demonstrated an accumulation of HSCs and a decrease in the frequency of LSK cells in the bone marrow compartment compared to LPS treated WT controls (Figure 3B). This skewing of hematopoietic progenitor output in miR-212/132^{-/-} mice may be characterized by an increase in the total number of long-term HSCs and a reduction in total number of short-term HSCs and MPPs in the bone marrow compartment (Supplemental Figure 5E). We can therefore mimic the aging-related hematopoietic defect

observed in miR-212/132^{-/-} by exposing younger mice to chronic inflammatory stimuli via repetitive LPS injections.

Loss of the miR-212/132 cluster reduces HSC cycling and improves engraftment potential

The cycling characteristics of HSCs are closely related to their ability to self-renew and differentiate into committed progenitors (Pietras et al., 2011). Furthermore, increased HSC quiescence and an increase in HSC number is characteristic of the aging hematopoietic system (Geiger et al., 2013). We thus sought to determine if the accumulation of HSCs and decrease in output of more committed progenitors in miR-212/132^{-/-} mice might be a result of altered cell cycling. We performed cell-cycling analysis using flow cytometry by staining for the proliferation marker Ki67 and utilizing the dsDNA dye Hoescht33342. Under steady-state conditions, we observed no major defect in cell cycling in 16-week old miR-212/132^{-/-} mice compared to age-matched WT mice (Supplemental Figure 5F). However, under conditions of inflammatory stress such as low-grade LPS stimulation, we found that miR-212/132^{-/-} HSCs were far less proliferative, with an almost 50% increase in the number of cells in the G₀ phase of the cell cycle compared to WT HSCs (Figure 3C-E). Importantly, we observed a substantial decrease in the number of HSCs in G₁ and only a small proportion of cells in S/M phases of the cell cycle in miR-212/132^{-/-} mice (Figures 3C-E). No change in p27 mRNA expression was observed at steady state between miR-212/132^{-/-} and WT HSCs. However, in mice treated with either LPS or 5-fluorouracil, which induce HSC proliferation, the expression of p27 in the bone marrow compartment was up-regulated in miR-212/132^{-/-} mice compared to WT mice (Supplemental Figure 5G,H). It follows that the loss of the miR-212/132 cluster leads to increased HSC

quiescence and an accumulation of HSCs, with a concomitant decrease in the number of more committed progenitors.

The majority of HSCs in the hematopoietic system remain in a dormant state, and disruption of this quiescence can have serious consequences for HSC function (Rossi et al., 2012). To investigate whether the alteration in cell cycling of aged miR-212/132^{-/-} HSCs might be related to altered HSC function, we performed competitive transplant assays. Aged (60-weeks) CD45.2 miR-212/132^{-/-} or WT^{-/-} HSCs were transplanted with equal numbers of CD45.1 WT HSCs into lethally irradiated CD45.2 recipient mice. The peripheral blood of these mice was analyzed 4 months post-reconstitution for repopulation of major mature cell types. The cells from aged miR-212/132^{-/-} mice were more effective at reconstituting most all immune cells than those from aged WT mice, as evidenced in total blood leukocytes (CD45+), B-cells (CD19+), myeloid cells (CD11b+), and granulocytes (Gr-1+) in the peripheral blood (Figure 4A). An insignificant difference in the relative proportion of T-cells (CD3e+) was observed (Figure 4A). Competitive transplant of young (12-weeks) miR-212/132^{-/-} HSCs yielded no observable functional difference compared to young WT HSCs except for defective repopulation of T-cells (Figure 4B); however, secondary transplantation of young miR-212/132^{-/-} HSCs yielded a similar phenotype to that observed with primary transplantation of aged miR-212/132^{-/-} HSCs (Supplemental Figure 5I). Consistent with the increased quiescence of aged miR-212/132^{-/-} HSCs compared to WT HSCs, miR-212/132^{-/-} cells performed better at long-term repopulation. Additionally, HSCs obtained from WT^{miR-132} mice, which ectopically over-express miR-132, were severely defective in long-term reconstitution in competitive transplant assays

compared to control HSCs obtained from WT^{MG} mice (Figure 4C). It therefore appears that the miR-212/132 cluster is important for tuning the interplay between quiescence and functional output of the aging hematopoietic system.

FOXO3 is a target of miR-132 in bone marrow cells

To understand the molecular mechanism of miR-132 action, we characterized the expression of the best computationally predicted targets of miR-132 from TargetScan under conditions of miR-132 over-expression (Friedman et al., 2009). RNA was extracted from lineage-depleted bone marrow cells of WT^{miR-132} and WT^{MG} mice and was subjected to quantitative polymerase chain reaction (qPCR) for target genes relevant to HSC function. The most significantly down-regulated targets under conditions of ectopic expression of miR-132 in WT^{miR-132} bone marrow, relative to control WT^{MG} bone marrow, were pursued for further analysis. Messenger RNA expression of several genes relevant to hematopoiesis was down regulated in WT^{miR-132} bone marrow samples, including AchE, FOXO3, Lin28B, MMP9, and SOX4 (Figure 5A). We sought to further investigate the role of FOXO3 in mediating the effect of miR-132 on HSCs as it contains a perfect 8-mer binding site for miR-132 (Figure 5B) and is the most significantly down regulated of these genes. Importantly, we also found a global upregulation of miR-132 targets in our RNA-sequencing analysis of miR-212/132^{-/-} and WT HSCs, and this included an upregulation of FOXO3 transcript expression as well as some of its downstream targets (Supplemental Figure 6B-D). We validated that miR-132 binds directly to the FOXO3 3'-untranslated region (3'UTR) using a luciferase reporter assay in which the FOXO3 3'UTR was

expressed immediately downstream of luciferase. We found that in the presence of miR-132 the expression of this reporter was significantly lower than from a vector lacking the FOXO3 3'UTR (Figure 5C). This binding was specific to miR-132 because mutating the miR-132 binding site on the FOXO3 3'UTR normalized luciferase expression (Figure 5C).

We next quantified FOXO3 protein expression in bone marrow cells from WT^{miR-132} and WT^{MG} mice. Consistent with FOXO3 being a target of miR-132, we found that protein expression was significantly down regulated in WT^{miR-132} mice compared to WT^{MG} mice (Figure 5D). Expression of FOXO1 and FOXO4, closely related family members of FOXO3, remained unchanged in WT^{miR-132} bone marrow cells (Supplemental Figure 7A). Importantly, we also found that FOXO3 mRNA and protein expression levels were elevated in lineage depleted bone marrow cells from miR-212/132^{-/-} mice compared to WT controls (Figure 5E,F). Expression of FOXO4 was also slightly elevated in miR-212/132^{-/-} cells and expression of FOXO1 was unchanged (Supplemental Figure 7B). We additionally performed intracellular staining of FOXO3 and phospho-FOXO3 (p-FOXO3) protein. As expected, we found elevated levels of FOXO3 in miR-212/132^{-/-} HSCs compared to WT controls. However, we saw only a marginal elevation in p-FOXO3 in miR-212/132^{-/-} HSCs, indicating that the majority of extra FOXO3 in these cells is likely in the nucleus in its active, un-phosphorylated state (Supplemental Figure 7C,D). Together, the data indicate that miR-132 is an important regulator of FOXO3 expression in bone marrow cells. As was observed with miR-132 expression, FOXO3 mRNA expression was increased in bone marrow cells from aged mice compared to those of young mice (Figure 6A), thus

suggesting that miR-132 might serve to maintain FOXO3 protein expression within a balanced range for normal hematopoietic function.

miR-132 regulates HSC cycling and function through FOXO3

To determine if FOXO3 is a key mediator of miR-132 function, we co-expressed FOXO3 with miR-132 in the bone marrow compartment of WT mice to see if it would rescue the phenotype observed with miR-132 expression alone. FOXO3 cDNA lacking a miR-132 target site was cloned into the MSCV-IRES-eGFP (MIG) vector immediately downstream of the MSCV promoter (Figure 6B). As previously described, miR-132 was cloned immediately downstream of eGFP. Lethally irradiated mice were reconstituted with bone marrow cells transduced with a control vector (WT^{MIG}), or a vector expressing both miR-132 and FOXO3 (WT^{FOXO3 + miR-132}), miR-132 only (WT^{miR-132}) or FOXO3 only (WT^{FOXO3}). The expression of miR-132 and FOXO3 from these vectors was validated by qPCR and Western Blot, respectively (Supplemental Figure 7E-F). We observed the mean fluorescence intensity of eGFP in bone marrow cells expressing only FOXO3 to be lower than that of the other vectors, suggesting that over-expression of FOXO3 above endogenous levels may have a toxic effect on these cells (Supplemental Figure 7G). We additionally observed that a larger fraction of bone marrow HSCs from WT^{FOXO3} mice expressed AnnexinV compared to WT^{MIG} controls (Supplemental Figure 7H). This effect was not observed when FOXO3 was co-expressed with miR-132, presumably because baseline levels of FOXO3 were already down regulated due to miR-132 over-expression.

As expected, a reduction in peripheral blood leukocytes was observed in $WT^{miR-132}$ mice compared to WT^{MIG} mice at 4-months post-reconstitution (Figure 6C). Co-expression of FOXO3 with miR-132, however, rescued this defect, as no significant change in peripheral blood leukocytes was observed in $WT^{FOXO3 + miR-132}$ mice compared to WT^{MIG} controls (Figure 6C). Examination of the bone marrow compartment of $WT^{FOXO3 + miR-132}$ mice revealed total numbers of HSCs and LSK cells comparable to WT^{MIG} controls, demonstrating a rescue of HSC depletion observed with the expression of miR-132 alone (Figure 6D,E). In addition, expression of FOXO3 alone resulted in a moderate elevation in the total number of bone marrow LSK cells compared to control mice (Figure 6E). HSCs from $WT^{FOXO3 + miR-132}$ mice also showed comparable proportions of Ki67 staining to HSCs from WT^{MIG} mice, indicating that these cells were not prone to cycling like $WT^{miR-132}$ cells (Figure 5F). WT^{FOXO3} HSCs demonstrated a significant albeit moderate decrease in the proportion of cycling HSCs compared to controls (Figure 6F). These experiments suggest that co-expression of FOXO3 can rescue the phenotype observed with expression of miR-132 alone. It seems likely that miR-132 regulates hematopoiesis primarily by directly modulating FOXO3 levels, although we cannot rule out that FOXO3 overexpression is able to override the miR-132 effect while the true targets of miR-132 in the bone marrow are other genes.

Loss of miR-212/132 affects HSC survival through protective autophagy

FOXO3 is critical for maintaining the hematopoietic stem cell pool by regulating HSC cell-cycling and resistance to oxidative stress (Miyamoto et al., 2007; Tothova et al., 2007). It is also implicated in maintaining the survival of aging HSCs by directing protective

autophagy (Warr et al., 2013). To this end, we found that several autophagy-related genes were up-regulated in miR-212/132^{-/-} HSCs compared to WT controls upon inspection of our RNA-sequencing dataset (Supplemental Figure 6E). Thus, to determine if miR-132 might play a role in altering survival of HSCs, we sorted HSCs from WT and miR-212/132^{-/-} mice and cultured them in the presence or absence of survival growth factors and cytokines, including mSCF, mIL6, mIL3, TPO, and Flt3L. We used a luciferase-based assay to monitor caspase 3 and caspase 7 activities after 12 hours in culture. In the presence of survival factors, minimal caspase activity was observed in both WT and miR-212/132^{-/-} HSCs. However, under starvation conditions, which induce protective autophagy in aged HSCs (Warr et al., 2013), miR-212/132^{-/-} HSCs demonstrated a significant reduction in induction of apoptosis compared to WT HSCs (Figure 7A). This is consistent with the more rapid induction of a protective autophagy program due to higher levels of FOXO3 in miR-212/132^{-/-} HSCs. Importantly, when autophagy was inhibited by Bafilomycin A (BafA), a known inhibitor of autophagosome fusion to lysosomes, miR-212/132^{-/-} and WT HSCs underwent comparable, higher levels of apoptosis (Figure 7A). As previously reported, FOXO3 expression levels had no major effect on autophagy and apoptosis of myeloid progenitors (Figure 7B).

To determine if miR-212/132^{-/-} HSCs indeed induce the autophagy machinery more potently than WT HSCs, we utilized a fluorescent reporter for autophagosome formation that was detectable by flow cytometry. The efficacy of this assay in detecting autophagosome formation was validated by comparing signal intensity in WT cells to autophagy deficient cells (Supplemental Figure 7I). WT and miR-212/132^{-/-} HSCs were

cultured under growth factor rich or starvation conditions as described above and were stained for the presence of autophagosomes. Under starvation conditions, miR-212/132^{-/-} HSCs demonstrated higher levels of autophagosome formation compared to WT HSCs (Figure 7C). In the presence of LY2940002, a PI3-kinase inhibitor and early inhibitor of autophagy, autophagosome formation was decreased to comparable levels in miR-212/132^{-/-} and WT HSCs (Figure 7C). We additionally sought to investigate whether the potent induction of autophagy in miR-212/132^{-/-} HSCs may improve survival by altering reactive-oxygen species (ROS) accumulation. We utilized a fluorescent detection system for ROS and found that miR-212/132^{-/-} HSCs had lower levels of ROS accumulation compared to WT HSCs under conditions of starvation (Figure 7D). The accumulation of ROS was elevated to comparable levels in WT and miR-212/132^{-/-} HSCs when autophagy was inhibited with BafA (Figure 7D).

We employed an shRNA knockdown strategy for FOXO3 to determine if it is the key mediator of autophagy in miR-212/132^{-/-} HSCs. WT and miR-212/132^{-/-} HSPCs were transduced with either a control vector (MB) or a FOXO3 shRNA construct (shFOXO3), and were subsequently used to reconstitute lethally irradiated WT mice. At 2 months post-reconstitution, we sorted HSCs from these mice and subjected them to the aforementioned assays for autophagy induction and caspase activation under conditions of growth factor starvation. WT HSCs expressing shFOXO3 demonstrated lower autophagy activity and higher levels of apoptosis compared to WT HSCs expressing MB (Figure 7E,F). Importantly, knockdown of FOXO3 in miR-212/132^{-/-} HSCs resulted in a significant reduction in autophagy induction and an increase in caspase activity compared to miR-

212/132^{-/-} HSCs expressing MB. However, this reduction did not reduce autophagy activity completely to that of WT HSCs expressing MB. This may be due to incomplete knockdown of FOXO3 in miR-212/132^{-/-} cells or may suggest that factors other than FOXO3 might be involved in mediating autophagy induction (Figure 7E,F).

Discussion

MicroRNAs are key regulators of lineage commitment and function in immune cells (Baltimore et al., 2008; Gangaraju and Lin, 2009; O'Connell et al., 2010b). Several microRNAs have been implicated in regulating diverse facets of normal HSC maintenance and function, such as cell-cycling (Lechman et al., 2012; Song et al., 2013), apoptosis (Guo et al., 2010), engraftment potential (O'Connell et al., 2010a; Ooi et al., 2010), and resistance to inflammatory stress (Zhao et al., 2013). While much has been done to characterize the functional differences between aged and young HSCs, little is known about how microRNAs might contribute to maintaining balanced hematopoietic output as an organism ages. Our findings suggest that the miR-212/132 cluster, particularly miR-132, is critical in regulating the balance between HSC survival, and proliferation and differentiation. We demonstrate that it does this primarily by buffering the expression of FOXO3 in the aging hematopoietic system. Deregulation of this cluster, and in turn FOXO3, can have negative consequences on the function of HSCs and the output of mature hematopoietic cells, leading to extramedullary hematopoiesis.

Because the expression of miR-132 was higher in HSCs compared to total bone marrow cells, we utilized both gain-of-function and loss-of-function approaches to investigate its role in HSC function and survival. Ectopic expression of miR-132 resulted in hyperproliferation and depletion of HSCs within the bone marrow compartment. Enforced expression of miR-212 produced a similar but less dramatic phenotype. This depletion of HSCs with miR-132 over-expression coincided with the onset of extramedullary hematopoiesis, including enlarged spleens and fibrotic bone marrow. We observed a drastic decrease in protein expression of the miR-132 target FOXO3 within the bone marrow compartment of miR-132 over-expressing mice. Consistent with our findings, a genetic deletion of FOXO3 in hematopoietic cells leads to increased HSC proliferation and an age-dependent depletion of the HSC pool with loss of HSC long-term reconstitution potential (Miyamoto et al., 2007). This phenotype is exacerbated by the concomitant deletion of the FOXO family members FOXO1 and FOXO4 (Tothova et al., 2007). We further found several FOXO3 target genes, particularly the negative cell-cycle regulators p21, p57, and p27, to be down regulated in miR-132 over-expressing bone marrow. Importantly, replenishing levels of FOXO3 during miR-132 over-expression rescued the phenotype we observed.

A genetic deletion of the miR-212/132 cluster led to higher basal expression of FOXO3 in bone marrow cells. Over time, this led to a dramatic increase in the number of HSCs, a decrease in production of more committed progenitors, and a defect in HSC cycling in response to environmental stress, such as lipopolysaccharide treatment. Consistent with the more quiescent state of miR-212/132^{-/-} HSCs, we found they were marginally better at

long-term reconstitution of the hematopoietic system than WT counterparts. FOXO3 is a known regulator of apoptosis, and we further demonstrated that ectopic expression of FOXO3 from a retroviral vector resulted in a selection for those cells expressing the lowest amount of the vector, presumably because higher levels of FOXO3 expression were toxic. We have therefore shown that the miR-212/132 cluster is important in regulating expression of FOXO3, and that when this target is either up-regulated or down regulated, there is a severe alteration in HSC function over time.

The expression of both miR-132 and FOXO3 transcripts is up-regulated with age in murine bone marrow cells and early progenitors. The role of FOXO3 as a longevity-associated gene remains unknown in the hematopoietic system. FOXO3 may be up-regulated in this context due to its vital role in survival through autophagy and in cell cycling. MicroRNAs play an important role in buffering perturbations in the expression of their targets in response to environmental stress (Ebert and Sharp, 2012; Kim et al., 2013). Such stress might include inflammation from repetitive exposure to environmental pathogens and hematopoietic aging. Importantly, the abundance of microRNAs in any given cell plays an important role in establishing a threshold for target expression (Mukherji et al., 2011); as such, up-regulation of the microRNA may require higher target expression to maintain important physiological functions. Given that both over-expression and deletion of miR-132 in bone marrow cells led to inappropriate hematopoiesis, we believe that miR-132 plays an important role in buffering FOXO3 expression levels within a defined range to maintain normal HSC function as an organism ages. The concomitant increase in the expression of miR-132 alongside FOXO3 in the aging hematopoietic system may be

critical for maintaining an important balance between known FOXO3-regulated processes, including cell-cycling and differentiation, and apoptosis of HSCs.

The aging hematopoietic system is characterized by an alteration of the balance between self-renewal and differentiation, which leads to the accumulation of less-functional HSCs, myeloid-biased differentiation, and a requirement for basal autophagy for survival (Geiger et al., 2013; Rossi et al., 2005; Warr et al., 2013). Of note is the fact that the loss of critical autophagy factors in the hematopoietic system leads to hyper-proliferation and poor survival of HSCs (Mortensen et al., 2011). Recently, it has also been demonstrated that FOXO3 plays a critical role in inducing protective autophagy of aging HSCs (Warr et al., 2013), which is critical for their survival in response to oxidative stress (Eijkelenboom and Burgering, 2013). The proposed mechanism of FOXO3 regulation of autophagy is through the transcription of glutamine synthase (van der Vos et al., 2012). Consistent with this role of FOXO3 in HSC survival, we found that miR-212/132^{-/-} HSCs, when compared to WT HSCs, demonstrated increased resistance to growth-factor starvation, as evidenced by the decrease in presence of reactive oxygen species, lower levels of apoptosis induction, and an increase in accumulation of autophagosomes. We observed an abrogation of this effect when we knocked down FOXO3 in miR-212/132^{-/-} HSCs, thus demonstrating that this phenotype is mostly due to the up-regulation of FOXO3 in these cells. Importantly, this improved survival of miR-212/132^{-/-} cells in response to environmental stress may contribute to the age-dependent accumulation of HSCs in miR-212/132^{-/-} mice compared to WT mice.

Our observations demonstrate that the miR-212/132^{-/-} cluster is an important regulator of HSC homeostasis by altering cell cycling, function, and survival. This is one of the first clear examples of a microRNA playing a physiological role in maintaining the balance of HSC functions during aging. The capacity of this microRNA to buffer expression of FOXO3 is critical given the multiple roles FOXO3 plays in regulating HSC biology. Our findings open the possibility of utilizing miR-132 mimics or antagonists to alter defects in HSC function that might lead to hematopoietic diseases late in life.

Experimental Procedures

DNA constructs

For *in-vivo* miR-132 over-expression and FOXO3 shRNA experiments, the mature miR-132 or FOXO3 shRNA sequence was placed in the microRNA-155 loop-and-arms format (O'Connell et al., 2010a) and cloned into the MSCV-eGFP (MG) and MSCV-TagBFP (MG) vectors, respectively. For FOXO3 rescue experiments, FOXO3 cDNA was cloned into the MSCV-IRES-eGFP (MIG) vector. See supplemental procedures for more details about these vectors. FOXO3 shRNA target sequences are given in Table S1.

For luciferase assays, the microRNA-132 expression cassette was sub-cloned into the pCDNA3 vector. The 3'untranslated regions of relevant gene targets containing the miR-132 binding region were cloned immediately downstream of luciferase in the pMiReport vector as previously described (Chaudhuri et al., 2012).

Cell culture

Cells were cultured in a sterile incubator that was maintained at 37⁰C and 5% CO₂. 293T cells were cultured in DMEM supplemented with 10% fetal bovine serum, 100 U/mL penicillin, and 100 U/mL streptomycin. Primary cells were cultured in complete RPMI supplemented with 10% FBS, 100 U/mL penicillin, 100 U/mL streptomycin, 50uM β-mercaptoethanol, and appropriate growth cytokines as needed for the experiment (see below).

Cell sorting for RNA extraction

For miR-132 expression profiling, bone marrow cells from C57BL/6 mice were depleted of RBCs and sorted for the respective cell populations at the Caltech Flow Cytometry Core Facility. Detailed procedures are provided in the supplemental procedures. RNA was harvested using the miRNAeasy RNA prep kit (Qiagen). For bone marrow samples from MG and miR-132 mice, bone marrow was harvested from the respective mice, lysed of red blood cells, and spun down. RNA was harvested as described above.

Expression profiling and qPCR

We performed real time qPCR (RT-qPCR) with a 7300 Real-Time PCR machine (Applied Biosystems) as previously described (Chaudhuri et al., 2012). TaqMan qPCR was performed for miR-132, miR-212 and snoRNA-202 (control) detection as per manufacturers instructions using TaqMan MicroRNA Assays (Life Technologies). SYBR Green-based RT-qPCR was performed for mRNA of mouse FOXO3, FOXO1, p27, p21, p57, and relevant miR-132 targets following cDNA synthesis using qScript cDNA SuperMix (Quanta) and detection with PerfeCTa qPCR Fastmix with ROX (Quanta) as per manufacturers instructions. Gene-specific primers used for qPCR are listed in Table S2. RNA-seq library construction and analysis are described in the Supplemental Information.

Target prediction and Luciferase reporter assays

Relevant targets for miR-132 were investigated using predictions from TargetScan Mouse 6.2 software (Friedman et al., 2009) and following sorting by probability of conserved targeting (P_{CT}). Luciferase assays for miR-132 targets were performed as previously

described (Chaudhuri et al., 2012). Briefly, 4×10^5 cells were plated in 12-well plates for 24 hours and subsequently transfected with either pCDNA or pCDNA-miR-132, a pMiReport vector, and a β -gal expression vector. 48 hours later, cells were lysed using Reporter Lysis Buffer (Promega) and luciferase and β -gal expression was analyzed, respectively, using a Dual Luciferase Kit (Promega) and a chemiluminescent β -gal reporter kit (Roche).

Immunoblotting

Bone marrow samples were prepared as described for RNA preparation. Cell extracts were collected using RIPA lysis buffer (Sigma), and were subjected to gel-electrophoresis and transfer onto a PVDF membrane. Antibody staining was performed using antibodies for FOXO3, p27, and actin. Detailed procedures are given in the supplemental information.

Animals

The California Institute of Technology Institutional Animal Care and Use Committee approved all experiments. C57BL/6 WT and miR-212/132^{-/-} mice were bred and housed in the Caltech Office of Laboratory Animal Resources (OLAR) facility. Bone marrow reconstitution experiments were performed as previously described (Chaudhuri et al., 2012) with the aforementioned vectors and are explained in more detail in the Supplemental Procedures. Recipient mice were monitored for health and peripheral blood was analyzed for mature blood cell types each month up till the experimental end-point at either 16 or 36 weeks post-reconstitution. At each end-point, immune organs were harvested for further analysis as described. The number of mice for each experimental cohort is described in the

figure legends. Each experiment was repeated at least twice, and in many cases three or four times.

Competitive transplant experiments

Bone marrow cells from age and gender-matched WT CD45.2+ C57BL/6 mice, miR-212/132^{-/-} CD45.2+ C57BL/6 mice, and WT CD45.1+ C57BL/6 mice were harvested and depleted of RBCs as described above. A 1:1 ratio of WT CD45.1+ HSCs with either WT or miR-212/132^{-/-} CD45.2+ HSCs were subsequently injected into lethally irradiated (1000 rads) WT CD45.2+ C57BL/6 mice. Mice were monitored for up to 20 weeks post-reconstitution and relevant tissues were harvested for further analysis by flow cytometry.

Flow cytometry

Relevant tissues were harvested and cells were homogenized and subsequently depleted of red blood cells as described above. Fluorophore-conjugated antibodies were used for the indicated markers, and detected using a MACSQuant10 Flow Cytometry machine (Miltenyi). Detailed procedures are given in the supplemental information.

Autophagy and reactive-oxygen species assays

HSCs were sorted as described above from either WT or miR-212/132^{-/-} C57BL/6 mice, or from reconstituted mice with donor WT or miR-212/132^{-/-} bone marrow infected with either MB or shFOXO3 retroviral constructs. Cells were then cultured with the appropriate growth factors and cytokines, or autophagy inhibitors, and processed for caspase activity

(Promega), the presence of ROS (Life Technologies), or autophagy activity (Enzo Life Sciences). Detailed procedures are given in the supplemental information.

Statistical tests

All statistical analysis was done in Graphpad Prism software using an unpaired Student's *t* test. Data was reported as mean \pm SEM. Significance measurements were marked as follows: * $p < 0.05$, ** $p < 0.01$, *** $p < 0.001$, or ns for not significant.

Data access

The RNA-seq data used in this study can be accessed from the Gene Expression Omnibus under the accession project ID GSE66352.

Figure legends

Figure 1. miR-132 is expressed in hematopoietic stem cells (HSCs) and over-expression alters hematopoiesis. (A) miR-132 expression in mature and progenitor hematopoietic cells. Cell populations were sorted by FACS directly into RNA lysis buffer and miR-132 expression was detected using TaqMan RT-qPCR (n=3). (B) – (G) WT C57BL/6 mice were lethally irradiated and reconstituted with donor bone marrow cells expressing either a control (MG) or a miR-132 over-expressing (miR-132) retroviral vector (n=8-12 mice per group). (B) Total numbers of mature leukocytes (CD45+) in the peripheral blood of MG and miR-132 mice at the indicated time points post-reconstitution. (C) Total number of HSCs (LSK CD150+ CD48-) in the bone marrow of MG and miR-132 mice at 8-weeks post-reconstitution. (D) Percentage of Ki-67+ bone marrow HSCs in MG and miR-132 mice at 8-weeks post-reconstitution. (E) Protein and RNA expression of p27 in the bone marrow of MG and miR-132 mice at 8-weeks post-reconstitution (n=3). (F) Representative spleen and bone marrow gross pathology of MG and miR-132 mice at 16-weeks post-reconstitution. (G) Total number of LSK cells and HSCs in the bone marrow of MG and miR-132 mice at 16-weeks post-reconstitution. Data represents at least three independent experiments and is represented as mean \pm SEM. See also Figures S1-S3. * denotes $p < 0.05$, ** denotes $p < 0.01$ and *** denotes $p < 0.001$ using a Student's *t* test.

Figure 2. Genetic deletion of the microRNA-212/132 cluster in mice alters hematopoietic output with age. (A) miR-132 expression in total bone marrow and LSK cells from 8-week old and 2-year old C57BL/6 WT mice. miR-132 expression was quantified by TaqMan

RT-qPCR (n=2). (B) – (D) Mice with a genetic deletion of the miR-212/132 cluster (miR-212/132^{-/-}) along with WT mice in the C57BL/6 background were analyzed. (B) Total number of HSCs (LSK CD150⁺ CD48⁻ and LSK EPCR⁺) and LSK cells in the bone marrow compartment of 60-64 week old WT and miR-212/132^{-/-} mice (n=7-12 mice per group). (C) Global expression profiling of WT and miR-212/132^{-/-} HSCs, as well as short-term HSCs and MPPs, from 16-week old mice using RNA-seq. The heat map represents the number of differentially expressed genes between the different WT and miR-212/132^{-/-} (KO) populations. (D) Enriched gene-ontology terms for differently expressed genes between WT and miR-212/132^{-/-} progenitors. Data represents at least two independent experiments and is represented as mean ± SEM. See also Figures S4-S6. * denotes p < 0.05, ** denotes p < 0.01 and *** denotes p < 0.001 using a Student's *t* test.

Figure 3. Genetic deletion of miR-212/132 in mice alters hematopoietic output and cycling in response to LPS stimulation. (A) – (E) 6-month old WT and miR-212/132^{-/-} mice were treated with 9 evenly-spaced low-dose (1mg/kg of body weight) LPS or PBS injections over one month. (A) Spleen weights of WT and miR-212/132^{-/-} mice treated with PBS or LPS. (B) Proportion of HSCs and LSK cells within the bone marrow compartment of WT and miR-212/132^{-/-} mice treated with LPS or PBS. (C) Representative FACS plots for cell cycle analysis of HSCs and LSK cells from WT and miR-212/132^{-/-} mice following LPS injection. (D) Proportion of bone marrow LSK cells and HSCs in each stage of the cell cycle (G0, G1, G2/M) from WT and miR-212/132^{-/-} mice following LPS injection. (E) Proportion of bone marrow LSK cells and HSCs expressing Ki67 from WT and miR-212/132^{-/-} mice following LPS injection. Data represents at least two independent

experiments and is represented as mean \pm SEM. See also Figures S4-S5. * denotes $p < 0.05$, ** denotes $p < 0.01$ and *** denotes $p < 0.001$ using a Student's *t* test.

Figure 4. The microRNA-212/132 cluster regulates long-term reconstitution potential of HSCs with age. (A) and (B) WT or miR-212/132^{-/-} CD45.2⁺ bone marrow cells, calibrated for the total number of phenotypically defined HSCs, were injected in a 1:1 ratio with CD45.1⁺ WT bone marrow cells into irradiated C57BL/6 CD45.2⁺ recipients. (A) Ratio of total CD45.2⁺ cells to CD45.1⁺ cells at 16-weeks post-reconstitution for various mature immune cell types in the peripheral blood of mice injected with aged WT and miR-212/132^{-/-} CD45.2⁺ cells. Data was normalized to proportion of WT CD45.2⁺ cells. (B) Ratio of total CD45.2⁺ cells to CD45.1⁺ cells at 16-weeks post-reconstitution for various mature immune cell types in the peripheral blood of mice injected with young WT and miR-212/132^{-/-} CD45.2⁺ cells. (C) Control (MG) or miR-132 over-expressing (miR-132) bone marrow HSCs, both expressing a retroviral vector containing eGFP, were injected in a 1:1 ratio with un-infected WT bone marrow HSCs into irradiated C57BL/6 mice. Graphs show the ratio of eGFP⁺ cells to eGFP⁻ cells for various immune cell types in the peripheral blood of recipients at 16-weeks post-reconstitution. Data represents at two independent experiments and is represented as mean \pm SEM. * denotes $p < 0.05$ using a Student's *t* test.

Figure 5. FOXO3 is a direct target of miR-132 in bone marrow cells. (A) mRNA expression by RT-qPCR of computationally predicted miR-132 targets in control (MG) or miR-132 over-expressing (miR-132) bone marrow cells. (B) Schematic of the predicted

miR-132 binding site in the FOXO3 3'UTR. (C) Relative luciferase expression in 293T cells transfected with a miR-132 over-expression vector and either a vector containing luciferase only (control), a vector containing luciferase and the FOXO3 3'UTR immediately downstream (FOXO3 3'UTR), or a vector containing luciferase and a FOXO3 3'UTR with a mutated miR-132 binding site (FOXO3 3'UTR mut). (D) FOXO3 protein expression in bone marrow cells from MG and miR-132 mice obtained by Western Blot. (E) FOXO3 transcript expression in lineage-depleted bone marrow cells obtained from WT or miR-212/132^{-/-} mice. (F) FOXO3 protein expression in lineage-depleted bone marrow cells obtained from WT or miR-212/132^{-/-} mice. See also Figure S7A-C. Data represents at least two independent experiments (n=2) and is represented as mean \pm SEM. * denotes $p < 0.05$, ** denotes $p < 0.01$, and *** denotes $p < 0.001$ using a Student-T test.

Figure 6. Co-expression of FOXO3 with miR-132 rescues the hematopoietic defects observed with expression of miR-132 alone. (A) FOXO3 mRNA expression by RT-qPCR in total bone marrow cells from 8-week old, 1-year old, and 2-year old C57BL/6 WT mice (n=2). (B) Schematic of retroviral vectors constructed for expression of FOXO3 only or for co-expression of FOXO3 along with miR-132. (C) – (F) WT C57BL/6 mice were lethally irradiated and reconstituted with donor bone marrow cells expressing either a control (MG), a miR-132 over-expressing (miR-132), a FOXO3 over-expressing (FOXO3), or a FOXO3 and miR-132 over-expressing (FOXO3 and miR-132) retroviral vector (n=10-12 mice per group). (C) Total peripheral blood CD45⁺ leukocytes in the respective animals at 16-weeks post-reconstitution. (D) Total LSK cells in the bone marrow compartment of the respective animals at 16-weeks post-reconstitution. (E) Total HSCs in the bone marrow

compartment of the respective animals at 16-weeks post-reconstitution. (F) Proportion of bone marrow HSCs expressing Ki-67 in the respective animals at 16-weeks post-reconstitution. Data represents at least two independent experiments and is represented as mean \pm SEM. See also Figure S7E-H. * denotes $p < 0.05$, ** denotes $p < 0.01$, and *** denotes $p < 0.001$ using a Student's *t* test.

Figure 7. Genetic deletion of the miR-212/132^{-/-} cluster results in a FOXO3 dependent alteration in autophagy and survival of HSCs. (A) and (B) Cells obtained from WT and miR-212/132^{-/-} mice were cultured with or without growth cytokines (mIL3, mIL6, mSCF, TPO, Flt3L, and G-CSF) or BafA. Caspase activation was measured using a luciferase based assay (n=6). (A) Caspase activation observed in HSCs from WT and miR-212/132^{-/-} mice with or without growth factor starvation and BafA treatment. (B) Caspase activation observed in myeloid progenitors from WT and miR-212/132^{-/-} mice with or without growth factor starvation and BafA treatment. (C) Autophagy activity in WT and miR-212/132^{-/-} HSCs with or without growth factor starvation and LY294002 treatment. Autophagy was measured using a dye that fluorescently labels autophagosomes (cyto-ID autophagy assay) (n=5). (D) ROS accumulation in WT and miR-212/132^{-/-} HSCs with or without growth factor starvation and BafA treatment measured using a fluorescence-based ROS detection system (CellROX assay) (n=5). (E) and (F) WT C57BL/6 mice were lethally irradiated and reconstituted with WT or miR-212/132^{-/-} donor bone marrow cells expressing either a control or FOXO3 shRNA knockdown vector. At 8-weeks post-reconstitution HSCs were sorted from bone marrow and assays were performed. (E) Autophagy activity measured in HSCs from the respective mice in response to growth factor starvation (n=6). (F) Caspase

activation measured in HSCs from the respective mice in response to growth factor starvation (n=6). Data represents two independent experiments and is represented as mean \pm SEM. See also Figure S7I. * denotes $p < 0.05$, ** denotes $p < 0.01$, and *** denotes $p < 0.001$ using a Student's *t* test.

References

- Baltimore, D., Boldin, M.P., O'Connell, R.M., Rao, D.S., and Taganov, K.D. (2008). MicroRNAs: new regulators of immune cell development and function. *Nature immunology* *9*, 839-845.
- Chaudhuri, A.A., So, A.Y., Mehta, A., Minisandram, A., Sinha, N., Jonsson, V.D., Rao, D.S., O'Connell, R.M., and Baltimore, D. (2012). Oncomir miR-125b regulates hematopoiesis by targeting the gene Lin28A. *Proceedings of the National Academy of Sciences of the United States of America* *109*, 4233-4238.
- Chen, C.Z., Li, L., Lodish, H.F., and Bartel, D.P. (2004). MicroRNAs modulate hematopoietic lineage differentiation. *Science (New York, N.Y.)* *303*, 83-86.
- Ebert, M.S., and Sharp, P.A. (2012). Roles for microRNAs in conferring robustness to biological processes. *Cell* *149*, 515-524.
- Eijkelenboom, A., and Burgering, B.M. (2013). FOXOs: signalling integrators for homeostasis maintenance. *Nature reviews. Molecular cell biology* *14*, 83-97.
- Esplin, B.L., Shimazu, T., Welner, R.S., Garrett, K.P., Nie, L., Zhang, Q., Humphrey, M.B., Yang, Q., Borghesi, L.A., and Kincade, P.W. (2011). Chronic exposure to a TLR ligand injures hematopoietic stem cells. *Journal of immunology (Baltimore, Md. : 1950)* *186*, 5367-5375.
- Filipowicz, W., Bhattacharyya, S.N., and Sonenberg, N. (2008). Mechanisms of post-transcriptional regulation by microRNAs: are the answers in sight? *Nature reviews. Genetics* *9*, 102-114.
- Flach, J., Bakker, S.T., Mohrin, M., Conroy, P.C., Pietras, E.M., Reynaud, D., Alvarez, S., Diolaiti, M.E., Ugarte, F., Forsberg, E.C., *et al.* (2014). Replication stress is a potent driver of functional decline in ageing haematopoietic stem cells. *Nature* *512*, 198-202.
- Frasca, D., and Blomberg, B.B. (2011). Aging affects human B cell responses. *Journal of clinical immunology* *31*, 430-435.
- Friedman, R.C., Farh, K.K., Burge, C.B., and Bartel, D.P. (2009). Most mammalian mRNAs are conserved targets of microRNAs. *Genome research* *19*, 92-105.
- Gangaraju, V.K., and Lin, H. (2009). MicroRNAs: key regulators of stem cells. *Nature reviews. Molecular cell biology* *10*, 116-125.
- Geiger, H., de Haan, G., and Florian, M.C. (2013). The ageing haematopoietic stem cell compartment. *Nature reviews. Immunology* *13*, 376-389.

Guo, S., Lu, J., Schlanger, R., Zhang, H., Wang, J.Y., Fox, M.C., Purton, L.E., Fleming, H.H., Cobb, B., Merckenschlager, M., *et al.* (2010). MicroRNA miR-125a controls hematopoietic stem cell number. *Proceedings of the National Academy of Sciences of the United States of America* *107*, 14229-14234.

Henry, C.J., Marusyk, A., and DeGregori, J. (2011). Aging-associated changes in hematopoiesis and leukemogenesis: what's the connection? *Aging* *3*, 643-656.

Kim, D., Grun, D., and van Oudenaarden, A. (2013). Dampening of expression oscillations by synchronous regulation of a microRNA and its target. *Nature genetics* *45*, 1337-1344.

Lagos, D., Pollara, G., Henderson, S., Gratrix, F., Fabani, M., Milne, R.S., Gotch, F., and Boshoff, C. (2010). miR-132 regulates antiviral innate immunity through suppression of the p300 transcriptional co-activator. *Nature cell biology* *12*, 513-519.

Lechman, E.R., Gentner, B., van Galen, P., Giustacchini, A., Saini, M., Boccalatte, F.E., Hiramatsu, H., Restuccia, U., Bachi, A., Voisin, V., *et al.* (2012). Attenuation of miR-126 activity expands HSC in vivo without exhaustion. *Cell stem cell* *11*, 799-811.

Miyamoto, K., Araki, K.Y., Naka, K., Arai, F., Takubo, K., Yamazaki, S., Matsuoka, S., Miyamoto, T., Ito, K., Ohmura, M., *et al.* (2007). Foxo3a is essential for maintenance of the hematopoietic stem cell pool. *Cell stem cell* *1*, 101-112.

Mortensen, M., Soilleux, E.J., Djordjevic, G., Tripp, R., Lutteropp, M., Sadighi-Akha, E., Stranks, A.J., Glanville, J., Knight, S., Jacobsen, S.E., *et al.* (2011). The autophagy protein Atg7 is essential for hematopoietic stem cell maintenance. *The Journal of experimental medicine* *208*, 455-467.

Mukherji, S., Ebert, M.S., Zheng, G.X., Tsang, J.S., Sharp, P.A., and van Oudenaarden, A. (2011). MicroRNAs can generate thresholds in target gene expression. *Nature genetics* *43*, 854-859.

Nakahama, T., Hanieh, H., Nguyen, N.T., Chinen, I., Ripley, B., Millrine, D., Lee, S., Nyati, K.K., Dubey, P.K., Chowdhury, K., *et al.* (2013). Aryl hydrocarbon receptor-mediated induction of the microRNA-132/212 cluster promotes interleukin-17-producing T-helper cell differentiation. *Proceedings of the National Academy of Sciences of the United States of America* *110*, 11964-11969.

Ni, B., Rajaram, M.V., Lafuse, W.P., Landes, M.B., and Schlesinger, L.S. (2014). Mycobacterium tuberculosis decreases human macrophage IFN-gamma responsiveness through miR-132 and miR-26a. *Journal of immunology (Baltimore, Md. : 1950)* *193*, 4537-4547.

- Novershtern, N., Subramanian, A., Lawton, L.N., Mak, R.H., Haining, W.N., McConkey, M.E., Habib, N., Yosef, N., Chang, C.Y., Shay, T., *et al.* (2011). Densely interconnected transcriptional circuits control cell states in human hematopoiesis. *Cell* *144*, 296-309.
- O'Connell, R.M., Chaudhuri, A.A., Rao, D.S., Gibson, W.S., Balazs, A.B., and Baltimore, D. (2010a). MicroRNAs enriched in hematopoietic stem cells differentially regulate long-term hematopoietic output. *Proceedings of the National Academy of Sciences of the United States of America* *107*, 14235-14240.
- O'Connell, R.M., Rao, D.S., Chaudhuri, A.A., and Baltimore, D. (2010b). Physiological and pathological roles for microRNAs in the immune system. *Nature reviews. Immunology* *10*, 111-122.
- Ooi, A.G., Sahoo, D., Adorno, M., Wang, Y., Weissman, I.L., and Park, C.Y. (2010). MicroRNA-125b expands hematopoietic stem cells and enriches for the lymphoid-balanced and lymphoid-biased subsets. *Proceedings of the National Academy of Sciences of the United States of America* *107*, 21505-21510.
- Orkin, S.H., and Zon, L.I. (2008). Hematopoiesis: an evolving paradigm for stem cell biology. *Cell* *132*, 631-644.
- Passegue, E., Wagers, A.J., Giuriato, S., Anderson, W.C., and Weissman, I.L. (2005). Global analysis of proliferation and cell cycle gene expression in the regulation of hematopoietic stem and progenitor cell fates. *The Journal of experimental medicine* *202*, 1599-1611.
- Pietras, E.M., Warr, M.R., and Passegue, E. (2011). Cell cycle regulation in hematopoietic stem cells. *The Journal of cell biology* *195*, 709-720.
- Rossi, D.J., Bryder, D., Zahn, J.M., Ahlenius, H., Sonu, R., Wagers, A.J., and Weissman, I.L. (2005). Cell intrinsic alterations underlie hematopoietic stem cell aging. *Proceedings of the National Academy of Sciences of the United States of America* *102*, 9194-9199.
- Rossi, L., Lin, K.K., Boles, N.C., Yang, L., King, K.Y., Jeong, M., Mayle, A., and Goodell, M.A. (2012). Less is more: unveiling the functional core of hematopoietic stem cells through knockout mice. *Cell stem cell* *11*, 302-317.
- Rubinsztein, D.C., Marino, G., and Kroemer, G. (2011). Autophagy and aging. *Cell* *146*, 682-695.
- Shaked, I., Meerson, A., Wolf, Y., Avni, R., Greenberg, D., Gilboa-Geffen, A., and Soreq, H. (2009). MicroRNA-132 potentiates cholinergic anti-inflammatory signaling by targeting acetylcholinesterase. *Immunity* *31*, 965-973.

- Song, S.J., Ito, K., Ala, U., Kats, L., Webster, K., Sun, S.M., Jongen-Lavrencic, M., Manova-Todorova, K., Teruya-Feldstein, J., Avigan, D.E., *et al.* (2013). The oncogenic microRNA miR-22 targets the TET2 tumor suppressor to promote hematopoietic stem cell self-renewal and transformation. *Cell stem cell* *13*, 87-101.
- Strovas, T.J., Rosenberg, A.B., Kuypers, B.E., Muscat, R.A., and Seelig, G. (2014). MicroRNA-based single-gene circuits buffer protein synthesis rates against perturbations. *ACS synthetic biology* *3*, 324-331.
- Suda, T., Takubo, K., and Semenza, G.L. (2011). Metabolic regulation of hematopoietic stem cells in the hypoxic niche. *Cell stem cell* *9*, 298-310.
- Sun, D., Luo, M., Jeong, M., Rodriguez, B., Xia, Z., Hannah, R., Wang, H., Le, T., Faull, K.F., Chen, R., *et al.* (2014). Epigenomic profiling of young and aged HSCs reveals concerted changes during aging that reinforce self-renewal. *Cell stem cell* *14*, 673-688.
- Takubo, K., Goda, N., Yamada, W., Iriuchishima, H., Ikeda, E., Kubota, Y., Shima, H., Johnson, R.S., Hirao, A., Suematsu, M., and Suda, T. (2010). Regulation of the HIF-1alpha level is essential for hematopoietic stem cells. *Cell stem cell* *7*, 391-402.
- Tothova, Z., Kollipara, R., Huntly, B.J., Lee, B.H., Castrillon, D.H., Cullen, D.E., McDowell, E.P., Lazo-Kallanian, S., Williams, I.R., Sears, C., *et al.* (2007). FoxOs are critical mediators of hematopoietic stem cell resistance to physiologic oxidative stress. *Cell* *128*, 325-339.
- Ucar, A., Gupta, S.K., Fiedler, J., Erikci, E., Kardasinski, M., Batkai, S., Dangwal, S., Kumarswamy, R., Bang, C., Holzmann, A., *et al.* (2012). The miRNA-212/132 family regulates both cardiac hypertrophy and cardiomyocyte autophagy. *Nature communications* *3*, 1078.
- van der Vos, K.E., Eliasson, P., Proikas-Cezanne, T., Vervoort, S.J., van Boxtel, R., Putker, M., van Zutphen, I.J., Mauthe, M., Zellmer, S., Pals, C., *et al.* (2012). Modulation of glutamine metabolism by the PI(3)K-PKB-FOXO network regulates autophagy. *Nature cell biology* *14*, 829-837.
- Warr, M.R., Binnewies, M., Flach, J., Reynaud, D., Garg, T., Malhotra, R., Debnath, J., and Passegue, E. (2013). FOXO3A directs a protective autophagy program in haematopoietic stem cells. *Nature* *494*, 323-327.
- Willcox, B.J., Donlon, T.A., He, Q., Chen, R., Grove, J.S., Yano, K., Masaki, K.H., Willcox, D.C., Rodriguez, B., and Curb, J.D. (2008). FOXO3A genotype is strongly associated with human longevity. *Proceedings of the National Academy of Sciences of the United States of America* *105*, 13987-13992.

Zhao, J.L., Rao, D.S., O'Connell, R.M., Garcia-Flores, Y., and Baltimore, D. (2013). MicroRNA-146a acts as a guardian of the quality and longevity of hematopoietic stem cells in mice. *eLife* 2, e00537.

Supplemental Figure Legends

Figure S1, related to Figure 1: Validation of microRNA-132 over-expression in bone marrow cells expressing control (MG) or a miR-132 over-expressing (miR-132) vector. (A) miR-212 expression in total bone marrow and HSCs. (B) Schematic of the retroviral construct used to over-express miR-132 and reconstitution efficiency of mice transplanted with MG or miR-132 donor bone marrow. Peripheral blood was analyzed at 8-weeks post-reconstitution for the proportion of eGFP⁺ CD45⁺ leukocytes. (C) Representative FACS plots and gating strategies used for sorting MG and miR-132 expressing bone marrow cells prior to transplantation into irradiated recipients. (D) Expression of miR-132 in bone marrow cells obtained from MG and miR-132 mice. Data is represented as mean \pm SEM.

Figure S2, related to Figure 1: Ectopic expression of microRNA-132 leads to deregulated hematopoiesis. (A) – (K) WT C57BL/6 mice were lethally irradiated and reconstituted with donor bone marrow cells expressing either a control (MG) or a miR-132 over-expressing (miR-132) retroviral vector (n=8-12 mice per group). (A) Total number of LSK cells in the bone marrow of MG and miR-132 mice at 8-weeks post-reconstitution. (B) Frequency of HSCs in the bone marrow of MG and miR-132 mice at 8-weeks post-reconstitution. (C) Frequency of LSK cells in the bone marrow of MG and miR-132 mice at 8-weeks post-reconstitution. (D) Percentage of Ki-67⁺ cells within the bone marrow LSK compartment of MG and miR-132 mice at 8-weeks post-reconstitution. (E) p27, p57, and p21 transcript expression in the bone marrow compartment of MG and miR-132 mice at 2-months post-reconstitution obtained by RT-qPCR. (F) p27 transcript expression in the bone marrow

compartment of MG and miR-132 mice at 4-months post-reconstitution. (G) Spleen weights for MG and miR-132 mice at 16-weeks post-reconstitution. (H) Percentage of Ter119+, CD11b+, and Gr-1+ cells in the spleen of MG and miR-132 mice at 16-weeks post-reconstitution. (I) Percentage of CD11b+ and Gr-1+ cells in the peripheral blood of MG and miR-132 mice at 16-weeks post-reconstitution. (J) Representative FACS plot and gating for HSCs (Lineage- Sca1+ cKit+ CD150+ CD48-) in the bone marrow compartment of MG and miR-132 mice at 16-weeks post-reconstitution. (K) Percentage of LSK cells and HSCs in the bone marrow of MG and miR-132 mice at 16-weeks post-reconstitution. Data represents at least three independent experiments and is represented as mean \pm SEM. * denotes $p < 0.05$, ** denotes $p < 0.01$, and *** denotes $p < 0.001$ using a Student's *t* test.

Figure S3, related to Figure 1: Ectopic expression of miR-132 and miR-212 leads to deficits in several early and late hematopoietic progenitor populations. (A) – (G) WT C57BL/6 mice were lethally irradiated and reconstituted with donor bone marrow cells expressing either a control (MG) or a miR-132 over-expressing (miR-132) retroviral vector (n=8-12 mice per group). Data represents at least three independent experiments. (A) Total number of LSK cells and HSCs in the bone marrow compartment of MG and miR-132 mice at 9-months post-reconstitution. (B) Total number of multipotent progenitors (MPPs) in the bone marrow compartment of MG and miR-132 mice at 16-weeks post-reconstitution. (C) Total number of lymphoid primed MPPs (LMPPs) in the bone marrow compartment of MG and miR-132 mice at 16-weeks post-reconstitution. (D) Total number of granulocyte-monocyte progenitors (GMPs) in the bone marrow compartment of MG and miR-132 mice at 16-weeks post-reconstitution. (E) Total number of common myeloid

progenitors (CMPs) in the bone marrow compartment of MG and miR-132 mice at 16-weeks post-reconstitution. (F) Total number of myeloid-erythroid progenitors (MEPs) in the bone marrow compartment of MG and miR-132 mice at 16-weeks post-reconstitution. (G) Percentage of HSCs in the bone marrow within the eGFP- population of bone marrow cells in MG and miR-132 mice at 16-weeks post-reconstitution. (H) WT C57BL/6 mice were lethally irradiated and reconstituted with donor bone marrow cells expressing either a control (MG) or a miR-132-mutant over-expressing (miR-132-mutant) retroviral vector in which the miR-132 seed sequence was mutated (n=5 mice per group). Graphs shows total peripheral blood CD45⁺ leukocytes and CD11b⁺ cells at 9-months post-reconstitution. (I) – (K) WT C57BL/6 mice were lethally irradiated and reconstituted with donor bone marrow cells expressing either a control (MG) or a miR-212 over-expressing (miR-212) retroviral vector (n=4 mice per group). (I) Total bone marrow CD45⁺ cells in MG and miR-212 mice. (J) Frequency and total number of LSK cells in the bone marrow of MG and miR-212 mice. (K) Frequency and total number of HSCs in the bone marrow of MG and miR-212 mice. Data represents two independent experiments and is represented as mean \pm SEM. * denotes $p < 0.05$, ** denotes $p < 0.01$, and *** denotes $p < 0.001$ using a Student's *t* test.

Figure S4, related to Figure 2 and 3: Genetic deletion of the microRNA-212/132 cluster has no observable effect on hematopoiesis in young mice. (A) – (C) Mice with a genetic deletion of the miR-212/132 cluster (miR-212/132^{-/-}) along with WT mice in the C57BL/6 background were analyzed to understand the physiological contribution of the miR-212/132 cluster on hematopoietic output (n=7-8 mice per group). (A) Total number of

peripheral blood CD45+, CD19+, and CD11b+ cells in WT and miR-212/132^{-/-} mice at 12-weeks of age. (B) Total number of splenic CD45+, CD19+, and CD11b+ cells in WT and miR-212/132^{-/-} mice at 12-weeks of age. (C) Total number of bone marrow CD45+, CD19+, and CD11b+ cells in WT and miR-212/132^{-/-} mice at 12-weeks of age. (D) Total number of HSCs in the bone marrow compartment of 12-week old WT and miR-212/132^{-/-} mice. Data represents two independent experiments and is represented as mean ± SEM.

Figure S5, related to Figures 2, 3 and 4: Genetic deletion of the microRNA-212/132 cluster in mice leads to deregulated hematopoiesis with age. (A) – (E) Mice with a genetic deletion of the miR-212/132 cluster (miR-212/132^{-/-}) along with WT mice in the C57BL/6 background were analyzed to understand the physiological contribution of the miR-212/132 cluster on hematopoietic output (n=7-12 mice per group). (A) Representative spleen gross pathology, spleen weight, and percentage of CD11b+, CD19+, and CD3e+ cells in the spleen of WT and miR-212/132^{-/-} mice at 60-64 weeks of age. (B) Total number of CD45+, CD11b+, CD19+, and CD3e+ cells in the bone marrow of WT and miR-212/132^{-/-} mice at 60-64 weeks of age. (C) WT or miR-212/132^{-/-} (KO) bone marrow cells were transplanted into lethally irradiated C57BL/6 mice. The relative ratio (KO/WT) of total numbers of various cell populations in the bone marrow of these mice at 60-weeks post-reconstitution is shown. (D) – (F) 6-month old WT and miR-212/132^{-/-} were treated with 9 evenly-spaced low-dose (1mg/kg of body weight) LPS or PBS injections over one month. (D) Total number of HSCs in the spleen of WT and miR-212/132^{-/-} mice treated with PBS or LPS. (E) Summary of relative proportions of early progenitors in the bone marrow of WT and miR-212/132^{-/-} mice treated with LPS. (F) Proportion of bone marrow

LSK cells and HSCs in each stage of the cell cycle (G0, G1, G2/M) from WT and miR-212/132^{-/-} mice following PPS injection. (G) Expression of p27 in the bone marrow compartment of mice treated with LPS as described above. (H) Expression of p27 in the bone marrow compartment of mice 5-days after a single treatment of 5-fluorouracil. (I) WT or miR-212/132^{-/-} CD45.2⁺ bone marrow cells from primary transplant experiments, calibrated for the total number of phenotypically defined HSCs, were injected in a 1:1 ratio with CD45.1⁺ WT bone marrow cells into irradiated C57BL/6 CD45.2⁺ recipients. The graph represents the relative ratio of mature cells in the peripheral blood of these secondary transplant mice at 16-weeks post-reconstitution. Data represents at least two independent experiments and is represented as mean \pm SEM. * denotes $p < 0.05$, ** denotes $p < 0.01$, and *** denotes $p < 0.001$ using a Student-T test.

Figure S6, related to Figure 2. Summary of RNA-sequencing analysis of WT and miR-212/132^{-/-} HSCs from 16-week old mice. (A) Summary of the number of detected protein coding genes and FPKM values for sequenced samples. LT-HSC: long-term HSCs, LSK CD150⁺ CD48⁻. SH-HSCs: short-term HSCs, LSK CD150⁻ CD48⁻. MPPs: multipotent progenitors, LSK CD150⁻ CD48⁺. WT: wildtype sample. KO: miR-212/132^{-/-} sample. (B) Box-plot showing enrichment of miR-132 targets in miR-212/132^{-/-} HSCs compared to WT HSCs. (C) Fold-change of several miR-132 targets in miR-212/132^{-/-} HSCs compared to WT HSCs. (D) Fold-change in several FOXO3 regulated genes in miR-212/132^{-/-} HSCs compared to WT HSCs. (E) Fold-change in several autophagy related genes in miR-212/132^{-/-} HSCs compared to WT HSCs. Data represents two replicate experiments.

Figure S7, related to Figures 6 and 7: Validation of microRNA-132 and FOXO3 over-expression in FOXO3 rescue experiment. (A) FOXO1 and FOXO4 expression in total bone marrow cells from WT^{MIG} and WT^{miR-132} mice. (B) FOXO1 and FOXO4 expression in lineage-depleted bone marrow cells from WT and miR-212/132^{-/-} mice. RNA was obtained from the respective cell populations and FOXO1 and FOXO4 expression was quantified by RT-qPCR (n=2-3 biological replicates). (C) Intracellular staining analyzed by FACS for FOXO3 protein expression in bone marrow HSCs obtained from WT and miR-212/132^{-/-} mice and starved for 12 hours *in-vitro*. (D) Intracellular staining analyzed by FACS for phosphorylated FOXO3 (p-FOXO3) protein expression in bone marrow HSCs obtained from WT and miR-212/132^{-/-} mice and starved for 12 hours *in-vitro*. (E) – (F) Bone marrow expressing either a control (MIG), a miR-132 over-expressing (MIG-miR-132), a FOXO3 over-expressing (MIG-FOXO3), or a FOXO3 and miR-132 over-expressing (MIG-FOXO3-miR-132) retroviral vector were analyzed using Taqman RT-qPCR for miR-132 expression or Western Blot for FOXO3 protein expression. (E) FOXO3 protein expression in bone marrow cells transduced with the indicated retroviral vectors. (F) Mature miR-132 expression in in bone marrow cells transduced with the indicated retroviral vectors. (G) eGFP expression in the bone marrow compartment of mice reconstitution with bone marrow cells transduced with the indicated retroviral vector. (H) AnnexinV staining performed on bone marrow HSCs from MIG and MIG-FOXO3 mice (n=3). (I) Detection of autophagy activity using the Cyto-ID autophagy detection assay in bone-marrow-derived dendritic cells treated with Rapamycin and obtained from WT and Atg16 deficient (Atg16 KO) mice. Data represents at least two independent experiments and is represented as mean \pm SEM.

Supplemental Experimental Procedures

DNA Constructs

The miR-132 over-expression construct was cloned into the MSCV-eGFP (MG) vector. In this modified vector, MG-miR-132, containing an MSCV promoter, the eGFP is placed immediately downstream of the 5' LTR, and the miR-132 expression cassette is placed immediately downstream of the eGFP stop codon. A miR-132-mutant vector was similar constructed with a mutated miR-132 seed sequence. For FOXO3 rescue experiments, FOXO3 cDNA was cloned into the MSCV-IRES-eGFP (MIG) vector, immediately downstream of the 5' LTR and upstream of the IRES. miR-132 was cloned downstream of eGFP as described above. For FOXO3 knockdown experiments, TagBFP was first subcloned into the MG vector, creating MSCV-TagBFP (MB). Several FOXO3 shRNA sequences were designed using the Invitrogen Block-iT RNAi Designer and cloned in the microRNA-155 loop-and-arms format immediately downstream of TagBFP in the MB vector.

Cell sorting for RNA extraction

Bone marrow cells were harvested from WT C57BL/6 mice and depleted of red blood cells (RBCs) using RBC lysis buffer (BioLegend). Cells were then spun down, resuspended in MACS separating buffer (Phosphate buffered saline, pH7.2, with 0.5% BSA and 2mM EDTA), and filtered through a 70uM cell-strainer. These cells were then blocked with FcBlock (Becton Dickinson) and depleted of mature cells on a magnetic column using biotin-conjugated mouse antibodies for CD3e, CD8, CD4, CD19, B220, CD11b, Gr-1, IL-

7Ra, and Ter119 (BioLegend) and streptavidin magnetic beads (Miltenyi), as suggested by the manufacturer (Miltenyi). Cells were subsequently stained with fluorophore-conjugated antibodies for lineage markers (CD3, CD19, CD11b, Gr-1, Ter119, Nk1.1), cKit, Sca1, CD150, CD48, and with 7-AAD, and several populations were sorted for analysis including HSCs (Lineage- cKit⁺ Sca1⁺ CD150⁺ CD48⁻), LSK cells (Lineage- cKit⁺ Sca1⁺), and other progenitor subsets as detailed in the text. Cells were sorted on a FACSAria IIu cell sorter (Becton Dickinson) at the Caltech Flow Cytometry Core Facility. Mature cell populations were sorted using a magnetic column as described above using positive-selection for the respective surface marker (Gr-1, CD11b, CD19). All cells were lysed using Qiazol lysis buffer (Qiagen) and processed using the miRNAeasy RNA prep kit (Qiagen). RNA was then subjected to qPCR.

Sample preparation for RNA-sequencing

LT-HSCs (LSK CD150⁺ CD48⁻), ST-HSCs (LSK CD150⁻ CD48⁻) and MPPs (LSK CD150⁻ CD48⁺) from WT and miR-212/132^{-/-} were sorted as described above. Cells were sorted directly into cell lysis buffer and processed using an RNAeasy kit (Qiagen) with *DNAseI* digestion (Qiagen) as per manufacturer's protocol. Libraries were prepared using the SMART-seq2 protocol (Picelli et al., 2013) modified to use Maxima H Minus enzyme for reverse transcription (Thermo Scientific). Amplified cDNA products were purified using AMPure XP SPRI beads (Beckman Coulter) and eluted in TE buffer (Teknova). Cleaned-up amplified cDNA was used for library construction using the Nextera XT DNA Sample Preparation Kit and Nextera XT Index Kit (Illumina). Libraries were then pooled

and cleaned-up using AMPure XP SPRI beads (Beckman Coulter Genomics). Final library quality and quantity were assessed using a DNA High Sensitivity chip (Agilent).

RNA-seq data generation and analysis

Libraries were sequenced on the Illumina HiSeq 2500. Paired-end 2x25bp reads were generated. The reads were filtered for rRNA contamination by aligning against mouse ribosomal sequences using Bowtie (version 0.12.7) (Langmead et al., 2009) and retaining unaligned read pairs. The refSeq annotation for the mm9 version of the mouse genome was used to create a transcriptome Bowtie index, to which read pairs were aligned with the following settings: “-v 2 -a -X 1000”. Gene expression levels were estimated using eXpress (version 1.5.1) (Roberts and Pachter, 2013), and the effective count values were used as input to DESeq (Anders and Huber, 2010) for evaluating differential expression. The targets of miR-132 were obtained from TargetScan (mouse release 6.2) (Friedman et al., 2009).

Immunoblotting

Pelleted cells were resuspended in RIPA lysis buffer (Sigma) containing protease inhibitors for 20 minutes on ice. Samples were spun down at max speed at 4°C for 10 minutes and the supernatant was processed immediately or flash-frozen on dry ice for analysis in the future. Total cell extracts were fractionated by gel-electrophoresis on a mini-PROTEAN TGX gradient (4-15%) gel (Bio-Rad) and electroblotted onto a PVDF membrane using a wet transfer apparatus (Bio-Rad). Protein detection was subsequently performed with the following antibodies: FoxO3a (75D8) (Cell Signaling Technologies), p27-HRP (sc-538)

(Santa Cruz Biotechnology), actin-HRP (sc-1616) (Santa Cruz Biotechnology), and goat anti-rabbit-IgG-HRP (sc-2030) (Santa Cruz Biotechnology).

Mice

All mice used in this study are of the C57BL/6 background. The miR-212/132^{-/-} mice were generated previously and are described elsewhere (Ucar et al., 2012). Briefly, these mice were generated by homologous recombination targeting the genomic cluster containing both microRNA-212 and microRNA-132. Mice obtained were backcrossed to the C57BL/6 background for at least 20 generations prior to the initiation of the reported studies.

Bone marrow reconstitution

WT C57BL/6 or miR-212/132^{-/-} mice were treated with 5-fluorouracil (10ug; Sigma) for 5 days to enrich for hematopoietic stem and progenitor cells (HSPCs) in the bone marrow. After 5 days, bone marrow cells were harvested, red blood cells (RBCs) were lysed with RBC lysis buffer (BioLegend), and cells were plated in HSPC media, which was composed of complete RPMI with mouse SCF (50 ng/mL), IL-3 (20 ng/mL), and IL-6 (50 ng/mL). Cells were then cultured in 24-wel plates for 24 hours and spin-infected with PCL-ecotropic pseudotyped gamma-retrovirus expressing the construct of interest, which was either a microRNA, shRNA, or a gene, as described in under the *DNA Constructs and Primers* section of the main text. Spin-infections were performed by removing supernatant carefully from cell culture plates and adding virus with 8 ug/mL Polybrene (Santa Cruz Biotechnology). Plates were then placed in a centrifuge for 2 hours at 30⁰C and 2500RPM. Immediately following infection, virus supernatant was removed and replaced with HSPC

media. 24 hours later a second identical spin infection was performed. After another 24 hours, recipient mice were lethally irradiated (1000 rads from Cs137 source) and 250,000 to a million virus-infected HSPCs were retro-orbitally delivered to reconstitute the immune system. Recipients were maintained on Septra and in autoclaved cages for at least one month post-reconstitution.

Virus production

To generate retrovirus for HSPC infection, 10 million HEK293T cells were first plated in a 15cm plate. 24 hours later, cells were transfected with both the pCL-Eco vector and either the pMG vector or the relevant variant described above for gene delivery. For transfection, we used BioT (Bioland Scientific) as per the manufacturers protocol. 36 hours after transfection, virus was collected, filtered through a 45uM syringe filter, and used for infection of HSPCs.

Flow cytometry

Cells were stained with fluorophore-conjugated antibodies (all from BioLegend unless indicated) for CD45.1, CD45.2, CD11b, Gr-1, CD19, B220, CD3e, Nk1.1, Ter119, cKit, Sca1, CD150, CD48, EPCR (Ebioscience), CD34, Flt3, FcRg or IL-7Ra in various combinations to characterize relevant hematopoietic cell populations. Intracellular staining was performed by first performing surface staining of cells, followed by fixation and permeabilization (Cytofix/Cytoperm kit; BD Biosciences) and subsequent staining with either Ki67 (BioLegend) and Hoescht33342 (Life Technologies) for cell-cycling analysis, or an anti-FoxO3a (75D8) (Cell Signaling Technologies) or anti-FoxO3a (phosphor S253)

(Abcam) primary antibody followed by an anti-Rabbit-IgG secondary antibody conjugated to Alexafluor488 (Cell Signaling Technologies). Samples were analyzed on a MACSQuant10 Flow Cytometry machine (Miltenyi). Gating and analysis was performed using FlowJo software.

Autophagy and reactive-oxygen species assays

HSCs were sorted as described above from either WT or miR-212/132^{-/-} C57BL/6 mice, or from reconstituted mice with donor WT or miR-212/132^{-/-} bone marrow infected with either MB or shFOXO3 retroviral constructs. For all *in-vitro* experiments, cells were sorted directly in a 96-wel plate containing cell culture media with the appropriate growth factors and cytokines (all from Ebioscience). For caspase activation assays and reactive oxygen species detection, 5000 cells were cultured with or without Bafilomycin A (5nM; Sigma) and with either no growth factors or cytokines, or with mSCF (50 ng/mL), IL-3 (20 ng/mL), IL-6 (50 ng/mL), Flt3L (25 ng/mL), TPO (25 ng/mL), and GM-CSF (10ng/mL). Cells were cultured for 12 hours and subsequently processed. Caspase activity was detected using the luciferase-based Caspase Glo 3/7 assay system as per manufactures instructions (Promega). Reactive-oxygen species were detected by flow cytometry using the CellROX Deep Red reagent (Life Technologies). For authophagy detection assays, 5000-8000 cells were cultured with or without LY294002 (20uM; Cell Signaling Technologies) and with or without aforementioned growth factors or cytokines. Autophagy activity was determined by flow cytometry using the CytoID autophagy detection kit as per manufacturers instructions (Enzo Life Sciences).

Supplemental Tables

Table S1: sequences for FOXO3 shRNA constructs.

FOXO3 shRNA sequence (in miR-155-arms-and-loop-format)	
mmu-FOXO3 shRNA #1	gaaggctgtaTGCTGCCATCATTGATTCATGGTGGTTTTGGCCACTGACTGACCACCATGACTGAATGATGGcaggacacaaggcctg
mmu-FOXO3 shRNA #2	gaaggctgtaTGCTGAACACGGTACTGTTGAAGGAGTTTTGGCCACTGACTGACCTCCTCAAGTACCGTGTTcaggacacaaggcctg
mmu-FOXO3 shRNA #3	gaaggctgtaTGCTGAAGAGAAGGTGGCTGGTCTGTGTTTTGGCCACTGACTGACACAGACCACACCTTCTTTcaggacacaaggcctg

Table S2: primer sequences used for qPCR.**Primer sequences**

AchE F	CTCCCTGGTATCCCCTGCATA
AchE R	GGATGCCAGAAAAGCTGAGA
BTG2 F	ATGAGCCACGGGAAGAGAAC
BTG2 R	GCCCTACTGAAAACCTTGAGTC
FOXO1 F	CCCAGGCCGGAGTTTAACC
FOXO1 R	GTTGCTCATAAAGTCGGTGCT
FOXO3 F	CTGGGGGAACCTGTCCTATG
FOXO3 R	TCATTCTGAACGCGCATGAAG
HMGA2 F	GAGCCCTCTCCTAAGAGACCC
HMGA2 R	TTGGCCGTTTTTCTCCAATGG
JARID1A F	CACAGACCCGCTGAGTTTTAT
JARID1A R	CTTCACAGCAAATGGAGGTT
Lin28b F	AGAATGCAGTCTACCTCCTCAG
Lin28b R	CCTCCCACTTCTCTTGGTGC
MAPK1 F	GGTTGTCCCAAATGCTGACT
MAPK1 R	CAACTTCAATCCTCTTGTGAGGG
MMP9 F	CTGGACAGCCAGACACTAAAG
MMP9 R	CTCGCGGCAAGTCTTCAGAG
p21 F	CCGCTGGAGGGCAACTTCGT
p21 R	TTTCGGCCCTGAGATGTTCC
p27 F	TCTCAGGCAAACCTCTGAGGAC
p27 R	TTCGGAGCTGTTTACGTCCTGG
p300 F	CTCGCACTTGCCCTTACCTTT
p300 R	GGTCGCAGTGGCTGGAGA
p57 F	TGATGAGCTGGGAAGTGAAGCC
p57 R	ACGTCGTTTCGACGCCTTGTTTC
PTBP2 F	GGATCTGACGAGCTACTCTCA
PTBP2 R	TTCTTACTATCGTTACCGTTGGC
RB1 F	TGCATCTTTATCGCAGCAGTT
RB1 R	GTTACACGTCCGTTCTAATTTG
SOX4 F	GACAGCGACAAGATTCCGTTTC
SOX4 R	GTTGCCCGACTTCACCTTC
SOX5 F	CCCGTGATCCAGAGCACTTAC
SOX5 R	CCGCAATGTGGTTTTTCGCT

Supplemental References

Anders, S., and Huber, W. (2010). Differential expression analysis for sequence count data. *Genome biology* *11*, R106.

Friedman, R.C., Farh, K.K., Burge, C.B., and Bartel, D.P. (2009). Most mammalian mRNAs are conserved targets of microRNAs. *Genome research* *19*, 92-105.

Langmead, B., Trapnell, C., Pop, M., and Salzberg, S.L. (2009). Ultrafast and memory-efficient alignment of short DNA sequences to the human genome. *Genome biology* *10*, R25.

Picelli, S., Bjorklund, A.K., Faridani, O.R., Sagasser, S., Winberg, G., and Sandberg, R. (2013). Smart-seq2 for sensitive full-length transcriptome profiling in single cells. *Nature methods* *10*, 1096-1098.

Roberts, A., and Pachter, L. (2013). Streaming fragment assignment for real-time analysis of sequencing experiments. *Nature methods* *10*, 71-73.

Ucar, A., Gupta, S.K., Fiedler, J., Erikci, E., Kardasinski, M., Batkai, S., Dangwal, S., Kumarswamy, R., Bang, C., Holzmann, A., *et al.* (2012). The miRNA-212/132 family regulates both cardiac hypertrophy and cardiomyocyte autophagy. *Nature communications* *3*, 1078.

Figures

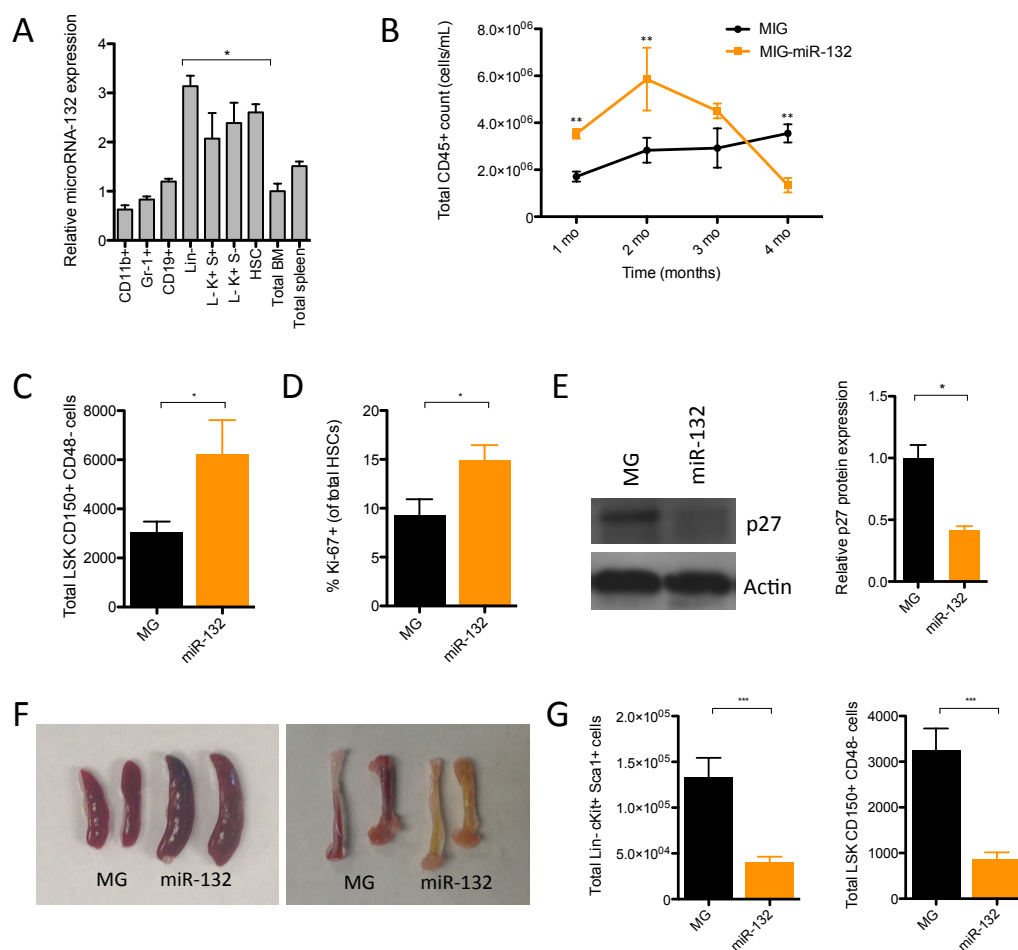


Figure 1: microRNA-132 is expressed in hematopoietic stem cells (HSCs) and over-expression alters hematopoiesis.

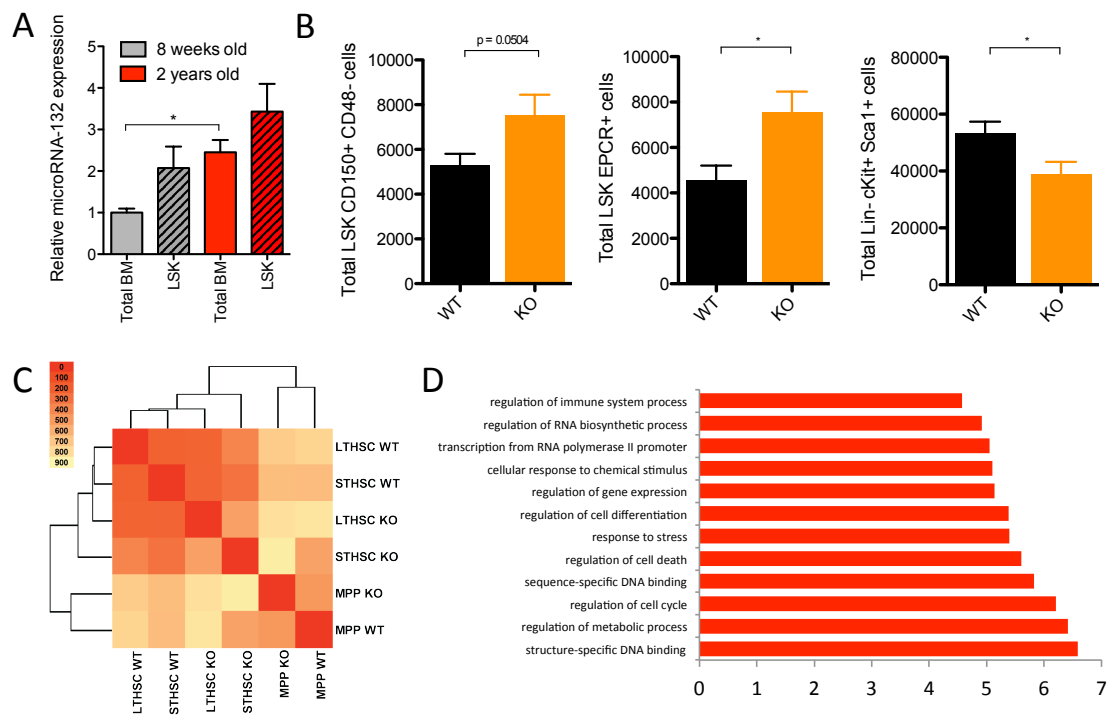


Figure 2: Genetic deletion of the microRNA-212/132 cluster in mice alters hematopoietic output with age.

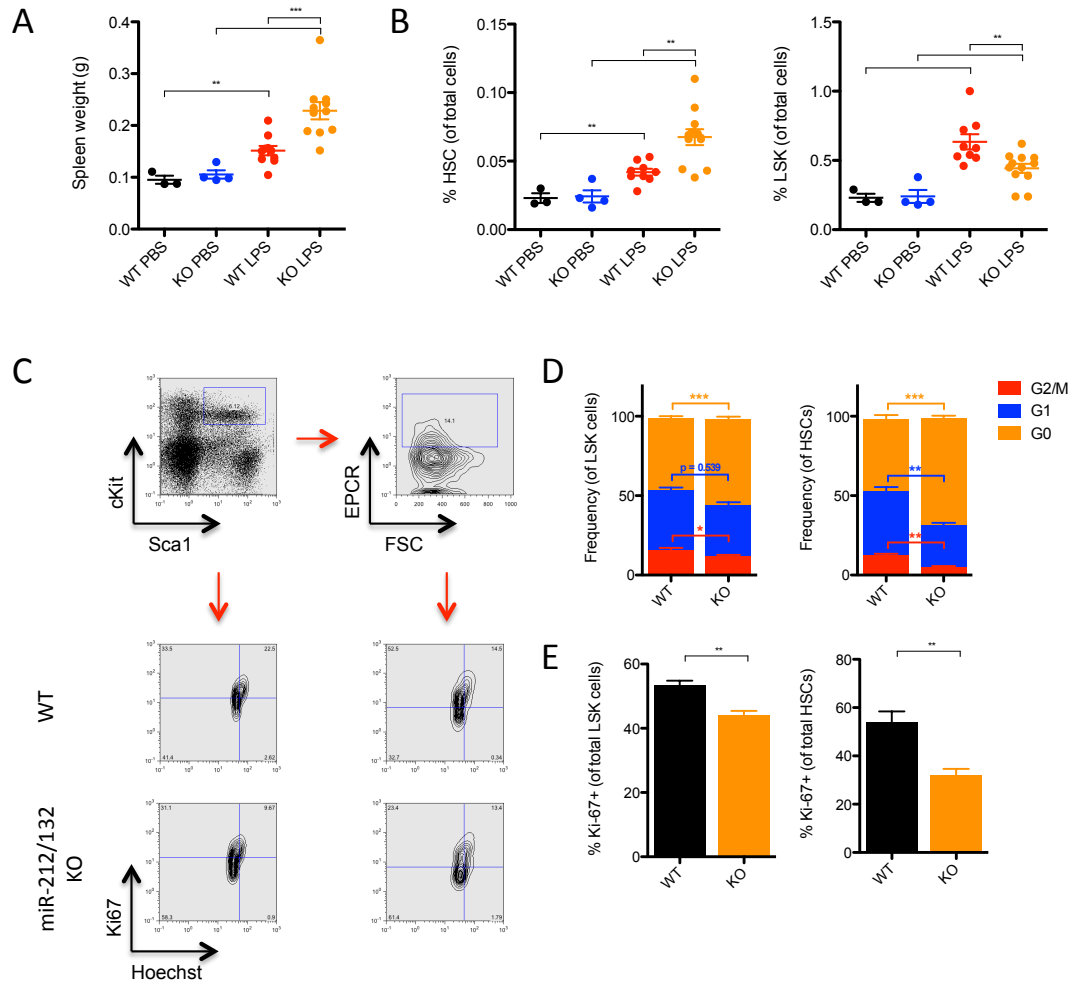


Figure 3: Genetic deletion of the microRNA-212/132 cluster in mice alters hematopoietic output and cycling in response to LPS stimulation.

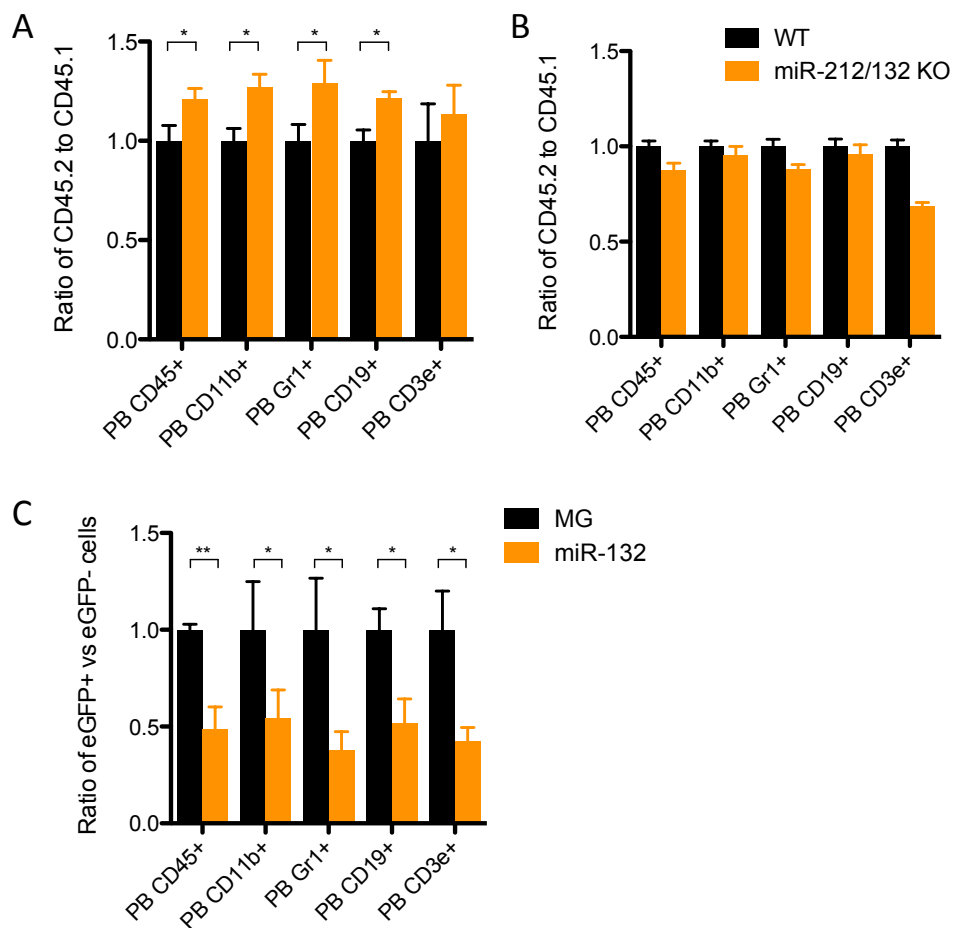


Figure 4: The microRNA-212/132 cluster regulates long-term reconstitution potential of HSCs with age.

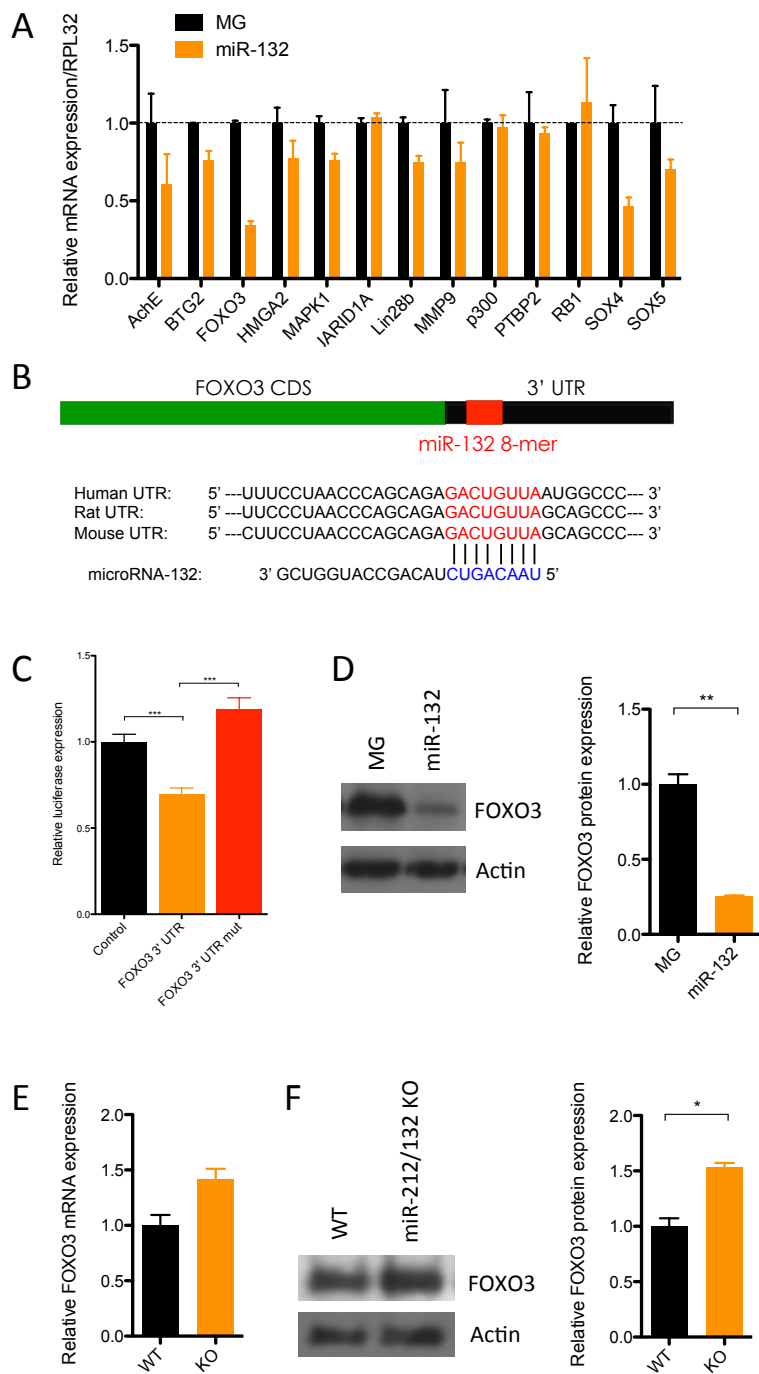


Figure 5: . FOXO3 is a direct target of microRNA-132 in bone marrow cells.

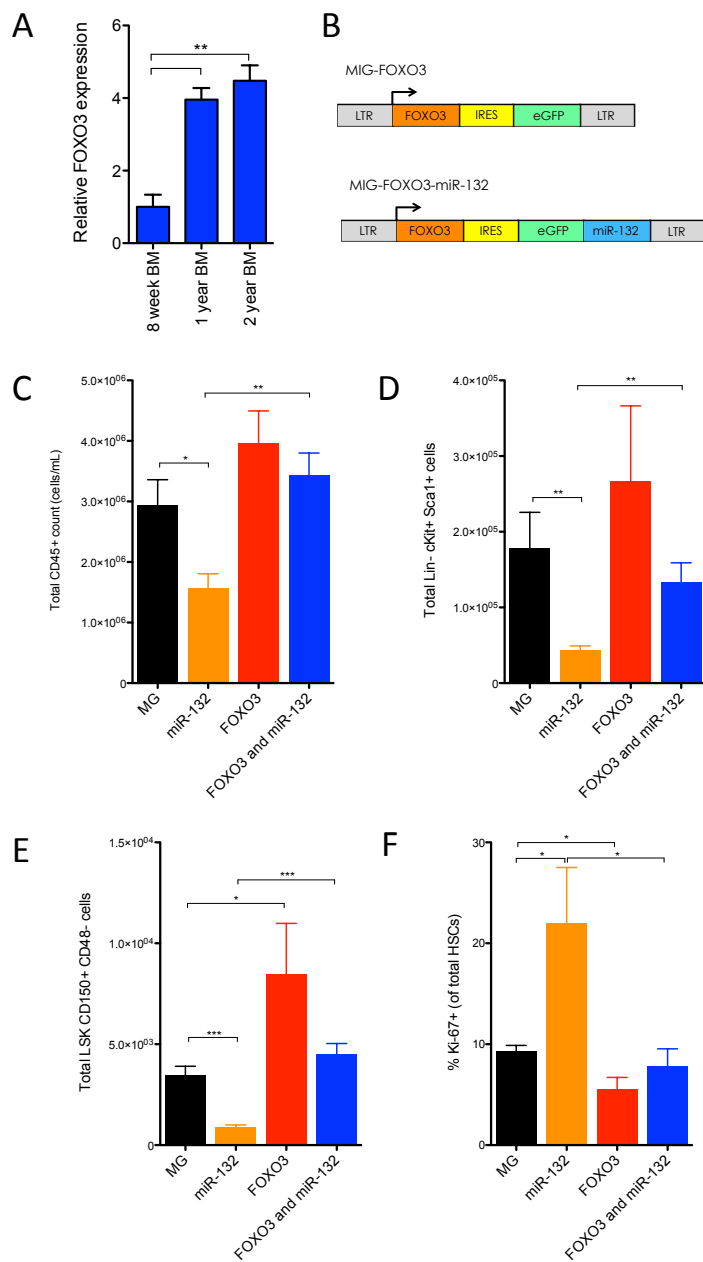


Figure 6: Co-expression of FOXO3 with miR-132 rescues the hematopoietic defects observed with expression of miR-132 alone.

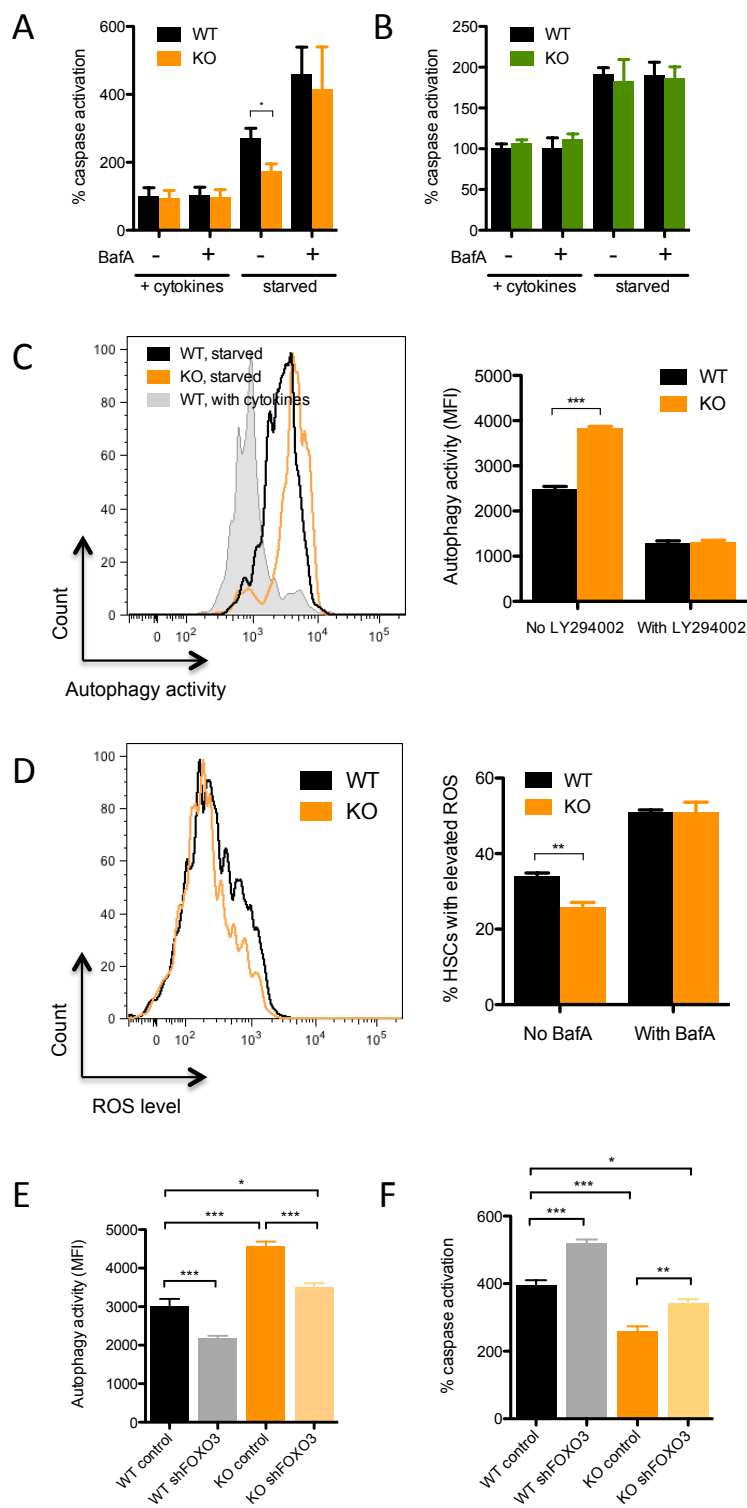


Figure 7: Genetic deletion of the miR-212/132^{-/-} cluster results in a FOXO3 dependent alteration in autophagy and survival of HSCs.

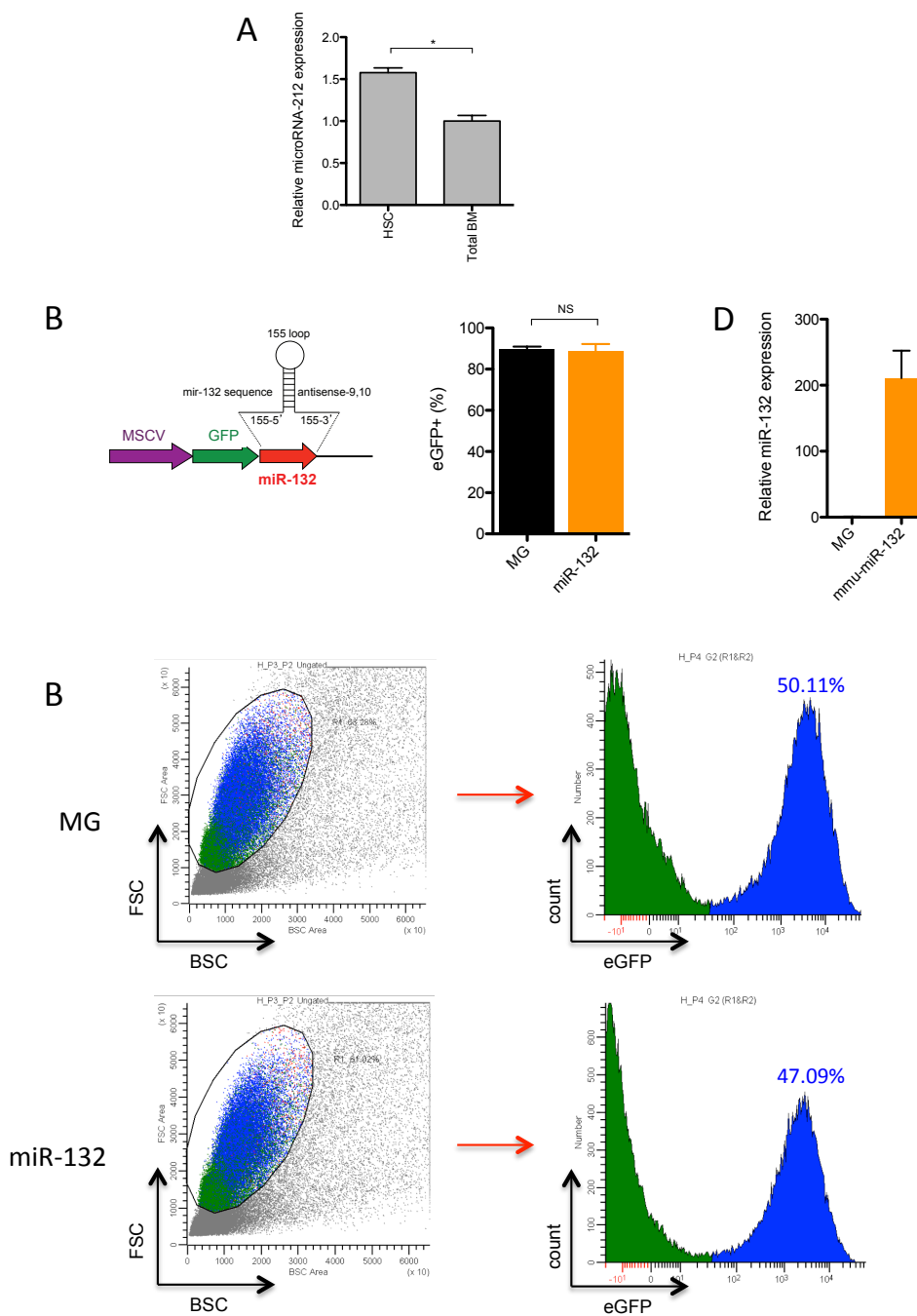


Figure S1: Validation of microRNA-132 over-expression in bone marrow cells expressing control (MG) or a miR-132 over-expressing (miR-132) vector.

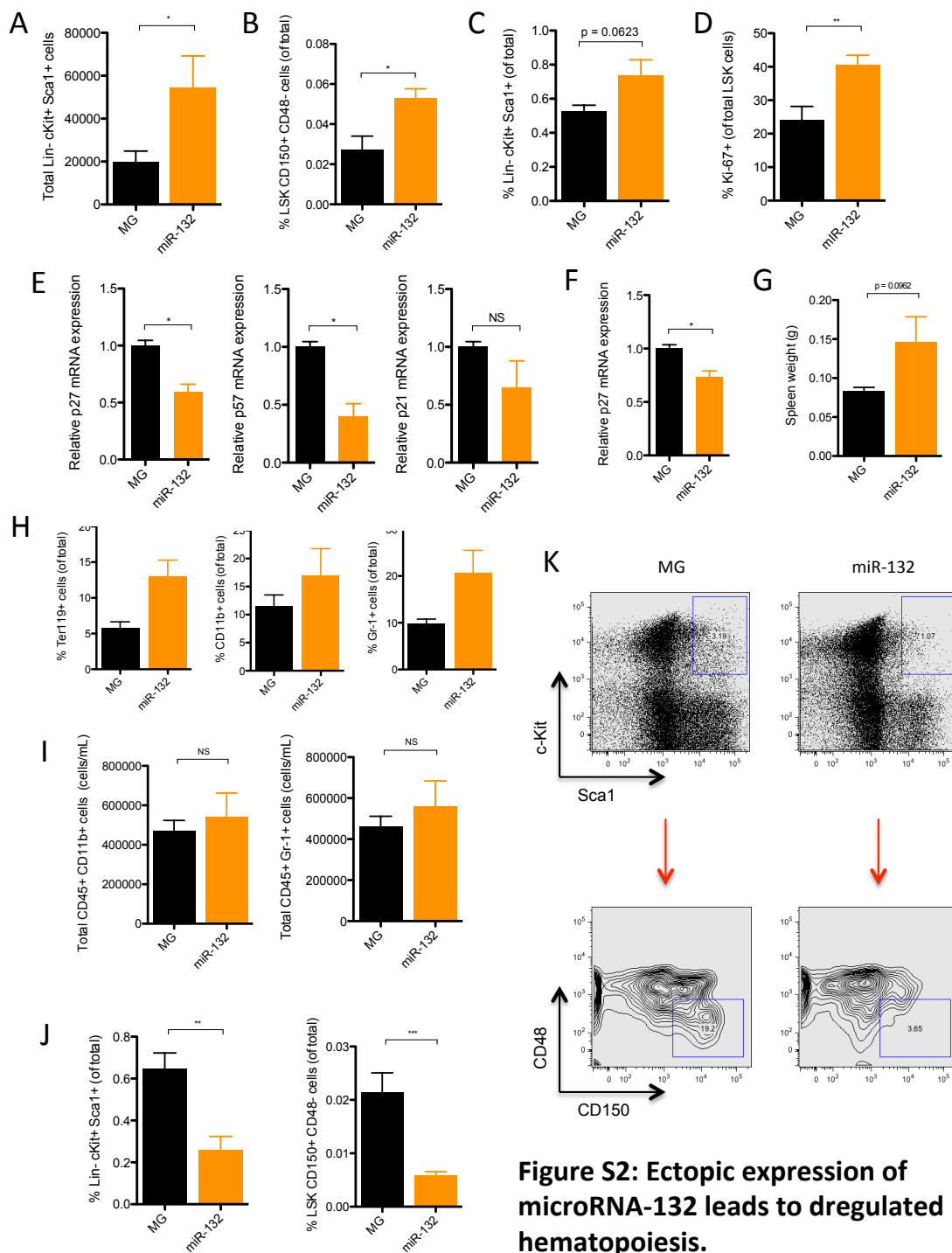


Figure S2: Ectopic expression of microRNA-132 leads to deregulated hematopoiesis.

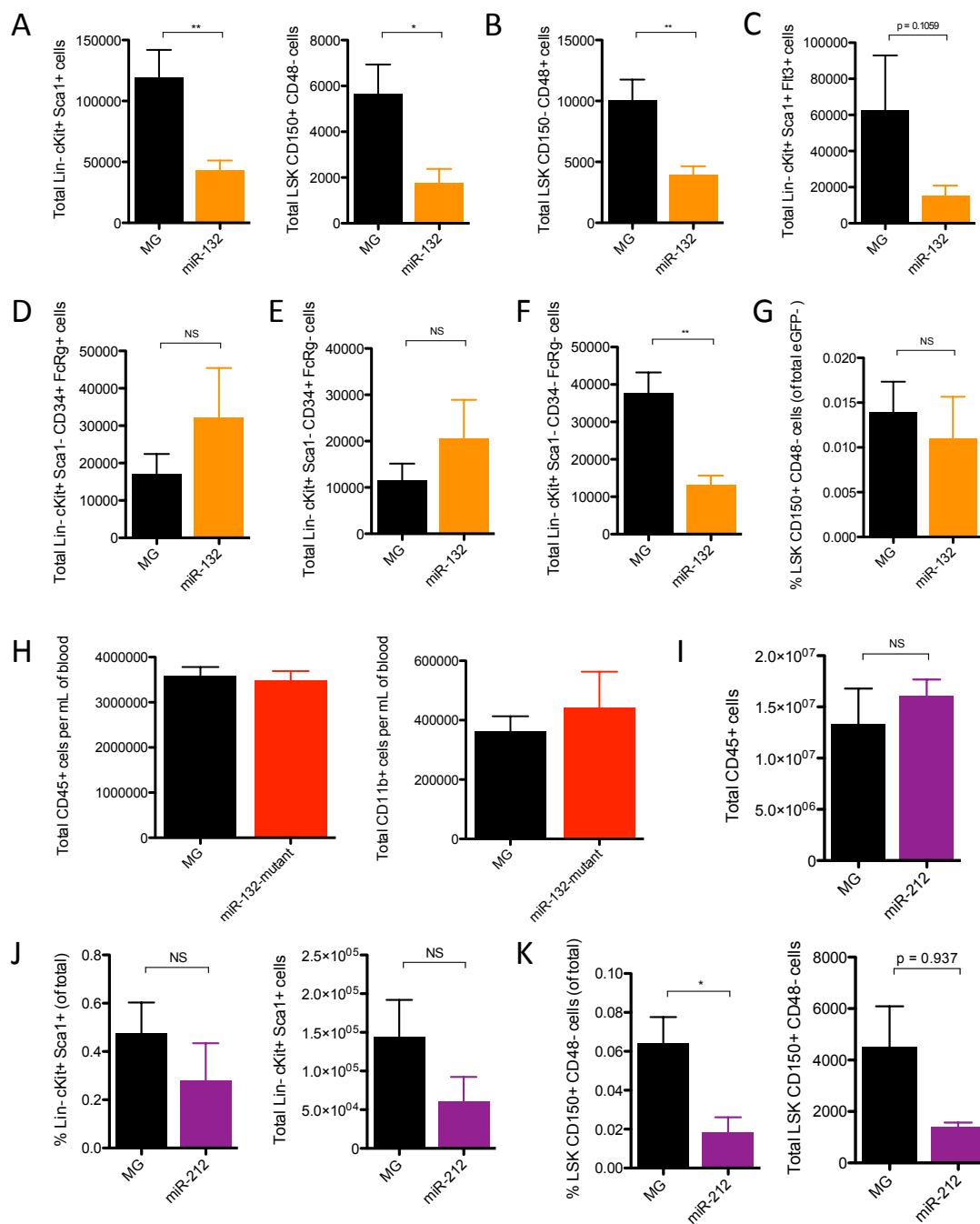


Figure S3: Ectopic expression of miR-132 leads to deficits in several early and late hematopoietic progenitor populations.

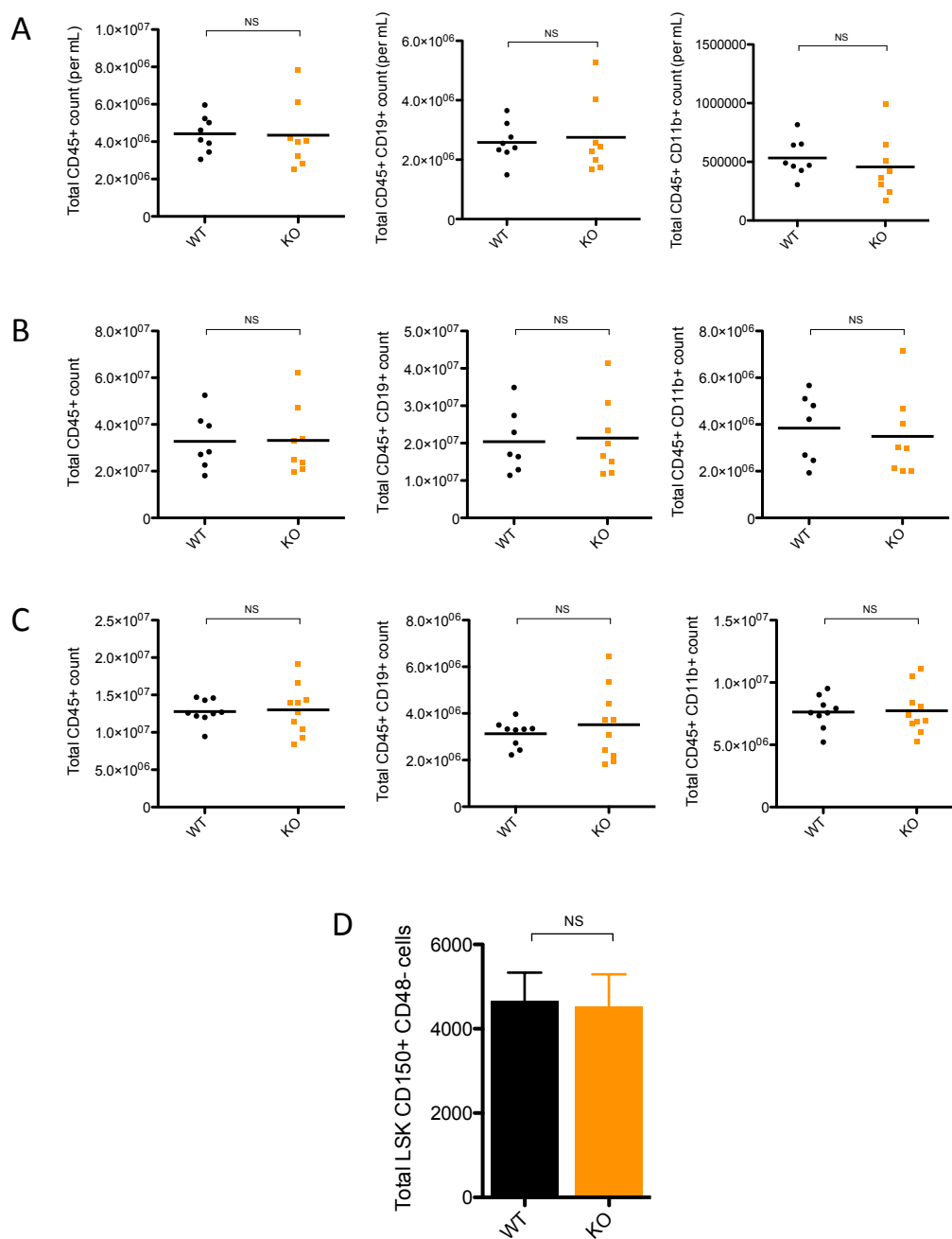


Figure S4: Genetic deletion of the microRNA-212/132 cluster has no observable effect on hematopoiesis in young mice.

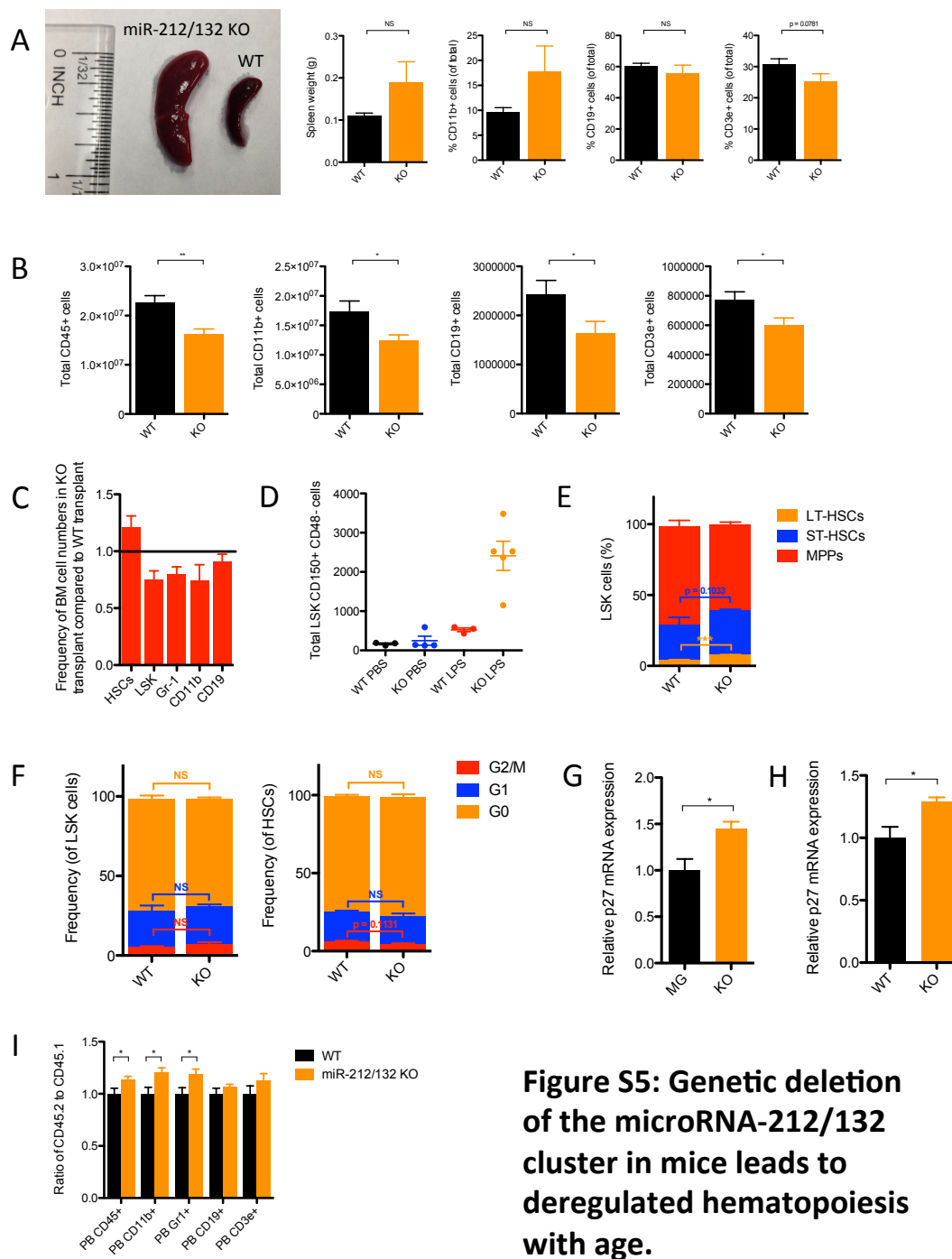


Figure S5: Genetic deletion of the microRNA-212/132 cluster in mice leads to deregulated hematopoiesis with age.

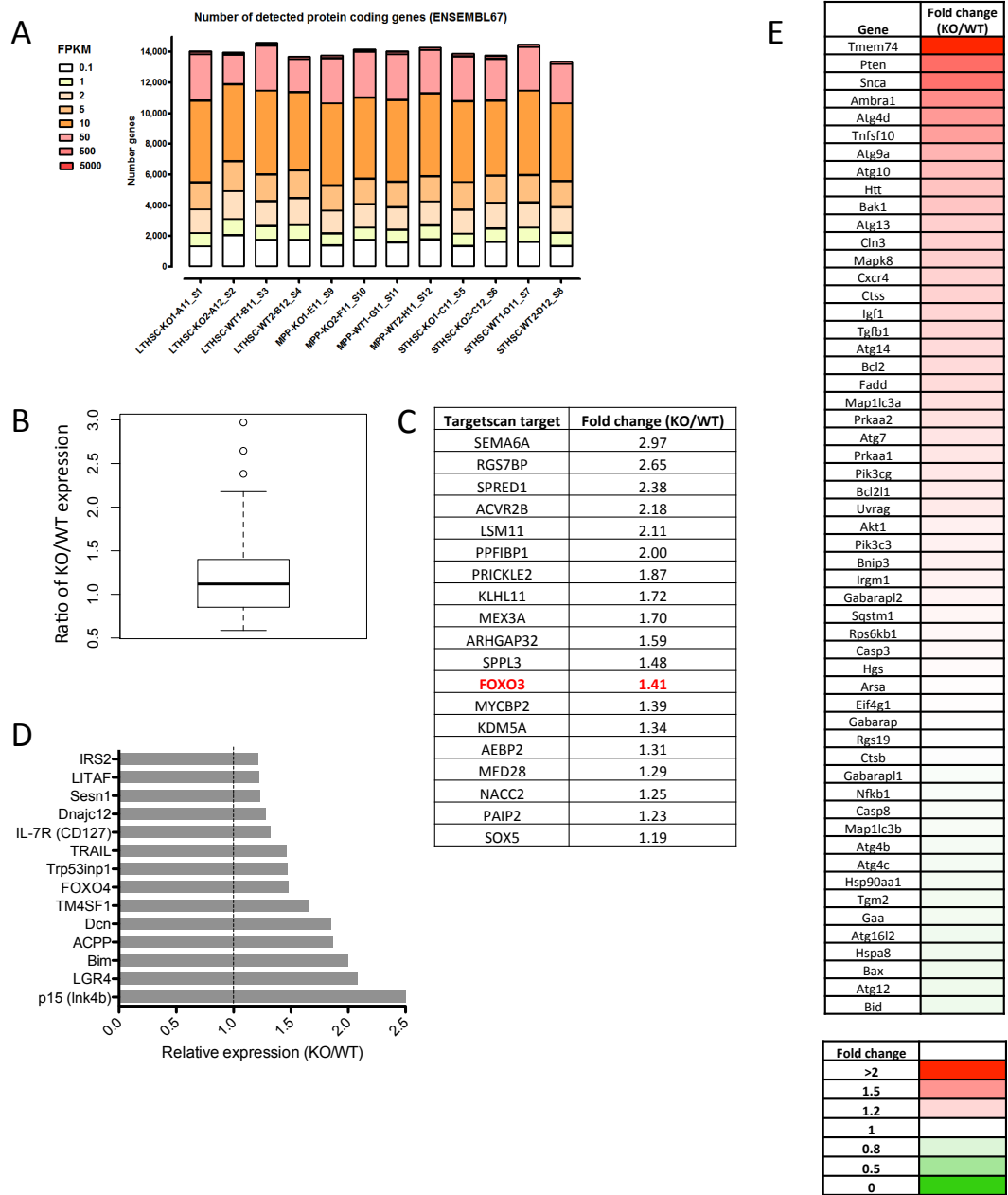


Figure S6: Summary of RNA-sequencing analysis on WT and miR-212/132^{-/-} HSCs from 16-week old mice.

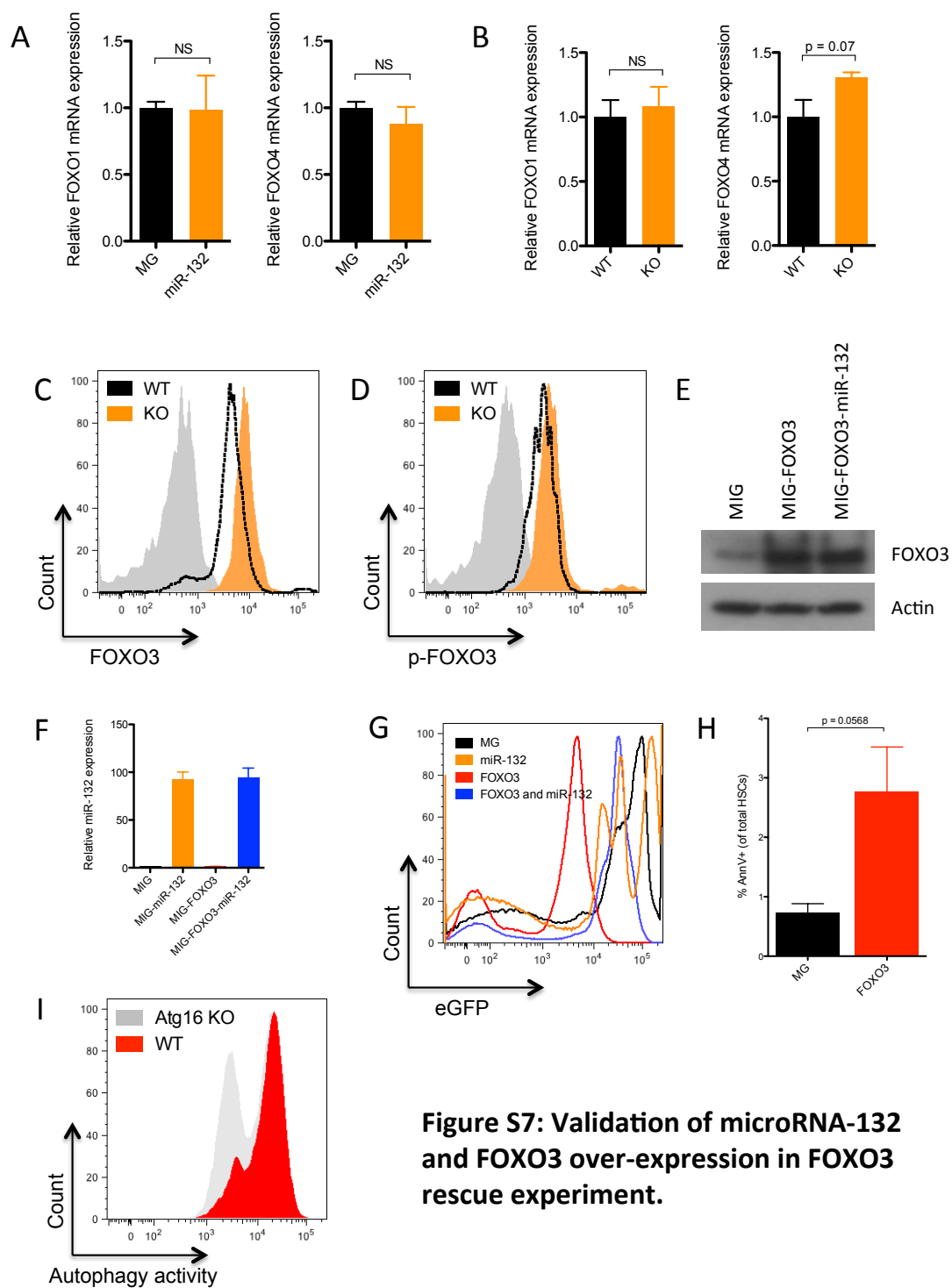


Figure S7: Validation of microRNA-132 and FOXO3 over-expression in FOXO3 rescue experiment.

Chapter 3: The microRNA-212/132 cluster regulates B cell development and apoptosis by targeting Sox4

Published as: A Mehta, M Mann, JL Zhao, GK Marinov, D Majumdar, Y Garcia-Flores, E Ericki, K Chowdhury, D Baltimore (2015). The microRNA-212/132 cluster regulates B cell development and apoptosis by targeting Sox4. *In review*.

Abstract

MicroRNAs have emerged as key regulators of B cell fate decisions and immune function. Deregulation of several microRNAs in B cells leads to the development of autoimmune disease and cancer in mice. We demonstrate that the microRNA-212/132 cluster (miR-212/132) is induced in B cells in response to B cell receptor signaling. Enforced expression of miR-132 results in a block in early B cell development at the pre-pro-B cell to pro-B cell transition and induces apoptosis in primary bone marrow B cells. Importantly, loss of miR-212/132 results in increased B cell output under non-homeostatic conditions. We find that miR-212/132 regulates B lymphopoiesis by targeting the transcription factor Sox4. Co-expression of SOX4 with miR-132 rescues the defect in B cell development from over-expression of miR-132 alone. In addition, we show that the expression of miR-132 can inhibit cancer development in cells that are prone to spontaneous B cell cancers, such as B cells expressing the c-Myc oncogene. We have thus uncovered a novel regulator of B cell lineage specification that may potentially have applications in B cell cancer therapy.

Introduction

Recently, the microRNA-212/132 cluster (miR-212/132) has emerged as an important regulator of anti-viral immunity (Lagos et al., 2010), as well as macrophage and T_H17 T cell immune function (Nahid et al., 2013; Nakahama et al., 2013; Shaked et al., 2009; Taganov et al., 2006). In addition, it has been shown that miR-132 plays a role in the proliferation and invasion of certain solid tumors (Jiang et al., 2015; Zhang et al., 2014), as well as in pathological angiogenesis (Anand et al., 2010), thus making it a potential candidate for cancer therapeutics. Recently, several groups have also identified miR-212/132 as deregulated in certain B cell cancers (Lawrie et al., 2008; Pede et al., 2013; Tavolaro et al., 2015). In this study, we uncover a novel role for miR-212/132 as a regulator of early B cell development by targeting the transcription factor Sox4. In addition, we find that miR-132 induces apoptosis in B cells and that this may be leveraged to inhibit the progression of B cell cancers, such as spontaneous B cell lymphomas in mice expressing the c-Myc oncogene driven by the IgH enhancer (Langdon et al., 1986).

Results

The microRNA-212/132 cluster is induced in B cells in response to B cell receptor activation

To investigate the role of the microRNA-212/132 cluster (miR-212/132) in B cells we first examined the expression of miR-212/132 in various sorted splenic and bone marrow cell populations obtained from wild-type (WT) C57BL/6 mice. RNA was extracted from these cells and we performed TaqMan qPCR to profile microRNA expression. We initially found

that miR-212/132 was not significantly enriched in either the splenic or bone marrow CD19⁺ B cell population (Fig. S1A). However, we found a significant upregulation of miR-132 in these cells in response to stimulation with mouse anti-IgM, which binds to and activates the B cell receptor (BCR) (Fig. 1A and S1B). This induction peaked at 24 hours, and was specific to BCR signaling through an NF- κ B independent pathway, since it could be replicated by stimulation with PMA and ionomycin, but not with activation of NF- κ B through TLR ligands or anti-CD40 (Fig. 1A and S1C). The level of miR-132 induction demonstrated a strong dependence on the concentration of anti-IgM used for stimulation (Fig. S1D). Importantly, we found that B cells from mice with a genetic deletion of miR-212/132 (miR-212/132^{-/-}) demonstrated no detectable expression of miR-132 at steady state and after anti-IgM stimulation (Fig. S1E).

Enforced expression of microRNA-132 inhibits B cell development

We next examined the result of miR-132 over-expression on B cell development. We chose to over-express miR-132 since it was the most strongly induced of the two microRNAs. Bone marrow from WT C57BL/6 mice that was enriched for hematopoietic stem and progenitor cells (HSPCs) was retrovirally transduced with control vector (WT^{MG}) or a miR-132 over-expression vector (WT^{miR-132}). These cells were then used to reconstitute the immune system of lethally irradiated C57BL/6 WT recipients, and we subsequently tracked the development of B cells. We found that WT^{miR-132} mice had a significant depletion in the frequency and total number of peripheral blood B cells compared to WT^{MG} controls at 3-4 months post-reconstitution (Fig. 1B,C). This was accompanied by a decrease in the total number of leukocytes (CD45⁺), B cells (CD19⁺), and plasma cells (CD138⁺) in the spleen

of WT^{miR-132} mice (Fig. 1D,E). The loss of B-cells was dramatically mirrored in the bone marrow compartment (Fig. 1F), where a minor increase in myeloid cells was also observed (Fig. 1G). A similar depletion in total leukocytes, B cells, and T cells was observed in the spleen of mice at 9-months post-reconstitution (Fig. S2A). The bone marrow compartment of these mice also demonstrated a loss in B cells and T cells, but no change in myeloid cells was apparent (Fig. S2B). Enforced expression of miR-212 alone resulted in slight decrease in B cells in the bone marrow compartment at 4 months post-reconstitution; however, no changes in the frequency of bone marrow B cell progenitors or splenic B cells was observed compared to controls (Fig. S3).

We next sought to better understand the underlying cellular mechanism for this defect in B cell development in WT^{miR-132} mice. To begin to address this question, we performed RNA-seq on immature B cells obtained from WT and miR-212/132^{-/-} mice under steady state conditions, and after 8-hours or 20-hours of anti-IgM stimulation. We found a number of differentially expressed genes between samples (Fig. S4A). These were enriched for genes related to cell death, calcium ion transport, B cell receptor signaling, and cytokine production when comparing anti-IgM stimulated cells to unstimulated cells (Fig. S4B). Clustering analysis of differentially expressed genes revealed that WT and miR-212/132^{-/-} cells from the same time-points were more closely related to each other than to any other sample (Fig. 2A). Importantly, among the genes that were differentially regulated between WT and miR-212/132^{-/-} cells at the same time-point, there was enrichment for genes related to B cell apoptosis and precursor-B (pre-B) cell differentiation (Fig. 2B).

To better understand the influence of miR-212/132 in early B cell commitment, we profiled the expression of miR-132 in B cell progenitors. We found a slight enrichment in miR-132 in progenitor B (pro-B) cells and precursor B (pre-B) cells compared to total bone marrow cells and common lymphoid progenitors (CLPs) (Fig. 2C). Consistent with this finding, we found that the bone marrow of WT^{miR-132} mice had a comparable frequency of CLPs (Lineage-cKit+Sca1+Flt3+IL7Ra+) and a slight, but not statistically significant, decrease in the frequency precursor-progenitor B (pre-pro-B) cells compared to WT^{MG} mice (Fig. 2D,E). However, we found a significant decrease in the frequency of both pre-B cells and pro-B cells in the bone marrow of WT^{miR-132} mice (Fig. 2F,G), which is indicative of a developmental block somewhere between the pre-pro-B cell to pro-B cell transition.

The microRNA-212/132 cluster regulates B cell survival

We next sought to investigate whether miR-132 may influence B cell development by altering the survival or proliferation of B cells. We found that primary splenic B cells in WT^{miR-132} at 2 months post-reconstitution demonstrated increased cell death compared to WT^{MG} controls, as measured by AnnexinV staining (Fig. 3A). This indicates that overexpression of miR-132 results in apoptosis in B cells of these mice. We next cultured primary splenic B cells from miR-212/132^{-/-} and WT mice with or without anti-IgM, and found in both conditions that miR-212/132^{-/-} B cells were more resistant to apoptosis (Fig. 3B and S5), as is consistent with the potential role of miR-212/132 in regulating cell death. Importantly, we found no difference in proliferation of splenic B cells from miR-212/132^{-/-} or WT mice in unstimulated conditions or in the presence of TLR ligands (Fig. 3C).

Loss of the microRNA-212/132 cluster enhances B cell development under non-homeostatic conditions

A close examination of the peripheral blood, spleen, and bone marrow of miR-212/132^{-/-} and WT mice at 16-weeks of age revealed no significant difference in the frequency of B cells present in these compartments, though a marginal elevation in CD19⁺ B cells in the peripheral blood was observed (Fig. S6A-C). We next challenged WT and miR-212/132^{-/-} mice with an anti-CD20 antibody to deplete all mature B cells (Sarikonda et al., 2013). We observed a rapid depletion of peripheral blood B cells in all mice treated with anti-CD20 compared to control mice treated with phosphate buffered saline (PBS) (Fig. 4). Within 3 days, the total number of B cells in both anti-CD20 treated cohorts was less than 1% of the total number of peripheral blood leukocytes. Interestingly, under these conditions, miR-212/132^{-/-} mice demonstrated a more rapid rebound in the frequency of peripheral blood B cells compared to WT mice about 21 days after anti-CD20 treatment (Fig. 4). This indicates a unique advantage of miR-212/132^{-/-} B cell progenitors to replenish the B cell pool under conditions of stress. We further corroborated this result by treating miR-212/132^{-/-} and WT mice with serial LPS injections to mimic aging under conditions of inflammatory stress. Consistent with the aforementioned result, we found that miR-212/132^{-/-} mice showed a large accumulation B cells in the spleen compared to WT mice (Fig. S6D).

Sox4 is a direct target of microRNA-132 in B cells and rescues defective B cell development with enforced expression of microRNA-132

We have previously shown that Sox4 mRNA expression levels are decreased in the bone marrow of WT^{miR-132} mice compared to WT^{MG} controls. Sox4 is a known regulator of B cell development (Laurenti et al., 2013; Mallampati et al., 2014; Sun et al., 2013) and has a conserved, computationally predicted 7mer-m8 binding site for miR-132 (Fig. 5A). We thus validated that it is a direct target of miR-132 and explored the possibility that miR-132 may regulate B cell development through Sox4. We transfected HEK293T cells with a construct that over-expressed miR-132 in the presence of a luciferase reporter immediately upstream of either the 3'-untranslated region (3'UTR) of Sox4, the 3'UTR of Sox4 with a mutated miR-132 binding site, or an irrelevant 3'UTR (control). We found decreased expression of luciferase when expressing the construct with an intact Sox4 3'UTR when compared to the control vector; however, this luciferase expression was restored upon mutating the miR-132 binding site (Fig. 5B). Examination of Sox4 protein expression in whole bone marrow lysates from WT^{miR-132} and WT^{MG} mice by Western Blot did not reveal significant differences (Fig. S7A). However, we found a significant decrease in Sox4 mRNA and protein expression levels in purified bone marrow B cells from WT^{miR-132} mice when compared to WT^{MG} controls (Fig. 5C,D). We further validated that enforced expression of miR-132 down-regulated Sox4 protein expression in the 70Z/3 B cell line (Fig. S7B). We also found a marginal decrease in Rag1 expression levels in purified bone marrow B cells from WT^{miR-132} when compared to WT^{MG} cells, but observed no changes in the expression levels of other genes critical for B cell development, including PU.1, Irf1, Ebf1, E2A, and Pax5 (Fig. S7C).

While it is known that a complete loss of Sox4 has dramatic consequences on B cell development, we explored whether a partial decrease in Sox4 protein levels, as might be expected by upregulation of a microRNA, may alter B cell fate. To do this, we reconstituted lethally irradiated C57BL/6 mice with HSPC enriched bone marrow cells transduced with either a control vector (WT^{MIG}) or a vector expressing an shRNA knockdown for Sox4 (WT^{shSOX4}) using a strategy previously described (Chaudhuri et al., 2012). WT^{shSOX4} mice, when compared to WT^{MIG} controls, demonstrated a significant depletion in the frequency of B cells in the spleen (Fig. 5E) and bone marrow compartment (Fig. 5F) at 4 months post-reconstitution. We observed no change in the frequency of pre-pro B cells (Fig. 5G); however, there was a significant decrease in the frequency of pro-B cells (Fig. 5H) and pre-B cells (Fig. 5I) in the bone marrow of WT^{shSOX4} mice.

To determine if Sox4 is the key target of miR-132 responsible for regulating B cell development, we attempted to rescue the defect in B cell development observed with enforced expression of miR-132 by co-expressing Sox4 in the same cells. To do this we reconstituted mice with HSPCs expressing an empty vector (WT^{MIG}), or with a vector expressing either miR-132 only (WT^{miR-132}), Sox4 only (WT^{SOX4}), or miR-132 and Sox4 together (WT^{miR-132-SOX4}) using a strategy previously described (Rao et al., 2010). We validated the expression of Sox4 and miR-132 in the respective samples by qPCR (Fig. 6A,B). Analysis of the peripheral blood of these mice at three months post-reconstitution revealed that co-expression of Sox4 partially rescues the loss of B cells observed with expression of miR-132 alone (Fig. 6C), thus suggesting that miR-132 regulates B cell

development in part by altering the expression of Sox4. Importantly, we also found that WT^{SOX4} mice had enhanced output of B cells compared to WT^{MG} controls (Fig. 6C).

MicroRNA-132 protects E μ -myc mice from spontaneous B cell leukemia development

Several groups have uncovered that the microRNA-212/132 cluster is deregulated in certain leukemia's of B cell origin (Pede et al., 2013; Tavolaro et al., 2015). Given our observation that miR-212/132 inhibits B cell development and induces B cell apoptosis, we investigated whether it may play a role in inhibiting B cell leukemias or lymphomas. To this end, we over-expressed miR-132 in 70Z/3 cells, a pre-B cell lymphoblast tumor line, and found increased AnnV⁺ staining in cells expressing miR-132 compared to a control vector (Fig. 7A). We next investigated whether delivering miR-132 to bone marrow cells from mice with a c-Myc transgene driven by an IgH enhancer (E μ -myc mice) (Langdon et al., 1986) could prevent the spontaneous occurrence of B cell cancers. To do this, we reconstituted lethally irradiated WT C57BL/6 mice with HSPC enriched bone marrow cells from WT or E μ -myc mice that were transduced with either a control vector or a miR-132 expressing vector. Over 4 months, none of the mice reconstituted with WT cells developed cancer and almost all of them survived. However, a significant majority of the mice that received cells from E μ -myc donors expressing the control vector developed spontaneous B cell lymphomas or leukemias, and quickly passed away (Fig. 7B). While approximately 50% of the mice receiving E μ -myc donor cells transduced with a miR-132 expression vector succumbed to cancer, there was a significant improvement in survival compared to mice receiving E μ -myc cells with the control vector (Fig. 7B). Importantly, surviving mice that received E μ -myc donor cells expressing miR-132 demonstrated a rescue in the

frequency of CD19⁺ B cells, CD11b⁺ myeloid cells and pre-B cells in the bone marrow compartment compared to mice that received E μ -myc donor cells with the control vector (Fig. 7C-E). Thus, the expression of miR-132 had a protective effect on cancer occurrence in mice that were given E μ -myc cells predisposed to forming B cell cancers.

Discussion

A handful of microRNAs have been implicated in regulating hematopoietic cell fate decisions, including B cell lineage commitment (O'Connell et al., 2010b; Rao et al., 2010; Xiao et al., 2007). As post-transcriptional regulators of gene expression, these microRNAs primarily serve to fine-tune the expression of their targets, and in turn confer robustness to biological processes (Ebert and Sharp, 2012). When deregulated, however, microRNAs can tip the balance between normal and pathologic function of a cell. In this study, we have uncovered a novel role for miR-212/132 in regulating the differentiation of pre-pro-B cells to pro-B cells by targeting the transcription factor Sox4. We found that deregulating miR-132 *in vivo* can affect survival of B cells, and this may be utilized for therapeutic purposes in combating B cell cancers.

We observed that miR-212/132 is highly induced in B cells in response to B cell receptor activation, but not to activation of TLR receptors or CD40, which result in a strong NF- κ B response. This highlights a potentially unique regulation of miR-212/132 in B cells, independent of what has been observed in macrophages, where a significant but less dramatic induction of miR-212/132 has been observed with TLR4 stimulation (Shaked et

al., 2009; Taganov et al., 2006). Importantly, this induction was replicated by stimulation with PMA, a DAG analog, but not with ionomycin, which mimics Ca^{2+} influx into a cell, thus suggesting that miR-212/132 may be regulated by CREB or a host of other factors in B cells, as has been observed in neurons (Klein et al., 2007; Wen et al., 2010). Importantly, we found that enforced expression of miR-132 blocks the development of pro-B cells, which express the pre-BCR. Thus, it remains to be seen whether miR-212/132 may be induced by pre-BCR signaling and what role this may play in the developmental process. We may hypothesize that high levels of miR-212/132 induction from strong pre-BCR induction may serve as a safety check to buffer aberrant B cell development and induce apoptosis in highly reactive cells.

A genetic deletion in miR-212/132 resulted in B cells that were more resistant to apoptosis. In addition, miR-212/132^{-/-} mice had an increased output of B cells compared to WT mice under non-homeostatic conditions, such as when B cells were depleted with a mouse anti-CD20 antibody. Aging these mice did not reveal the occurrence of B cell cancers; however, it may be possible that deregulation of miR-212/132 may aid in the progression of cancers once they have been established. In fact, it has been demonstrated that miR-212/132 is deregulated in cancers of various forms, including B cell leukemias, and that upregulation of miR-212/132 in lung cancers inhibits proliferation and progression of the disease (Jiang et al., 2015; Pede et al., 2013; Tavolaro et al., 2015; Zhang et al., 2014). We found that enforced expression of miR-132 in donor cells from E μ -myc mice, which are prone to develop spontaneous B cell lymphomas, had a strong protective effect on cancer development. Importantly, as was observed in primary B cells, the delivery of miR-132 to

70Z/3 cells, a B cell cancer line, induced apoptosis in these cells. We note, however, that this contrasts the role of miR-132 promoting pathological angiogenesis (Anand et al., 2010), thus requiring targeted delivery of miR-132 specifically to the tumor cells only and complicating treatment of solid tumors.

Our work also led to the discovery of Sox4 as a novel target for miR-132. We demonstrated that Sox4 is a key player in mediating the B cell development defect observed with miR-132 over-expression. A genetic deletion of Sox4 in mice has been shown to completely abolish the development of pro-B cells (Sun et al., 2013). Consistent with this, we found a dramatic loss of pro-B cells with miR-132 over-expression and a concomitant increase in B cell apoptosis. Importantly, we demonstrated that sub-threshold levels of Sox4, either by miR-132 over-expression or by shRNA knockdown of Sox4, are sufficient to recreate the defect in pro-B cell development. We found that over-expression of miR-132 also affected downstream targets of Sox4 (Mallampati et al., 2014), particularly Rag1.

We have thus identified miR-212/132 as a novel player in regulating B cell development. While much remains to be understood about the role of miR-212/132 in pro-B cell differentiation, we have identified a novel target for miR-212/132 in Sox4, and together these findings provide unique insight into the post-transcriptional mechanisms that govern B cell fate. Furthermore, our current work also suggests a potential role for miR-212/132 in combating cancers of B cell origin.

Experimental Procedures

DNA constructs

For *in-vivo* miR-132 expression and Sox4 shRNA experiments, we cloned either the mature miR-132 or Sox4 shRNA sequence in the microRNA-155 loop-and-arms format (O'Connell et al., 2010a) and into the MSCV-eGFP (MG) vector. For Sox4 rescue experiments, Sox4 lacking its 3'UTR was cloned into the MSCV-IRES-eGFP (MIG) vector using a strategy previously described (Rao et al., 2010). Sox4 shRNA target sequences are given in Table S1.

For luciferase assays, the microRNA-132 expression cassette was sub-cloned into the pCDNA3 vector. The 3'UTR of Sox4 containing either the intact or mutated miR-132 binding site was cloned immediately downstream of luciferase in the pMiReport vector as previously described (Chaudhuri et al., 2012).

Cell culture

Cells were cultured in a sterile incubator that was maintained at 37°C and 5% CO₂. HEK293T cells were cultured in DMEM supplemented with 10% fetal bovine serum, 100 U/mL penicillin, and 100 U/mL streptomycin. Primary splenic B cells were cultured in complete RPMI supplemented with 10% FBS, 100 U/mL penicillin, 100 U/mL streptomycin, 50uM β-mercaptoethanol, and the indicated stimulants. All stimulants, including anti-IgM (goat F(ab')₂ anti-mouse IgM; Southern Biotech), lipopolysaccharide (055:B5; Sigma Aldrich), CpG (ODN 1826; Invivogen), mouse IL-4 (Biolegend), mouse

CD40 ligand (eBioscience), phorbol-12-myristate-13-acetate (PMA; Calbiochem), and ionomycin (Calbiochem) were prepared as per manufacturers instructions and used at the indicated concentration in the text.

Cell sorting for RNA extraction

For miR-132 expression studies, we sorted cells either using MACS columns (Miltenyi) or by FACS. To isolate B cells, RBC depleted bone marrow or spleen samples were sorted on MACS columns (Miltenyi). Briefly, bone marrow or spleen cells were incubated first with biotin-conjugated CD19 (positive-selection) or CD43 (negative selection) antibodies (BioLegend) in MACS sorting buffer (Miltenyi), followed by incubation with streptavidin-conjugated magnetic beads (Miltenyi) as per manufacturers protocol, before being separated on the columns. For profiling studies on B cell progenitors, cells were sorted on a FACS Aria IIu cell sorter (Becton Dickinson) at the Caltech Flow Cytometry Core Facility after surface staining with fluorescent antibodies for B220, CD19, CD43, CD24, IgM, CD11b, CD3e, Gr-1, Ter119, Nk1.1, Sca1, cKit, Flt3, and IL7Ra (BioLegend). RNA was then harvested from these cells using the miRNAeasy RNA prep kit (Qiagen).

Expression profiling and qPCR

RNA harvested from the respective cell populations was analyzed as previously described (Chaudhuri et al., 2012) by real time qPCR (RT-qPCR) with a 7300 Real-Time PCR machine (Applied Biosystems). We used TaqMan MicroRNA Assays (Life Technologies) for miR-132, miR-212 and snoRNA-202 (control) to perform TaqMan qPCR as per manufacturers instructions. We performed SYBR Green-based RT-qPCR for mRNA

expression of mouse Sox4, Ikzf1, Ebf1, E2A, Pax5, PU.1, and Rag1 following cDNA synthesis using qScript cDNA SuperMix (Quanta) and detection with PerfeCTa qPCR Fastmix with ROX (Quanta) as per manufacturers instructions. Table S2 lists primers used for qPCR.

Luciferase reporter assays

We performed luciferase assays for the SOX4 3'UTR as has been previously described (Rao et al., 2010). 4×10^5 cells HEK293T cells, plated for 24 hours, were transfected with either pCDNA or pCDNA-miR-132, a β -gal expression vector, and a pMiReport vector containing either no 3'UTR, the Sox4 3'UTR, or a Sox4 3'UTR with a mutant miR-132 binding site. 48 hours later, cells were lysed using Reporter Lysis Buffer (Promega) and luciferase and β -gal expression was analyzed, respectively, using a Dual Luciferase Kit (Promega) and a chemiluminescent β -gal reporter kit (Roche), respectively.

Immunoblotting

Whole bone marrow samples and bone marrow B cells were sorted using the procedure described for RNA preparation using MACS columns (Miltenyi). Whole protein lysates were collected using RIPA lysis buffer (Sigma), and were subjected to gel-electrophoresis on a mini-PROTEAN TGX gradient (4-15%) gel (Bio-Rad), and then transferred onto a PVDF membrane. Proteins were detected using the following antibodies: anti-Sox4 (154C4a) (Abcam), actin-HRP (sc-1616) (Santa Cruz Biotechnology), and goat anti-mouse-IgG-HRP (sc-2005) (Santa Cruz Biotechnology).

Flow cytometry

Respective tissue samples were collected from the appropriate mice as indicated in the text, RBC lysed (BioLegend), and processed as previously described (Chaudhuri et al., 2012). They were subsequently stained with a combination of fluorephore-conjugated antibodies (all from BioLegend), such as CD45, B220, CD19, CD43, CD24, IgM, CD11b, CD3e, Gr-1, Ter119, Nk1.1, Sca1, cKit, Flt3, and IL7Ra. Surface markers were detected and analyzed using a MACSQuant10 Flow Cytometry machine (Miltenyi). Gating and analysis was performed using FlowJo software.

Animals

All experiments were approved by the California Institute of Technology Institutional Animal Care and Use Committee (IACUC). C57BL/6 WT and miR-212/132^{-/-} mice were bred and housed in the Caltech Office of Laboratory Animal Resources (OLAR) facility. Bone marrow reconstitution experiments were performed as previously described (Chaudhuri et al., 2012) using donor cells from C57BL/6 WT mice or E μ -myc mice, and with the appropriate retroviral vectors as described in the text. *In vivo* B cell depletion studies were performed by intraperitoneal delivery of 50 μ g of mouse anti-CD20 (5D2) (Genentech) in 250 μ L of phosphate buffered saline (PBS). Treated mice were subsequently bled at the indicated time points and cell populations in the peripheral blood were analyzed using FACS as described above.

RNA-seq data generation and analysis

RNA-seq libraries were prepared from polyA⁺ selected RNA using the TruSeq RNA Sample Preparation Kit at the Millard and Muriel Jacobs Genetics and Genomics Laboratory at Caltech. Libraries were sequenced on the Illumina HiSeq 2500 generating single-end 50bp reads. The refSeq annotation for the mm9 version of the mouse genome was used to create a transcriptome Bowtie (version 0.12.7) (Langmead et al., 2009) index, to which reads were aligned with the following settings: “-v 3 -a”. Gene expression levels were estimated using eXpress (version 1.2.2) (Roberts and Pachter, 2013), and the effective count values were used as input to DESeq (Anders and Huber, 2010) for evaluating differential expression.

Statistical tests

All statistical analysis was done in Graphpad Prism software using an unpaired Student's *t* test. Data was reported as mean \pm SEM. Significance measurements were marked as follows: * $p < 0.05$, ** $p < 0.01$, *** $p < 0.001$, or NS for not significant.

Figure Legends

Figure 1. miR-132 is induced in B cells and over-expression of miR-132 in mice alters B-cell development. (A) Relative miR-132 expression in primary splenic B cells stimulated with anti-IgM (5 μ g/mL), LPS (20 μ g/mL), CD40L (2 μ g/mL), IL-4 (10ng/mL), or CpG (0.5 μ M) for the indicated durations. miR-132 expression was detected using Taqman RT-qPCR (n=3). (B)-(G) WT C57BL/6 mice were lethally irradiated and reconstituted with donor HPSCs expressing either a control (MG) or a miR-132 over-expressing (miR-132) vector. Mice were analyzed at 4 months post-reconstitution (n>10 mice per group). (B) Frequency of peripheral blood B cells (B220+) in MG and miR-132 mice. (C) Total number of peripheral blood B cells (B220+) in MG and miR-132 mice. (D) Total number of leukocytes (CD45+) and B cells (CD19+) in the spleen of MG and miR-132 mice. (E) Total number of plasma cells (CD138+) in the spleen of MG and miR-132 mice. (F) Total number of B cells (CD19+) in the bone marrow of MG and miR-132 mice. (G) Total number of myeloid cells (CD11b+) and granulocytes (Gr-1+) in the bone marrow of MG and miR-132 mice. Data represent at least three independent experiments. The mean \pm SEM is shown. * denotes $p < 0.05$, ** denotes $p < 0.01$ and *** denotes $p < 0.001$ using a Student's *t* test.

Figure 2. miR-132 causes a block in early B cell development. (A)-(B) B cells were purified from miR-212/132^{-/-} and WT mice and subsequently either left unstimulated, or stimulated for 8 hours or 20 hours with anti-IgM (5 μ g/mL). RNA was harvested from the cells and RNA-seq libraries were generated and sequenced. (A) Heat map and clustering

indicating the number of differentially expressed genes between each sample. (B) Enriched functional annotations for genes differentially expressed between miR-212/132^{-/-} and WT B cells at any of the time points. (C) miR-132 expression in various bone marrow B cell progenitor populations. Cells were sorted by FACS directly into RNA lysis buffer and miR-132 expression was detected using Taqman RT-qPCR (n=2). (D)-(G) Analysis of MG and miR-132 mice at 4 months post-reconstitution (n>10 mice per group). (D) Frequency of CLPs (Lineage-cKit+Sca1+Flt3+IL7Ra+) in the bone marrow MG and miR-132 mice. (E) Frequency of pre-pro-B cells (B220+IgM-CD43+CD24-) in the bone marrow of MG and miR-132 mice. (F) Frequency of pro-B cells (B220+IgM-CD43+CD24+) in the bone marrow of MG and miR-132 mice. (G) Frequency of pre-B cells (B220+IgM-CD43-) in the bone marrow of MG and miR-132 mice. Data represent at least three independent experiments. The mean \pm SEM is shown. * denotes $p < 0.05$, ** denotes $p < 0.01$, and *** denotes $p < 0.001$ using a Student's *t* test.

Figure 3. miR-212/132 regulates B cell apoptosis. (A) Frequency of bone marrow B cells (CD19+) and myeloid cells (CD11b+) from MG and miR-132 mice that demonstrated positive staining for AnnexinV and 7-AAD. (B) miR-212/132^{-/-} and WT splenic B cells were isolated and cultured *in vitro* for the indicated durations. Graph demonstrates the frequency of AnnV+ cells at each time point. (C) miR-212/132^{-/-} or WT splenic B cells were cultured in the presence of no stimulation, or with LPS (20 μ g/mL) or CpG (0.5 μ M). Proliferation of these cells was measured at the indicated time points using the WST-1 cell proliferation assay (see methods). Data represent two independent experiments. The mean

± SEM is shown. * denotes $p < 0.05$, ** denotes $p < 0.01$, and *** denotes $p < 0.001$

using a Student's *t* test.

Figure 4. Loss of miR-212/132 alters B cell development under non-homeostatic conditions. 16-week old miR-212/132^{-/-} (KO) and WT mice were treated with either an anti-CD20 antibody (30µg/mouse) or phosphate buffered saline (PBS) (n=3-4 mice per group). Graph indicates the frequency of B cells (B220+) in the peripheral blood at each of the indicated time points after anti-CD20 antibody treatment. Data represent two independent experiments. The mean ± SEM is shown. * denotes $p < 0.05$ using a Student's *t* test.

Figure 5. SOX4 is a direct target of miR-132 and is a key regulator of B cell development. (A) Schematic of the predicted miR-132 binding site in the Sox4 3' UTR. (B) Relative luciferase expression in HEK293T cells transfected with a miR-132 over-expression vector and either a vector containing luciferase only (control), luciferase and the Sox4 3' UTR immediately downstream (Sox4 3' UTR), or a vector containing luciferase and a Sox4 3' UTR with a mutated miR-132 binding site (Sox4 3' UTR mut). (C) Sox4 transcript expression level, obtained by RT-qPCR, in B cells purified from the bone marrow of MG and miR-132 mice. (D) Sox4 protein expression levels, obtained by Western Blot, in B cells purified from the bone marrow of MG and miR-132 mice. (E)-(I) WT C57BL/6 mice were lethally irradiated and reconstituted with donor bone marrow cells transduced with either a control (MG) or Sox4 shRNA expressing (shSOX4) retroviral vector. Mice were analyzed at 4 months post-reconstitution. (E) Frequency of B cells (CD19+) in the spleen

of MG and shSOX4 mice. (F) Frequency of B cells (B220+) in the bone marrow of MG and shSOX4 mice. (G) Frequency of pre-pro-B cells in the bone marrow of MG and shSOX4 mice. (H) Frequency of pro-B cells in the bone marrow of MG and shSOX4 mice. (I) Frequency of pre-B cells in the bone marrow of MG and shSOX4 mice. Data represent two independent experiments. The mean \pm SEM is shown. * denotes $p < 0.05$, ** denotes $p < 0.01$, and *** denotes $p < 0.001$ using a Student's *t* test.

Figure 6. Co-expression of Sox4 rescues the defect in B cell development with expression of miR-132 alone. WT C57BL/6 mice were lethally irradiated and reconstituted with donor bone marrow cells expressing either a control (MIG), a miR-132 over-expressing (MIG-miR-132), a SOX4 over-expressing (MIG-SOX4), or a SOX4 and miR-132 over-expressing (MIG-SOX4-miR-132) retroviral vector (n=5 mice per group). (A) Validation of miR-132 over-expression in donor HSPCs transduced with the labeled constructs. (B) Validation of Sox4 expression in donor HSPCs transduced with the labeled constructs. (C) Frequency of B cells in the peripheral blood of MIG, MIG-miR-132, MIG-SOX4, and MIG-SOX4-miR-132 mice at 3 months post-reconstitution. Data represent the combination of two independent experiments. The mean \pm SEM is shown. * denotes $p < 0.05$, ** denotes $p < 0.01$, and *** denotes $p < 0.001$ using a Student's *t* test.

Figure 7. Enforced expression of miR-132 inhibits the development of spontaneous B cell cancers in cells with the E μ -myc transgene. (A) Cells from a pre-B cell lymphoblastic leukemia line, 70Z/3, were transduced with a control vector (MGP) or a miR-132 over-expressing vector (miR-132) and cultured for 48 hours with or without LPS (20 μ g/mL).

The frequency of cells expressing AnnV was then measured by FACS. (B)-(E) C57BL/6 mice were reconstituted with donor HSPCs from WT or E μ -myc mice that were either transduced with a control vector (MG) or miR-132 over-expressing vector (miR-132). These mice were followed for 4 months and harvested for analysis at this time point (n=8-10 mice). (B) Survival curve for all experimental cohorts. Frequency of (C) bone marrow B cells (CD19+), (D) myeloid cells (CD11b+), and (E) pre-B cells (B220+IgM-CD43-) in all cohorts. Data represent two independent experiments. The mean \pm SEM is shown. * denotes $p < 0.05$, ** denotes $p < 0.01$, and *** denotes $p < 0.001$ using a Student's *t* test.

References

Anand, S., Majeti, B.K., Acevedo, L.M., Murphy, E.A., Mukthavaram, R., Scheppke, L., Huang, M., Shields, D.J., Lindquist, J.N., Lapinski, P.E., *et al.* (2010). MicroRNA-132-mediated loss of p120RasGAP activates the endothelium to facilitate pathological angiogenesis. *Nature medicine* *16*, 909-914.

Anders, S., and Huber, W. (2010). Differential expression analysis for sequence count data. *Genome biology* *11*, R106.

Calin, G.A., Cimmino, A., Fabbri, M., Ferracin, M., Wojcik, S.E., Shimizu, M., Taccioli, C., Zanesi, N., Garzon, R., Aqeilan, R.I., *et al.* (2008). MiR-15a and miR-16-1 cluster functions in human leukemia. *Proceedings of the National Academy of Sciences of the United States of America* *105*, 5166-5171.

Chaudhuri, A.A., So, A.Y., Mehta, A., Minisandram, A., Sinha, N., Jonsson, V.D., Rao, D.S., O'Connell, R.M., and Baltimore, D. (2012). Oncomir miR-125b regulates hematopoiesis by targeting the gene Lin28A. *Proceedings of the National Academy of Sciences of the United States of America* *109*, 4233-4238.

Cobaleda, C., Schebesta, A., Delogu, A., and Busslinger, M. (2007). Pax5: the guardian of B cell identity and function. *Nature immunology* *8*, 463-470.

Costinean, S., Zanesi, N., Pekarsky, Y., Tili, E., Volinia, S., Heerema, N., and Croce, C.M. (2006). Pre-B cell proliferation and lymphoblastic leukemia/high-grade lymphoma in E(mu)-miR155 transgenic mice. *Proceedings of the National Academy of Sciences of the United States of America* *103*, 7024-7029.

de Yebenes, V.G., Belver, L., Pisano, D.G., Gonzalez, S., Villasante, A., Croce, C., He, L., and Ramiro, A.R. (2008). miR-181b negatively regulates activation-induced cytidine deaminase in B cells. *The Journal of experimental medicine* *205*, 2199-2206.

DeKoter, R.P., Lee, H.J., and Singh, H. (2002). PU.1 regulates expression of the interleukin-7 receptor in lymphoid progenitors. *Immunity* *16*, 297-309.

Ebert, M.S., and Sharp, P.A. (2012). Roles for microRNAs in conferring robustness to biological processes. *Cell* *149*, 515-524.

Eis, P.S., Tam, W., Sun, L., Chadburn, A., Li, Z., Gomez, M.F., Lund, E., and Dahlberg, J.E. (2005). Accumulation of miR-155 and BIC RNA in human B cell lymphomas. *Proceedings of the National Academy of Sciences of the United States of America* *102*, 3627-3632.

- Igarashi, H., Gregory, S.C., Yokota, T., Sakaguchi, N., and Kincade, P.W. (2002). Transcription from the RAG1 locus marks the earliest lymphocyte progenitors in bone marrow. *Immunity* *17*, 117-130.
- Jiang, X., Chen, X., Chen, L., Ma, Y., Zhou, L., Qi, Q., Liu, Y., Zhang, S., Luo, J., and Zhou, X. (2015). Upregulation of the miR-212/132 cluster suppresses proliferation of human lung cancer cells. *Oncology reports* *33*, 705-712.
- Jordan, M.A., Zhao, J.L., Casellas, R., Athanasopoulos, V., Vinuesa, C.G., Porstner, M., Winkelmann, R., Daum, P., Schmid, J., Pracht, K., *et al.* (2015). miR-148a promotes plasma cell differentiation and targets the germinal center transcription factors Mitf and Bach2. *Nature communications*.
- Klein, M.E., Liroy, D.T., Ma, L., Impey, S., Mandel, G., and Goodman, R.H. (2007). Homeostatic regulation of MeCP2 expression by a CREB-induced microRNA. *Nature neuroscience* *10*, 1513-1514.
- Koralov, S.B., Muljo, S.A., Galler, G.R., Krek, A., Chakraborty, T., Kanellopoulou, C., Jensen, K., Cobb, B.S., Merkenschlager, M., Rajewsky, N., and Rajewsky, K. (2008). Dicer ablation affects antibody diversity and cell survival in the B lymphocyte lineage. *Cell* *132*, 860-874.
- Lagos, D., Pollara, G., Henderson, S., Gratrix, F., Fabani, M., Milne, R.S., Gotch, F., and Boshoff, C. (2010). miR-132 regulates antiviral innate immunity through suppression of the p300 transcriptional co-activator. *Nature cell biology* *12*, 513-519.
- Langdon, W.Y., Harris, A.W., Cory, S., and Adams, J.M. (1986). The c-myc oncogene perturbs B lymphocyte development in E-mu-myc transgenic mice. *Cell* *47*, 11-18.
- Langmead, B., Trapnell, C., Pop, M., and Salzberg, S.L. (2009). Ultrafast and memory-efficient alignment of short DNA sequences to the human genome. *Genome biology* *10*, R25.
- Laurenti, E., Doulatov, S., Zandi, S., Plumb, I., Chen, J., April, C., Fan, J.B., and Dick, J.E. (2013). The transcriptional architecture of early human hematopoiesis identifies multilevel control of lymphoid commitment. *Nature immunology* *14*, 756-763.
- Lawrie, C.H., Saunders, N.J., Soneji, S., Palazzo, S., Dunlop, H.M., Cooper, C.D., Brown, P.J., Troussard, X., Mossafa, H., Enver, T., *et al.* (2008). MicroRNA expression in lymphocyte development and malignancy. *Leukemia* *22*, 1440-1446.
- Mallampati, S., Sun, B., Lu, Y., Ma, H., Gong, Y., Wang, D., Lee, J.S., Lin, K., and Sun, X. (2014). Integrated genetic approaches identify the molecular mechanisms of Sox4 in early B-cell development: intricate roles for RAG1/2 and CK1epsilon. *Blood* *123*, 4064-4076.

- Mandel, E.M., and Grosschedl, R. (2010). Transcription control of early B cell differentiation. *Current opinion in immunology* 22, 161-167.
- Matthias, P., and Rolink, A.G. (2005). Transcriptional networks in developing and mature B cells. *Nature reviews. Immunology* 5, 497-508.
- Mauri, C., and Bosma, A. (2012). Immune regulatory function of B cells. *Annual review of immunology* 30, 221-241.
- Nahid, M.A., Yao, B., Dominguez-Gutierrez, P.R., Kesavalu, L., Satoh, M., and Chan, E.K. (2013). Regulation of TLR2-mediated tolerance and cross-tolerance through IRAK4 modulation by miR-132 and miR-212. *Journal of immunology (Baltimore, Md. : 1950)* 190, 1250-1263.
- Nakahama, T., Hanieh, H., Nguyen, N.T., Chinen, I., Ripley, B., Millrine, D., Lee, S., Nyati, K.K., Dubey, P.K., Chowdhury, K., *et al.* (2013). Aryl hydrocarbon receptor-mediated induction of the microRNA-132/212 cluster promotes interleukin-17-producing T-helper cell differentiation. *Proceedings of the National Academy of Sciences of the United States of America* 110, 11964-11969.
- Nutt, S.L., and Kee, B.L. (2007). The transcriptional regulation of B cell lineage commitment. *Immunity* 26, 715-725.
- O'Connell, R.M., Chaudhuri, A.A., Rao, D.S., Gibson, W.S., Balazs, A.B., and Baltimore, D. (2010a). MicroRNAs enriched in hematopoietic stem cells differentially regulate long-term hematopoietic output. *Proceedings of the National Academy of Sciences of the United States of America* 107, 14235-14240.
- O'Connell, R.M., Rao, D.S., Chaudhuri, A.A., and Baltimore, D. (2010b). Physiological and pathological roles for microRNAs in the immune system. *Nature reviews. Immunology* 10, 111-122.
- O'Riordan, M., and Grosschedl, R. (1999). Coordinate regulation of B cell differentiation by the transcription factors EBF and E2A. *Immunity* 11, 21-31.
- Pede, V., Rombout, A., Vermeire, J., Naessens, E., Mestdagh, P., Robberecht, N., Vanderstraeten, H., Van Roy, N., Vandesompele, J., Speleman, F., *et al.* (2013). CLL cells respond to B-Cell receptor stimulation with a microRNA/mRNA signature associated with MYC activation and cell cycle progression. *PloS one* 8, e60275.
- Puissegur, M.P., Eichner, R., Quelen, C., Coyaud, E., Mari, B., Lebrigand, K., Broccardo, C., Nguyen-Khac, F., Bousquet, M., and Brousset, P. (2012). B-cell regulator of immunoglobulin heavy-chain transcription (Bright)/ARID3a is a direct target of the oncomir microRNA-125b in progenitor B-cells. *Leukemia* 26, 2224-2232.

- Rao, D.S., O'Connell, R.M., Chaudhuri, A.A., Garcia-Flores, Y., Geiger, T.L., and Baltimore, D. (2010). MicroRNA-34a perturbs B lymphocyte development by repressing the forkhead box transcription factor Foxp1. *Immunity* 33, 48-59.
- Roberts, A., and Pachter, L. (2013). Streaming fragment assignment for real-time analysis of sequencing experiments. *Nature methods* 10, 71-73.
- Sarikonda, G., Sachithanatham, S., Manenkova, Y., Kupfer, T., Posgai, A., Wasserfall, C., Bernstein, P., Straub, L., Pagni, P.P., Schneider, D., *et al.* (2013). Transient B-cell depletion with anti-CD20 in combination with proinsulin DNA vaccine or oral insulin: immunologic effects and efficacy in NOD mice. *PloS one* 8, e54712.
- Shaked, I., Meerson, A., Wolf, Y., Avni, R., Greenberg, D., Gilboa-Geffen, A., and Soreq, H. (2009). MicroRNA-132 potentiates cholinergic anti-inflammatory signaling by targeting acetylcholinesterase. *Immunity* 31, 965-973.
- Souabni, A., Cobaleda, C., Schebesta, M., and Busslinger, M. (2002). Pax5 promotes B lymphopoiesis and blocks T cell development by repressing Notch1. *Immunity* 17, 781-793.
- Sun, B., Mallampati, S., Gong, Y., Wang, D., Lefebvre, V., and Sun, X. (2013). Sox4 is required for the survival of pro-B cells. *Journal of immunology (Baltimore, Md. : 1950)* 190, 2080-2089.
- Taganov, K.D., Boldin, M.P., Chang, K.J., and Baltimore, D. (2006). NF-kappaB-dependent induction of microRNA miR-146, an inhibitor targeted to signaling proteins of innate immune responses. *Proceedings of the National Academy of Sciences of the United States of America* 103, 12481-12486.
- Tavolaro, S., Colombo, T., Chiaretti, S., Peragine, N., Fulci, V., Ricciardi, M.R., Messina, M., Bonina, S., Brugnoletti, F., Marinelli, M., *et al.* (2015). Increased chronic lymphocytic leukemia proliferation upon IgM stimulation is sustained by the upregulation of miR-132 and miR-212. *Genes, chromosomes & cancer* 54, 222-234.
- Teng, G., Hakimpour, P., Landgraf, P., Rice, A., Tuschl, T., Casellas, R., and Papavasiliou, F.N. (2008). MicroRNA-155 is a negative regulator of activation-induced cytidine deaminase. *Immunity* 28, 621-629.
- Thai, T.H., Calado, D.P., Casola, S., Ansel, K.M., Xiao, C., Xue, Y., Murphy, A., Frendewey, D., Valenzuela, D., Kutok, J.L., *et al.* (2007). Regulation of the germinal center response by microRNA-155. *Science (New York, N.Y.)* 316, 604-608.
- Wen, A.Y., Sakamoto, K.M., and Miller, L.S. (2010). The role of the transcription factor CREB in immune function. *Journal of immunology (Baltimore, Md. : 1950)* 185, 6413-6419.

Xiao, C., Calado, D.P., Galler, G., Thai, T.H., Patterson, H.C., Wang, J., Rajewsky, N., Bender, T.P., and Rajewsky, K. (2007). MiR-150 controls B cell differentiation by targeting the transcription factor c-Myb. *Cell* *131*, 146-159.

Xiao, C., Srinivasan, L., Calado, D.P., Patterson, H.C., Zhang, B., Wang, J., Henderson, J.M., Kutok, J.L., and Rajewsky, K. (2008). Lymphoproliferative disease and autoimmunity in mice with increased miR-17-92 expression in lymphocytes. *Nature immunology* *9*, 405-414.

Yoshida, T., Ng, S.Y., Zuniga-Pflucker, J.C., and Georgopoulos, K. (2006). Early hematopoietic lineage restrictions directed by Ikaros. *Nature immunology* *7*, 382-391.

Zhang, Z.G., Chen, W.X., Wu, Y.H., Liang, H.F., and Zhang, B.X. (2014). MiR-132 prohibits proliferation, invasion, migration, and metastasis in breast cancer by targeting HN1. *Biochemical and biophysical research communications* *454*, 109-114.

Zhou, B., Wang, S., Mayr, C., Bartel, D.P., and Lodish, H.F. (2007). miR-150, a microRNA expressed in mature B and T cells, blocks early B cell development when expressed prematurely. *Proceedings of the National Academy of Sciences of the United States of America* *104*, 7080-7085.

Supplemental Figure Legends

Figure S1, refers to Figure 1. miR-212/132 is induced in B cells by activation of the B cell receptor (BCR). (A) miR-132 expression in various splenic and bone marrow cell populations. RNA was harvested from the indicated cell populations and miR-132 expression was detected using Taqman RT-qPCR (n=3). (B)-(E) Splenic B cells were purified from C57BL/6 mice and cultured in the presence of the indicated stimulants for the indicated duration of time. The expression of miR-132 and miR-212 was detected using Taqman RT-qPCR (n=3). (B) Relative expression of miR-212 in splenic B cells stimulated with LPS (20 μ g/mL) or anti-IgM (aIgM; 5 μ g/mL) for the indicated times. (C) Relative expression of miR-132 in splenic B cells stimulated for 8 hours with a combination of PMA (15ng/mL), ionomycin (0.5 μ g/mL), and anti-IgM (5 μ g/mL) as indicated. (D) Relative expression of miR-132 in splenic B cells stimulated for 8 hours with varying concentrations of anti-IgM as indicated. (E) Relative expression of miR-132 in splenic B cells obtained from miR-212/132^{-/-} or WT mice and stimulated with LPS (20 μ g/mL) or anti-IgM (5 μ g/mL) for the indicated time points. Data represents two independent experiments and is represented as mean \pm SEM.

Figure S2, refers to Figure 1 and 2. Enforced expression of miR-132 alters B cell output in mice up to 9 months post-reconstitution. WT C57BL/6 mice were lethally irradiated and reconstituted with donor HPSCs expressing either a control (MG) or a miR-132 over-expressing (miR-132) vector. Mice were analyzed at 9 months post-reconstitution (n>6 mice per group). (A) Total number of leukocytes (CD45+), B cells (CD19+) and T cells

(CD3e+) in the spleen of MG and miR-132 mice. (B) Total number of myeloid cells (CD11b+), B cells (CD19+), and T cells (CD3e+) in the bone marrow of MG and miR-132 mice. Data represents at least three independent experiments and is represented as mean \pm SEM. * denotes $p < 0.05$, ** denotes $p < 0.01$, and *** denotes $p < 0.001$ using a Student's *t* test.

Figure S3, refers to Figures 1 and 2. Enforced expression of miR-212 has a marginal effect on B cell output. WT C57BL/6 mice were lethally irradiated and reconstituted with donor HPSCs expressing either a control (MG) or a miR-212 over-expressing (miR-212) vector. Mice were analyzed at 4 months post-reconstitution (n=4-5 mice per group). (A) Frequency of B cells (CD19+) in the spleen of MG and miR-212 mice. (B) Frequency of B cells (B220+) in the bone marrow of MG and miR-212 mice. (C) Frequency of pre-pro-B cells (B220+IgM-CD43+CD24-) in the bone marrow of MG and miR-212 mice. (D) Frequency of pro-B cells (B220+IgM-CD43+CD24+) in the bone marrow of MG and miR-212 mice. (E) Frequency of pro-B cells (B220+IgM-CD43-) in the bone marrow of MG and miR-212 mice. Data represents at least three independent experiments and is represented as mean \pm SEM. * denotes $p < 0.05$, ** denotes $p < 0.01$, and *** denotes $p < 0.001$ using a Student's *t* test.

Figure S4, refers to Figure 2. Stimulation of B cells through the B cell receptor (BCR) results in dramatic gene expression changes. B cells were purified from miR-212/132^{-/-} and WT mice and subsequently either left unstimulated, or stimulated for 8 hours or 20 hours with anti-IgM (5 μ g/mL). RNA was harvested from the cells and processed for RNA-

sequencing. (A) Summary of differential gene expression analysis between samples.

Table shows the number of upregulated genes in the described row sample compared to the described column sample. (B) Functional annotations for differentially expressed genes between WT stimulated B cells (8 hours or 20 hours with anti-IgM) compared to WT unstimulated B cells.

Figure S5, refers to Figure 3. miR-212/132 regulates B cell apoptosis. miR-212/132^{-/-} and WT splenic B cells were isolated and cultured *in vitro* with anti-IgM stimulation (5ug/mL) for the indicated durations. Graph demonstrates the frequency of AnnV⁺ cells at each time point. Data represents two independent experiments and is represented as mean \pm SEM. * denotes $p < 0.05$ using a Student's *t* test.

Figure S6, refers to Figure 4. miR-212/132^{-/-} mice demonstrate no observable defect in B cell output under steady state conditions. (A)-(C) miR-212/132^{-/-} and WT mice were analyzed at 12-16 weeks of age to understand the physiological contribution of miR-212/132 on B cell output (n=7-10 mice per group). (A) Frequency of B cells (CD19⁺) in the peripheral blood of miR-212/132^{-/-} and WT mice. (B) Frequency of B cells (CD19⁺) in the spleen of miR-212/132^{-/-} and WT mice. (C) Frequency of B cells (CD19⁺) in the bone marrow of miR-212/132^{-/-} and WT mice. (D) 6-month old miR-212/132^{-/-} and WT mice were treated with 9 evenly-spaced LPS (1mg/kg of body weight) or PBS injections over one month. Graphs shows the total number of B cells (CD19⁺) in the spleen after the last injection. * denotes $p < 0.05$ using a Student's *t* test.

Figure S7, refers to Figure 5. miR-212/132 targets Sox4 in B cells. (A) Sox4 protein expression by Western Blot in whole bone marrow lysate from MG and miR-132 mice. (B) Sox4 protein expression by Western Blot in 70Z/3 cells transduced with a control vector (MG) or a miR-132 over-expression vector (miR-132). (C) Transcript expression levels of PU.1, Ikzf1, Ebf1, E2A, Pax5, and Rag1 obtained by RT-qPCR from B cells purified from the bone marrow of MG and miR-132 mice. Data represents two independent experiments and is represented as mean \pm SEM.

Supplemental Tables

Table S1: sequences for SOX4 shRNA constructs.

SOX4 shRNA sequence (in miR-155-arms-and-loop-format)	
mmu-FOXO3 shRNA #1	gaaggctgtaTGCTGTTGAGCAGCTTCCAGCGTTTGGTTTTGGCCACTGACTGACCAAACGCTAAGCTGCTCAAc ggacacaaggcctg
mmu-FOXO3 shRNA #2	gaaggctgtaTGCTGTTCACTTTCTTGTCGGCAGGGGTTTTGGCCACTGACTGACCCCTGCCGAAGAAAGTGAAc ggacacaaggcctg
mmu-FOXO3 shRNA #3	gaaggctgtaTGCTGTTTAGAAGCTTGCTTGCTTGGCTTGTGGTTTTGGCCACTGACTGACAAGCCAAGAAGCTTCTAAc ggacacaaggcctg

Table S2: primer sequences used for qPCR.**Primer sequences**

SOX4 F	GACAGCGACAAGATTCCGTTTC
SOX4 R	GTTGCCCGACTTCACCTTC
EBF1 F	GCATCCAACGGAGTGGAAAG
EBF1 R	GATTTCCGCAGGTTAGAAGGC
E2A F	GGGTGCCAGCGAGATCAAG
E2A R	ATGAGCAGTTTGGTCTGCGG
PAX5 F	CCATCAGGACAGGACATGGAG
PAX5 R	GGCAAGTTCCACTATCCTTTGG
PU.1 F	ATGTTACAGGCGTGCAAAATGG
PU.1 R	TGATCGCTATGGCTTTCTCCA
IL-7R F	GCGGACGATCACTCCTTCTG
IL-7R R	AGCCCCACATATTTGAAATTCCA
Rag1 F	ACCCGATGAAATTCAACACCC
Rag1 R	CTGGA ACTACTGGAGACTGTTCT
Ikzf1 F	ATGTCCCAAGTTTCAGGAAAGG
Ikzf1 R	GCACGCCCATCTCTTCATC

Figures

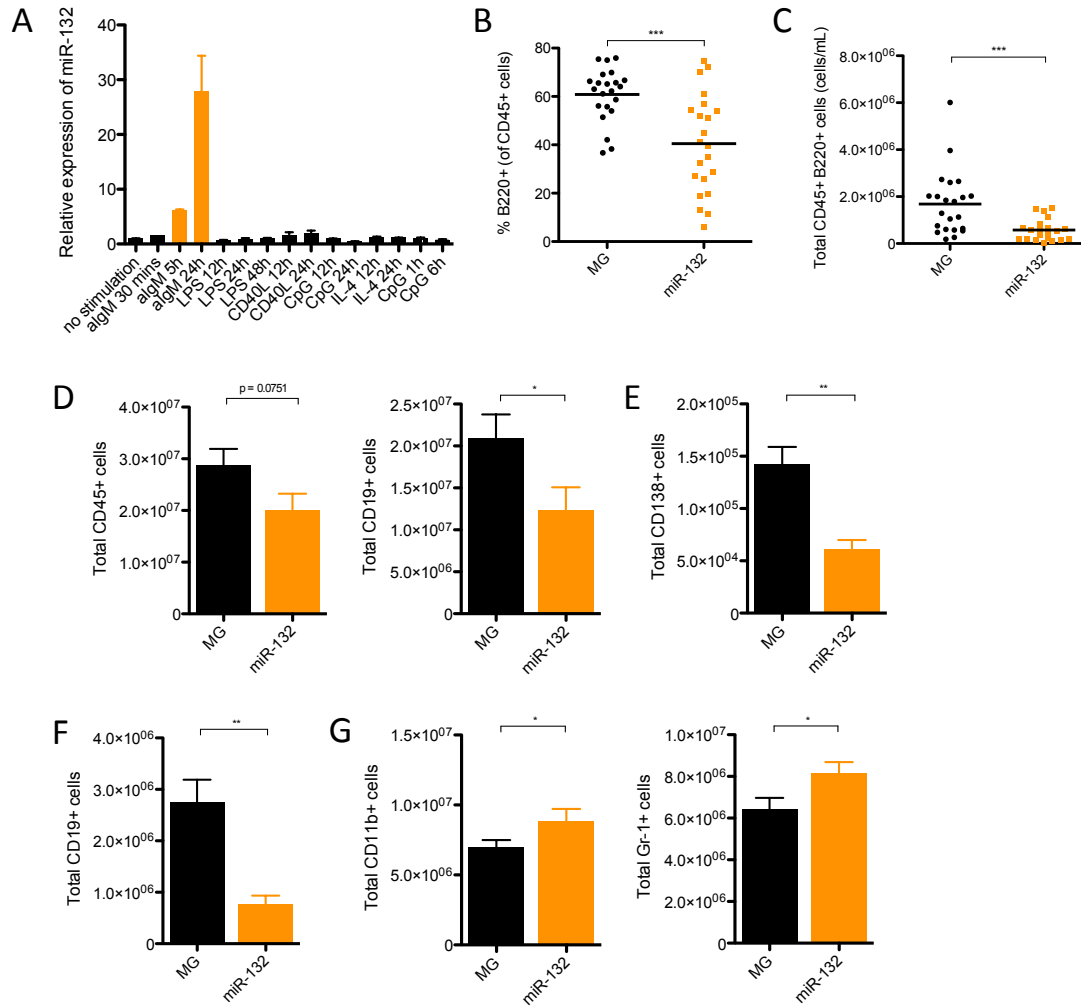


Figure 1. miR-132 is induced in B cells and over-expression of miR-132 in mice alters B-cell development.

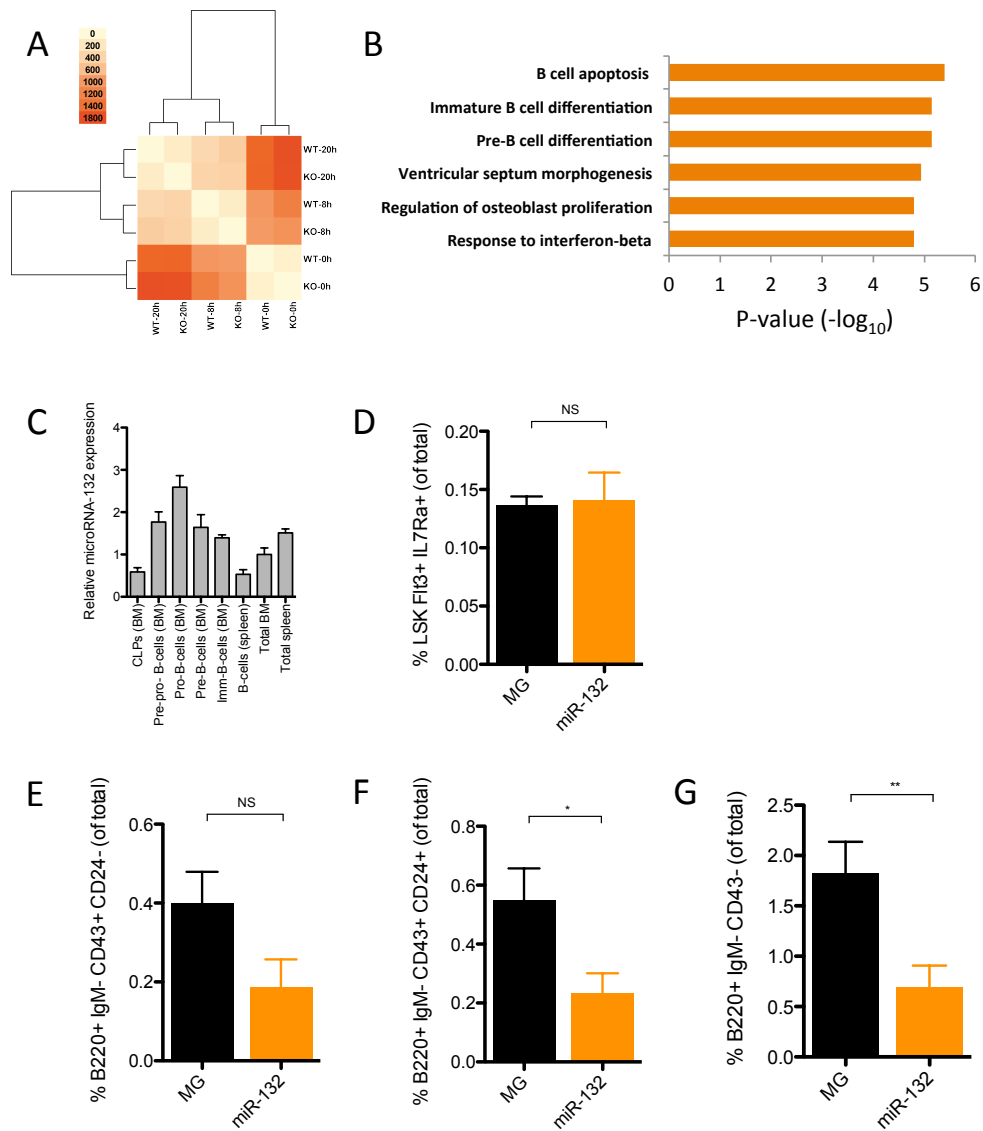


Figure 2. miR-132 causes a block in early B cell development.

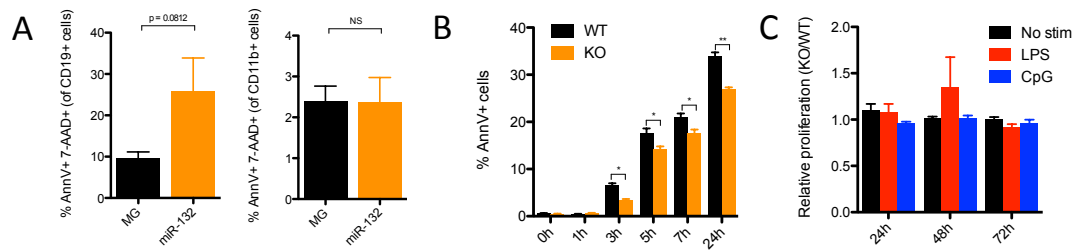


Figure 3. miR-212/132 regulates B cell apoptosis.

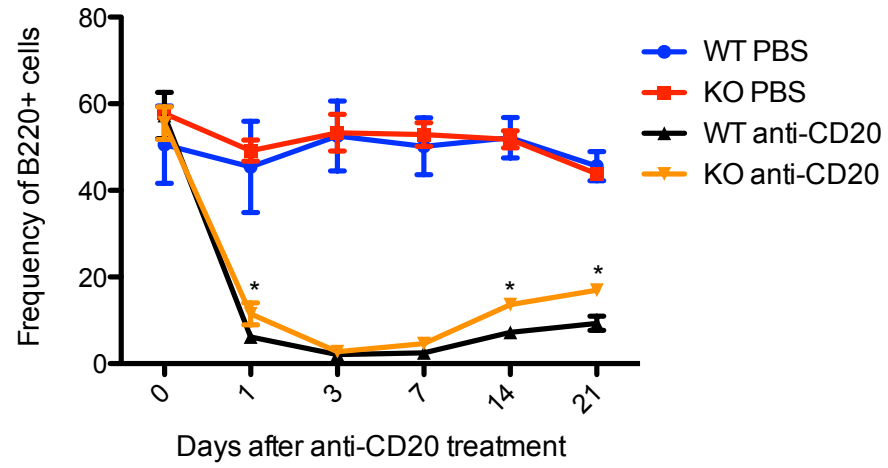


Figure 4. Loss of miR-212/132 alters B cell development under non-homeostatic conditions.

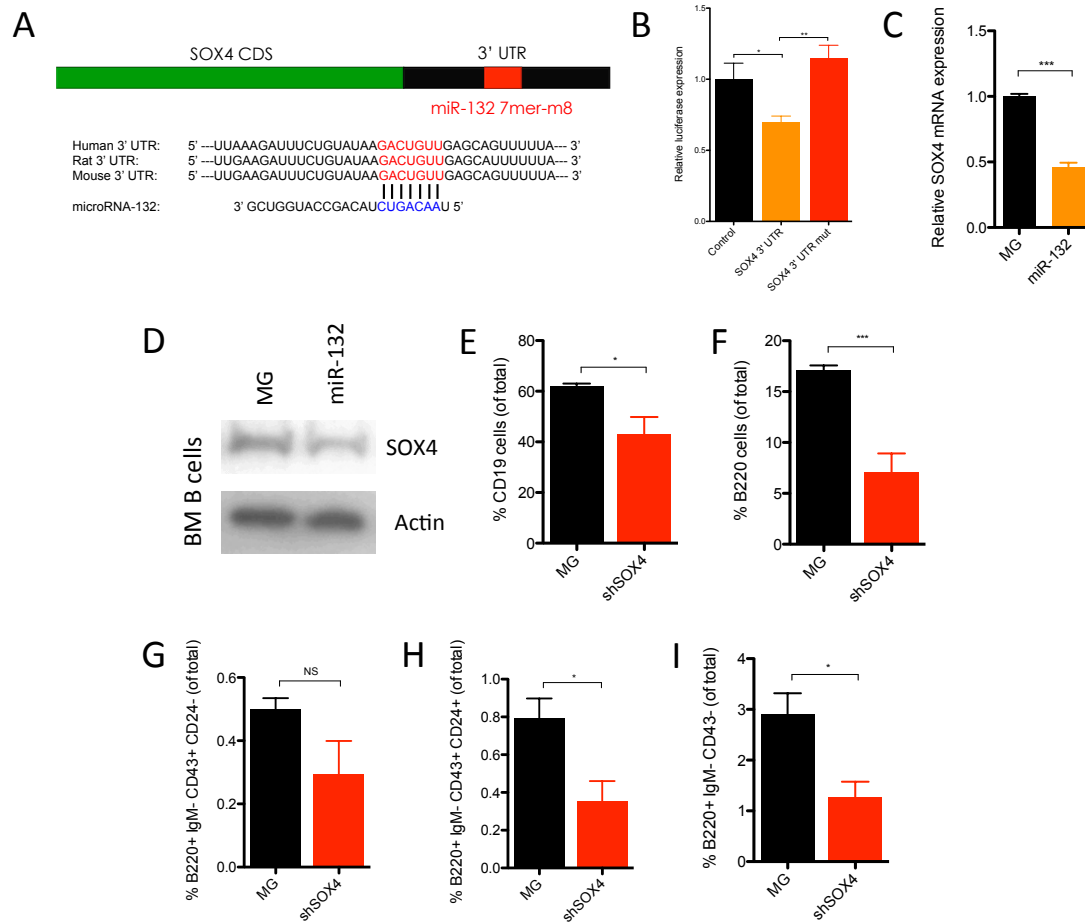


Figure 5. SOX4 is a direct target of miR-132 and is a key regulator of B cell development.

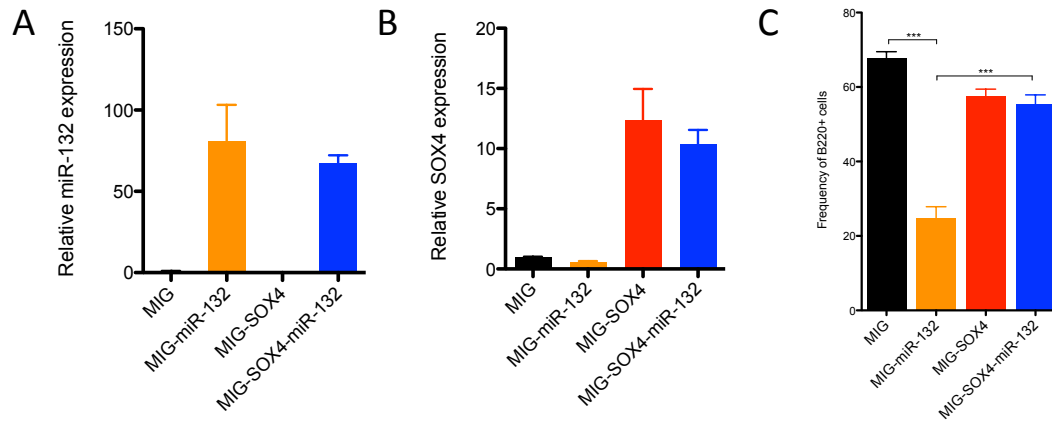


Figure 6. Co-expression of SOX4 rescues the defect in B cell development with expression of miR-132 alone.

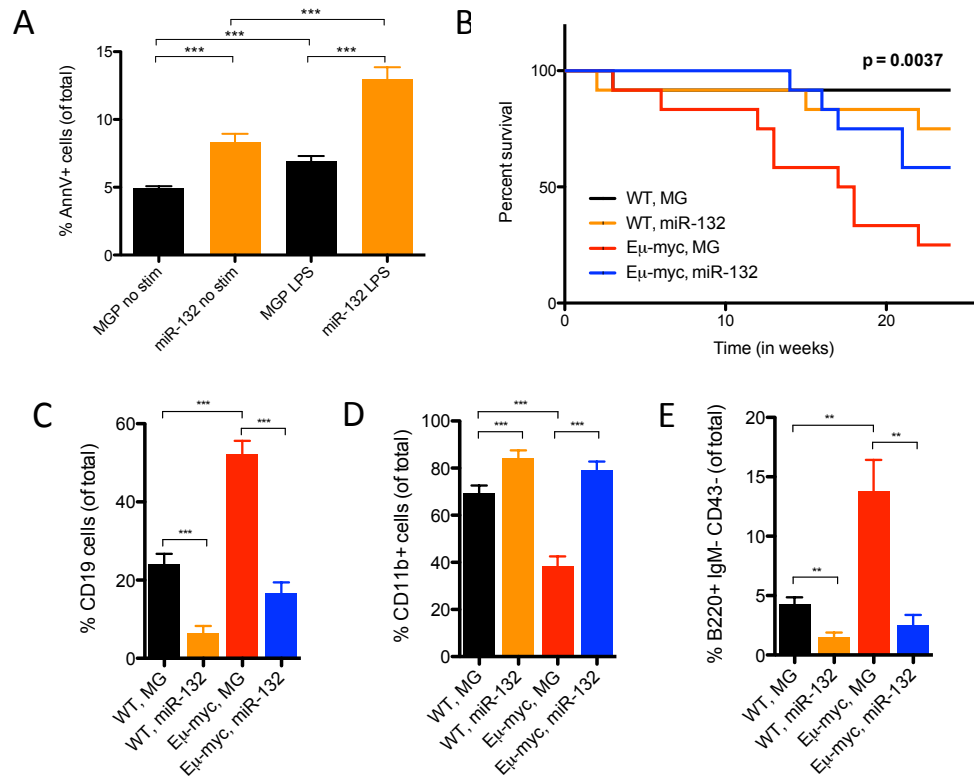


Figure 7. Enforced expression of miR-132 inhibits the development of spontaneous B cell cancers in cells with the Eμ-myc transgene.

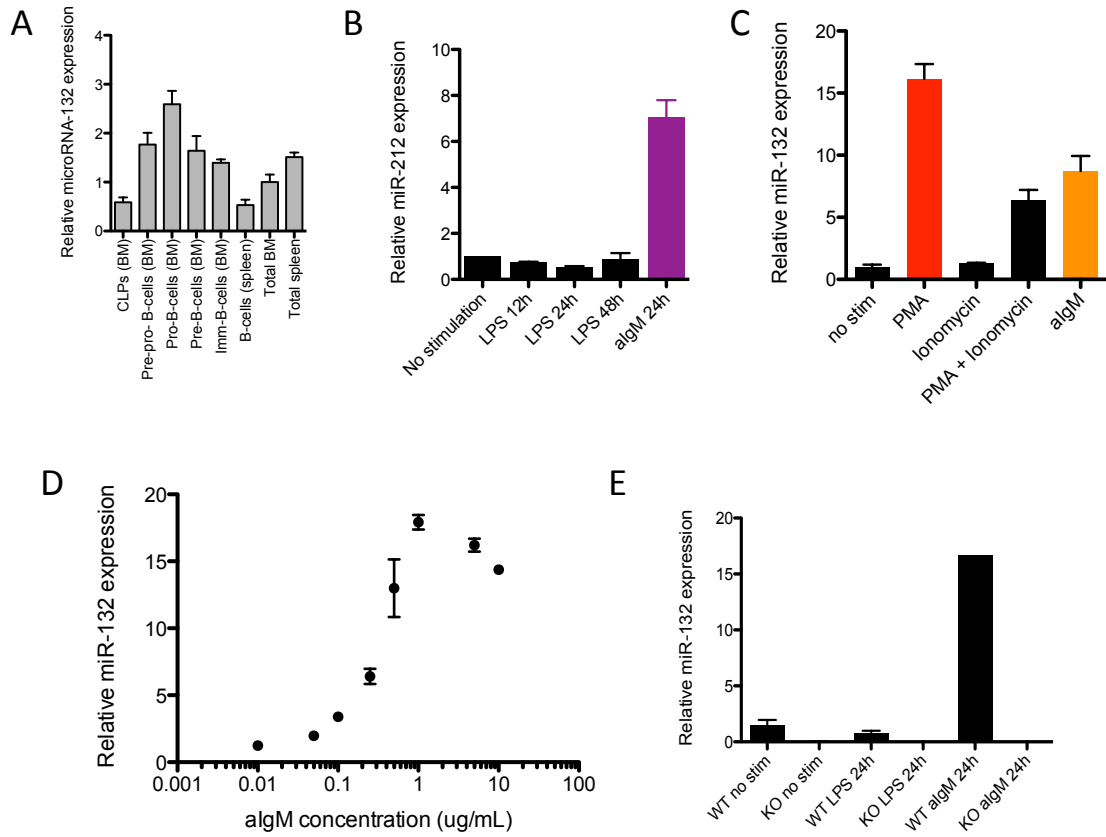


Figure S1. miR-212/132 is induced in B cells by activation of the B cell receptor (BCR).

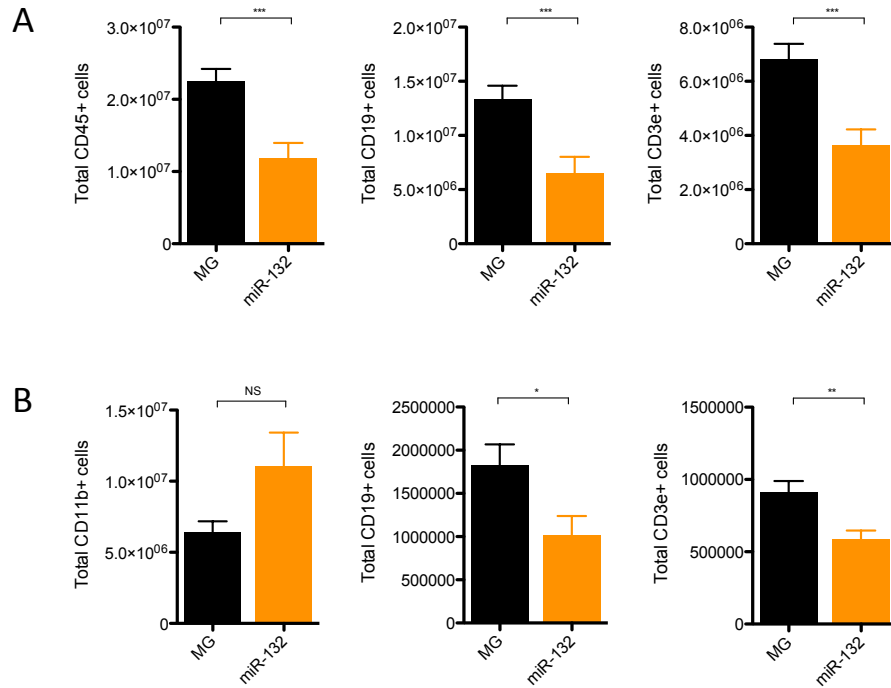


Figure S2. Enforced expression of miR-132 alters B cell output in mice up to 9 months post-reconstitution.

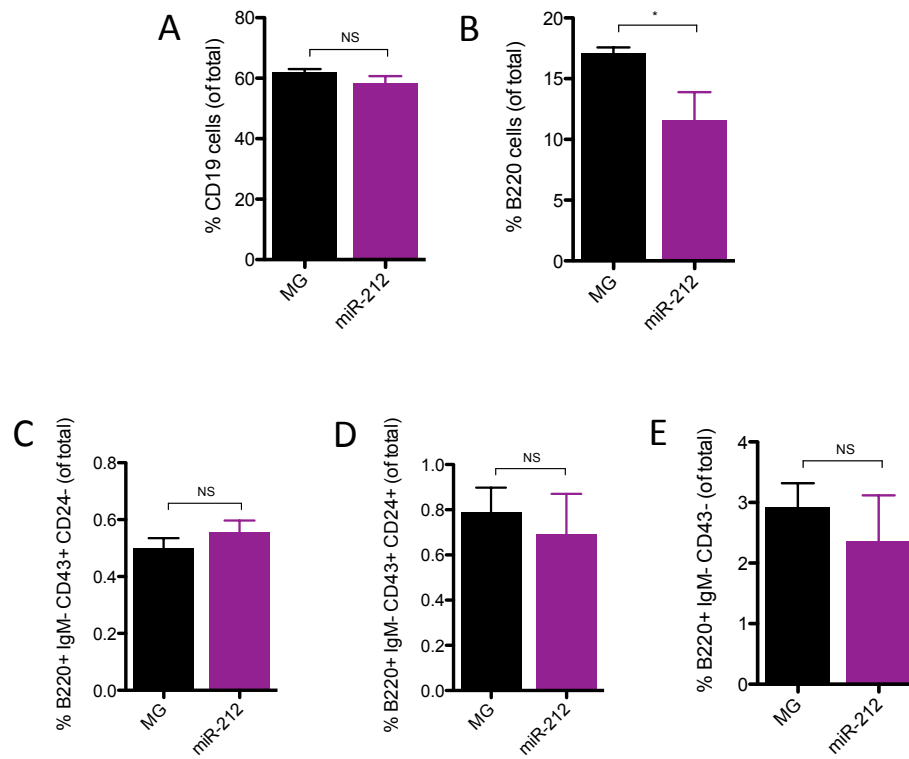


Figure S3. Enforced expression of miR-212 has a marginal effect on B cell output.

A

Number of genes	WT unstim	WT anti-IgM 8h	WT anti-IgM 20h	KO unstim	KO anti-IgM 8h	KO anti-IgM 20h
WT unstim	0	326	491	63	330	472
WT anti-IgM 8h	717	0	121	823	70	117
WT anti-IgM 20h	1036	227	0	1136	300	59
KO unstim	54	448	695	0	378	653
KO anti-IgM 8h	666	83	163	707	0	123
KO anti-IgM 20h	1060	279	88	1124	293	0

B

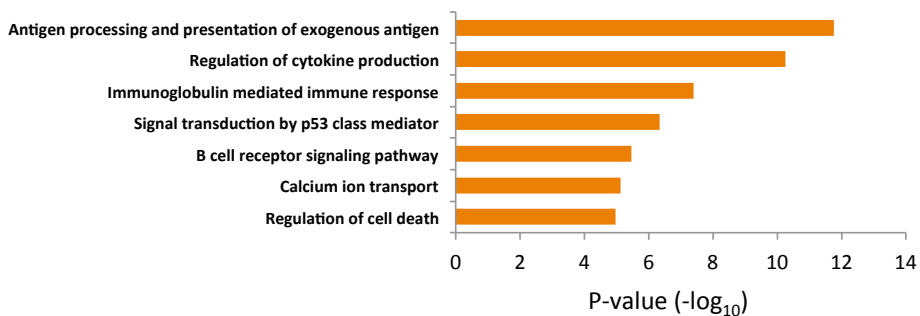


Figure S4. Stimulation of B cells through the B cell receptor (BCR) results in dramatic gene expression changes.

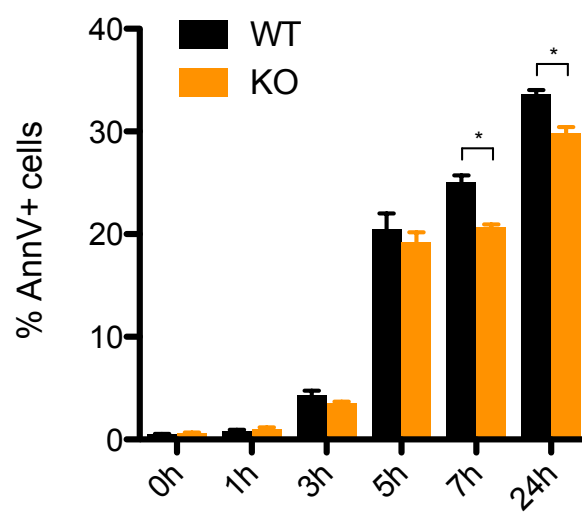


Figure S5. miR-212/132 regulates B cell apoptosis.

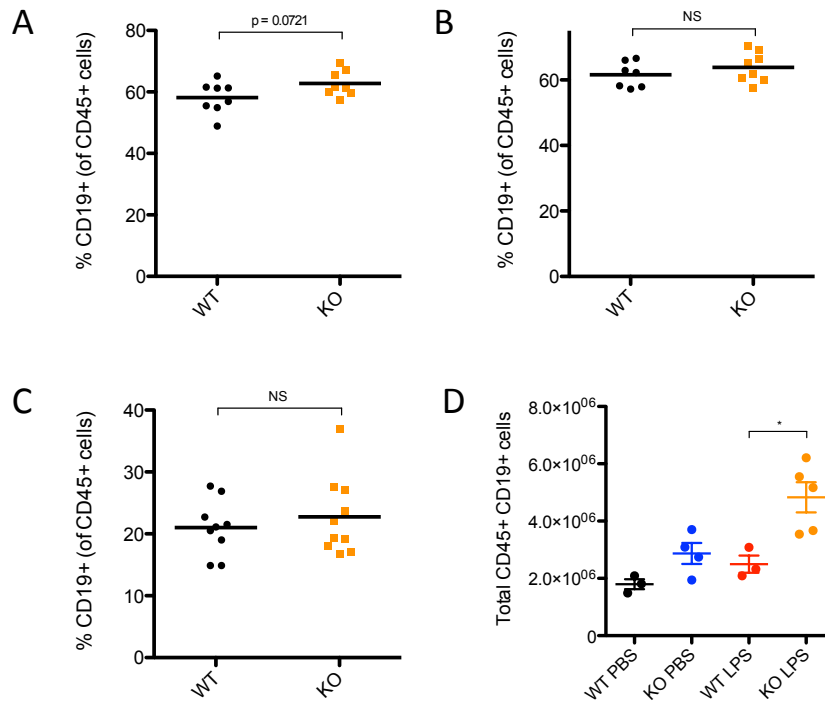


Figure S6. miR-212/132^{-/-} mice demonstrate no observable defect in B cell output under steady state conditions.

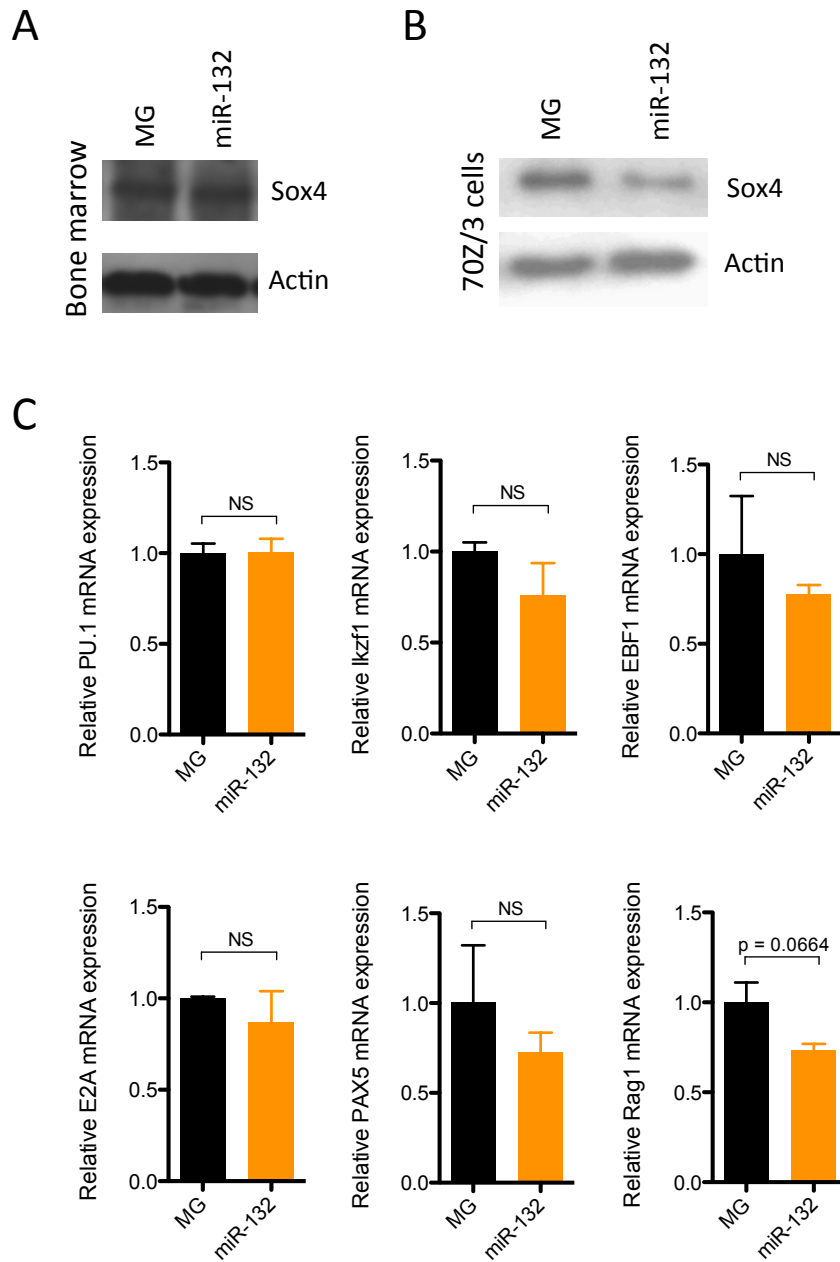


Figure S7. miR-212/132 targets SOX4 in B cells.

Chapter 4: microRNA-125b regulates hematopoiesis by targeting Lin28A

Published as: AA Chaudhuri, AYL So, A Mehta, A Minisandaram, N Sinha, VD Jonsson, DS Rao, RM O'Connell, D Baltimore (2012). Oncomir miR-125b regulates hematopoiesis by targeting Lin28A. *Proceedings of the National Academy of Sciences*. **109**(11), 4233-4238.

Abstract

MicroRNA-125b is upregulated in patients with leukemia. Overexpression of miR-125b alone in mice causes a very aggressive, transplantable myeloid leukemia. Prior to leukemia, these mice do not display elevation of white blood cells in the spleen or bone marrow; rather, the hematopoietic compartment shows lineage-skewing with myeloid cell numbers dramatically increased and B cell numbers severely diminished. MiR-125b exerts this effect by upregulating the number of common myeloid progenitors while inhibiting development of pre-B cells. We applied a miR-125b 'sponge' loss-of-function system in vivo to show that miR-125b physiologically regulates hematopoietic development. Investigating the mechanism by which miR-125b regulates hematopoiesis, we found that among a panel of candidate targets, the mRNA for Lin28A, an induced pluripotent stem cell (iPSC) gene, was most repressed by miR-125b in mouse hematopoietic stem and progenitor cells. Overexpressing Lin28A in the mouse hematopoietic system mimicked the phenotype observed upon inhibiting miR-125b function, leading to a decrease in hematopoietic development. Relevant to the miR-125b overexpression phenotype, we also found that knockdown of Lin28A led to hematopoietic lineage-skewing, with increased myeloid and decreased B cell numbers. Thus, the miR-125b target Lin28A is an important regulator of hematopoiesis and a primary target of miR-125b in the hematopoietic system.

Introduction

Lin28A is an important regulator in early embryogenesis in mice and humans (Viswanathan and Daley, 2010). The levels of Lin28A are enriched in embryonic stem (ES) cells and decrease as these cells differentiate (Viswanathan and Daley, 2010). Ectopic expression of Lin28A along with three other genes (Oct4, Sox2, and Nanog) causes de-differentiation of mature human cells into induced pluripotent stem (IPS) cells (Yu et al., 2007). This demonstrates the power of Lin28A to endow cells with pluripotent qualities. Still, it remains to be seen whether Lin28A also plays developmental roles in biological systems arising from adult stem cells, such as hematopoiesis.

In this study, we examine the role of miR-125b in inducing cancer and show that overexpression of this microRNA induces a pre-leukemic state before the aggressive frank leukemia is evident. This pre-leukemic state is characterized by overproduction of myeloid cells and their precursors as well as inhibition of B cell development. We then show that the most affected target gene of miR-125b is Lin28A and that Lin28A downregulation can mimic the pre-leukemic state induced by miR-125b. Furthermore, downregulation of miR-125b has profound effects on normal hematopoiesis and Lin28A overexpression mimics those effects.

Results

MiR-125b ectopic expression favors myeloid differentiation and causes a highly invasive myeloid leukemia

Previously, we showed that over-expression of miR-125b in bone marrow transplanted

recipient mice causes a myeloid leukemia 4-6 months after bone marrow reconstitution (O'Connell et al., 2010). Here, we found that the neoplastic myeloid cells infiltrate non-hematopoietic organs, including the brain, and overwhelm the periphery (Fig 1, Fig S1). Also, mice over-expressing miR-125a developed an aggressive leukemia, as demonstrated by enlarged spleen and infiltration into the liver and kidneys (Fig S2). These mice died by six months post-reconstitution. Thus, dysregulated expression of miR-125b or its paralogue leads to an aggressive leukemia that efficiently invades non- hematopoietic organs.

To understand the initial events that precede the frank leukemia, we examined the spleen and bone marrow at seven weeks after reconstitution, a time well before the onset of cancer, as indicated by similar white blood cell counts in the spleen and bone marrow of MG and MG-125b animals (Fig 2A, Fig S3, Fig S4A-B). At this time, MG- 125b animals showed dramatic increases in all myeloid lineages, including granulocytes, macrophages, and dendritic cells with T cell numbers being similar to those in the MG mice (Fig 2A, S4C-E). However, B cell numbers were significantly decreased in these miR-125b over-expressing animals (Fig 2A, S4F). Whether miR- 125b physiologically regulates B cell development will require further studies. Thus, miR-125b over-expression at the pre-cancerous stage causes a lineage-skewing of the hematopoietic compartment with myeloid cell numbers elevated and B cells diminished.

To investigate the developmental stage at which miR-125b over-expression promotes myelopoiesis and compromises B cell development, we analyzed hematopoietic stem and progenitor cell (HSPC) numbers in the bone marrow at 7 weeks following bone marrow transplantation. In these mice, the numbers of hematopoietic stem cell (HSC) numbers

were similar in MG-125b animals compared to MG controls (Fig S4G, H). Progenitors directly downstream of HSCs, however, including multipotent progenitors (MPPs), common myeloid progenitors and granulocyte macrophage progenitors (CMP/GMPs), myeloid-erythroid progenitors (MEPs), and common lymphoid progenitors (CLPs), were all significantly increased however (Fig 2B). Of these, CMP/GMPs were the most drastically augmented, being up 8.4-fold in MG-125b animals compared to controls (Fig 2B). Notably, pre-B cell numbers were severely decreased (Fig 2B), providing a developmental basis for the decreased B cell numbers we observed in MG-125b animals. This also indicates that miR-125b overexpression causes a developmental block between the CLP and pre-B cell stages. In summary, we show here that prior to the onset of leukemic disease, miR-125b skews hematopoietic differentiation towards the myeloid lineage, likely by increasing CMP/GMP and blocking B cell development.

Physiological regulation of hematopoiesis by miR-125b

While over-expression studies are relevant to the role of miR-125b as an oncomiR, we developed a loss-of-function system to assess the potential physiological role of miR-125b in hematopoiesis. We generated a ‘sponge’ decoy to competitively inhibit miR-125b binding to its natural targets (Fig 5SA) (Ebert et al., 2007; Ebert and Sharp, 2010; Starczynowski et al., 2010; Wang et al., 2011). Of note is that the ‘sponge’ does not decrease miR-125b expression but rather serves as a decoy to compete miR-125b away from endogenous targets. Indeed, the sponge decoy (MG-sponge) was capable of significantly de-repressing a luciferase reporter vector containing an artificial 3’ UTR with two perfect miR-125b complementary sequences (Fig S5B). Demonstrating the

effectiveness of this approach, a UTR-less reporter vector was not de-repressed by the sponge (Fig S5C). To determine the hematopoietic effect of miR-125b loss-of- function, recipient mice were reconstituted with equal numbers of sorted GFP⁺ MG and MG-sponge transduced bone marrow cells (Fig S5D). The MG-sponge mice at one month post-reconstitution had significantly fewer white blood cells (CD45⁺), myeloid cells (CD45⁺ CD11b⁺), pre-erythrocytes (CD45⁺ Ter119⁺), and granulocytes (CD45⁺ Gr1⁺) and compared to the MG controls (Fig 3). The blood was also noticeably thinner in the sponge mice compared to controls, indicating that mature erythrocytes were decreased as well. The sponge data indicates an important physiological role for miR- 125b in hematopoietic development, while the overexpression data shows that excess levels lead to cancer.

Lin28A is a primary target of miR-125b in the hematopoietic system

To identify miR-125b targets that might regulate hematopoietic development, we performed a nonbiased screen using Targetscan (Friedman et al., 2009; Grimson et al., 2007; Lewis et al., 2005) to isolate putative miR-125b targets with P_{Conserved Targeting} > 0.8 (P < 0.2 that the putative microRNA site is evolutionarily maintained due to selective microRNA targeting rather than chance) (Friedman et al., 2009). Application of this screen yielded 192 genes. Gene ontology analyses indicate that these genes are functionally enriched for biological processes that include transcriptional regulation, vasculature development, proteolysis, and apoptosis (David Functional Annotation Bioinformatics, P < 0.05). We focused on those that were pro- apoptotic or involved with stem cell regulation as these processes have been correlated with leukemic development. This yielded four

candidate genes, Bak1, Trp53inp1, BMF and Lin28A, which independently have been previously validated as miR-125b targets by other groups (Enomoto et al., 2011; Shi et al., 2007; Wu and Belasco, 2005; Xia et al., 2009). We examined and confirmed by qPCR that miR-125b represses these genes, including Lin28A, in 5-FU treated bone marrow hematopoietic cells enriched for HSPCs (Fig 4A). As evidence of these genes being miR-125b direct targets, we found that the 3' UTR luciferase reporter of all of these genes, but not the negative control Picalm, were significantly repressed by miR-125b over-expression (Fig 4B). Notably, endogenous expression of Lin28A, Trp53inp1, and BMF were de-repressed by the miR-125b sponge decoy in HSPC-enriched bone marrow (Fig S6A). The miR-125b sponge decoy also de-repressed 5-fold a luciferase reporter containing the mouse Lin28A 3' UTR (Fig 4C), which contains a 9 nucleotide miR-125b seed sequence (Fig S6B). Demonstrating that the miR-125b:Lin28A interaction exhibits species conservation between mouse and human hematopoietic cells, human myeloid K562 cells transduced with either MGP, MGP-125b-1, MGP-125b-2, or a seed mutant of miR-125b exhibited seed-dependent repression of Lin28A by both miR-125b species at both the RNA and protein level (Fig 4D, Fig S6C-E). Of note, the expression of Lin28B isoform was not repressed by miR-125b (Fig S6F, G). In summary, miR-125b directly represses Lin28A in hematopoietic cells, an interaction conserved between mouse and human. Previously, up-regulation of Lin28A and Lin28B has been associated with cancer development. Thus, we examined the expression of these genes in leukemic samples over-expressing miR-125b but found that Lin28A and Lin28B expression was similar in the cancer samples and control cells (Fig S7).

Lin28A regulates aspects of hematopoiesis that mirror those controlled by miR-125b

The regulation of Lin28A by miR-125b is highly conserved across species. The *C. elegans* homologue of miR-125b Lin-4 also represses the RNA-binding protein Lin28A. The Lin-4:Lin28A cascade has been shown to be critical for proper worm development. However, a potential critical developmental function of miR-125b:Lin28A signaling in mammals has not yet been explored. In addition, Lin28A is known to be involved in maintaining pluripotency of embryonic stem cells, but its role in other biological events, such as hematopoiesis, has not been fully characterized. Thus, we were interested in determining whether miR-125b-mediated repression of Lin28A has a role in the hematopoietic system. We bypassed the repressive effect exerted by endogenous miR-125b by over-expressing Lin28A lacking its 3'UTR. We utilized the MSCV-IRES-GFP (MIG) vector system (Bousquet et al., 2008), which allowed the co-expression of Lin28A and GFP from the same vector. A Western blot was performed to confirm expression of Lin28A from the MIG-Lin28A vector in transfected 293T cells (Fig S8A). Next we performed bone marrow transplant experiments with HSPC-enriched bone marrow cells transduced with either MIG or MIG-Lin28A. We achieved over 80% transduction efficiency as measure by GFP-positive cells (Fig S8B). Similar to mice reconstituted with the miR-125b sponge decoy (Fig 3), animals with Lin28A over-expression had significant decreases in total white blood cells ($CD45^+$), total myeloid cells ($CD45^+ CD11b^+$), granulocytes ($CD45^+ Gr1^+$), and erythrocytes ($Ter119^+ CD11b^-$) (Fig 5A-D). Also similar to the sponge mice, the blood was noticeably thinner from MIG-Lin28A animals compared to MIG controls, likely due to

the diminished erythrocyte numbers we observed. Of importance, whereas all the controls remained healthy, the Lin28A over-expressing mice with the thinnest blood (2 out of 15) died at five weeks post-reconstitution, likely as a consequence of impaired hematopoietic development. Thus, over-expressing Lin28A in the hematopoietic system mirrored the phenotypes observed upon miR-125b inhibition (Fig 3).

Next, we used Lin28A loss-of-function studies to examine whether Lin28A physiologically regulates hematopoiesis. Also, loss-of-function assays allowed us to determine whether inhibiting Lin28A function would mimic specific aspects of hematopoietic development observed upon over-expressing miR-125b. Thus we transduced HSPC-enriched bone marrow with Lin28A shRNA and achieved ~70% transduction with a 2-fold knockdown of Lin28A as assessed by qPCR (Fig 6A-B), less than the level of repression exerted by miR-125b over-expression (Fig 4A). Strikingly, mice reconstituted with shLin28A exhibited similar but less dramatic features of hematopoietic development to those caused by over-expression of miR-125b at the pre-cancerous stage: expansion of myeloid cells ($CD45^+ CD11b^+$, $CD45^+ Gr1^+$) and a decrease of B cells ($CD19^+ CD11b^-$) (Fig 6C-E). The Lin28A knockdown mimicked the alteration of the hematopoietic system that we observed in miR-125b over-expressers (Fig 2A), namely increased myeloid cells and decreased B cells (Fig 6C-E). Thus, we show that Lin28A is a primary target of miR-125b in hematopoiesis and that its levels influence development of the hematopoietic system.

Discussion

We demonstrate here that 1) miR-125b over-expression causes a highly invasive myeloid

leukemia; 2) in the pre-leukemic stage of disease, miR-125b induces a skewing of the hematopoietic system favoring myeloid development; 3) before terminal leukemia development, miR-125b drastically increases CMP/GMP numbers; 4) In addition to the pathological role of miR-125b, it also physiologically regulates hematopoiesis as shown by downregulating it with a 'sponge' construct; 5) Lin28A is a bona fide primary target of miR-125b in hematopoietic cells; and 6) Lin28A over-expression and knockdown mimic important aspects of miR-125b loss-of-function and gain-of-function, respectively. We conclude that miR-125b physiologically regulates hematopoiesis, and that constitutive over-expression of miR-125b in our experimental system leads to uncontrolled generation of myeloid progenitors and mature myeloid cells that subsequently causes a myeloid leukemia. We also conclude that the miR-125b primary target Lin28A is an important regulator of hematopoietic development.

In this study, we observed that miR-125b over-expression induces an aggressive myeloid leukemia that is highly invasive. Of note, two mice out of the fourteen analyzed in two cohorts exhibited significantly increased lymphoid cells as well, supporting studies by Bousquet et al., Ooi et al., and Enomoto et al. that miR-125b is capable of causing leukemias involving lymphoid cell types (Bousquet et al., 2010; Enomoto et al., 2011; Ooi et al., 2010). Interestingly, Enomoto et al. confirms the remarkable potency of miR-125b as an oncomiR by showing that B-cell restricted ectopic expression of miR-125b can drive lymphoid leukemia (Enomoto et al., 2011). In our system, miR-125b and GFP is expressed from the same transcript. Interestingly, the GFP intensity in the CD11b⁺ myeloid cells of

the MG-125b mice was much higher than that of CD19⁺ B cells (geometric mean fluorescence of 85.2±7.3 versus 15.7±0.8, respectively), suggesting that miR-125b is expressed more highly in the former lineages. This might explain the predominance of myeloid leukemia observed in our system. Of importance, miR-125b has been found to be over-expressed in a variety of human leukemias, including AML (Bousquet et al., 2010; Enomoto et al., 2011), CML (Enomoto et al., 2011), AmkL (Gefen et al., 2010), and ALL (Enomoto et al., 2011; Gefen et al., 2010), suggesting that deregulated miR-125b expression in different contexts can lead to distinct types of cancer.

Interestingly, Ooi et al. showed that recipient mice reconstituted with miR-125b over-expression display elevated HSC numbers (Ooi et al., 2010). Although we did not observe an increase in HSC number, our study does not exclude that miR-125b regulates HSC development; the discrepancy likely reflects differences in experimental models used between the two studies. Ooi et al. overexpressed miR-125b in purified HSCs using a lentiviral system, whereas we ectopically expressed the microRNAs in unsorted progenitor-enriched bone marrow hematopoietic cells using a retroviral system. It is possible that our retroviral system may not adequately over-express miR-125b in HSCs to observe a phenotype in these cells. Nonetheless, we show here that miR-125b over-expression is capable of inducing an aggressive myeloid leukemia and increases levels of MPP, CMP/GMP, MEP, and CLPs independent of HSC numbers. In the future, it will be interesting to investigate whether miR-125b overexpression drives tumorigenesis in myeloid progenitors and/or the mature myeloid cells.

We show here that miR-125b is an important regulator of hematopoiesis both physiologically and pathologically. Searching for a mechanism by which miR-125b exerts its effects on the hematopoietic system, we found that miR-125b's direct target Lin28A is also a regulator of hematopoiesis. The miR-125b seed sequence within 3'UTR of Lin28A has been previously identified and shown to be functionally important for miR-125b repression (Wu and Belasco, 2005). In our study, manipulating Lin28A expression levels in mice mimicked the hematopoietic phenotypes of those with modulated miR-125b levels. Of note, shRNA-mediated knockdown of Lin28A was less effective than miR-125b mediated knockdown, indicating that a better specific knockdown of Lin28A might more precisely mimic the miR-125b overexpression phenotype. Although we demonstrate Lin28A as a miR-125b target important for hematopoiesis, we do not exclude that other miR-125b targets might play a role as well. Indeed, Le et al. have recently demonstrated that miR-125b regulates a panel of genes in the p53 pathway (Le et al., 2011). Potentially, Lin28A knockdown by miR-125b may help setting the stage for myeloid leukemia. We did not, however, observe obvious signs of leukemia in the shLin28A mice after three months following bone marrow transplantation, suggesting that either cancer will occur later or that repression of other targets such as the pro-apoptotic genes Bak1, Trp53inp1, and BMF, may collaborate with Lin28A inhibition during miR-125b mediated cancer.

In summary, this work links two molecules shown in different contexts to be important in development, miR-125b and Lin28A, and indicates that their interaction serves as a fundamental regulator of hematopoietic physiology and pathology. Indeed, the interplay between miR-125b and Lin28A is one that might be toggled therapeutically to ameliorate

hematopoietic disorders such as leukemia and bone marrow failure.

Experimental Procedures

Cell Culture. 293T cells were cultured in complete DMEM with 10% FBS, 100 units/ml penicillin, and 100 units/ml streptomycin. K562 cells and splenocytes from mice were cultured in complete RPMI with 10% FBS, 100 units/ml penicillin, 100 units/ml streptomycin and 50 μ M 2-Mercaptoethanol.

DNA Constructs. The retroviral vectors MG, MGP, MGP-125b-1 and MGP-125b-2 have been described previously (O'Connell et al., 2009; O'Connell et al., 2010; O'Connell et al., 2008; Rao et al., 2010). Both Lin28A shRNA and MGP-125b-Mutant were cloned using a miR-155 arms-and-loop format, which has been previously described (O'Connell et al., 2009; O'Connell et al., 2010; O'Connell et al., 2008; Rao et al., 2010). The Lin28A shRNA sequence was predicted using the Invitrogen BlockiT RNAi Designer. The 3' UTRs for mouse Lin28A, Trp53inp1, Bak1, and BMF as well as the antisense 2mer were cloned downstream of luciferase in the pMIR-REPORT vector (Ambion). For the Lin28A overexpression vector, the mouse Lin28A coding sequence (Open Biosystems) was cloned downstream of the LTR and preceding the IRES-GFP of the MSCV Ires GFP (MIG) vector (Cherry et al., 2000). All primers are listed in Table S1.

Retroviral Transduction and Bone Marrow Reconstitution Experiments. C57Bl/6 mice were bred and housed in the Caltech Office of Laboratory Animal Resources (OLAR) facility. The Caltech Institutional Animal Care and Use Committee (IACUC) approved all experiments related to mice. Virus production and reconstitution experiments were

performed as previously described (O'Connell et al., 2009; O'Connell et al., 2010; O'Connell et al., 2008; Rao et al., 2010). K562 cells were transduced with VSV-G pseudotyped MGP, MGP-125b-1, MGP-125b-2, and MGP-125b- Mut as described previously (O'Connell et al., 2010).

Cell Counting and Flow Cytometry. Cells were counted using a Coulter Counter (Beckman Coulter) or a MACSQuant flow cytometer (Miltenyi Biosciences). Absolute cell counts in the blood were obtained by FACS-staining equivalent volumes of blood, resuspending the stained samples in equivalent volumes of FACS buffer, and running equal volumes of each sample using the MACSQuant. For flow cytometry, cells were harvested, homogenized, and red blood cells were lysed. Cells were stained with the following fluorophore-conjugated antibodies that were purchased from Biolegend, Ebioscience, or BD Pharmingen and assayed using MACSQuant (Miltenyi Biosciences) or a FACSCalibur (Becton Dickinson). All data was analyzed with FlowJo software (Treestar). Specific gating strategies are available upon request.

Cell Sorting for Sponge Reconstitution. 5-FU enriched bone marrow was transduced with retroviral vectors as previously described (O'Connell et al., 2009; O'Connell et al., 2010; O'Connell et al., 2008; Rao et al., 2010). Prior to IV injection into mice, GFP-positive MG, and MG-Sponge transduced samples were sorted using an iCyt cell sorter. Equal numbers of cells were then injected into lethally irradiated recipient animals.

Target Analysis. Predicted miR-125b targets in H. Sapien were downloaded from Targetscan and rank-ordered by their Probability of Conserved Targeting (PCT) scores.

Repeated target genes were removed from this list using a PERL script (available upon request). Literature search was performed on the resulting list in order to identify candidate target genes. For one target, Lin28A, the 3' UTR for the mouse version of the gene was obtained and aligned with miR-125b using TargetScan.

Luciferase Reporter Assays. Reporter assays to measure microRNA-based repression of target 3' UTRs were performed as previously described (O'Connell et al., 2009; O'Connell et al., 2010; O'Connell et al., 2008). For de-repression assays with the sponge construct, we added MG (empty vector) or MG- Sponge to the transfection mix. After 24 hours, cells were lysed with Passive Lysis Buffer (Promega) and luciferase assays were performed as previously described (O'Connell et al., 2009; O'Connell et al., 2010; O'Connell et al., 2008).

RNA Preparation and Quantitation. RNA was isolated with TRIzol (Invitrogen) as per the manufacturer's instructions. We performed SYBR Green (Quanta Biosciences) based quantitative real-time PCR (qPCR) with a 7300 Real-Time PCR machine (Applied Biosystems) to assay mRNA levels. A Taqman approach was used to quantify miR- 125b and snoRNA-202 expression (Applied Biosystems). All mRNA levels were normalized to L32 whereas microRNA-125b levels were normalized to snoRNA-202. Sequence specific primers are listed in Table S1.

Immunoblotting. Total cell extracts were fractionated by electrophoresis on a 12% SDS polyacrylamide gel and electroblotted onto a Trans-Blot nitrocellulose membrane with a semidry transfer apparatus. Protein detection was performed using the following

antibodies: Lin28A (A177) (Cell Signaling), β -Actin (A1978) (Sigma), anti-rabbit HRP- conjugated secondary antibody (Santa Cruz Biotechnology), and anti-mouse HRP- conjugated secondary antibody (Santa Cruz Biotechnology).

Statistical Tests. Statistical tests were performed using Graphpad PRISM software or Microsoft Excel. The two-tailed student's T test was used to determine P values.

Figure Legends

Figure 1: MiR-125b over-expression causes an aggressive invasive myeloid leukemia. A)

Infiltration of GFP⁺ CD45⁺ and GFP⁺ CD11b⁺ cells into the brain. (Top) Representative flow cytometric plots are shown. (Bottom) Average percent GFP⁺ CD45⁺ and GFP⁺ CD11b⁺ in the brain are shown from three MG and two MG-125b mice. B) Leukemic cell infiltration into non-hematopoietic organs. Sections from the kidney, lung, and liver were stained with hematoxylin and eosin. The normal structures of the MG- 125b mouse kidney, lung and liver are effaced by a dramatic infiltrate of leukemic cells. A representative image for each tissue is shown. The brain, kidney, lung, and liver were harvested from animals five months after bone marrow reconstitution. During the time of harvest, the average %GFP⁺ cell in the spleen of MG and MG-125b mice were 49±9.7 and 91±2.9 %, respectively. All plots shown depict the mean with standard error of the mean (SEM). All data is representative of two independent experiments. Abbreviations: Inf, Infiltrate; G, Glomerulus; A, alveolar space; CV, central vein.

Figure 2: MiR-125b over-expression causes a skewing of the hematopoietic system at seven weeks post-bone marrow reconstitution. A)

Flow cytometric analyses of the spleens were used to quantify the percent of granulocytes (GR-1⁺ CD19⁻), macrophages (F4/80⁺ CD68⁺), dendritic cells (CD11b⁺ CD11c⁺), T cells (CD3ε⁺ CD19⁻), and B cells (CD19⁺ GR-1⁻). The total leukocyte counts in the spleen were similar between MG and MG-125b mice. B) The percent of MPPs and total numbers of CMP/GMPs, MEP, CLP, and pre-B

cells in the bone marrow were measured by flow cytometry. Horizontal lines represent the mean and each dot represents an individual mouse. Data is representative of 2-3 independent experiments with 4-5 mice per group.

Figure 3: Inhibiting miR-125b function decreases hematopoietic output. Equal numbers of sorted GFP⁺ MG and MG-Sponge transduced progenitor-enriched BMCs were injected into recipient animals. A) Total numbers of white blood cells, B) myeloid cells, C) granulocytes, and erythroid cells (Ter119⁺) were measured by flow cytometry. Data represent Mean number of cells / ml of blood (SEM shown). P values were calculated using unpaired Student's T test. All results are representative of two independent experiments with 9-10 animals per group.

Figure 4: MiR-125b represses Lin28A expression in mouse and human hematopoietic cells. A) Relative expression of miR-125b candidate targets in miR-125b over-expressing progenitor-enriched BMCs compared to MG control. Bone marrow cells from 5-FU treated mice were infected with miR-125b over-expressing vector and RNA was subsequently harvested for expression level analysis. The relative expression level was measured by qPCR. B) 3'UTR reporter analyses. The 3'UTR of the indicated genes were cloned into a luciferase reporter and co-transfected with a miR-125b expression vector. Relative luminescence of the luciferase reporters was measured and normalized to an empty vector control. The Picalm 3' UTR, which contains no miR-125b putative binding sites, is shown. The 2mer positive control, which consists of two adjacent miR-125b antisense sites, is also shown. C) Relative luminescence of the Lin28A 3' UTR reporter co-transfected with either

MG or miR-125b sponge decoy vector into 293T cells. D) Protein expression of Lin28A transduced with either MGP empty vector or MGP expressing miR-125b-1, miR-125b-2, or a miR-125b seed mutant in K562 cells. Protein levels were obtained by Western blot and β -actin was included as a loading control. All data shown represent mean with SEM. * indicates $p < 0.02$; ** indicates $p < 0.01$.

Figure 5: Lin28A over-expression inhibits hematopoiesis. Recipients were transplanted with progenitor-enriched BMCs transduced with MIG-Lin28A or MIG. Five weeks post-reconstitution, the number of A) white blood cells, B) myeloid cells, C) granulocytes, and D) erythrocytes per ml in the blood were measured by flow cytometry. We did not observe an increase in B-cells in the MIG-Lin28A animals. Data is pooled from two independent groups of MIG-Lin28A animals, each with 7-8 animals and compared to MIG (6 animals). Data shown graphically represents the mean and SEM.

Figure 6: Inhibition of Lin28A increases the number of myeloid cells but decreases B cells. A) Flow cytometry of progenitor-enriched bone marrow transduced with MG- Lin28A shRNA or MG control vector was performed and the percent GFP^+ cells is indicated. B) Lin28A mRNA expression was obtained by qPCR on the samples shown in A, and the results were normalized to L32. Representative of two independent experiments with 4 samples per group. C) Total myeloid, D) granulocytes, and E) B cells were measured from blood five weeks post-bone marrow reconstitution with 7-8 animals per group. Data shown represents mean and SEM. P values are indicated.

References

- Bousquet, M., Harris, M.H., Zhou, B., and Lodish, H.F. (2010). MicroRNA miR-125b causes leukemia. *Proceedings of the National Academy of Sciences of the United States of America* *107*, 21558-21563.
- Bousquet, M., Quelen, C., Rosati, R., Mansat-De Mas, V., La Starza, R., Bastard, C., Lippert, E., Talmant, P., Lafage-Pochitaloff, M., Leroux, D., *et al.* (2008). Myeloid cell differentiation arrest by miR-125b-1 in myelodysplastic syndrome and acute myeloid leukemia with the t(2;11)(p21;q23) translocation. *The Journal of experimental medicine* *205*, 2499-2506.
- Cherry, S.R., Biniszkiwicz, D., van Parijs, L., Baltimore, D., and Jaenisch, R. (2000). Retroviral expression in embryonic stem cells and hematopoietic stem cells. *Molecular and cellular biology* *20*, 7419-7426.
- Ebert, M.S., Neilson, J.R., and Sharp, P.A. (2007). MicroRNA sponges: competitive inhibitors of small RNAs in mammalian cells. *Nature methods* *4*, 721-726.
- Ebert, M.S., and Sharp, P.A. (2010). MicroRNA sponges: progress and possibilities. *RNA (New York, N.Y.)* *16*, 2043-2050.
- Enomoto, Y., Kitaura, J., Hatakeyama, K., Watanuki, J., Akasaka, T., Kato, N., Shimanuki, M., Nishimura, K., Takahashi, M., Taniwaki, M., *et al.* (2011). Emu/miR-125b transgenic mice develop lethal B-cell malignancies. *Leukemia* *25*, 1849-1856.
- Friedman, R.C., Farh, K.K., Burge, C.B., and Bartel, D.P. (2009). Most mammalian mRNAs are conserved targets of microRNAs. *Genome research* *19*, 92-105.
- Gefen, N., Binder, V., Zaliova, M., Linka, Y., Morrow, M., Novosel, A., Edry, L., Hertzberg, L., Shomron, N., Williams, O., *et al.* (2010). Hsa-mir-125b-2 is highly expressed in childhood ETV6/RUNX1 (TEL/AML1) leukemias and confers survival advantage to growth inhibitory signals independent of p53. *Leukemia* *24*, 89-96.
- Grimson, A., Farh, K.K., Johnston, W.K., Garrett-Engele, P., Lim, L.P., and Bartel, D.P. (2007). MicroRNA targeting specificity in mammals: determinants beyond seed pairing. *Molecular cell* *27*, 91-105.
- Gururajan, M., Haga, C.L., Das, S., Leu, C.M., Hodson, D., Josson, S., Turner, M., and Cooper, M.D. (2010). MicroRNA 125b inhibition of B cell differentiation in germinal centers. *International immunology* *22*, 583-592.

Klusmann, J.H., Li, Z., Bohmer, K., Maroz, A., Koch, M.L., Emmrich, S., Godinho, F.J., Orkin, S.H., and Reinhardt, D. (2010). miR-125b-2 is a potential oncomiR on human chromosome 21 in megakaryoblastic leukemia. *Genes & development* 24, 478-490.

Le, M.T., Shyh-Chang, N., Khaw, S.L., Chin, L., Teh, C., Tay, J., O'Day, E., Korzh, V., Yang, H., Lal, A., *et al.* (2011). Conserved regulation of p53 network dosage by microRNA-125b occurs through evolving miRNA-target gene pairs. *PLoS genetics* 7, e1002242.

Lewis, B.P., Burge, C.B., and Bartel, D.P. (2005). Conserved seed pairing, often flanked by adenosines, indicates that thousands of human genes are microRNA targets. *Cell* 120, 15-20.

O'Connell, R.M., Chaudhuri, A.A., Rao, D.S., and Baltimore, D. (2009). Inositol phosphatase SHIP1 is a primary target of miR-155. *Proceedings of the National Academy of Sciences of the United States of America* 106, 7113-7118.

O'Connell, R.M., Chaudhuri, A.A., Rao, D.S., Gibson, W.S., Balazs, A.B., and Baltimore, D. (2010). MicroRNAs enriched in hematopoietic stem cells differentially regulate long-term hematopoietic output. *Proceedings of the National Academy of Sciences of the United States of America* 107, 14235-14240.

O'Connell, R.M., Rao, D.S., Chaudhuri, A.A., Boldin, M.P., Taganov, K.D., Nicoll, J., Paquette, R.L., and Baltimore, D. (2008). Sustained expression of microRNA-155 in hematopoietic stem cells causes a myeloproliferative disorder. *The Journal of experimental medicine* 205, 585-594.

Ooi, A.G., Sahoo, D., Adorno, M., Wang, Y., Weissman, I.L., and Park, C.Y. (2010). MicroRNA-125b expands hematopoietic stem cells and enriches for the lymphoid-balanced and lymphoid-biased subsets. *Proceedings of the National Academy of Sciences of the United States of America* 107, 21505-21510.

Rao, D.S., O'Connell, R.M., Chaudhuri, A.A., Garcia-Flores, Y., Geiger, T.L., and Baltimore, D. (2010). MicroRNA-34a perturbs B lymphocyte development by repressing the forkhead box transcription factor Foxp1. *Immunity* 33, 48-59.

Rossi, R.L., Rossetti, G., Wenandy, L., Curti, S., Ripamonti, A., Bonnal, R.J., Birolo, R.S., Moro, M., Crosti, M.C., Gruarin, P., *et al.* (2011). Distinct microRNA signatures in human lymphocyte subsets and enforcement of the naive state in CD4⁺ T cells by the microRNA miR-125b. *Nature immunology* 12, 796-803.

Shi, X.B., Xue, L., Yang, J., Ma, A.H., Zhao, J., Xu, M., Tepper, C.G., Evans, C.P., Kung, H.J., and deVere White, R.W. (2007). An androgen-regulated miRNA suppresses Bak1 expression and induces androgen-independent growth of prostate cancer cells.

Proceedings of the National Academy of Sciences of the United States of America
104, 19983-19988.

Starczynowski, D.T., Kuchenbauer, F., Argiropoulos, B., Sung, S., Morin, R., Muranyi, A., Hirst, M., Hogge, D., Marra, M., Wells, R.A., *et al.* (2010). Identification of miR-145 and miR-146a as mediators of the 5q- syndrome phenotype. *Nature medicine* *16*, 49-58.

Viswanathan, S.R., and Daley, G.Q. (2010). Lin28: A microRNA regulator with a macro role. *Cell* *140*, 445-449.

Wang, L., Toomey, N.L., Diaz, L.A., Walker, G., Ramos, J.C., Barber, G.N., and Ning, S. (2011). Oncogenic IRFs provide a survival advantage for Epstein-Barr virus- or human T-cell leukemia virus type 1-transformed cells through induction of BIC expression. *Journal of virology* *85*, 8328-8337.

Wu, L., and Belasco, J.G. (2005). Micro-RNA regulation of the mammalian lin-28 gene during neuronal differentiation of embryonal carcinoma cells. *Molecular and cellular biology* *25*, 9198-9208.

Xia, H.F., He, T.Z., Liu, C.M., Cui, Y., Song, P.P., Jin, X.H., and Ma, X. (2009). MiR-125b expression affects the proliferation and apoptosis of human glioma cells by targeting Bmf. *Cellular physiology and biochemistry : international journal of experimental cellular physiology, biochemistry, and pharmacology* *23*, 347-358.

Yu, J., Vodyanik, M.A., Smuga-Otto, K., Antosiewicz-Bourget, J., Frane, J.L., Tian, S., Nie, J., Jonsdottir, G.A., Ruotti, V., Stewart, R., *et al.* (2007). Induced pluripotent stem cell lines derived from human somatic cells. *Science (New York, N.Y.)* *318*, 1917-1920.

Supplemental Figure Legends

Figure S1: MiR-125b overexpressing animals exhibit myeloid infiltration into peripheral organs five months post-reconstitution. Moribund MG-125b animals were sacrificed and their organs harvested. Flow cytometry on GFP⁺ CD45⁺ and GFP⁺ CD11b⁺ populations were performed for the A) kidney, C) lung, and E) liver. A representative FACS plot is shown for each organ. Gross pathology comparing MG and MG-125b B) kidney and D) lung are also shown. F) A representative MG-125b liver is shown. G) Blood smear. Wright stain was performed when miR-125b overexpressing mice were moribund. All data is representative of 8 MG animals and 5 MG-125b animals.

Figure S2: MiR-125a overexpression causes an aggressive leukemia six months post-reconstitution. Mice overexpressing miR-125a became moribund six months post-reconstitution, at which point they were euthanized. Gross pathology from A) spleen, B) liver, and C) kidneys are shown. Arrows show the infiltration of cancer cells into the kidneys in the miR-125a mice. Representative of two animals. Note: Pictures for MG and miR-125a overexpressing mice were obtained on separate days and the colors are thus not to be used for direct comparison.

Figure S3: MiR-125b overexpression increases leukocyte count five months post-reconstitution. Spleens from MG and MG-125b animals were harvested, RBC-lysed, and the relative leukocyte count was determined by flow cytometry. Each dot represents a mouse; the Mean and SEM are also indicated. Data is from four MG and five MG-125b animals and is representative of two independent experiments.

Figure S4: Bone marrow and peripheral blood from MG-125b animals early post-reconstitution display hematopoietic reconfiguration. At seven weeks post-reconstitution, A) total white blood cell counts and B) total GFP⁺ white blood cells were measured in MG and MG-125b mouse bone marrow. Total number of C) GFP⁺ granulocytes (GFP⁺ Gr1⁺ Ter119⁻), D) dendritic cells (GFP⁺ CD11b⁺ CD11c⁺), E) macrophages (GFP⁺ F480⁺), F) B cells (GFP⁺ CD19⁺ CD11c⁻), G), GFP⁺ long term HSCs (LT HSC, Lin⁻ Sca1⁺ cKit⁺ CD48⁻ CD150⁺), and H) short term HSCs (ST HSC, Lin⁻ Sca1⁺ cKit⁺ CD48⁻ CD150⁻) were also measured in MG and MG-125b mouse bone marrow at this time point. Each dot represents an individual mouse and a horizontal line indicates the mean. P values are also shown. Data is representative of two independent experiments.

Figure S5: Inhibiting miR-125b function decreases hematopoietic output. A) Design and testing of the miR-125b ‘sponge’ decoy system. MiR-125b sponge decoy was constructed by placing four miR-125b complementary sites downstream of GFP in the MG vector with a 4-6 nt spacer between each site. A 3 nt mismatch region was placed in each miRNA binding site, since it has been shown to increase the effectiveness of sponge decoys (11-14). B) Sponge de-represses a miR-125b reporter vector comprised of 2 perfect antisense sites placed downstream of luciferase in 293T cells. C) Sponge does not de-repress the pMiR-Report negative control vector in 293T cells. Luciferase values were measured and normalized to the loading control β-gal. Assays were performed with three samples per group; Mean and SEM are plotted. Results are representative of three independent experiments. Abbreviations: nt, nucleotide; miRNA, microRNA. Note: The sponge de-

represses the 2mer reporter by 30%. D) GFP⁺ cells were isolated from MG and MG-Sponge transduced progenitor- enriched bone marrow by fluorescent activated cell sorting (FACS). Equal numbers of GFP⁺ cells were injected into recipient animals. (Left) Oval indicates gating on the primary population of cells based on forward (FSC) and side scatter (BSC). (Right) GFP⁺ cells within the primary population were sorted as indicated by the blue arrow.

Figure S6: MiR-125b represses Lin28 expression in mouse and human hematopoietic cells. A) Relative expression of Lin28, Trp53inp1, and BMF expression in miR-125b sponge-transduced progenitor-enriched bone marrow, normalized to MG transduced controls. The percent expression relative to MG is shown. Broken line demarcates 100%. B) MiR-125b seed sequence in the 3'UTR of Lin28 is shown. Depiction is not drawn to scale. C) MiR-125b mutant vector expresses a seed mutant version of miR-125b. MGP-125b-Mutant vector was designed to express a seed mutant version of miR-125b by utilizing a miR- 155 arms-and-loop format (top). Sequences expressed by wild type miR-125b and the mutant are shown below. D) Quantitative PCR shows relative expression of the mutant version of miR-125b (normalized to L32) in K562 cells transduced with MGP-125b-Mutant or MGP control. E) RNA expression of Lin28 transduced with either MGP empty vector or MGP expressing miR-125b-1, miR-125b-2, or a miR-125b seed mutant in K562 cells. F) Immunoblot of Lin28B transduced with either MGP empty vector or MGP expressing miR-125b-1 or miR-125b-2 in K562 cells. G) qPCR of Lin28B after transduction with either MG empty vector or MG- miR-125b in bone marrow cells

harvested from 5-FU injected mice.

Figure S7: Lin28A and Lin28B expression in miR-125b over-expressing leukemic samples. RNA from peripheral blood mononuclear (PBMC) of cancer mice, which was transplanted with miR-125b over-expressing leukemic cells, was harvested. Equal amounts of RNA were used for RT-qPCR analyses. The control samples were PBMC from recipients of MG mice that did not develop cancer. The relative expressions of Lin28A, Lin28B, and the control Rpl19 gene are displayed. Each dot represents an individual animal. Student T-test was for statistical analyses.

Figure S8: Lin28 over-expression inhibits hematopoiesis. A) Lin28 over-expression was confirmed by western blot with B-actin as loading control. Note: We confirmed by qPCR that Lin28 is over-expressed using this vector system in mouse primary bone marrow cells. B) Recipients were transplanted with progenitor-enriched BMCs that were transduced MIG-Lin28 or MIG with similar efficiency.

Figures

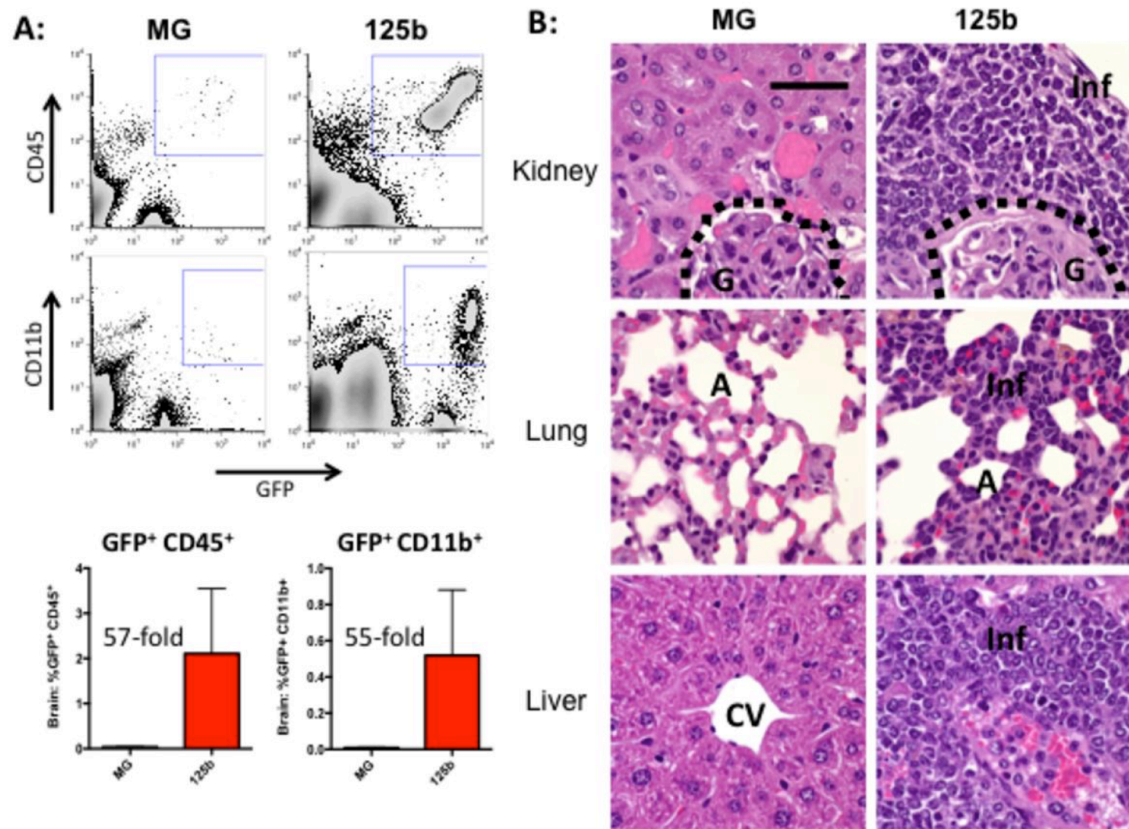


Figure 1: MiR-125b over-expression causes an aggressive invasive myeloid leukemia.

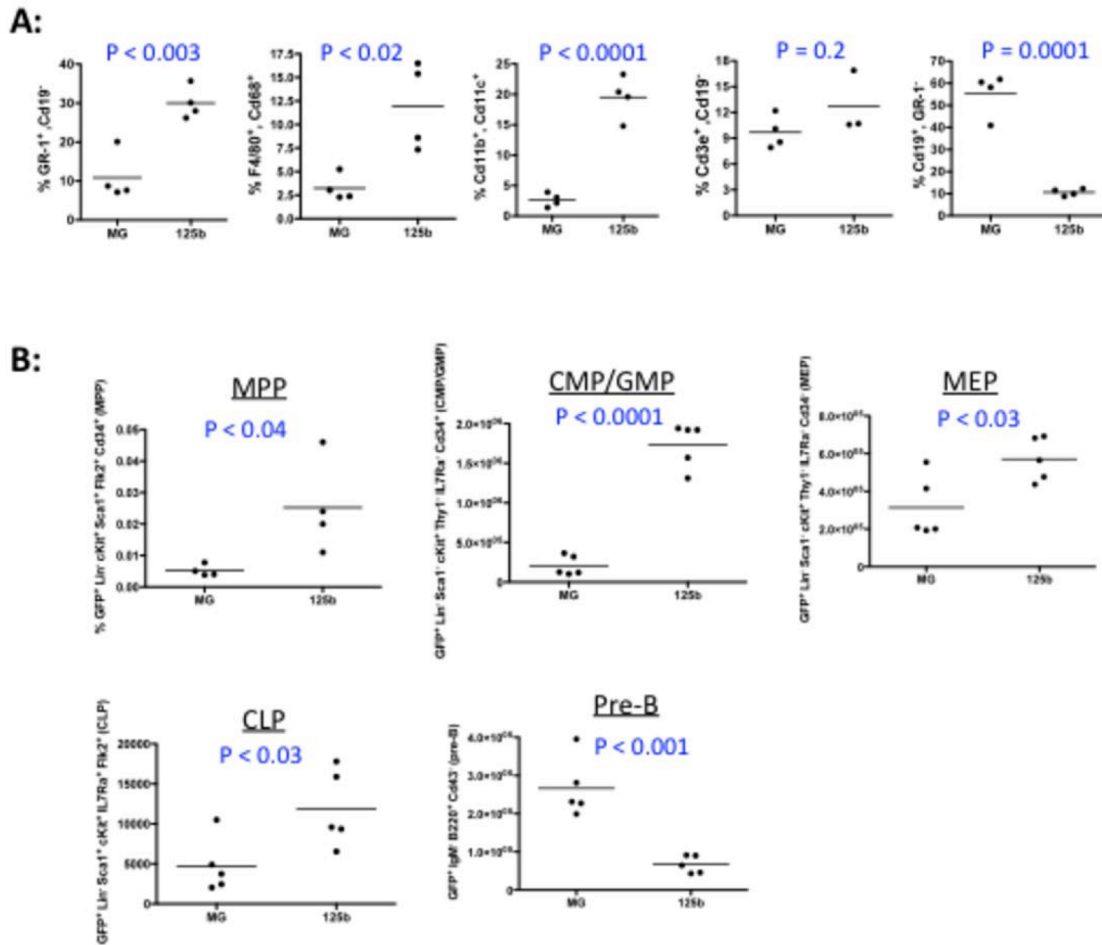


Figure 2: MiR-125b over-expression causes a skewing of the hematopoietic system at seven weeks post-bone marrow reconstitution.

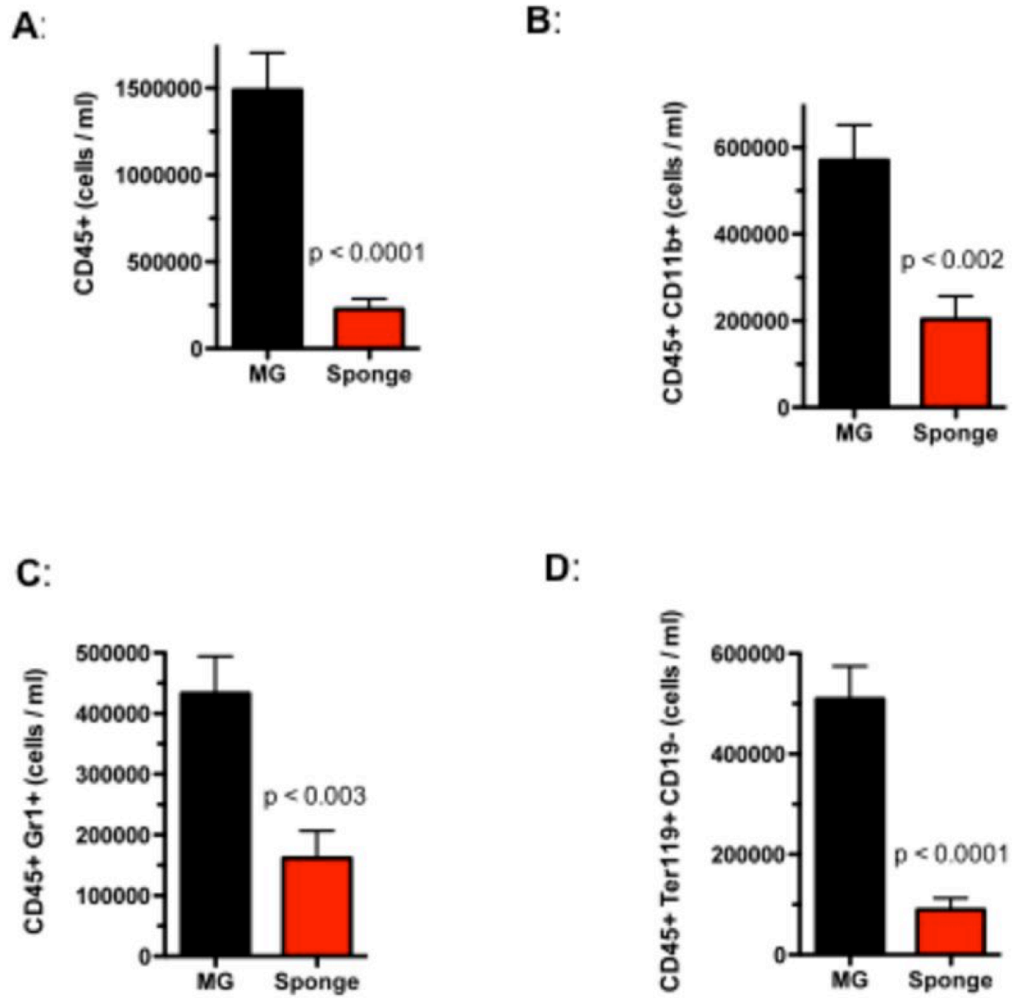


Figure 3: Inhibiting miR-125b function decreases hematopoietic output.

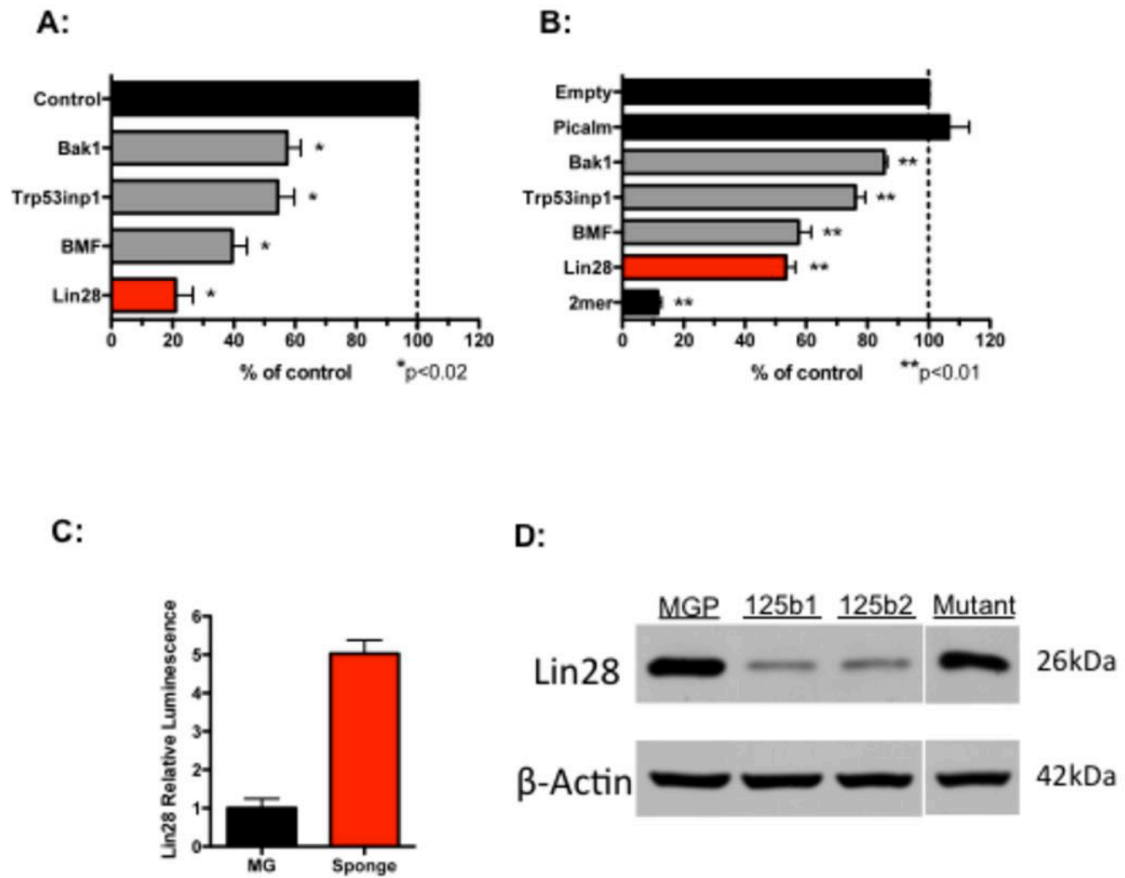


Figure 4: MiR-125b represses Lin28A expression in mouse and human hematopoietic cells.

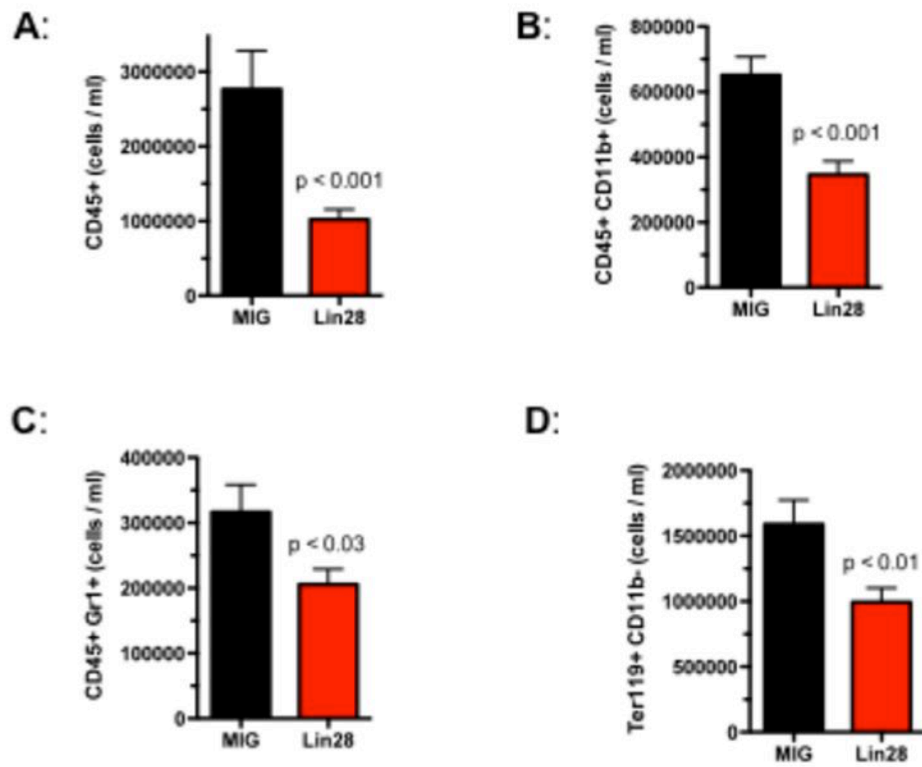


Figure 5: Lin28A over-expression inhibits hematopoiesis.

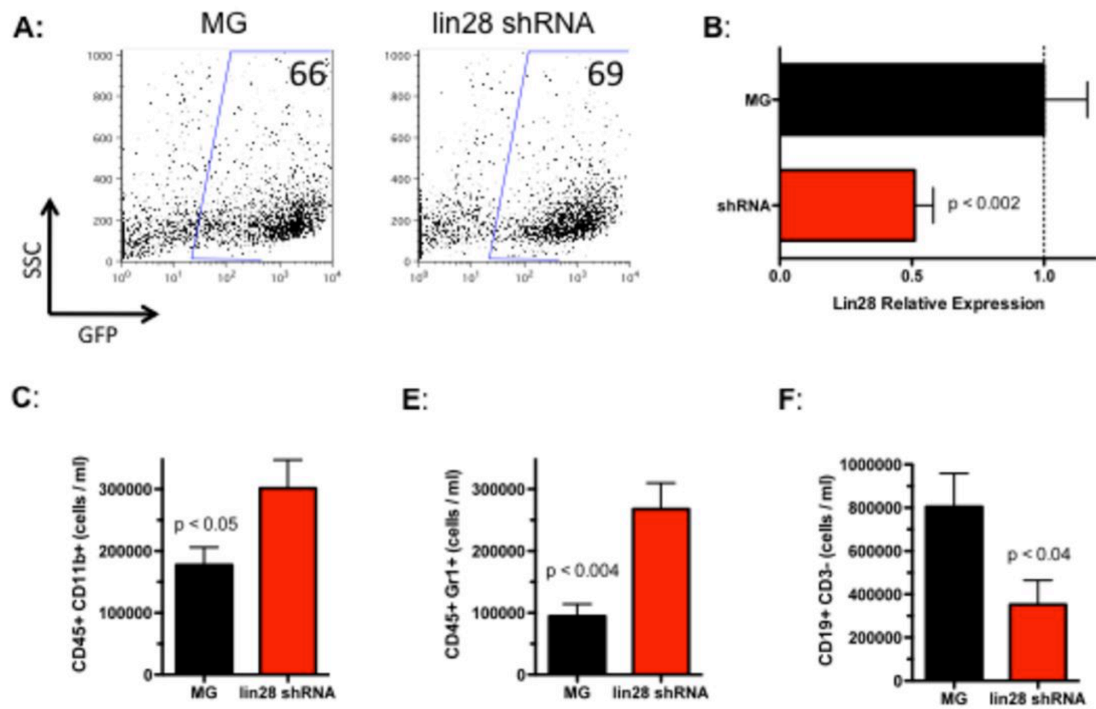


Figure 6: Inhibition of Lin28A increases the number of myeloid cells but decreases B cells.

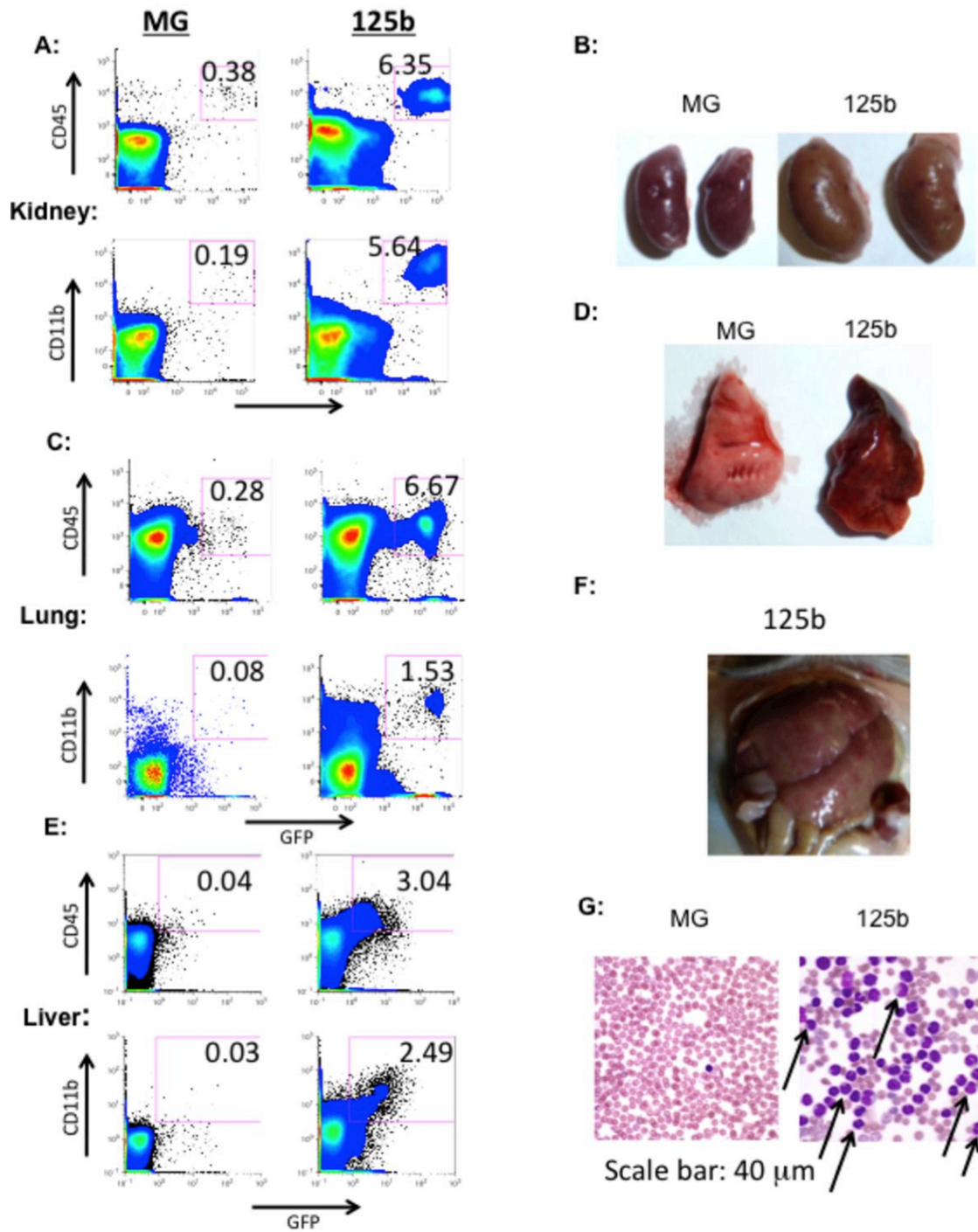


Figure S1: MiR-125b overexpressing animals exhibit myeloid infiltration into peripheral organs five months post-reconstitution.

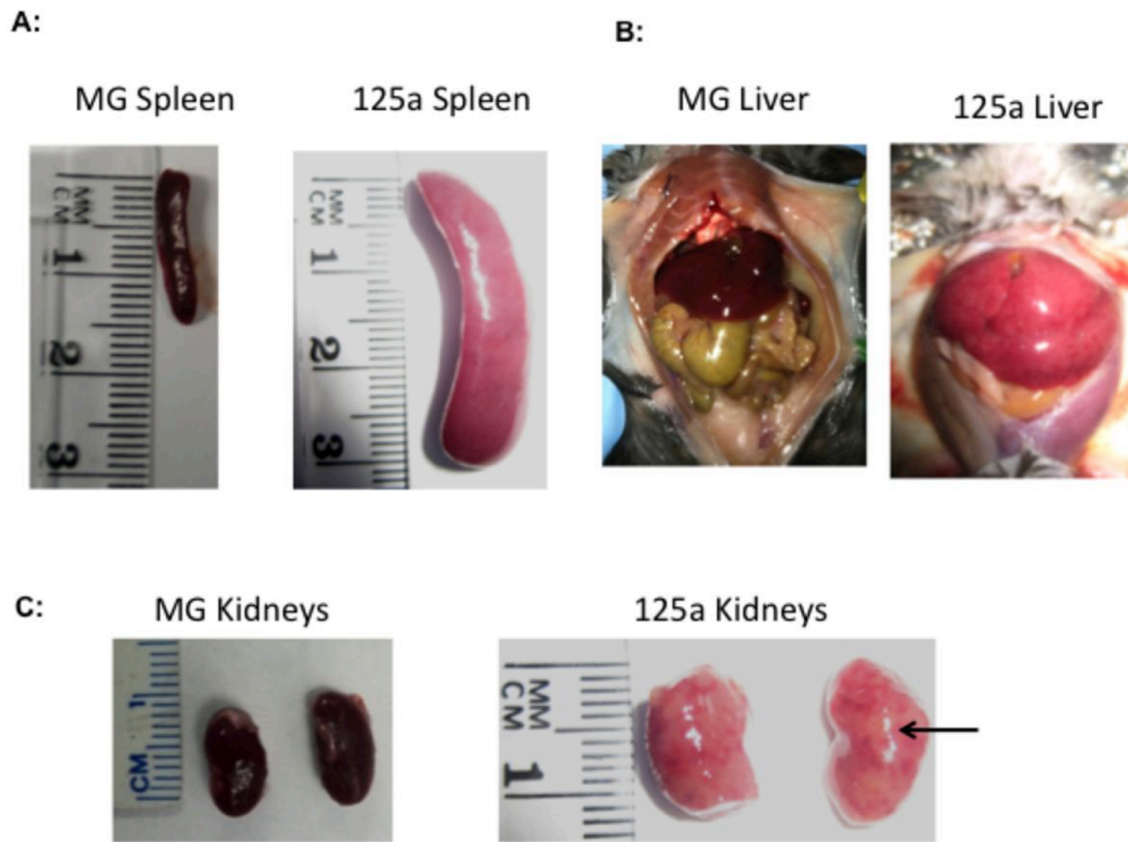


Figure S2: MiR-125a overexpression causes an aggressive leukemia six months post-reconstitution.

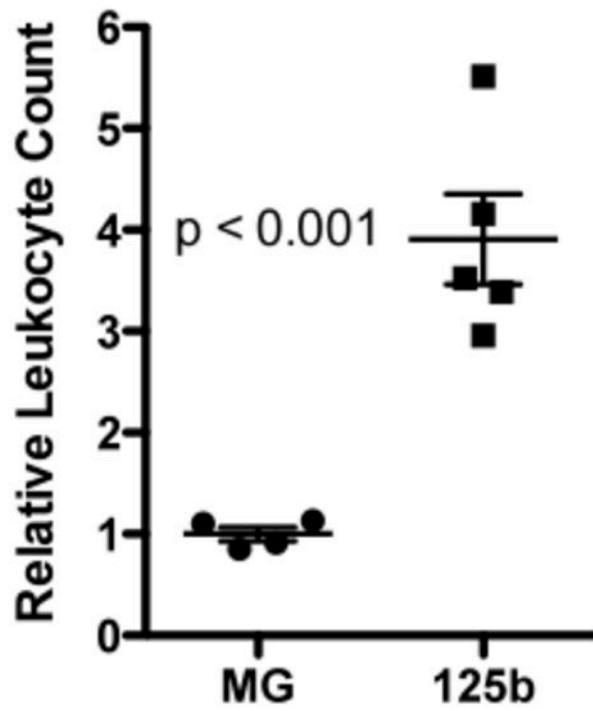


Figure S3: MiR-125b overexpression increases leukocyte count five months post-reconstitution.

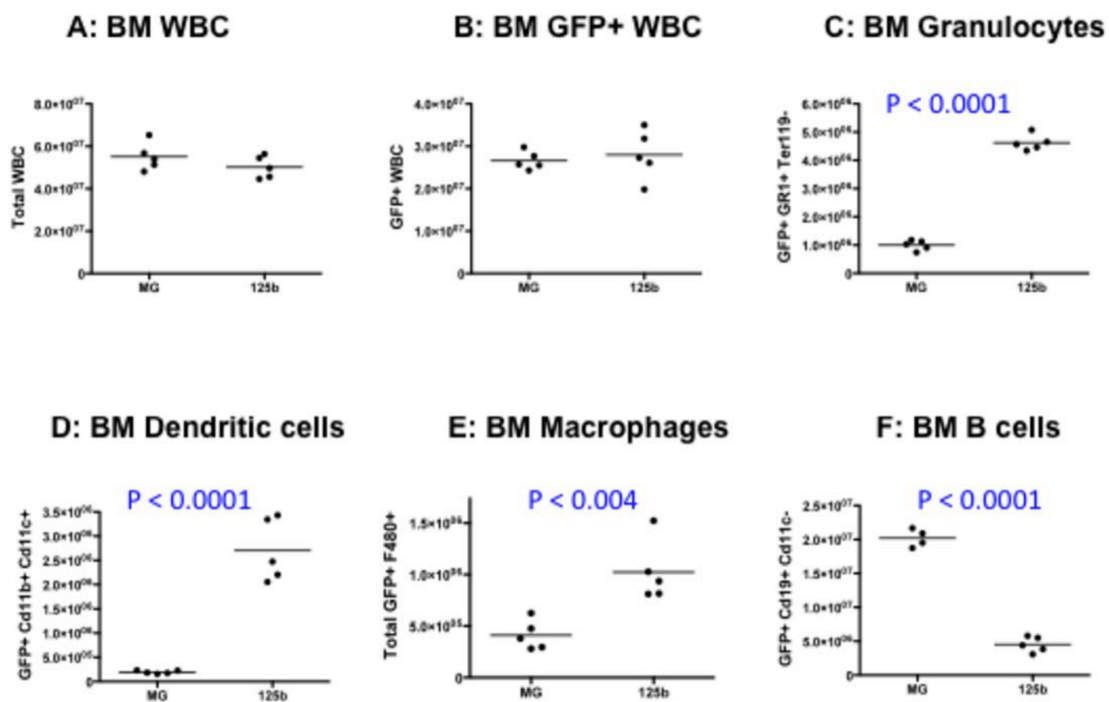


Figure S4: Bone marrow and peripheral blood from MG-125b animals early post-reconstitution display hematopoietic reconfiguration.

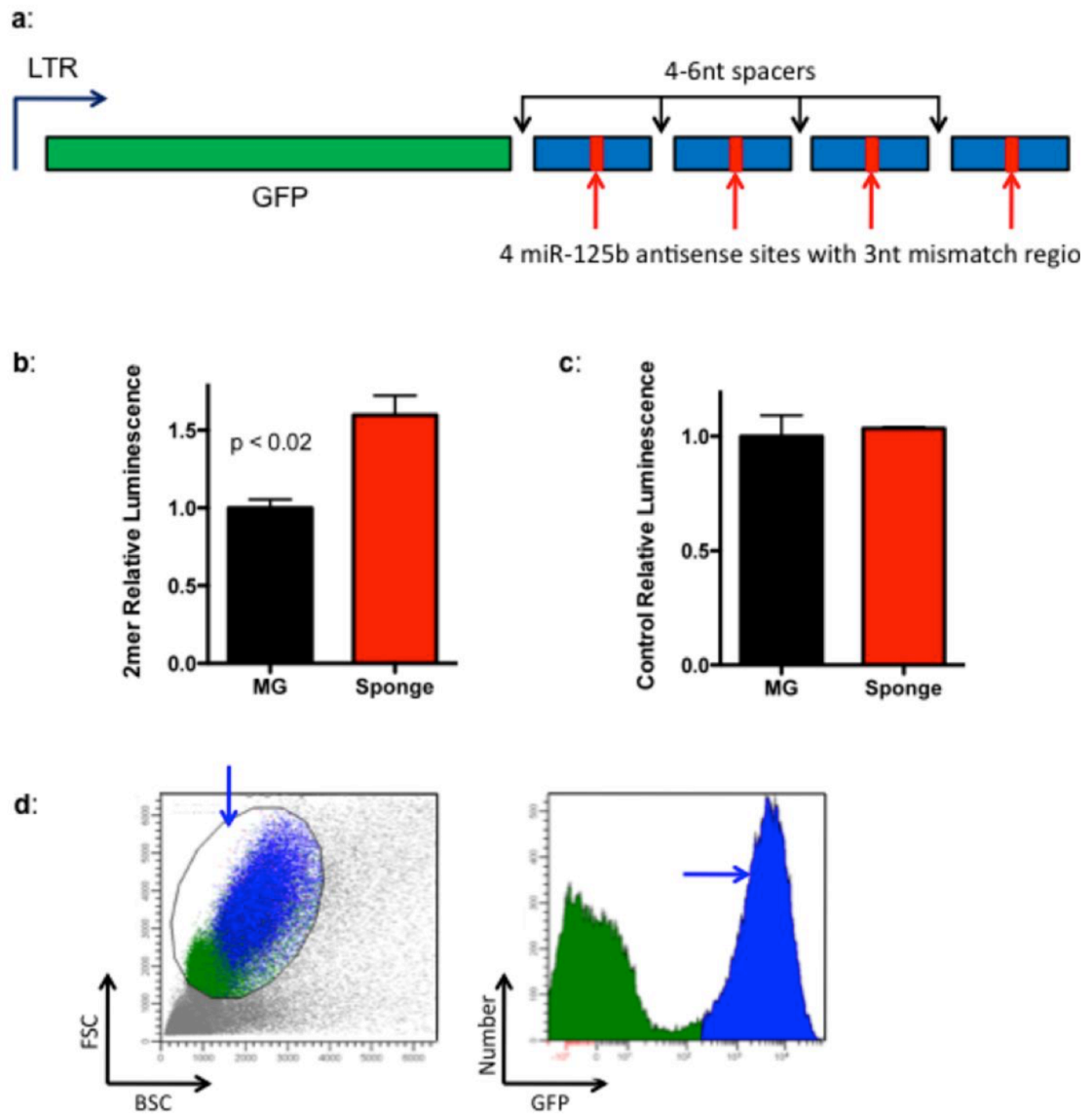


Figure S5: Inhibiting miR-125b function decreases hematopoietic output.

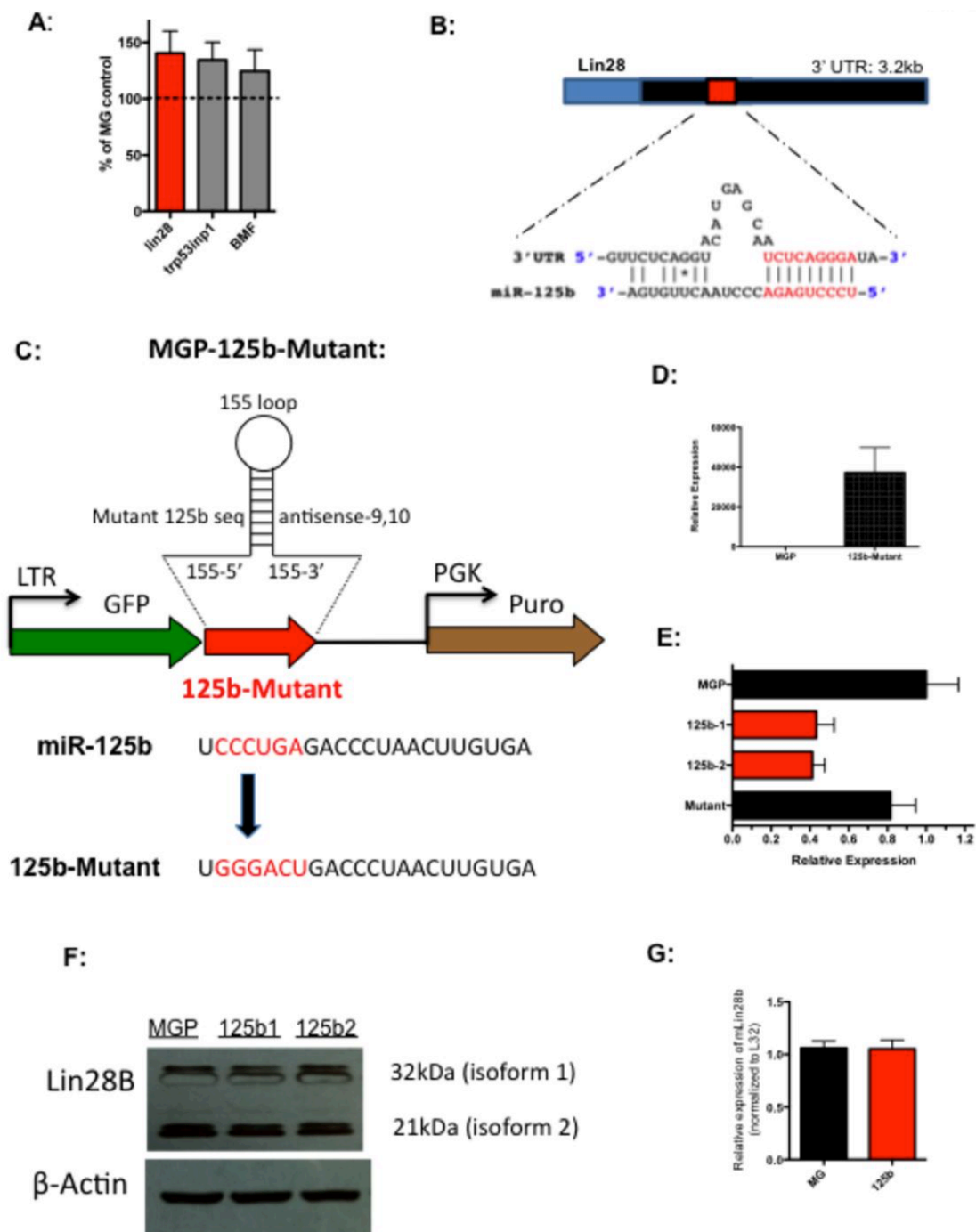


Figure S6: MiR-125b represses Lin28 expression in mouse and human hematopoietic cells.

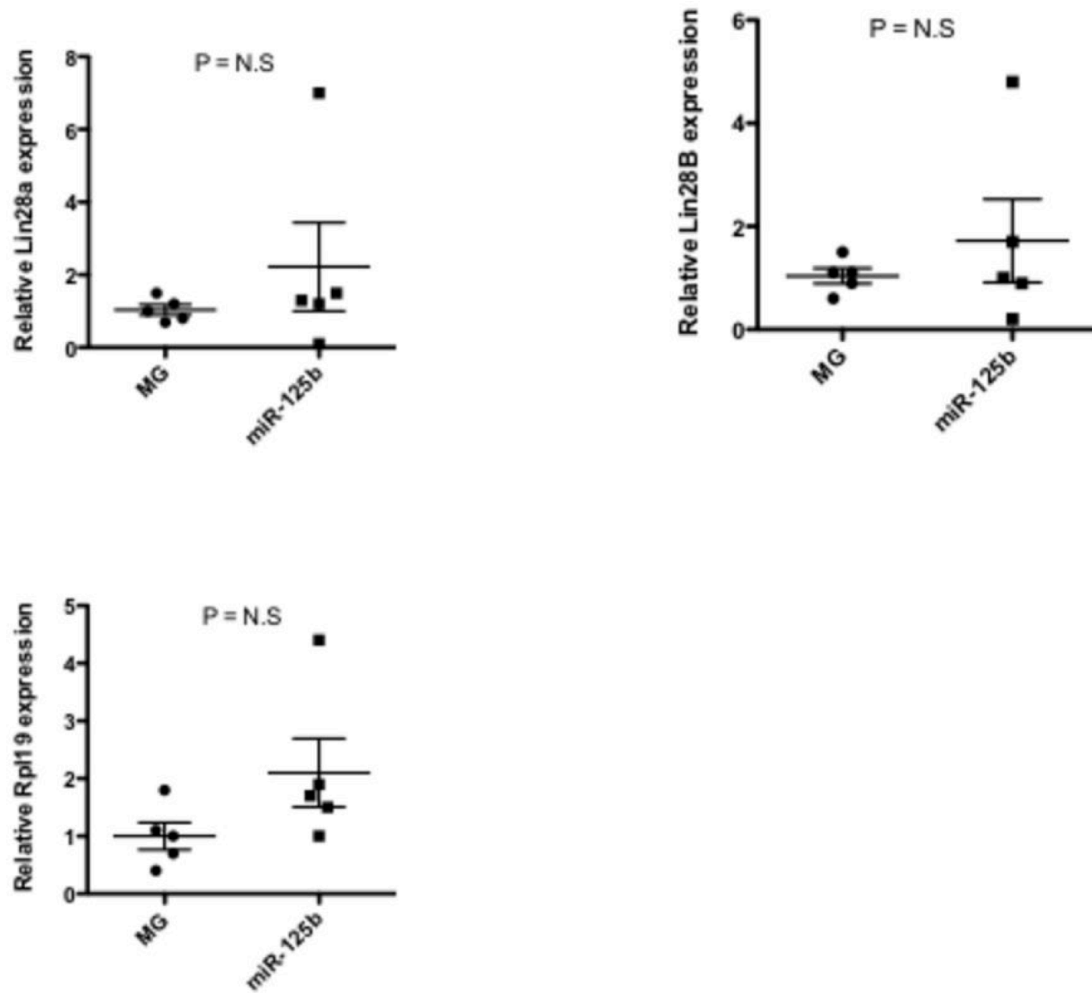


Figure S7: Lin28A and Lin28B expression in miR-125b over-expressing leukemic samples.

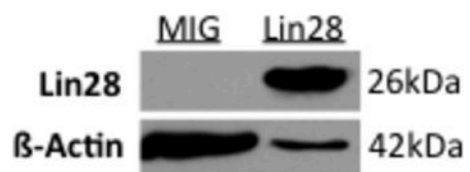
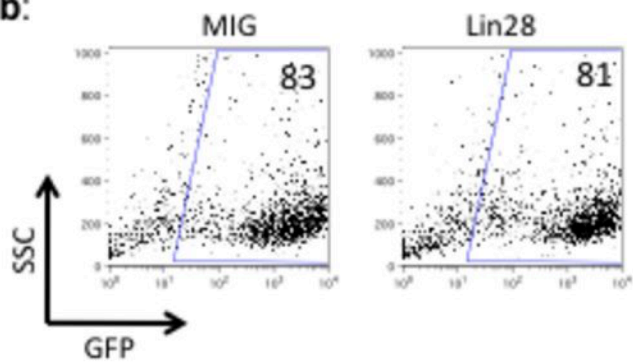
a:**b:**

Figure S8: Lin28 over-expression inhibits hematopoiesis.

Chapter 5: Conclusions and Future Directions

A putative role of miR-132 in maintaining HSC function with age

In this thesis I have uncovered a novel role of miR-132 in HSC and B cell function. We observed that miR-132 buffers the expression of the transcription factor FOXO3 in order to maintain balanced hematopoietic output of aging HSCs. Deregulation of miR-132 results in altered HSC cell cycling, function, and survival through protective autophagy. Several open questions remain about the role of miR-132 in HSCs:

- 1) What regulates the expression of miR-132 in HSCs? And why is it up regulated with age?
- 2) What is the molecular mechanism by which a loss in protective autophagy leads to decreased HSC survival? What cellular and molecular changes in HSCs result in survival through autophagy becoming more important with age?
- 3) What are the other critical targets of miR-132 that regulate HSC function with age?
- 4) Can we alter age-related functional decline of HSCs? Can we use this to prevent age-associated hematopoietic disease?

Uncovering potential roles of miR-132 in normal and malignant B cell development

We have additionally shown that miR-132 regulates B cell development by targeting the transcription factor Sox4. We found that delivery of miR-132 can also inhibit B cancer progression in mice. Several open questions remain about the role of miR-132 in B cell

development. Our current efforts seek to understand the following:

- 1) How is miR-132 induced in early B cell progenitors? Can we induce miR-132 with pre-BCR signaling? What regulates this induction?
- 2) What roles does Sox4 play in altering pro-B cell fate? What is the molecular mechanism by which Sox4 regulates B cell fate decisions? How does Sox4 alter B cell apoptosis?
- 3) Finally, we observed in our studies that the induction of miR-132 is 3-fold higher than that of miR-212. Thus, an open question remains as to how miR-132 and miR-212, expressed in a cluster, are differentially regulated in B cells.

A proposal to better understand HSC aging with age at single-cell resolution

To better understand how molecular changes in aging HSCs may lead to age-associated hematopoietic disease, we are currently investigating the molecular characteristics of hematopoietic progenitors using single-cell proteomic and transcriptomic experiments. Below is a proposal for future work in this area.

Significance

Aging is a progressive degenerative process, tightly integrated with chronic inflammation. However, the molecular link between chronic inflammation and aging is still poorly understood. This proposed study aims to make fundamental advances in defining the key molecular regulators of hematopoietic aging and their relationship to chronic inflammation.

Using single cell analysis, we will determine the molecular signature of specific subpopulations within the hematopoietic stem and progenitor cells (HSPC) pool from young and aged mice, and chronically inflamed mouse models. We will further characterize the relative contribution of these molecular factors to the aging process.

Our combined study of chronic inflammation models and the molecular signature of aging will enable us elucidate the molecular pathways responsible for immune aging and understand the relationship between chronic inflammation and aging. This proposed study might also reveal potential therapeutic approaches for treating immune-aging related malignancies, such as cancer, autoimmunity, and anemia.

Innovation

To date, cellular and molecular properties are largely investigated by utilizing bulk methods that measure the average values for population of cells. Bulk analysis of these cells masks an understanding of the way each individual cell behaves, and is often insufficient for characterizing the biological processes in which cellular heterogeneity plays a key role. The hematopoietic stem and progenitor cell compartment is heterogeneous by nature, enabling many cell fate decisions for each cell. In this proposed study, we will determine the molecular signature of specific subpopulations within the HSPC pool by using single cell cytokine secretion and transcriptome analysis. This methodology will enable us to determine the key molecular regulators of hematopoietic aging and chronic inflammation. This approach will also allow us further characterize the contribution of these molecular pathways to immune aging, inflammation, and homeostasis.

Approach

Aim 1: Define the molecular signature of the hematopoietic stem and progenitor cell compartment in young and aged mice in response to inflammatory signals.

Background: Aging alters the cellular composition of the hematopoietic system, leading to more myeloid-biased hematopoietic stem and progenitor cells (HSPCs), pro-inflammatory macrophages, and T cells, as well as expansion of memory B cells. These alterations contribute to the increased susceptibility to infectious diseases, autoimmunity, vaccine failure, and cancers such as leukemia (Morrison et al., 1996). Similarly, changes observed during chronic inflammation are reminiscent of hematopoietic stem cell (HSC) aging, including alterations in HSC cycling, impairment in the capacity of HSCs to repopulate and self-renew in transplanted animals, and skewing of differentiation towards myeloid cell types (Morrison et al., 1996; Rossi et al., 2005). We hypothesize that a molecular signature exists within HSPCs that reflects the aging-dependent response of the hematopoietic system to chronic or acute challenges. We further hypothesize that by characterizing the proteome and transcriptome of single hematopoietic cells, we will resolve the molecular networks that are associated with how aging influences the hematopoietic system.

The goal of this aim is to discover key regulators of hematopoietic aging and their relationship to diseases of age; as such, we are using a global, unbiased approach to studying the gene and protein expression networks of hematopoietic cells. We recently demonstrated the remarkable ability of HSPCs to produce cytokines, especially in response to direct inflammatory stimulation (Zhao et al., 2014). Of note is that the types and

abundance of cytokines produced by HSPCs varied significantly, with some producing myeloid-biased cytokine profiles and others lymphoid-biased profiles. This, in turn, is reflective of the inherent heterogeneity of hematopoietic progenitors. In this Aim, we propose to elaborate on these measurements in context of the aging hematopoietic system at steady state and after exposure to inflammatory stimuli. In doing so, we will build a resource tool of molecular pathways that reflect the aging process at the single cell level.

Subaim 1.1. Define a molecular signature of hematopoietic progenitors that reflects the altered response to danger signals during the process of aging.

We seek to define a molecular signature of the hematopoietic system that reflects the process of aging and how aging influences the capacity of the hematopoietic system to deal with chronic or acute inflammation. Our preliminary results indicate that early progenitors demonstrate a robust response to the bacterial components lipopolysaccharide (LPS) + Pam3csk4, ligands for toll-like receptor 4 (TLR4) and toll-like receptor 2 (TLR2), respectively (Figure 1A,B). However, it remains unclear whether this response is analogous to that of more mature immune cell types and how this response is altered with age. We first seek to investigate the molecular pathways that are altered in bulk populations of young and aged HSPCs in response to critical danger signals, such as bacterial components.

Approach: In order to investigate the molecular pathways that are critical for HSPC response to danger signals, we will perform RNA-sequencing on bulk populations of various hematopoietic progenitors from young and aged mice over a comprehensive time-course. Long-term HSCs (Lineage- cKit+ Sca1+ CD150+ CD48-), short-term HSCs (Lineage- cKit+ Sca1+ CD150- CD48-), MPPs (Lineage- cKit+ Sca1+ CD150- CD48+),

and more committed hematopoietic progenitors will be sorted from young (12 weeks) and aged (> 22 months) mice by fluorescence activated cell sorting (FACS). These cells will subsequently be cultured without stimulants, or stimulated with LPS + Pam3csk4 for 30 minutes, 1 hour, 2 hours, 4 hours, 8 hours, 12 hours, and 24 hours. Samples will then be processed for bulk RNA-sequencing as shown in the preliminary data (Figure 1A,B). Briefly, RNA will be harvested using a commercially available kit (Qiagen), and processed for cDNA double-strand synthesis, whole-transcriptome amplification, and library preparation (Shalek et al., 2014). Samples will be sequenced at the Caltech's Milliard and Muriel Jacobs Genetics and Genomics Core Facility on a HiSeq2500 machine (Illumina), using 50 base-pair paired-end sequencing. Sequencing reads will be aligned using TopHat and quantified using Cufflinks (Trapnell et al., 2010). Reads will then be analyzed in several ways, including analysis for differentially expressed genes between time points, enrichment of gene-ontology terms, and for expression of co-expressed gene networks in order to characterize the differences between cells with different durations of stimulation, and cells from young and aged mice. In this way, we seek to understand the transcriptional response of hematopoietic progenitors to acute inflammatory stimuli, and to elucidate the differences between how young and aged HSPCs respond to bacterial infections. Preliminary results from young progenitors suggest a clear and unique cell type transcriptional response to LPS + Pam3csk4, with differential changes in proliferation, differentiation, and inflammatory related genes (Figure 1 A, B).

Anticipated results: We expect a strong transcriptional response from aged and young progenitors alike, and a robust upregulation of several NF- κ B activated genes, since both LPS + Pam3csk4 are potent activators of the NF- κ B pathway. Importantly, we expect that

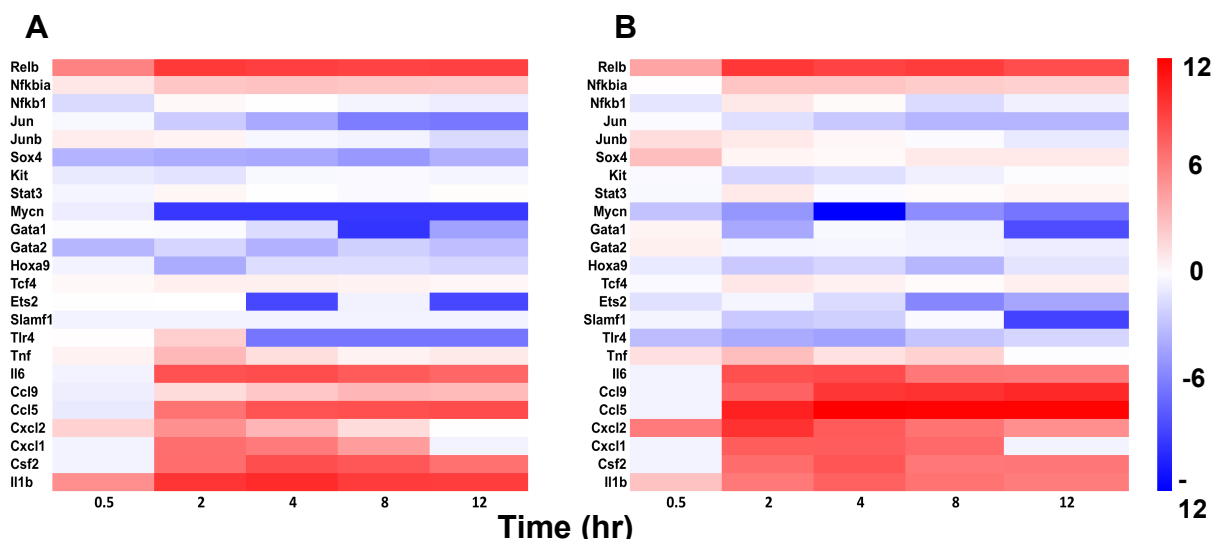


Figure 1. Transcriptomic analysis of bulk hematopoietic progenitors. Comparison between selected expressed genes in (A) ST-HSCs (LSK CD150⁻ CD48⁻) and (B) LT-HSCs (LSK CD150⁺ CD48⁻) in response to LPS + Pam3csk4 stimulation. Each cell type show a robust up-regulation of several known inflammatory genes, including cytokines such as IL-6, IL-1 β and TNF- α . Blue coloring indicates genes that are downregulated after stimulation, and red coloring indicates genes that are upregulated after stimulation, compared to no stimulation. Color bar represent fold change from no stimulation.

aged mice will show a strong predisposition to the production of myeloid-biased transcripts, including major cytokines such as IL-6 and TNF- α , which would be consistent with their well-established bias towards myeloid cell differentiation.

Potential pitfalls and solutions: We might find that there are few transcriptional differences between young and aged progenitor cells in response to TLR stimulation, in which case we will still have learned a significant amount about how these cells respond to acute inflammatory stimuli, and how this response changes with age. In addition, TLR2 and TLR4 ligands might not be the best acute inflammatory stimulants for early progenitors, in which case we will explore the expression of other TLR receptors, as well as cytokine and growth factor receptors on these cells and stimulate with their respective ligands for further analysis of the response of these progenitors to an inflammatory environment.

Subaim 1.2. Investigate the differences in gene expression and cytokine secretion between young and aged HSPCs in response to danger signals at the single-cell level.

Bulk analysis of HSPCs, while useful, masks an understanding of the way each individual cell behaves in an ageing hematopoietic system. By studying single cells, we are able to examine whether there is a transcriptionally-primed, clonally expanded subset of myeloid biased cells in an aged mouse, or if in fact all cells have similar molecular signatures, and specific environmental cues influence the differentiation potential of the cell.

Our preliminary work has demonstrated that young HSPCs are inherently heterogeneous in their secretion of inflammatory cytokines in response to LPS + Pam3csk4 stimulation (Figure 2A,B (Zhao et al., 2014)). Looking at multipotent progenitors (MPPs), we find that aged MPPs are less potent cytokine producers and secrete fewer cytokines per cell compared to young MPPs (Figure 2C). Importantly, aged cells secrete myeloid-biased cytokines, and do so in a much more homogenous manner than their young counterparts (Figure 2D). While these differences might reflect the lineage potential of these cells, this remains largely unexplored, especially in the context of aging. To better understand the molecular characteristics of the response of HSPCs, especially earlier progenitors like LT-HSCs and ST-HSCs, to danger signals, we will perform single-cell proteomic analysis of secreted cytokines, with concomitant single-cell transcriptome analysis using RNA-sequencing and single-molecule RNA fluorescent *in situ* hybridization (FISH) (Figure 2E,F).

Approach: To understand the process of aging at the single cell level we will apply a two-pronged approach for both young and aged hematopoietic progenitors: 1) we will

determine the relevant functional secreted and intracellular proteins from each individual cell using a single-cell barcode chip (SCBC) (Figure 2A) (Ma et al., 2011; Zhao et al., 2014) and 2) we will determine the transcriptional landscape of these same cells using parallel single-cell RNA-sequencing and single-molecule RNA FISH (in collaboration with Dr. Long Cai, Caltech) (Figure 2E,F). Cells from bone marrow, spleen, peripheral blood, and thymus will be collected from young (12 weeks) and aged (18-24months) mice. Hematopoietic cell populations will be characterized by FACS. We will then use the SCBC to analyze the secretion profile of up to 15 cytokines important in hematopoietic differentiation and immune cell function from long-term hematopoietic stem cells (Lineage-Sca1+cKit+CD150+CD48-), short-term hematopoietic stem cells (Lineage-Sca1+cKit+CD150-CD48-), multipotent progenitors (Lineage-Sca1+cKit+CD150-CD48+), as well as more committed progenitors such as lymphoid-primed multipotent progenitor (LMPPs), common myeloid progenitors (CMPs), granulocyte-macrophage progenitors (GMPs), common lymphoid progenitor cells (CLPs), and megakaryocyte-erythroid progenitor cell (MEPs). Cytokines of interest include but are not limited to GM-CSF, M-CSF, TGF- β , TNF- α , IL-2, IL-4, IL-6, IL-10, IL-12, and IFN- γ . Single cells are then indexed, picked, and processed for single-cell massive parallel RNA-sequencing (in collaboration with Dr. Aviv Regev, Broad Institute of MIT and Harvard) (Shalek et al., 2013; Yosef et al., 2013). This methodology allows us the unique ability to obtain proteomic and transcriptional information for the same single hematopoietic cell. This in turn can be used to determine the relationship between the transcriptional landscape of young and aged hematopoietic stem cells and their functional output, in terms of cytokine secretion. We have demonstrated the detection of both transcripts and proteins from the

same single cells (Figure 2C-F). Comprehensive transcriptomics will allow us to elucidate unique molecular events that govern hematopoietic cell fate decisions in old and young mice. Once gene networks have been identified, we will use single-molecule RNA FISH to validate our results and do absolute quantitation of genes of interest. Single-molecule RNA FISH enables us to analyze vast number of cells in different conditions and get absolute counts of RNA abundance for each gene within a cell (Singer et al., 2014). This allows us to obtain extremely high-resolution data that, along with RNA-sequencing, will help define the entire transcriptional landscape of young and aged progenitors. By utilizing single-molecule RNA FISH, we can focus our efforts on specific signaling pathways in a high-throughput manner that allows us to test many cells and experimental conditions.

Anticipated results: We anticipate, as our proteomic data already suggests (Figure 2), that aged hematopoietic stem cells have a myeloid biased gene expression signature, reflected in an expansion of single hematopoietic stem cells with biased myeloid differentiation potential. Importantly, we anticipate that several pathways implicated in ageing of the hematopoietic system, including TGF-signaling and cell-cycling, will be deregulated in aged hematopoietic stem cells.Potential pitfalls and solutions: It is possible that culturing cells for 12 hours to perform proteomic studies might severely alter the transcriptome of these cells; this in turn, might not be reflective of the transcriptome of hematopoietic stem cells *in vivo*. If we find that this is the case, we will significantly shorten the incubation time to 3-6 hours, as required. If necessary, we will also perform single-cell RNA-sequencing on cells directly sorted into RNA lysis buffer. While we won't get proteomic and transcriptome information from the same cell in this case, we will still learn a

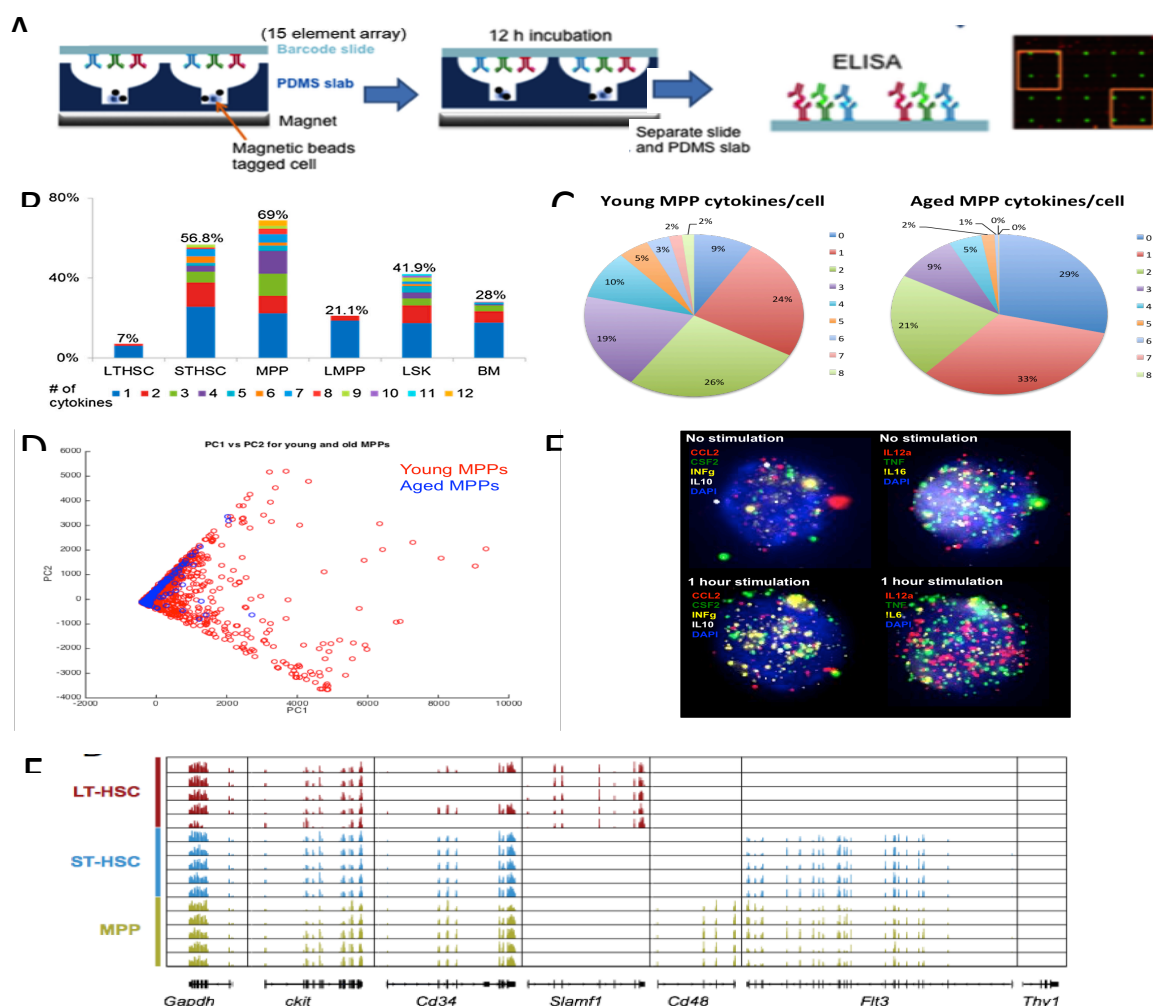


Figure 2. Transcriptomic and proteomic analysis of hematopoietic progenitors (A) Single-cell barcode chip (SCBC) analysis of hematopoietic progenitors. The SCBC contains >6000 microchambers, each designed with a central well in which a cell is localized. The microchip surface is coated with a cocktail of magnetic beads conjugated to anti-mouse-CD34, anti-mouse-cKit, or anti-mouse-Sca1 antibodies to hold the cells in place over a magnet. Unbound cells are washed off and the chip is sealed and incubated at 37°C in 5% CO₂ for 12 hrs. During incubation, secreted proteins are captured on a miniature 12-element antibody array, which is later developed using sandwich ELISA to record those secreted protein levels. Single cells are indexed by location and cytokine production, and may then be processed for RNA-sequencing. (B) Data from SCBC analysis. The six cell groups analyzed are BM (total BM cells), LSK cells, LMPPs (LSK CD34⁺Flt3^{hi}), MPPs (LSK CD34⁺Flt3^{int}), ST-HSCs (LSK CD34⁺Flt3⁻), and LT-HSCs (LSK CD34⁻Flt3⁻), all under LPS + Pam3CSK4 stimulation for 12 hrs. (C) Proportion of young and aged MPPs secreting certain numbers of cytokines. (D) Principal component analysis of young and aged MPPs: each data point represents a single cell and principal component 1 (PC1) explains the highest variation in cytokine secretion in the data set. Young MPPs are highly heterogeneous and aged MPPs are more uniform in their cytokine secretion profile. (E) Single-molecule RNA FISH performed on LT-HSCs for various cytokines before stimulation or after 1 hr of LPS + Pam3csk4 stimulation. (F) Single-cell RNA-sequencing traces from HSPCs processed as described in the text.

tremendous amount about the heterogeneous responses of aged and young HSPCs to danger signals.

Subaim 1.3. Elucidate the functional and lineage potential of young vs. old as well as acute and chronically inflamed HSPCs.

Our basic premise is that the hematopoietic stem cell pool changes its composition during mammalian aging: a change from a balanced HSC pool in young animals to a myeloid-biased pool in older animals. This change in HSC composition is one of the direct factors leading to a pro-inflammatory milieu in aging organisms.

It is uncertain, however, how each cell from the HSC pool contributes to this myeloid bias. We seek to determine if all old HSCs are programmed to be myeloid biased, or if a fraction of “youthful” cells within that population that behave like young HSCs exists. In this Subaim, we will further examine the change of the HSC pool at the proteomic and transcriptomic level during aging, as done in Subaim 1.2. We will use this information to define a precise cytokine production signature of different HSC subsets in young and aged mice. Once we are able to define different HSC subsets, we will isolate them for lineage and functional analysis in transplant studies *in vivo*. This methodology enables us to determine the differentiation potential of single cells with a known molecular signature, and has the potential to reveal new, un-described subpopulations within the HSC compartment.

Approach: We will isolate various subsets of hematopoietic stem and progenitor cells from young and old WT mice, define their cytokine secretion signature and examine their lineage potential and functional properties. From Subaim 1.2, we will have obtained the cytokine and transcriptomic signature of individual HSPCs and will be able to correlate different cytokine production profiles with transcriptomic signatures. To further understand the functional significance of HSPCs with different cytokine production profiles and transcriptomic signatures, we will recover individual cells based on their cytokine profile for measurement of their lineage potential and functional properties *in vivo*. We will use competitive repopulation assays, where we inject distinguishable cell mixtures (HSPCs with a known signature together with control young or old HSPCs) into irradiated recipients and measure the percentage of differentiated cells produced by each cell type. Blood will be collected from mice every month after injection, and analyzed for mature immune cell populations (such as with the surface markers CD11b, CD19, CD3 ϵ , and CD45) by flow cytometry. After 12 weeks, mice will be sacrificed and the homing and repopulation potential of HSPCs will be analyzed by quantifying long-term hematopoietic stem cells (Lineage-Sca1+cKit+CD150+CD48-), short-term hematopoietic stem cells (Lineage-Sca1+cKit+CD150-CD48-), and multipotent progenitors (Lineage-Sca1+cKit+CD150-CD48+), as well as more committed progenitors (such as LMPPs, CMPs, GMPs, CLPs, and MEPs). We will then determine whether HSPCs with different cytokine profiles display different functions and lineage potential in competitive repopulation studies carried out with acute as well as chronic inflammation environments. To this end, cells will be challenged *in vitro* prior to being transplanted into WT mice, to mimic challenge with an acute inflammatory stimulus, or be transplanted into recipient

mice in an established chronic inflammatory state. In particular, we will utilize recipient mice that have a genetic deletion in the interleukin-10 gene or the microRNA-146a gene, both of which have higher basal inflammatory state in most of their tissues (see Aim 2).

Anticipated Results: We expect to find disparate differentiation potential for HSPCs with the same membrane markers but different molecular signatures. We believe our approach will discover many different subpopulations with different functional properties and differentiation potential within each HSPCs population examined.

Potential pitfalls and solution: Single cell repopulation assays have low success rate and high rate of false negatives. If this will be the case, we will be able to inject up to 100 cells with similar cytokine signatures to each mouse. In addition, we will perform *in vitro* methycellulose differentiation assays for cells of similar cytokine signatures. Also, we note that LPS + Pam3csk4 stimulation may change the repopulation capacity of HSCs. If this becomes a major obstacle, we will utilize cells that have not been stimulated but express differing levels of basal cytokine secretion. Unstimulated cells tend to express fewer cytokines at much lower abundance; however, we will still be able to identify subsets of secreting cells by screening a much larger number of them.

Subaim 1.4. Characterize the cardinal molecular components associated with HSPCs aging.

Using the approaches described in Subaims 1.1 and 1.2, we will establish a comprehensive database of the molecular pathways important for the aging process of different HSPCs, in both normal and inflamed environments. We then plan to further understand the relevant contribution of selected pathways and genes to aging using genetic and pharmacologic manipulations. Using this approach, we will build an integrated model to capture the molecular basis of the aging process and might find potential pathways that can be used as targets for drug development.

Approach: We will first apply one of several approaches to identifying pathways important in regulating HSPC behavior with age. We will begin by studying differentially expressed genes using TopHat for sequence alignment, and Cufflinks for quantitation of genes (Trapnell et al., 2012). Of the genes that are differentially expressed, we will perform gene-ontology and gene-set enrichment analysis to identify pathways particularly affected by age and inflammatory status (Huang da et al., 2009; Subramanian et al., 2005). We will further identify modules of co-expression networks (working closely with Aviv Regev, MIT) as potential targets for perturbation (Novershtern et al., 2011). We will then apply loss and gain of function studies using a retroviral delivery system on the most differentially expressed molecular pathways and targets between young and aged mice identified from Subaims 1.1 and 1.2. Bone marrow cells from donor mice will be infected with retroviruses expressing the examined genes of interest for gain of function, or shRNA knockdown constructs for loss of function studies. The cells will then be injected into lethally irradiated mice. We will then determine whether genetic manipulation at these nodes may attenuate the detrimental effects of aging mice by repopulation assays as described in Subaim 1.3.

We will also test pharmacologic interventions that can act along these nodes as effective and safe anti-inflammatory drugs in aged mice, and compare their HSPC molecular signature to non-treated mice. During both genetic and pharmacologic interventions, we will study both the positive and negative effects of blocking inflammation on aging by regulating key inflammatory pathways. Importantly, we will investigate the effects of these perturbations in preventing age-related onset of immune diseases, such as autoimmunity and blood cancers, by using mouse models of chronic inflammation, as described in Subaim 2.1 and 2.2. Mice with a genetic deletion in the interleukin-10 gene or the microRNA-146a gene both have a predisposition to develop autoimmune disease, and in the case of microRNA-146a deletion, these mice develop myeloproliferative disorder and myeloid leukemias.

Anticipated results: We expect to reveal that genetic manipulation of a few discovered genetic nodes will lead to a phenotypic attenuation of the aging process both in WT and chronically inflamed mice.

Potential pitfalls and solution: It is reasonable to believe that some of the pathways discovered in this Subaim will also have a crucial role in the normal immune response, making them unsuitable for drug design. Nonetheless, understanding of the contribution of these pathways to HSPC function and aging is of great importance, and will lead us and others to further characterize the relevance of each gene in this process to HSPC aging.

References

- Huang da, W., Sherman, B.T., and Lempicki, R.A. (2009). Systematic and integrative analysis of large gene lists using DAVID bioinformatics resources. *Nature protocols* 4, 44-57.
- Ma, C., Fan, R., Ahmad, H., Shi, Q., Comin-Anduix, B., Chodon, T., Koya, R.C., Liu, C.C., Kwong, G.A., Radu, C.G., *et al.* (2011). A clinical microchip for evaluation of single immune cells reveals high functional heterogeneity in phenotypically similar T cells. *Nature medicine* 17, 738-743.
- Morrison, S.J., Wandycz, A.M., Akashi, K., Globerson, A., and Weissman, I.L. (1996). The aging of hematopoietic stem cells. *Nature medicine* 2, 1011-1016.
- Novershtern, N., Subramanian, A., Lawton, L.N., Mak, R.H., Haining, W.N., McConkey, M.E., Habib, N., Yosef, N., Chang, C.Y., Shay, T., *et al.* (2011). Densely interconnected transcriptional circuits control cell states in human hematopoiesis. *Cell* 144, 296-309.
- Rossi, D.J., Bryder, D., Zahn, J.M., Ahlenius, H., Sonu, R., Wagers, A.J., and Weissman, I.L. (2005). Cell intrinsic alterations underlie hematopoietic stem cell aging. *Proceedings of the National Academy of Sciences of the United States of America* 102, 9194-9199.
- Shalek, A.K., Satija, R., Adiconis, X., Gertner, R.S., Gaublomme, J.T., Raychowdhury, R., Schwartz, S., Yosef, N., Malboeuf, C., Lu, D., *et al.* (2013). Single-cell transcriptomics reveals bimodality in expression and splicing in immune cells. *Nature* 498, 236-240.
- Shalek, A.K., Satija, R., Shuga, J., Trombetta, J.J., Gennert, D., Lu, D., Chen, P., Gertner, R.S., Gaublomme, J.T., Yosef, N., *et al.* (2014). Single-cell RNA-seq reveals dynamic paracrine control of cellular variation. *Nature* 510, 363-369.
- Singer, Z.S., Yong, J., Tischler, J., Hackett, J.A., Altinok, A., Surani, M.A., Cai, L., and Elowitz, M.B. (2014). Dynamic heterogeneity and DNA methylation in embryonic stem cells. *Molecular cell* 55, 319-331.
- Subramanian, A., Tamayo, P., Mootha, V.K., Mukherjee, S., Ebert, B.L., Gillette, M.A., Paulovich, A., Pomeroy, S.L., Golub, T.R., Lander, E.S., and Mesirov, J.P. (2005). Gene set enrichment analysis: a knowledge-based approach for interpreting genome-wide expression profiles. *Proceedings of the National Academy of Sciences of the United States of America* 102, 15545-15550.
- Trapnell, C., Roberts, A., Goff, L., Pertea, G., Kim, D., Kelley, D.R., Pimentel, H., Salzberg, S.L., Rinn, J.L., and Pachter, L. (2012). Differential gene and transcript expression analysis of RNA-seq experiments with TopHat and Cufflinks. *Nature protocols* 7, 562-578.

Trapnell, C., Williams, B.A., Pertea, G., Mortazavi, A., Kwan, G., van Baren, M.J., Salzberg, S.L., Wold, B.J., and Pachter, L. (2010). Transcript assembly and quantification by RNA-Seq reveals unannotated transcripts and isoform switching during cell differentiation. *Nature biotechnology* 28, 511-515.

Yosef, N., Shalek, A.K., Gaublomme, J.T., Jin, H., Lee, Y., Awasthi, A., Wu, C., Karwacz, K., Xiao, S., Jorgolli, M., *et al.* (2013). Dynamic regulatory network controlling TH17 cell differentiation. *Nature* 496, 461-468.

Zhao, J.L., Ma, C., O'Connell, R.M., Mehta, A., DiLoreto, R., Heath, J.R., and Baltimore, D. (2014). Conversion of danger signals into cytokine signals by hematopoietic stem and progenitor cells for regulation of stress-induced hematopoiesis. *Cell stem cell* 14, 445-459.

Conversion of Danger Signals into Cytokine Signals by Hematopoietic Stem and Progenitor Cells for Regulation of Stress-Induced Hematopoiesis

Jimmy L. Zhao,^{1,5,*} Chao Ma,^{2,5} Ryan M. O'Connell,⁴ Arnab Mehta,¹ Race DiLoreto,² James R. Heath,^{2,3,*} and David Baltimore^{1,*}

¹Division of Biology and Biological Engineering, California Institute of Technology, 1200 East California Boulevard, Pasadena, CA 91125, USA

²NanoSystems Biology Cancer Center, California Institute of Technology, 1200 East California Boulevard, Pasadena, CA 91125, USA

³Kavli Nanoscience Institute, California Institute of Technology, 1200 East California Boulevard, Pasadena, CA 91125, USA

⁴Department of Pathology, University of Utah, 15 North Medical Drive East, Salt Lake City, UT 84112, USA

⁵These authors contribute equally to this work

*Correspondence: jzhao@caltech.edu (J.L.Z.), heath@caltech.edu (J.R.H.), baltimo@caltech.edu (D.B.)

<http://dx.doi.org/10.1016/j.stem.2014.01.007>

SUMMARY

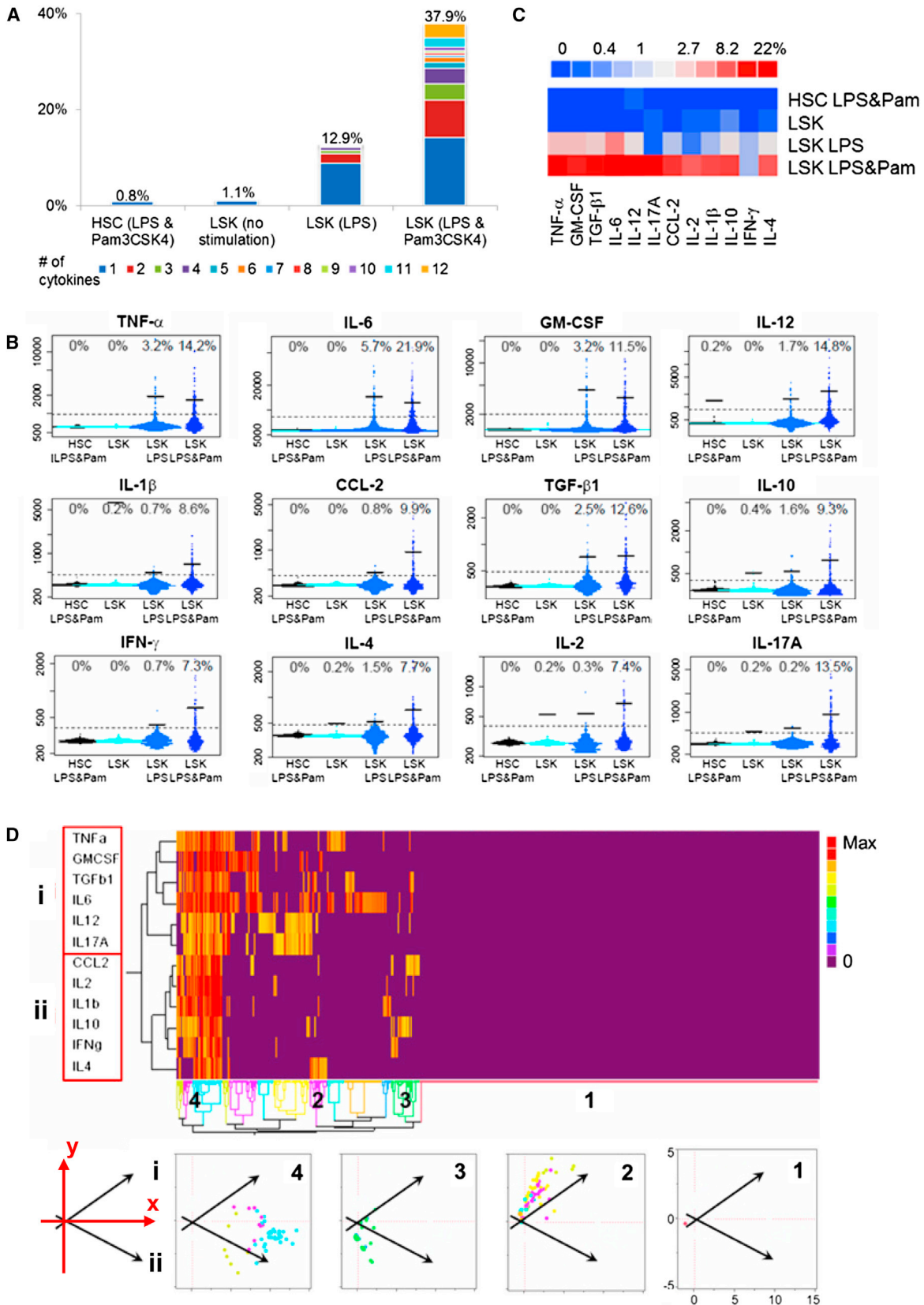
During an infection, the body increases the output of mature immune cells in order to fight off the pathogen. Despite convincing evidence that hematopoietic stem and progenitor cells (HSPCs) can sense pathogens directly, how this contributes to hematopoietic cell output remains unknown. Here, we have combined mouse models with a single-cell proteomics platform to show that, in response to Toll-like receptor stimulation, short-term HSCs and multipotent progenitor cells produce copious amounts of diverse cytokines through nuclear factor κ B (NF- κ B) signaling. Interestingly, the cytokine production ability of HSPCs trumps mature immune cells in both magnitude and breadth. Among cytokines produced by HSPCs, IL-6 is a particularly important regulator of myeloid differentiation and HSPC proliferation in a paracrine manner and in mediating rapid myeloid cell recovery during neutropenia. This study has uncovered an important property of HSPCs that enables them to convert danger signals into versatile cytokine signals for the regulation of stress hematopoiesis.

INTRODUCTION

Immune cells of the myeloid lineage are often considered the first responders of host defense against bacterial infection; meanwhile, hematopoietic stem and progenitor cells (HSPCs) may respond in a delayed fashion to ensure sufficient production of myeloid cells consumed during an infection. The response by HSPCs was originally thought to be of a passive response to the depletion of downstream immune cells, but more recent evidence suggests that HSPCs may participate directly by sensing systemically elevated cytokines through cytokine receptors and bacterial and viral components through Toll-like receptors (TLRs) (King and Goodell, 2011; Nagai et al., 2006).

It is well known that immune cells are potent cytokine producers upon encountering bacteria and viruses. When cytokines produced by immune cells and nonhematopoietic tissues accumulate to sufficient quantity, they circulate back to the bone marrow (BM) niche via blood circulation to activate HSPCs. Numerous cytokines, including IL-6, TNF- α , IFN- α , IFN- γ , TGF- β , and M-CSF, with the ability to regulate proliferation and differentiation of HSPCs have been identified (Baldrige et al., 2010, 2011; Challen et al., 2010; Essers et al., 2009; Maeda et al., 2009; Mossadegh-Keller et al., 2013; Pronk et al., 2011). On the other hand, it is clear now that HSPCs can also respond to TLR stimulation directly, leading to accelerated myeloid cell production in vitro (Nagai et al., 2006) and most likely in vivo as well (Megias et al., 2012). However, it remains unclear how direct pathogen sensing by HSPCs translates into signals directing myeloid differentiation under the stressed conditions. Conventional wisdom would suggest that TLR signaling activates lineage-specific transcriptional factors that can directly regulate differentiation within HSPCs. Currently, little is known about what transcription factors downstream of TLR activation might mediate this process. An alternative, but not mutually exclusive, hypothesis is that TLR stimulation activates a general proinflammatory program within HSPCs in order to induce cytokine production, which can act in an autocrine or paracrine manner to regulate differentiation.

In this study, we have combined extensive mouse genetics and a microfluidic single-cell proteomics platform to show that HSPCs can directly respond to bacterial components via the TLR/necrosis nuclear factor κ B (NF- κ B) axis, and, in response, HSPCs, specifically short-term HSCs (ST-HSCs) and multipotent progenitor cells (MPPs), produce copious amounts of cytokines. In addition, single-cell analysis shows that HSPCs contain heterogeneous subsets based on their different cytokine production profiles. The cytokine production ability of HSPCs is shown to be regulated by NF- κ B activity, given that p50-deficient HSPCs have significantly attenuated cytokine production, whereas miR-146a-deficient HSPCs display significantly enhanced cytokine production. Interestingly, HSPCs are significantly more potent cytokine producers in both breadth and quantity than the conventional known cytokine producers of the immune system, such as myeloid cells and lymphocytes.



(legend on next page)

Cell Stem Cell

HSPCs Regulate Myelopoiesis via Cytokines

Furthermore, we have shown that HSPCs possess TLRs, functional NF- κ B signaling, and cytokine receptors—an entire cascade of molecules necessary for translating danger signals into cytokine signals. Lastly, we have demonstrated the functional significance of HSPC-produced cytokines, especially IL-6, in promoting myelopoiesis *in vitro* and *in vivo* in neutropenic mice after chemotherapeutic treatment or BM transplant. We believe that this represents a previously underappreciated mechanism by which HSPCs convert danger signals encountered during an infection into a range of versatile cytokine signals in order to ensure efficient stress-induced hematopoiesis. This circumvents both the delay associated with having to wait for systemic cytokine accumulation and the need to “reinvent” the molecular circuitry within HSPCs in order to convert TLR activation into specific differentiation signals.

RESULTS

Heterogeneity in Cytokine Production Profile among Purified HSPCs

To test whether any of the HSPC populations have the capability of cytokine production, we adapted a high-throughput, microfluidic-based technology to quantify a panel of up to 15 secreted proteins at the single-cell level (Ma et al., 2011). HSPCs are rare cells in BM, with LSK cells (defined as Lin⁻Sca1⁺cKit⁺), a mixed population of long-term HSCs (LT-HSCs), ST-HSCs, MPPs, and lymphoid-biased MPPs (LMPPs) accounting for less than 1% and LT-HSCs accounting for less than 0.1% of the total nucleated BM cells. This microfluidic platform allowed us to simultaneously measure a large number of secreted proteins at the single-cell level from thousands of phenotypically defined cells. After sorting LSK cells and LT-HSCs (defined as LSK CD150⁺CD48⁻) with stringent gating criteria and reanalyzing the sorted fraction for purity (Figure S1A available online), we loaded the cells onto chips containing several thousand microchambers. After 12 hr of incubation with culture medium containing either lipopolysaccharide (LPS), a TLR-4 ligand, alone or with Pam3CSK4, a TLR-2 ligand, secreted proteins were quantified by an ELISA-based method (Ma et al., 2011). At this time, nearly all LSK cells remained undifferentiated by fluorescence-activated cell sorting (FACS) analysis (Figure S2). Interestingly,

although very few stimulated LT-HSCs produced cytokines, a significant fraction of LSK cells produced a wide range of cytokines upon TLR stimulation (Figures 1A–1C and S3). Cytokine production by LSK cells was stimulation dependent, given that few LSK cells had detectable secretion in the absence of stimulation. Furthermore, although LPS alone was sufficient to stimulate 12.9% of LSK cells to produce cytokines, a combination of LPS and Pam3CSK4 boosted the percentage to 37.9%, and many more cells secreted multiple cytokines, suggesting an additive effect of simultaneously stimulating multiple TLRs (Figures 1A–1C). Among the 12 cytokines studied, IL-6 was the most prominently induced and was secreted by 21.9% of LPS and Pam3CSK4-stimulated LSK cells, whereas the production of the other cytokines ranged from 7%–15% (Figures 1B and 1C).

Among the 12 cytokines in the panel, most are produced by multiple immune cell types. However, some cytokines, such as IL-2, IL-4, IL-17, and IFN- γ are mainly produced by lymphocytes, whereas IL-1 β , IL-6, IL-12, TNF- α , and GM-CSF are more abundantly produced by cells of the myeloid lineage (Janeway et al., 2001). Interestingly, when unsupervised clustering analysis was performed on LSK cells, it identified two main cytokine clusters: a cytokine cluster (group i) including IL-6, TNF- α , IL-12, and GM-CSF that resembles the production profile of myeloid cells, and a cytokine cluster (group ii) including IL-2, IL-4, IL-10, and IFN- γ that resembles the production profile of lymphocytes (Figure 1D). LSK cells were divided into multiple functional subsets differing in their ability to produce group i and group ii cytokines, ranging from nonproducers (Figure 1D, subset 1), group i producers (Figure 1D, subset 2), group ii producers (Figure 1D, subset 3), to superproducers of all cytokines (Figure 1D, subset 4). When the cells from the four subsets were plotted onto the 2D principal component plane with the two vectors representing the two cytokine groups, subset 2 cells fell into the group i direction, and subset 3 cells fell into the group ii direction, whereas subset 4 cells fell between the two vector directions (Figure 1D, bottom), demonstrating once again the differential cytokine secretion profiles among LSK cells.

LSK cells represent a heterogeneous population comprising LT-HSCs, ST-HSCs, MPPs, and LMPPs. They represent cells along a differentiation tree with successive loss of self-renewal ability while still retaining the full potential to replenish most, if

Figure 1. Single-Cell Analysis of Cytokine Production by WT HSPCs in Response to TLR Stimulation

(A–D) Data from single-cell cytokine chip analysis. The four cell groups analyzed are HSCs with LPS and Pam3CSK4, LSK cells with medium only, LSK cells with LPS, and LSK cells with LPS and Pam3CSK4 stimulation for 12 hr. LSK is defined by Lin⁻Sca1⁺cKit⁺, and HSC is defined by LSK CD150⁺CD48⁻.

(A) Polyfunctionality and population-level statistics of the cell types analyzed. The percentage of cells secreting different number of cytokines is shown for each cell type studied. Different colors represent cells producing different number of cytokines from 1 to 12 (labeled with different colors); the number on top of each cell type shows the total percentage of cells secreting detectable amount of any of the 12 cytokines.

(B) Comparison of HSCs and LSK cells by individual cytokine. Each plot is composed of several thousand individual dots from several thousand single cells. The four cell groups arranged from left to right are HSCs under LPS and Pam3CSK4 stimulation (black), LSK cells with no stimulation (cyan), LSK cells with LPS stimulation only (light blue), and LSK cells with LPS and Pam3CSK4 stimulation (dark blue). The numbers on top represent the percentage of cytokine-producing cells identified by the gate (the dotted line), and the bars represent the mean intensity of only the cytokine-producing cells (average intensity of the cells above the dotted line).

(C) A summary heat map showing the percentage of HSCs and LSK cells that secrete any individual cytokine under different stimulations.

(D) Clustering analysis of WT LSK cells under LPS and Pam3CSK4 stimulation with results presented as heat maps and scatter plots. The data are analyzed by two-way hierarchical clustering that groups similar proteins and cells together. The grouping is shown by the tree structure for both proteins and cells. Each row represents an individual cytokine, and each column represents an individual cell. The result is presented by a heat map with colors representing the amount of cytokine secretion from purple (undetectable) to yellow (intermediate) to red (maximum). Two major groups of proteins (i and ii) and four main groups of cells (1 to 4) are identified. Each cell group is replotted onto the 2D principal component plane. This reduced space is the one that can explain the largest fraction (65%) of the information from the data. The arrows indicate the directions of the two cytokine functional groups aligned to the x and y axes.

See also Figures S1–S3.

not all, hematopoietic cells (Adolfsson et al., 2005; Forsberg et al., 2006). Next, we asked whether the LSK heterogeneity based on cytokine production profile correlates with known HSPC subsets. To study this, we separately purified LT-HSCs (LSK Flt3⁻CD34⁻), ST-HSCs (LSK Flt3⁻CD34⁺), MPPs (LSK Flt3^{int}CD34⁺), and LMPPs (LSK Flt3^{hi}CD34⁺) from the LSK population and analyzed their cytokine secretion with the single-cell microfluidic chips (Figures 2 and S4). We confirmed that LT-HSCs lacked cytokine production with the use of a set of stem cell markers different from those used in Figure 1 because of controversy over what set of markers best defines HSCs. In comparison, ST-HSCs and MPPs were potent cytokine producers, whereas more differentiated LMPPs produced rather modest levels of cytokines (Figures 2A–2C and S4). Furthermore, similar to unfractionated LSK cells, ST-HSCs and MPPs remained heterogeneous in terms of cytokine production profile (Figure S4A). These results were succinctly summarized with principal component analysis in order to reduce the 12-dimensional cytokine intensity data set from six different BM subsets down to two principal components (Figures 2D and 2E). Principal component 1 (PC1) represents a measure of the overall cytokine secretion ability of a cell and is positively correlated with the intensity of each of the 12 cytokines (Figure S4C). When LT-HSCs, ST-HSCs, MPPs, and LMPPs along with unfractionated LSK cells and total BM were compared along PC1, a majority of LT-HSCs and LMPPs were clustered at the lower end of PC1, indicating very low overall cytokine secretions, whereas ST-HSCs and MPPs contained a large fraction of high cytokine secretors (Figure 2D). Principal component 2 (PC2) is a measure of cytokine secretion bias and is positively correlated with lymphoid cytokines (Figure S4D) but negatively correlated with myeloid cytokines (Figure S4E). When the six cell types were compared along PC2, LSK cells, ST-HSCs, and MPPs were heterogeneous with relatively even distribution across PC2, indicating that they contained a mixture of nonproducers, myeloid cytokine-biased, lymphoid cytokine-biased, and balanced producers. In comparison, unfractionated BM cells showed moderate myeloid-cytokine bias, and LMPPs showed moderate lymphoid-cytokine bias (Figure 2E). It is known that HSCs defined by current best cell-surface markers represent a heterogeneous population with biased myeloid or lymphoid lineage potential (Beerman et al., 2010; Challen et al., 2010; Copley et al., 2012). A recent study using a single-cell barcode technology also demonstrated the highly heterogeneous nature of the LMPP population (Naik et al., 2013). To add to the complexity, we have now shown that ST-HSCs and MPPs contain heterogeneous subsets based on their cytokine secretion profile. It is reasonable to speculate that the skewed cytokine production ability of ST-HSCs and MPPs may also reflect a biased lineage potential. Unfortunately, the current chip design does not allow us to recover the various cell subsets on the basis of their cytokine secretion profile for functional and lineage potential analysis. The possible relationship between the heterogeneous cytokine production ability and their lineage potential and functional capacity represents a future direction for research.

Regulation of HSPC Cytokine Production by NF- κ B

NF- κ B is a family of transcription factors central to the regulation of inflammation and immune cell activation. Almost three de-

acades of research has elucidated many key physiological functions of NF- κ B in innate and adaptive immune cells as well as its involvement in the pathogenesis of many immunological diseases (Baltimore, 2011). However, much less is known about the physiological function of NF- κ B in HSPCs during inflammation. Because both LPS and Pam3CSK4 can activate NF- κ B, which in turn can upregulate the transcription of many inflammatory cytokines in mature immune cells, we suspected that NF- κ B might also regulate cytokine production in HSPCs. To test this, we first determined whether the important components of the TLR/NF- κ B pathway were expressed at the protein level in HSPCs. Using a transgenic mouse that has a knockin of a RELA-GFP fusion protein at the endogenous locus (De Lorenzi et al., 2009), we found that all LT-HSCs and LSK cells were GFP⁺, indicating that all HSPCs express RELA (also known as p65) protein, a key subunit of NF- κ B (Figure 3A). Then, we showed that both TLR-2 and TLR-4 receptors were expressed on the surface of LSK cells, and a subset of them express both receptors (Figure 3B), a finding consistent with previous reports (Nagai et al., 2006). Next, we asked whether HSPCs have functional NF- κ B activity upon TLR stimulation. To study this, we took advantage of a different transgenic NF- κ B-GFP reporter mouse, one with GFP expression under the control of the NF- κ B regulatory elements (Magnez et al., 2004). LPS stimulation *in vivo* upregulated GFP expression from 8% basally to 35%–40% in both LSK cells and LT-HSCs (Figures 3C and 3D). More directly, when purified LSK cells and LT-HSCs were stimulated with LPS and Pam3CSK4 *in vitro*, NF- κ B activation was again evident by both the percent of GFP⁺ cells and mean fluorescence intensity (Figures 3E and 3F). These results demonstrate that both LSK cells and LT-HSCs contain functional TLR/NF- κ B signaling that can be directly activated by TLR-4 and TLR-2 ligands.

To determine whether NF- κ B regulates cytokine production in LSK cells, we took advantage of mice deleted for genes important to the NF- κ B pathway. NFKB1 (also known as p50) is one of the main subunits of the NF- κ B family of transcription factors, and p50 deficiency results in defective NF- κ B activity in various immune cells (Sha et al., 1995). In contrast, miR-146a is an important negative regulator of NF- κ B activation by targeting its upstream signaling transducers TRAF6 and IRAK1. Thus, deficiency in miR-146a leads to enhanced NF- κ B activity (Boldin et al., 2011; Zhao et al., 2011, 2013). When we subjected LSK cells from *Nfkb1*^{-/-} mice (p50 knockout [KO]) and *Mir146a*^{-/-} mice (miR KO) to the single-cell chip analysis, we found that production of all 12 cytokines was significantly attenuated in p50 KO LSK cells and enhanced in miR KO LSK cells in comparison to wild-type (WT) LSK cells (Figures 4A–4C and S3). Although 37.9% of WT LSK cells produced cytokines under costimulation, the percentage rose to an impressive 69.7% in miR KO and dropped to a mere 2.4% in p50 KO LSK cells (Figure 4A). Furthermore, the percentage of cytokine-producing LSK cells in *Mir146a*^{-/-} *Nfkb1*^{-/-} (miR/p50 double knockout [DKO]) mice was less than in WT mice, indicating that the lack of p50 is dominant over miR-146a deficiency (Figures 4A–4C and S3). In addition to the percentage of responding cells, the amount of cytokines produced on a per-cell basis was also enhanced in miR KO LSK cells and reduced in p50 LSK cells for all the proinflammatory cytokines (Figure 4B). These data demonstrate that cytokine production in LSK cells is regulated by the level of

Cell Stem Cell

HSPCs Regulate Myelopoiesis via Cytokines

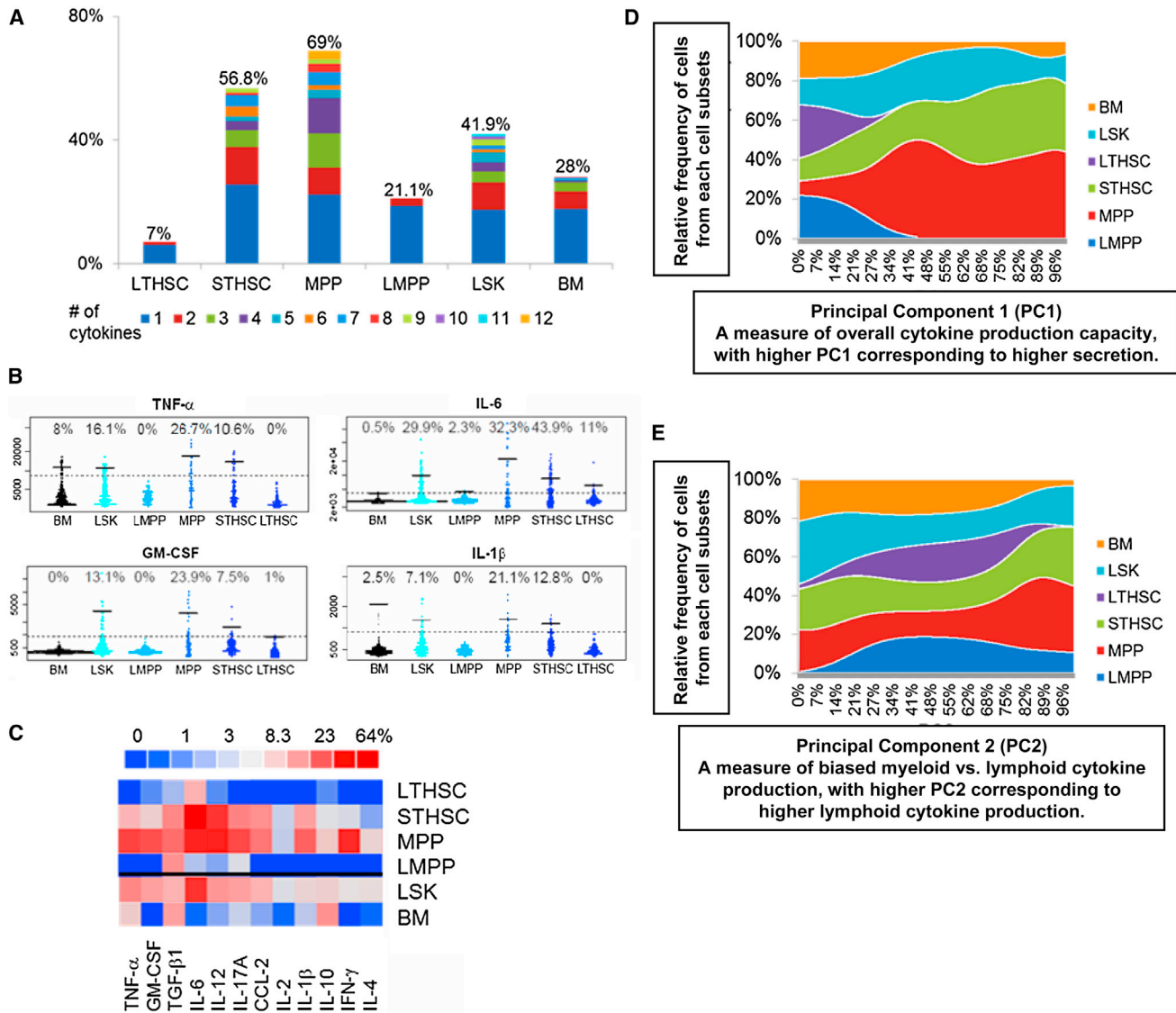


Figure 2. Single-Cell Analysis of Cytokine Production by Various HSPC Subsets in Response to TLR Stimulation

(A–E) Data from single-cell cytokine chip analysis. The six cell groups analyzed are BM (total BM cells), LSK cells, LMPPs (LSK CD34⁺Flt3^{hi}), MPPs (LSK CD34⁺Flt3^{int}), ST-HSCs (LSK CD34⁺Flt3⁻), and LT-HSCs (LSK CD34⁻Flt3⁻), all under LPS and Pam3CSK4 stimulation for 12 hr.

(A) Polyfunctionality and population-level statistics of the cell types analyzed. The percentage of cells secreting different number of cytokines is shown for each cell type studied. Different colors represent cells producing different number of cytokines from 1 to 12 (labeled with different colors); the number on top of each cell type represents the total percentage of cells secreting detectable amount of any of the 12 cytokines.

(B) Comparison of HSPC subsets by individual cytokines. Four out of 12 cytokines are shown here, and the rest are shown in Figure S4B. Each plot is composed of several thousand individual dots from several thousand single cells. The six cell groups arranged from left to right are total BM, LSK cells, LMPPs, MPPs, ST-HSCs, and LT-HSCs under LPS and Pam3CSK4 stimulation. The numbers on top represent the percentage of cytokine-producing cells identified by the gate (the dotted line), and the bars represent the mean intensity of only the cytokine-producing cells (average intensity of the cells above the dotted line).

(C) A summary heat map showing the percentage of the six groups of cells that secrete any individual cytokine under different stimulations.

(D and E) Principal component analysis of all six cell groups that reduce a 12-dimensional cytokine data set from six different cell groups into two principal components (PC1 and PC2).

(D) PC1 represents the overall cytokine production capacity of a cell and is positively correlated to the overall intensity of all 12 cytokines (see Figure S4C). After all 12 cytokine intensities of each cell are converted into a single PC1 value, the relative frequency of cells with each PC1 value is calculated for all six cell subsets. Graphs show the relative frequency of cells (y axis) of the six cell groups against PC1 (x axis). Each cell type is represented by a different color.

(E) PC2 represents the level of biased cytokine production profile and is positively correlated to the lymphoid group of cytokines, including IL-2, IL-17a, IL-4, IL-12, IL-1 β , and IFN- γ , but is negatively correlated to the myeloid group of cytokines, including TNF- α , IL-6, and GM-CSF (see Figures S4D and S4E). Graphs show the relative frequency of cells (y axis) of the six cell groups against PC2 (x axis). Each cell type is represented by a different color.

See also Figure S4.

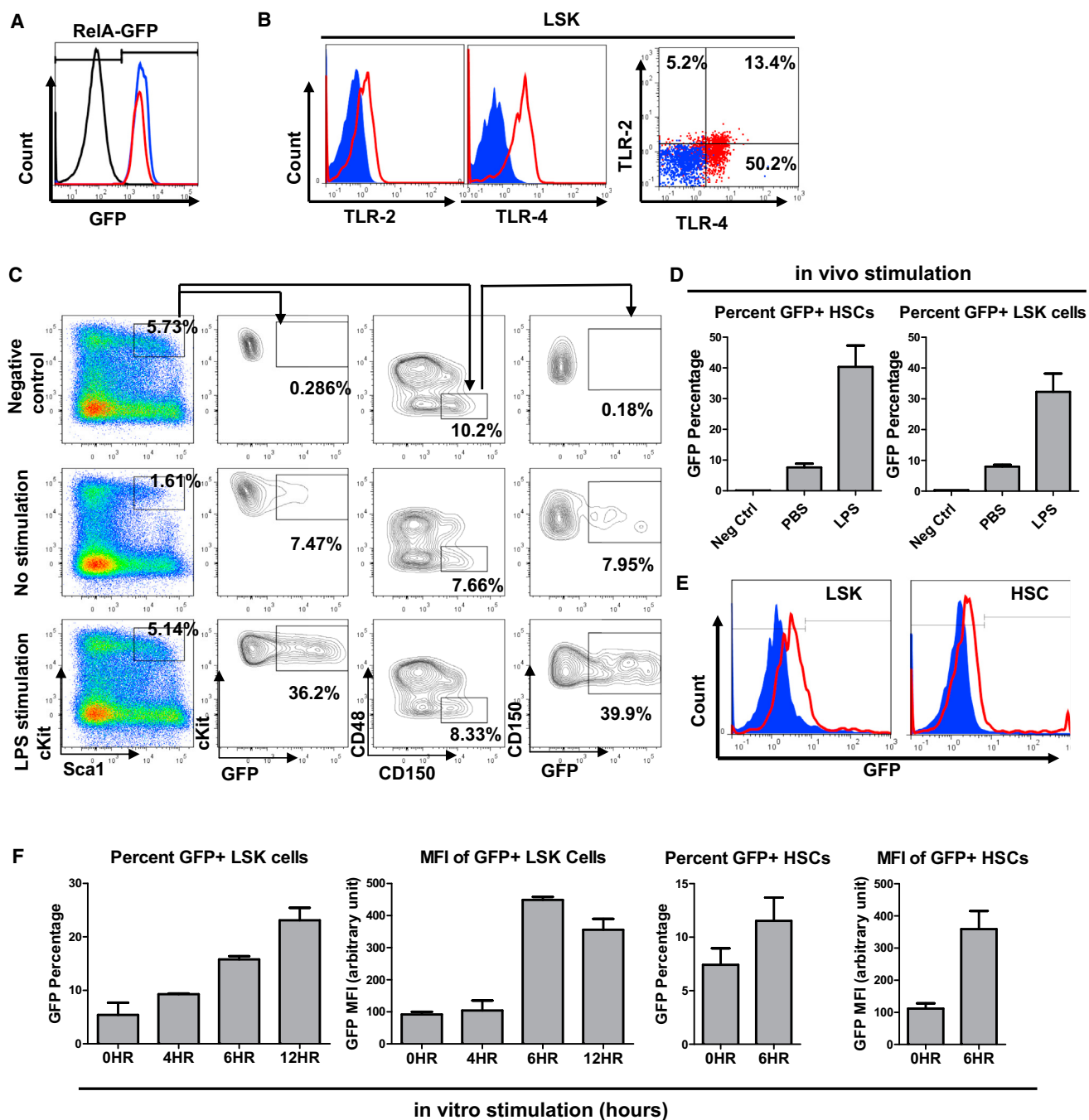


Figure 3. NF-κB Activation through TLRs in HSPCs

(A–F) Data from FACS analysis.

(A) Representative FACS histogram of LSK cells (blue) and HSCs (LSK CD150⁺CD48⁻; red) from RELA-GFP transgenic mice. LSK cells from a WT C57Bl/6 mice were used as a negative control (black).

(B) Representative FACS plots of TLR-2 and TLR-4 surface expression of WT LSK cells. Blue represents isotype antibody control, and red represents fluorescence-conjugated antibodies against TLR-2 (left), TLR-4 (middle), or both (right).

(C–F) Determination of TLR and NF-κB functionality in LSK cells and HSCs with mice in which GFP production is under NF-κB regulatory control.

(C and D) Experiments from in vivo stimulation.

(C) LPS-stimulated WT mouse is used as a negative control (top row) for GFP expression. No stimulation (middle row) corresponds to PBS-treated NF-κB-GFP transgenic reporter mice. LPS stimulation (bottom row) corresponds to LPS-stimulated NF-κB-GFP transgenic reporter mice (2 mg/kg body weight LPS for 6 hr).

(D) Quantification of GFP⁺ percentages in LSK cells and HSCs from negative control, unstimulated, and LPS-stimulated NF-κB-GFP transgenic reporter mice (n = 3).

(E and F) Experiments from in vitro stimulation of purified LSK cells and HSCs.

(legend continued on next page)

Cell Stem Cell

HSPCs Regulate Myelopoiesis via Cytokines

NF- κ B activity. Tuning the NF- κ B activity up or down is sufficient to increase or decrease the cytokine production of LSK cells in response to TLR stimulation. We also measured the coproduction of any two cytokines at the single-cell level (Figures 4D and 4E). Correlation coefficients (R values) were calculated for all cytokine pairs for WT, p50 KO, and miR KO LSK cells, higher R values indicating tighter coregulation. In general, WT LSK cells showed higher correlation coefficients than either p50 KO or miR KO LSK cells, indicating a better coregulation of these cytokines (Figure 4E, green blocks). This may be functionally important, given that many of these cytokines are often produced together by a single cell; e.g., myeloid cells produce TNF- α , IL-6, and IL-12 during an inflammatory response, and CD4 T_{H1} cells produce IL-2 and IFN- γ . Imbalance in cytokine levels could lead to undesired effects and pathologies. When we performed a principal component analysis on LSK cells of all genotypes, a myeloid cytokine group including IL-6, TNF- α , IL-1 β , and GM-CSF and a lymphoid cytokine group including IL-2, IL-4, and IL-17a were again identified (Figure 4F). Plotting the measurements onto the dominant 2D principal component space revealed diminished production of both groups of cytokines in p50 KO LSK cells and enhanced production in miR KO LSK cells. Interestingly, enhancement in the myeloid component was even more prominent in miR KO LSK cells, suggesting miR-146a-deficient LSK cells have especially enhanced myeloid cytokine production. Overall, these results demonstrate that TLR-stimulation-mediated cytokine production in HSPCs is exquisitely regulated by the level of NF- κ B activity.

Functional Significance of HSPC-Produced Cytokines in Regulating Myelopoiesis In Vitro

Cytokines produced by HSPCs are also produced by mature immune cells in the BM and periphery. However, we hypothesize that the location of HSPCs in the stem cell niche may represent an inherent advantage, allowing HSPC-produced cytokines to efficiently regulate their own fate in a more timely fashion during an infection or inflammatory challenge. To assess the functional significance of HSPC-produced cytokines, we first compared the cytokine production capacity of LSK cells with that of more differentiated progenitor cells and mature immune cells. To this end, purified LSK cells and lineage-committed progenitor cells (Lin⁻cKit⁺Sca1⁻ and Lin⁻cKit⁻Sca1⁺) from BM as well as CD11b⁺ myeloid, CD4⁺ T, CD8⁺ T, and B220⁺ B cells from spleen were stimulated with LPS plus Pam3CSK4 for 24 hr. Then, culture medium was collected for multiplexed ELISA in order to measure a panel of 15 cytokines. Surprisingly, in the absence of survival and proliferative advantage after stimulation (Figure S5A), LSK cells produced far more cytokines in both quantity and breadth than mature myeloid and lymphoid cells in 24 hr with LPS and Pam3CSK4 stimulation. More impressively, even with much stronger stimuli, such as CpG, anti-CD3 and anti-CD28, or 100-fold more LPS, T, B, and myeloid cells were still significantly less potent cytokine producers than LSK cells (Figure 5A). In addition, LSK cells produced a wide range of myeloid and

lymphoid cytokines, whereas mature myeloid cells and lymphocytes showed narrower cytokine production profile.

Next, we determined whether the cytokines produced by HSPCs are able to influence hematopoiesis in vitro. First, we showed that a fraction of LT-HSCs, LSK cells, and myeloid progenitor cells expressed various cytokine receptors, including IL-6R α , IFN- γ R, TNF-R1, and TNF-R2, on their surfaces (Figure S6A). This is consistent with previous studies that provided direct and indirect evidence of cytokine receptor expression in HSPCs (Baldridge et al., 2010, 2011; Maeda et al., 2009; Pronk et al., 2011). Next, we measured myeloid differentiation of LSK cells under LPS and Pam3CSK4 stimulation. Using an IL-6 neutralizing antibody, we were able to determine the effect of taking away IL-6 produced by LSK cells on myelopoiesis (Figures 5B and 5C). Interestingly, in comparison to the isotype antibody control, the neutralization of IL-6 had a significant effect on myeloid differentiation. Specifically, the percent of CD11b⁺ cells produced from LSK cells decreased by about 50%, and the number of CD11b⁺ cells showed a 2-fold reduction over a 4-day period (Figures 5B and 5C). To extend the study to include several other abundantly produced cytokines, we found that the neutralization of TNF- α or GM-CSF, but not IFN- γ , also had an inhibitory effect on the generation of myeloid cells (Figures 5D and 5E). Interestingly, neutralization of IL-6, IFN- γ , or GM-CSF all decreased the number of LSK cells, suggesting that these cytokines produced by LSK cells have a positive effect on their own proliferation and/or survival (Figure 5E). It is worth noting that we have previously shown that IL-6 can directly induce LSK cell proliferation by BrdU incorporation (Zhao et al., 2013). To further demonstrate the functional importance of HSPC-produced cytokines, we compared cytokines produced by BM cells that were depleted of HSPCs to that of total BM cells in inducing myelopoiesis. To this end, we stimulated equal number of total BM cells and Sca1-depleted BM cells with LPS and Pam3CSK4 in vitro for 24 hr and then used the conditioned media to stimulate LSK cells. We saw up to 40% reduction in the number CD11b⁺ myeloid cells after only 2 days of incubation with conditioned medium from Sca1-depleted BM cells (Figure 5F). This suggests that HSPCs, accounting for less than 1% of total BM cells, make a significant contribution to the cytokine milieu and have a stimulatory effect on myelopoiesis. Instead of depleting cytokine, we next asked whether increased cytokine production by LSK cells could enhance myelopoiesis. To this end, we used miR-146a-deficient LSK cells that showed exaggerated cytokine production (Figure 4). Purified LSK cells from WT or miR KO mice were stimulated with LPS and Pam3CSK4 in vitro for 24 hr, and then the conditioned media were used to stimulate newly purified WT LSK cells. After 2 days, we saw a modest but consistent increase in numbers of both LSK cells and CD11b⁺ cells when WT LSK cells were cultured with miR KO-LSK-cell-conditioned medium in comparison to WT-LSK-cell-conditioned medium (Figure 5G). This suggests that with just 24 hr of cytokine accumulation, the exaggerated cytokine production by miR KO LSK

(E) Representative FACS histograms of LSK cells and HSCs sorted from NF- κ B-GFP transgenic reporter mice. Blue represents unstimulated LSK cells or HSCs and red represents cells stimulated in vitro with LPS (100 ng/ml) for 6 hr.

(F) Quantification of GFP⁺ percentages and GFP mean fluorescence intensity of LSK cells at 0, 4, 6, and 12 hr and HSCs at 0 and 6 hr (n = 3). Data are presented as mean \pm SEM.

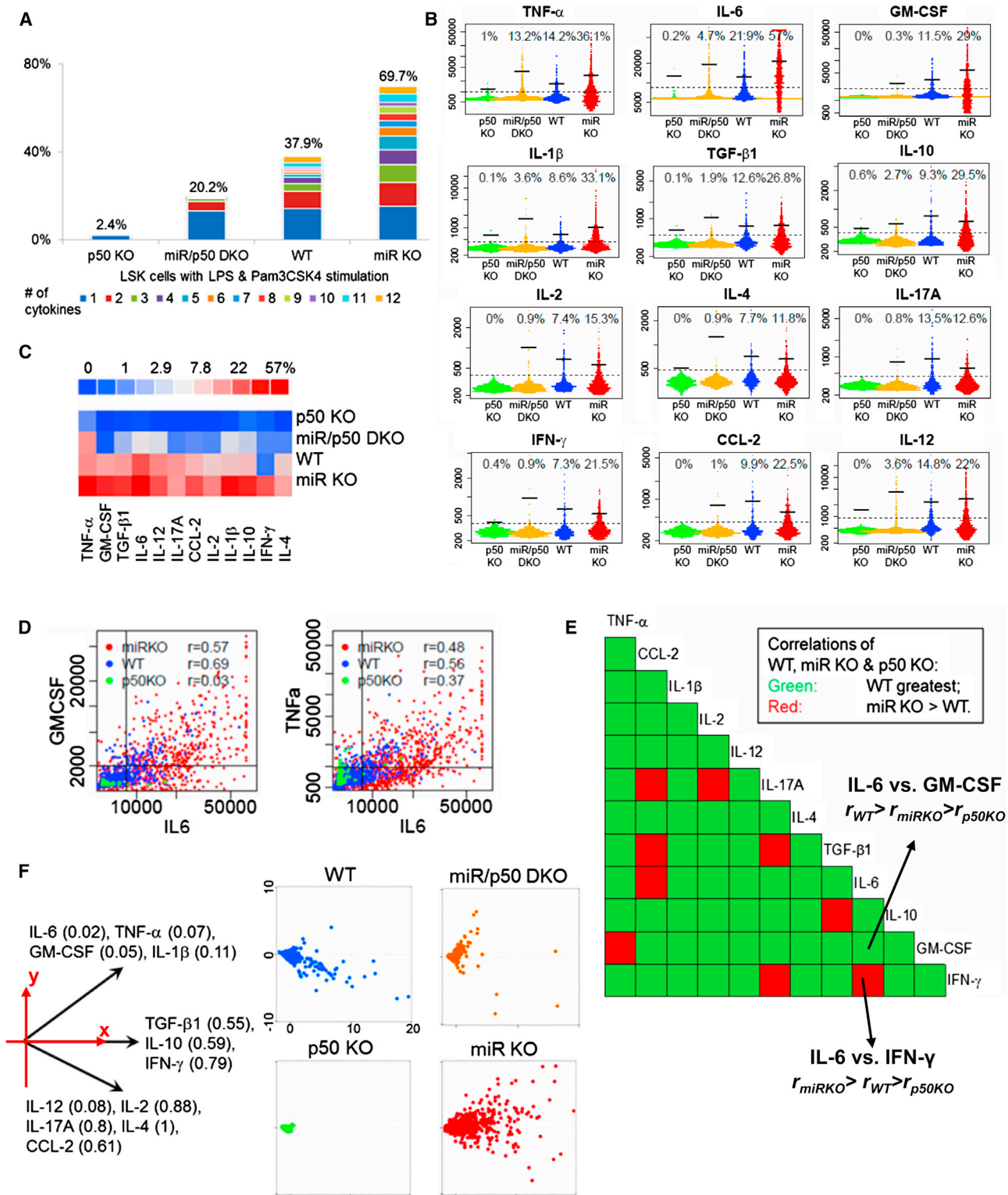


Figure 4. Regulation of HSPC Cytokine Production by NF- κ B

(A–F) Data from single-cell cytokine chip analysis. LSK cells were sorted from WT, *Nfkb1*^{-/-} (p50 KO), *Mir146a*^{-/-} (miR KO), and *Nfkb1*^{-/-}*Mir146a*^{-/-} (miR/p50 DKO) mice and were stimulated with LPS and Pam3CSK4 for 12 hr.

(A) Polyfunctionality and population level statistics of LSK cells of different genetic models. The percentage of LSK cells secreting a different number of cytokines is shown for each cell type studied. Different colors represent cells producing different number of cytokines from 1 to 12 (labeled by different colors); the number on top of each cell type represents the total percentage of cells secreting detectable amount of any cytokine.

(legend continued on next page)

cells is sufficient to support enhanced myelopoiesis and LSK cell proliferation and/or survival. Consistent with this *in vitro* finding, miR KO mice exhibit a significant myeloproliferative disease after chronic inflammatory stimulation as a result of enhanced HSPC proliferation and myeloid differentiation, whereas deleting IL-6 in miR KO mice effectively ameliorates the myeloproliferative condition (Zhao et al., 2013). Complementing our previous reports that have shown the involvement of hyperactivated T cells and myeloid cells in miR-146a-deficiency-mediated pathologies (Zhao et al., 2011, 2013), this study shows that exaggerated cytokine production by miR-146a-deficient HSPCs is also a contributor to enhanced myelopoiesis in miR-146a KO mice.

Functional Significance of HSPC-Produced Cytokines in Regulating Myelopoiesis *In Vivo*

In addition to *in vitro* functional significance, we next determined whether HSPC-produced cytokines are important in regulating hematopoiesis *in vivo*. Because current technology does not allow us to delete a cytokine specifically and selectively in stem and progenitor cells while allowing cytokine production in mature cells, to overcome this hurdle, we have created leucopenic conditions *in vivo* in which mature myeloid and lymphoid cells are severely depleted, whereas stem and progenitor cells are preserved. We created these conditions in mice by injecting a chemotherapeutic drug, 5-fluorouracil (5-FU) (Figures 6A–6C) or by transplanting stem and progenitor cells after lethal irradiation (Figures 6D–6F). LPS was injected into mice in order to stimulate myelopoiesis when neutropenia became the most severe, as measured by periodic sampling of peripheral blood. 5-FU is a chemotherapeutic drug that induces a significant reduction in mature cells in both BM and periphery while stimulating stem and progenitor cells to cycle (Harrison and Lerner, 1991). After 5-FU injection, myeloid cells started to decline, and, by day 5, 80% of myeloid cells were depleted in WT, miR-146a KO, IL-6 KO, and miR-146a/IL-6 DKO mice (Figure 6A). At this time, low-dose LPS was injected in order to stimulate myelopoiesis. Consistent with *in vitro* studies, IL-6 KO mice showed a 2-fold decrease in CD11b⁺ and Gr1⁺ myeloid cells, whereas miR KO mice showed a modest increase in comparison to WT mice (Figures 6B and 6C). In addition, DKO mice showed a similar level of reduction as IL-6 KO mice, indicating that loss of IL-6 is the dominant factor. To perform stem cell transplant, 500,000 purified Lin[−]cKit⁺ cells from WT, miR KO, IL-6 KO, or miR/IL-6 DKO

mice were injected into lethally irradiated WT recipient mice. All four groups of mice showed severe leucopenia 6 days after irradiation and cell injection, and approximately 8,000 myeloid cells and 20,000 total white blood cells were left in the peripheral blood. This represented less than 1% of the normal level and 4% of the number of transplanted HSPCs (Figures 6D–6F). LPS stimulation promoted myelopoiesis that was mildly increased in mice receiving miR KO HSPCs but was significantly attenuated in mice receiving IL-6 KO or miR/IL-6 DKO HSPCs, indicating that IL-6 produced by HSPCs is an important factor in promoting myeloid cell recovery during neutropenia (Figures 6D–6F). Overall, these *in vivo* experiments show that, in mice with severe leucopenia, LPS-stimulated production of cytokines, especially IL-6, by endogenous or transplanted HSPCs has a significant positive impact on stress-induced myelopoiesis.

Within the BM niche, we speculate that the cytokines released by HSPCs upon TLR stimulation can act on themselves or neighboring HSPCs. To further delineate whether HSPC-produced cytokines mediate hematopoiesis predominantly through an autocrine or paracrine fashion, we injected NF- κ B-GFP reporter mice with both LPS and BrdU in order to determine the relationship between cytokine-producing HSPCs and proliferating HSPCs. GFP expression, an indicator of NF- κ B activation and cytokine production, and BrdU incorporation, a marker of proliferation, were costained in myeloid progenitor cells, LSK cells, and LT-HSCs at 4, 12, and 24 hr (Figure 6G). The result showed that LSK cells and LT-HSCs rapidly turned on NF- κ B in response to LPS stimulation, whereas myeloid progenitor cells went into cycle quickly. As time elapsed, LT-HSCs and LSK cells started to proliferate, whereas NF- κ B activity gradually dampened. Interestingly, throughout the stimulation, cells with NF- κ B activity and cells that rapidly proliferated represented two largely nonoverlapping populations in all the stem and progenitor subsets. Although this result has multiple potential interpretations, the fact that we have been unable to capture a large fraction of cells that are simultaneously positive for BrdU and GFP throughout the 24 hr interval suggests to us the following mechanism: LPS-mediated NF- κ B activation in HSPCs does not appear to directly turn on a proliferation program, and, instead, cytokines are induced that, in turn, act on cytokine receptors on neighboring HSPCs to stimulate proliferation and differentiation. The nature of this type of paracrine signaling and the distinction between the proliferative and the NF- κ B-activated subsets within HSPCs require further investigation.

(B) Comparison of the cytokine secretion capacity of LSK cells from different genetic models. Each plot represents cytokine intensity scatter plots for a single protein with the four different mouse models arranged from left to right (p50 KO, green; miR/p50 DKO, yellow; WT, blue; miR KO, red). Each plot is composed of several thousand individual dots from several thousand single cells. The numbers on top represent the percentage of cytokine-producing cells above the gate (the dotted line), and the bars represent the mean intensity of only the positive cytokine-producing cells (average intensity of the cells above the dotted line).

(C) A summary heat map showing the percentage of LSK cells that secrete any individual cytokine.

(D) 2D scatter plots showing protein pair correlations. Results from p50 KO (green), WT (blue), and miR KO (red) LSK cells are plotted. Correlation coefficients (R value) of the two cytokines for the different mouse models are shown on the plots.

(E) A half matrix summarizing the comparison of correlation coefficients (R values) of any given cytokine pairs between WT, p50 KO, and miR KO LSK cells. Each square block, intercepted by two cytokines with one on the top and one to the right, represents correlation coefficients between the two cytokines. Green represents the case when WT LSK has the highest correlation, such as IL-6 versus GM-CSF, and red represents when miR KO LSK has the highest correlation, such as IL-6 versus IFN- γ . Correlations for all protein pairs from the p50 KO LSK cells are always lower than either WT or miR KO.

(F) Principal component analysis of LSK cells from the four genetic models. The data are plotted onto the 2D space by the top two principal components. This reduced space is the one that can explain the most (>60%) information of the data. The directions of the two protein groups are represented by the two vectors aligned to the x and y axes.

See also Figure S3.

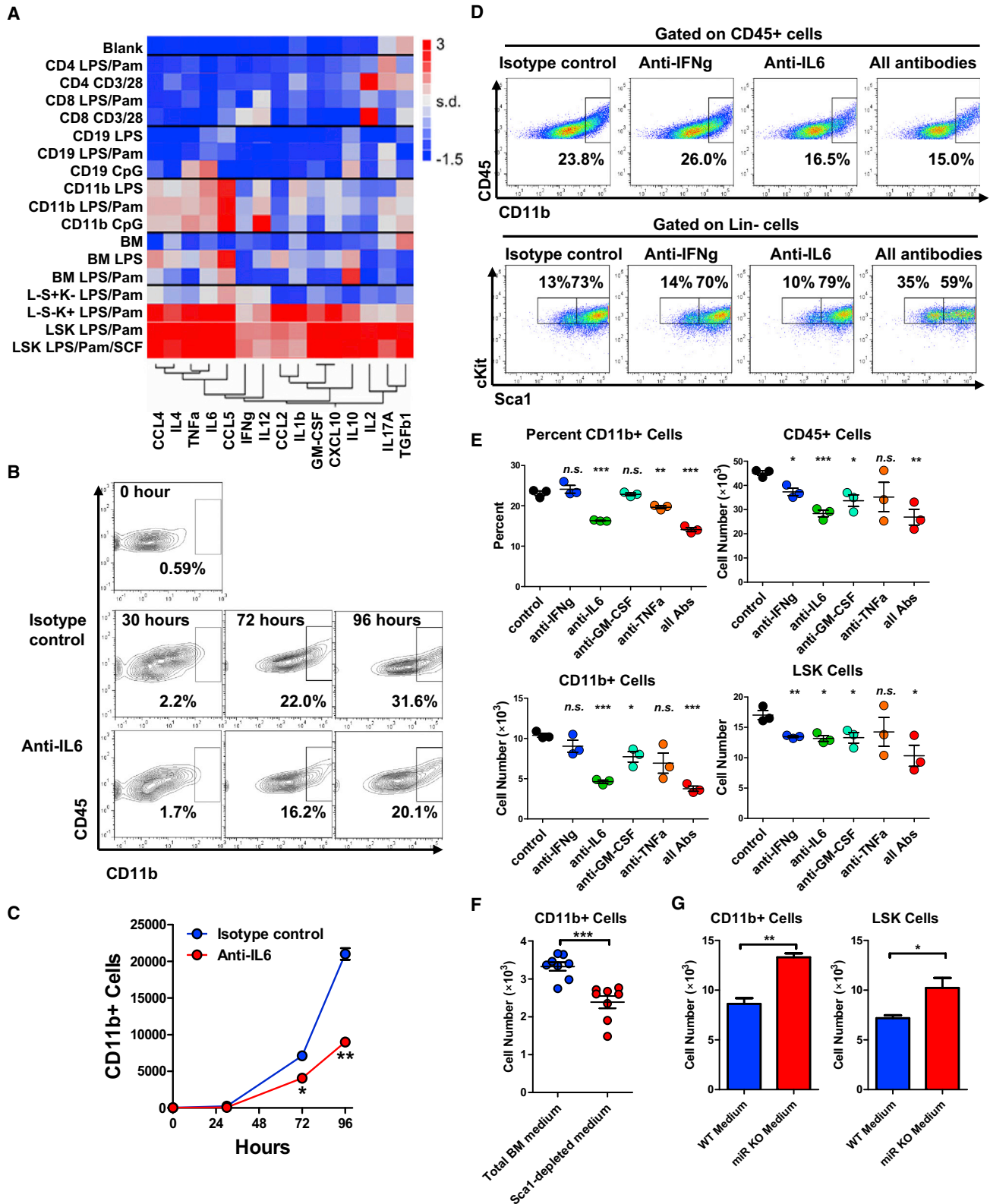


Figure 5. In Vitro Analysis of Functional Significance of HSPC-Produced Cytokines

(A) Multiplexed ELISA quantification of cytokines in bulk cell-culture medium in order to compare cytokine production of different FACS-purified cell subsets stimulated for 24 hr with various stimulations. Cell types include LSK cells, L⁻S⁻K⁺ (Lin⁻Sca1⁻cKit⁺), and L⁻S⁺K⁻ (Lin⁻Sca1⁺cKit⁻) sorted from BMs and CD4⁺T, CD8⁺T, CD19⁺B, and CD11b⁺ myeloid cells sorted from spleens. Stimulations include LPS/Pam (100 ng/ml LPS and 1 μ g/ml Pam3CSK4), LPS/Pam/stem cell (legend continued on next page)

DISCUSSION

In this study, we have shown that ST-HSCs and MPPs can translate danger signals arising from an infection into cytokine signals that can directly regulate stress-induced hematopoiesis. Significantly, the cytokine production ability of HSPCs trumps both mature myeloid and lymphoid cells in terms of speed, magnitude, and breadth. In the BM stem cell niche, this property of HSPCs may play an important role in providing a rapid response time from the encounter of an infection to the output of myeloid cells. In addition to residing in the BM, HSPCs are known to egress from the marrow and traffic through the blood and lymphatic circulation to peripheral organs, including spleen, liver, lymph nodes, gut, and adipose tissues, where they may be exposed to a heavy burden of danger signals. These extramedullary sites may provide excellent opportunities for HSPCs to coordinate rapid stress-induced hematopoiesis upon TLR stimulation (Han et al., 2010; Jaiswal and Weissman, 2009; Massberg et al., 2007; Wesemann et al., 2013).

Given that all the cytokines produced by HSPCs are also produced by mature immune cells and some nonhematopoietic cells, isolating the effect of cytokines produced by HSPCs from mature cells *in vivo* is difficult, if not impossible, given current technical limitations in specifically deleting a gene in HSCs while turning it back on in mature cells. Therefore, we have relied on *in vitro* studies to demonstrate the functional importance of HSPC-produced cytokines in regulating myelopoiesis. In addition, there are situations when mature immune cells are significantly depleted, such as during sepsis, after chemotherapy, and during the initial recovering phase of stem cell transplant. During these situations, when mature immune cells are depleted and HSPCs are overrepresented, the ability of HSPCs to respond to stress directly in order to produce cytokines may become critical in mediating rapid hematopoietic cell recovery. We have created these situations in mice to mimic neutropenic conditions after chemotherapy or stem cell transplant and have shown that the ability of HSPCs to produce IL-6 is particularly important in mediating stress-induced myelopoiesis. In clinical practice, G-CSF and GM-CSF are used in certain situations after chemotherapy or stem cell transplant to stimulate neutrophil recovery in neutropenic patients who are susceptible to fatal infections (Bennett et al., 2013). A better understanding of the cytokine-mediated hematopoiesis in neutropenic conditions

will provide insight in the development of potentially more effective hematopoietic stimulating factors.

In addition to neutropenic conditions, we reason that this stem and progenitor cell property is also important under physiological conditions, despite of the rarity of HSPCs among differentiated hematopoietic cells. First, the speed, magnitude, and breadth of the cytokines produced by HSPCs in comparison to mature immune cells are impressive. Furthermore, this has not taken into the account the unique location of HSPCs in the stem cell niche. Location and organization of HSPCs within the BM niche have long been appreciated to play an important role in their self-renewal and proliferative properties (Shen and Nilsson, 2012). Perhaps groups of HSPCs residing in close proximity represent a unique advantage for rapid autocrine or paracrine-mediated hematopoiesis. Through BrdU incorporation in NF- κ B-GFP reporter mice, we have shown that HSPCs with NF- κ B activity and that are actively proliferating are largely two distinct populations. We speculate that a potential paracrine regulatory signaling may be at work within the BM that involves one subset of HSPCs responding to TLR stimulation by rapidly turning on NF- κ B and producing copious amounts of cytokines and a neighboring cell population with cytokine receptors that can undergo rapid proliferation and differentiation in response to cytokine stimulation. In support of the notion, although some LSK cells express both TLR-4 and IL-6R α , it appears that a fraction of LSK cells express only the TLR or the cytokine receptor (Figure S6B), suggesting that HSPCs contain heterogeneous subsets with intrinsic differences in their ability to respond to TLR and cytokine stimuli.

The questions regarding the extent of involvement of HSPC-produced cytokines in hematopoiesis in a nonneutropenic host and the nature of HSPC heterogeneity on the basis of differential cytokine production or receptor expression remain open and will be an area of significant interest for future studies. In addition, we are also currently redesigning the microfluidic platform in order to recover individual cells from the chip after proteomic analysis for subsequent lineage and functional analysis. Furthermore, there are perhaps limitations in the *in vitro* on-chip stimulation, which may not provide the optimal conditions for culturing undifferentiated HSPCs. This may result in a reduction in the cells' functional robustness and an underestimate of the true percentage of cytokine-producing cells *in vivo*, despite our poststimulation analysis to ensure that HSPCs remain phenotypically

factor (SCF; 100 ng/ml LPS, 1 μ g/ml Pam3CSK4, and 50 ng/ml SCF), CpG (1 μ M), LPS (10 μ g/ml), CD3/28 (1 μ g/ml anti-CD3 and 1 μ g/ml anti-CD28). Blank, fresh medium; BM, culture medium from unstimulated total BM cells. Data are presented as a heat map with low cytokine level represented in blue, intermediate level represented in white, and high level represented in red. Cytokines are clustered into groups.

(B–E) Analysis of *in vitro* myelopoiesis from WT LSK cells by FACS. Sorted WT LSK cells were stimulated with LPS (100 ng/ml), Pam3CSK4 (1 μ g/ml), and SCF (50 ng/ml) in the presence of cytokine-neutralizing antibodies. Control, isotype antibody control; all Abs, a combination of anti-IL-6, anti-IFN- γ , anti-GM-CSF, and anti-TNF- α neutralizing antibodies.

(B and C) Time course of myelopoiesis from WT LSK cells in the presence of anti-IL-6 neutralizing antibody.

(D and E) Myelopoiesis from WT LSK cells in the presence of various neutralizing antibodies. Cells were analyzed on day 3 by FACS for percent and number of myeloid cells and LSK cells. The representative FACS plots (B and D); quantification (n = 3; C and E).

(F and G) FACS analysis of *in vitro* myelopoiesis from WT LSK cells in the presence of conditioned medium.

(F) WT total BM cells or WT BM cells depleted of Sca1⁺ cells were stimulated with LPS and Pam3CSK4 for 24 hr in order to induce cytokine production into the culturing medium. Then, the culturing medium was used to stimulate freshly purified WT LSK cells. Number of myeloid and LSK cells was analyzed on day 2 (n = 8).

(G) WT or miR-146a KO LSK cells were stimulated with LPS and Pam3CSK4 for 24 hr in order to induce cytokine production into the culturing medium. Then, the culturing medium was used to stimulate freshly purified WT LSK cells. The number of myeloid and LSK cells was analyzed on day 2 (n = 3). Data are presented as mean \pm SEM.

See also Figure S5.

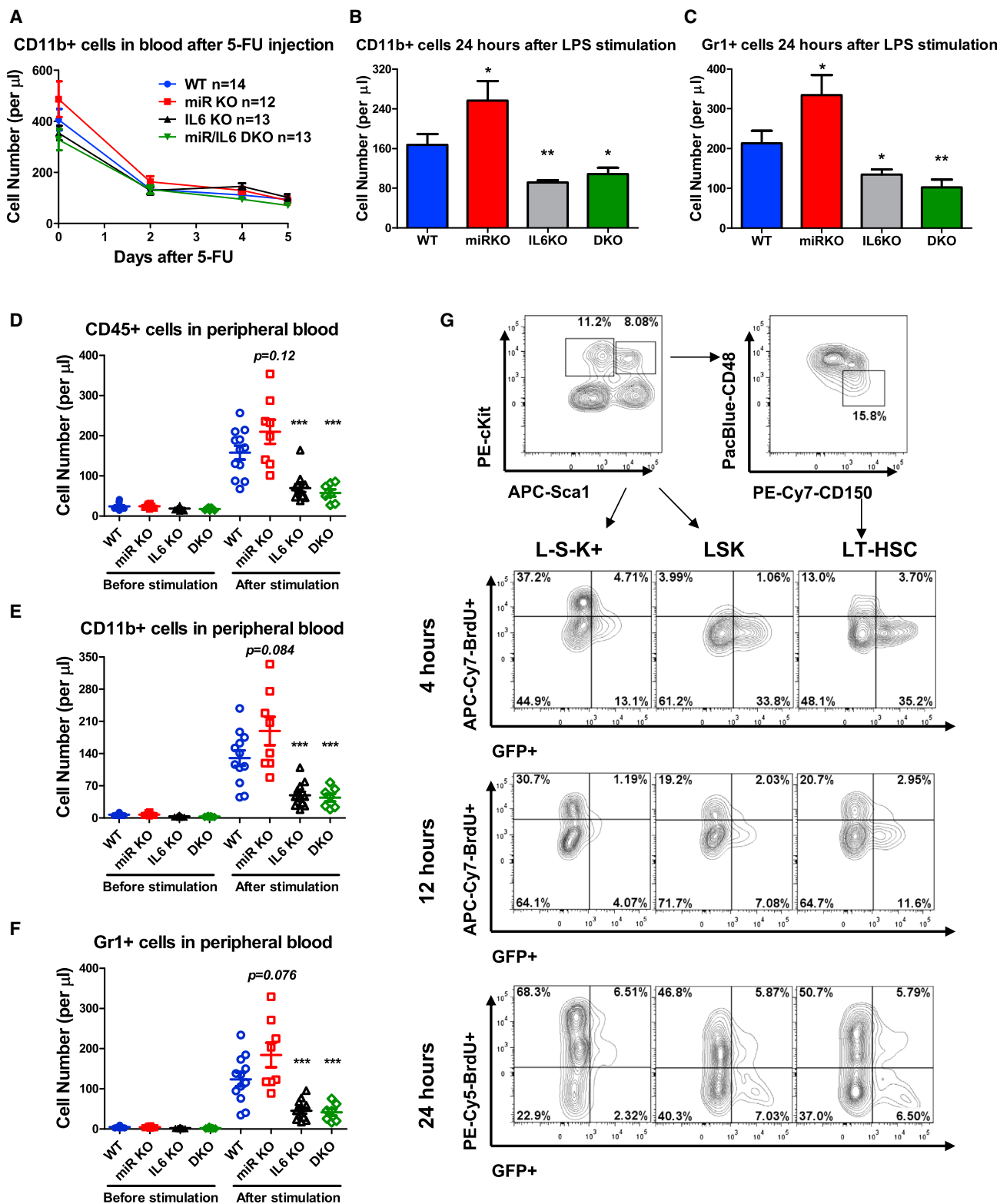


Figure 6. In Vivo Analysis of Functional Significance of HSPC-Produced Cytokines

(A–C) For 5-FU-induced neutropenia, WT, miR-146a KO, IL-6 KO, and miR-146a/IL-6 DKO mice were injected with 5-FU (250 mg/kg of body weight, i.p.). (A) Peripheral blood was analyzed on days 0, 2, 4, and 5 by FACS in order to determine the number of CD11b⁺ myeloid cells. On day 5, LPS (0.3 mg/kg of body weight, i.p.) was injected, and mice were bled 24 hr later in order to study LPS-induced myelopoiesis by analyzing the number of CD11b⁺ (B) or Gr1⁺ (C) cells.

(legend continued on next page)

Cell Stem Cell

HSPCs Regulate Myelopoiesis via Cytokines

undifferentiated by FACS and morphologically intact by microscopy. The ability to recover individual cells poststimulation will allow us to better assess cell viability.

Functions of NF- κ B in immune cells have been extensively studied. However, knowledge of the functional role of NF- κ B in HSPCs has been limited. In this study, we have connected a known function of NF- κ B, the regulation of cytokine production, to two unexpected multipotent hematopoietic cell populations, ST-HSCs and MPPs. What is also intriguing is that some LT-HSCs appear able to respond to TLR stimulation by the activation of NF- κ B, and all HSCs appear to have at least the p65 subunit of NF- κ B. Thus, despite NF- κ B by itself being insufficient to enable cytokine secretion in LT-HSCs, NF- κ B is present from the inception of hematopoiesis and may regulate other aspects of HSC biology.

EXPERIMENTAL PROCEDURES

Animal Models

All mice (WT, *Nfkb1*^{-/-}, *Mir146a*^{-/-}, *Il6*^{-/-}, *Nfkb1*^{-/-}*Mir146a*^{-/-}, *Il6*^{-/-}*Mir146a*^{-/-}, RELA-GFP knockin, and NF- κ B-eGFP reporter mice) were on a C57BL/6 genetic background and housed under a specific pathogen-free condition at the California Institute of Technology. Mice used for all experiments were age- and sex-matched 6- to 8-week-old female mice. All experiments were approved by the institutional Animal Care and Use Committee of the California Institute of Technology.

FACS Sort

In general, 15 to 20 mice of the same genotype were used for FACS sorting in order to obtain sufficient stem and progenitor cells. First, BM cells were subjected to magnetic bead selection (Miltenyi Biotec) according to manufacturer's protocol in order to deplete lineage-positive cells, and then they were sorted on a BD FACSAria sorter at the California Institute of Technology FACS Core. More details can be found in the [Supplemental Experimental Procedures](#).

Single-Cell Cytokine Chip Analysis

We integrated upstream FACS purification techniques with the single-cell barcode chip in order to study the functional proteomics from phenotypically defined single cells. The chips used in this study have > 5,000 microchambers of about 100 picoliter volume to enable sensitive detection of proteins. Within each microchamber, a panel of 12 cytokines (TNF- α , GM-CSF, IL-6, IL-12p40, IFN- γ , IL-2, IL-4, IL-10, TGF- β 1, CCL-2, IL-17A, and IL-1 β) can be simultaneously measured by sandwich ELISA-like assay. The manufacture procedure of the chip has been described in our previous study ([Ma et al., 2011](#)), and the detailed experimental steps can be found in the [Supplemental Experimental Procedures](#). In brief, FACS-purified cells were cultured at 37°C in 5% CO₂ cell incubator with medium alone, medium plus LPS, or medium plus LPS and Pam3CSK4 for 12 hr. At the end of stimulation, the chip was imaged with a high-resolution bright-field microscope. Cell number in each chamber was counted, and cell viability was assessed to exclude fragmented or non-light-reflective cells by trained personnel in a blind manner. Then, cells were washed off, and the chips were developed via an immuno-sandwich assay. A GenePix 4400A microarray scanner was used to scan slides, and data were analyzed with GenePix Pro 7. Each single-cell chip analysis of a specific cell subset, genotype, and stimulating condition was performed at least two times.

Multiplexed Cytokine Analysis of Bulk Cell-Culture Medium

For multiplexed cytokine analysis of bulk cell-culture medium, 100,000 cells of each FACS-purified subset were stimulated in 100 μ l medium with various stimulations for 24 hr in a 96-well plate. Then, the medium was collected and concentrated by 4-fold before being subjected to multiplexed ELISA quantification of 15 different cytokines and chemokines. For multiplexed ELISA quantification, the detection method was identical to the single-cell chip analysis described above. The difference is that the sample here consists of culturing medium only. In brief, the ELISA chip was first blocked with 3% BSA in PBS buffer and then hybridized with an antibody-single-stranded DNA conjugate cocktail and washed with 3% BSA in PBS followed by the application of a medium sample. The assay was completed by applying secondary biotinylated antibodies and streptavidin-cy3 in sequence. Multiplexed cytokine analysis of a specific cell subset, genotype, and stimulating condition was performed at least two times.

In Vitro Analysis of Myeloid Differentiation

For analysis of myeloid differentiation under cytokine-neutralizing antibodies, sorted LSK cells (15,000 cells per 100 μ l medium) were stimulated with LPS (100 ng/ml), Pam3CSK4 (1 μ g/ml), and stem cell factor (50 ng/ml) in the presence of various cytokine-neutralizing antibodies. Antibody concentrations used were isotype control (1 μ g/ml), anti-IFN- γ (1 μ g/ml), anti-IL-6 (1 μ g/ml), anti-GM-CSF (5 μ g/ml), and anti-TNF- α (5 μ g/ml; eBioscience). Cells were analyzed on day 3 by FACS for the percent and number of myeloid cells and LSK cells. For the analysis of myeloid differentiation under conditioned medium, WT or miR-146a KO LSK cells (30,000 cells per 100 μ l medium) were stimulated with LPS (100 ng/ml) and Pam3CSK4 (1 μ g/ml) for 24 hr in order to induce cytokine production into the culturing medium. Then, the culturing medium from either WT or miR KO LSK cells was collected and used to stimulate freshly purified WT LSK cells. The number of myeloid and LSK cells was analyzed after 2 days by FACS. All experiments were performed two times with three biological replicates, each of which was sorted from pooled BM cells of six to ten mice.

In Vivo Analysis of Myeloid Differentiation

For 5-FU-induced leucopenia, WT, miR-146a KO, IL-6 KO, and miR-146a/IL-6 DKO mice were injected with 5-FU (250 mg/kg of body weight, intraperitoneally [i.p.] injected; Sigma-Aldrich). Peripheral blood was obtained on days 0, 2, 4, and 5 for FACS analysis in order to determine the severity of neutropenia. On day 5, LPS (0.3 mg/kg of body weight, i.p.) was injected, and mice were bled 24 hr later for FACS analysis. For stem cell transplant study after lethal irradiation, Lin⁻cKit⁺ cells were purified from the BM of WT, miR-146a KO, IL-6 KO, and miR-146a/IL-6 DKO mice. 500,000 cells were injected intravenously into each lethally irradiated (1,000 rad in one dose) WT recipient mice. On day 6, mice were bled for FACS analysis and LPS injection (0.3 mg/kg of body weight, i.p.) was given; 48 hr later, mice were bled again for FACS analysis. Data represent cumulative results from two independent mouse experiments.

Computational Algorithm and Statistical Analysis

In [Figures 3 and 5](#), F tests were used to compare variances, and then the appropriate two-sided Student's t tests were applied. All figures with error bars were graphed as mean \pm SEM. For all heat maps, scale bars represent mean \pm SD. *p < 0.05; **p < 0.01; ***p < 0.001.

For all single-cell cytokine chip analysis, custom-written software routines in R language were used to process, analyze, and visualize the single-cell functional assay results. In brief, the algorithm converts raw fluorescence images into numerical fluorescence intensity values for each assayed protein within a given microchamber matched with the number of cells. The number of cells within each microchamber was determined manually by microscopy.

(D-F) For stem cell transplant studies, Lin⁻cKit⁺ cells were purified from the BM of WT, miR-146a KO, IL-6 KO, and miR-146a/IL-6 DKO mice. 500,000 cells per mouse were injected intravenously into lethally irradiated WT recipient mice. On day 6, mice were bled for FACS analysis in order to determine the degree of neutropenia. LPS was injected (0.3 mg/kg of body weight, i.p.), and, 48 hr later, mice were bled in order to study LPS-induced myelopoiesis by analyzing the number of total white blood cells (D), CD11b⁺ cells (E), and Gr1⁺ cells (F).

(G) LPS (2 mg/kg of body weight, i.p.) and BrdU (1 mg, i.p.) were injected into NF- κ B-GFP transgenic reporter mice, which were harvested for FACS analysis at 4, 12, and 24 hr. Representative FACS plots of GFP expression and BrdU incorporation of L⁻S⁻K⁺ cells, LSK cells, and HSCs. Data are presented as mean \pm SEM. See also [Figure S6](#).

The average background signal levels from all zero-cell microchambers were used to set the gate in order to separate nonproducing cells from cytokine-producing cells. Detailed statistical analysis method for principal component analysis (Figures 1D, 2D, 2F, and 4F) can be found in the [Supplemental Experimental Procedures](#) and our previous publication (Ma et al., 2011). These types of statistical analysis and graphical representations are routinely used to analyze large-scale multidimensional data sets from numerous cell subsets (Bendall et al., 2011).

SUPPLEMENTAL INFORMATION

Supplemental Information contains Supplemental Experimental Procedures and six figures and can be found with this article online at <http://dx.doi.org/10.1016/j.stem.2014.01.007>.

AUTHOR CONTRIBUTIONS

J.L.Z., D.B., C.M., R.M.O., and J.R.H. conceived the study. J.L.Z., C.M., and A.M. designed and performed the experiments. R.D. helped with data collection. J.L.Z., D.B., C.M., and J.R.H. analyzed the data. J.L.Z. and D.B. wrote the manuscript.

ACKNOWLEDGMENTS

The authors wish to thank Caltech animal facility and flow cytometry core facility and Drs. Alejandro Balazs, Devdoot Majumdar, and Michael Bethune of the D.B. lab for their help. RELA-GFP knockin and NF- κ B-eGFP reporter mice were obtained from Dr. Manolis Pasparakis of the University of Cologne and Dr. Christian Jobin of the University of North Carolina, respectively. The work was supported by research grants R01AI079243 (D.B.), R01CA170689 (J.R.H.), National Research Service Award F30HL110691 (J.L.Z.), UCLA/Caltech Medical Scientist Training Program (J.L.Z. and A.M.), Rosen Fellowship (C.M.), NIH New Innovator Award DP2GM111099 (R.M.O.), the Pathway to Independence Award R00HL102228 (R.M.O.), and an American Cancer Society Research grant (R.M.O.) with core facilities support from 5U54CA119347 (J.R.H.).

Received: October 1, 2013
Revised: November 28, 2013
Accepted: January 14, 2014
Published: February 20, 2014

REFERENCES

Adolfsson, J., Månsson, R., Buza-Vidas, N., Hultquist, A., Liuba, K., Jensen, C.T., Bryder, D., Yang, L., Borge, O.J., Thoren, L.A., et al. (2005). Identification of Flt3⁺ lympho-myeloid stem cells lacking erythro-megakaryocytic potential: a revised road map for adult blood lineage commitment. *Cell* 121, 295–306.

Baldrige, M.T., King, K.Y., Boles, N.C., Weksberg, D.C., and Goodell, M.A. (2010). Quiescent haematopoietic stem cells are activated by IFN- γ in response to chronic infection. *Nature* 465, 793–797.

Baldrige, M.T., King, K.Y., and Goodell, M.A. (2011). Inflammatory signals regulate hematopoietic stem cells. *Trends Immunol.* 32, 57–65.

Baltimore, D. (2011). NF- κ B is 25. *Nat. Immunol.* 12, 683–685.

Beerman, I., Bhattacharya, D., Zandi, S., Sigvardsson, M., Weissman, I.L., Bryder, D., and Rossi, D.J. (2010). Functionally distinct hematopoietic stem cells modulate hematopoietic lineage potential during aging by a mechanism of clonal expansion. *Proc. Natl. Acad. Sci. USA* 107, 5465–5470.

Bendall, S.C., Simonds, E.F., Qiu, P., Amir, A.D., Krutzik, P.O., Finck, R., Bruggner, R.V., Melamed, R., Trejo, A., Ornatsky, O.I., et al. (2011). Single-cell mass cytometry of differential immune and drug responses across a human hematopoietic continuum. *Science* 332, 687–696.

Bennett, C.L., Djulbegovic, B., Norris, L.B., and Armitage, J.O. (2013). Colony-stimulating factors for febrile neutropenia during cancer therapy. *N. Engl. J. Med.* 368, 1131–1139.

Boldin, M.P., Taganov, K.D., Rao, D.S., Yang, L., Zhao, J.L., Kalwani, M., Garcia-Flores, Y., Luong, M., Devrekanli, A., Xu, J., et al. (2011). miR-146a is a significant brake on autoimmunity, myeloproliferation, and cancer in mice. *J. Exp. Med.* 208, 1189–1201.

Challen, G.A., Boles, N.C., Chambers, S.M., and Goodell, M.A. (2010). Distinct hematopoietic stem cell subtypes are differentially regulated by TGF- β 1. *Cell Stem Cell* 6, 265–278.

Copley, M.R., Beer, P.A., and Eaves, C.J. (2012). Hematopoietic stem cell heterogeneity takes center stage. *Cell Stem Cell* 10, 690–697.

De Lorenzi, R., Gareus, R., Fengler, S., and Pasparakis, M. (2009). GFP-p65 knock-in mice as a tool to study NF- κ B dynamics in vivo. *Genesis* 47, 323–329.

Essers, M.A., Offner, S., Blanco-Bose, W.E., Waibler, Z., Kalinke, U., Duchosal, M.A., and Trumpp, A. (2009). IFN α activates dormant haematopoietic stem cells in vivo. *Nature* 458, 904–908.

Forsberg, E.C., Serwold, T., Kogan, S., Weissman, I.L., and Passegué, E. (2006). New evidence supporting megakaryocyte-erythrocyte potential of flk2/flt3⁺ multipotent hematopoietic progenitors. *Cell* 126, 415–426.

Han, J., Koh, Y.J., Moon, H.R., Ryoo, H.G., Cho, C.H., Kim, I., and Koh, G.Y. (2010). Adipose tissue is an extramedullary reservoir for functional hematopoietic stem and progenitor cells. *Blood* 115, 957–964.

Harrison, D.E., and Lerner, C.P. (1991). Most primitive hematopoietic stem cells are stimulated to cycle rapidly after treatment with 5-fluorouracil. *Blood* 78, 1237–1240.

Jaiswal, S., and Weissman, I.L. (2009). Hematopoietic stem and progenitor cells and the inflammatory response. *Ann. N Y Acad. Sci.* 1174, 118–121.

Janeway, C.A., Jr., Travers, P., Walport, M., and Shlomchik, M.J. (2001). *Immunobiology: The Immune System in Health and Disease*. Appendix III. Cytokines and Their Receptors, Fifth Edition. (New York: Garland Science).

King, K.Y., and Goodell, M.A. (2011). Inflammatory modulation of HSCs: viewing the HSC as a foundation for the immune response. *Nat. Rev. Immunol.* 11, 685–692.

Ma, C., Fan, R., Ahmad, H., Shi, Q., Comin-Anduix, B., Chodon, T., Koya, R.C., Liu, C.C., Kwong, G.A., Radu, C.G., et al. (2011). A clinical microchip for evaluation of single immune cells reveals high functional heterogeneity in phenotypically similar T cells. *Nat. Med.* 17, 738–743.

Maeda, K., Malykhin, A., Teague-Weber, B.N., Sun, X.H., Farris, A.D., and Coggeshall, K.M. (2009). Interleukin-6 aborts lymphopoiesis and elevates production of myeloid cells in systemic lupus erythematosus-prone B6.Sle1.Yaa animals. *Blood* 113, 4534–4540.

Magness, S.T., Jijon, H., Van Houten Fisher, N., Sharpless, N.E., Brenner, D.A., and Jobin, C. (2004). In vivo pattern of lipopolysaccharide and anti-CD3-induced NF- κ B activation using a novel gene-targeted enhanced GFP reporter gene mouse. *J. Immunol.* 173, 1561–1570.

Massberg, S., Schaerli, P., Knezevic-Maramica, I., Köllnberger, M., Tubo, N., Moseman, E.A., Huff, I.V., Junt, T., Wagers, A.J., Mazo, I.B., and von Andrian, U.H. (2007). Immunosurveillance by hematopoietic progenitor cells trafficking through blood, lymph, and peripheral tissues. *Cell* 131, 994–1008.

Megias, J., Yáñez, A., Moriano, S., O'Connor, J.E., Gozalbo, D., and Gil, M.L. (2012). Direct Toll-like receptor-mediated stimulation of hematopoietic stem and progenitor cells occurs in vivo and promotes differentiation toward macrophages. *Stem Cells* 30, 1486–1495.

Mossadegh-Keller, N., Sarrazin, S., Kandalla, P.K., Espinosa, L., Stanley, E.R., Nutt, S.L., Moore, J., and Sieweke, M.H. (2013). M-CSF instructs myeloid lineage fate in single haematopoietic stem cells. *Nature* 497, 239–243.

Nagai, Y., Garrett, K.P., Ohta, S., Bahrun, U., Kouro, T., Akira, S., Takatsu, K., and Kincaid, P.W. (2006). Toll-like receptors on hematopoietic progenitor cells stimulate innate immune system replenishment. *Immunity* 24, 801–812.

Naik, S.H., Perić, L., Swart, E., Gerlach, C., van Rooij, N., de Boer, R.J., and Schumacher, T.N. (2013). Diverse and heritable lineage imprinting of early haematopoietic progenitors. *Nature* 496, 229–232.

Pronk, C.J., Veiby, O.P., Bryder, D., and Jacobsen, S.E. (2011). Tumor necrosis factor restricts hematopoietic stem cell activity in mice: involvement of two distinct receptors. *J. Exp. Med.* *208*, 1563–1570.

Sha, W.C., Liou, H.C., Tuomanen, E.I., and Baltimore, D. (1995). Targeted disruption of the p50 subunit of NF-kappa B leads to multifocal defects in immune responses. *Cell* *80*, 321–330.

Shen, Y., and Nilsson, S.K. (2012). Bone, microenvironment and hematopoiesis. *Curr. Opin. Hematol.* *19*, 250–255.

Wesemann, D.R., Portuguese, A.J., Meyers, R.M., Gallagher, M.P., Cluff-Jones, K., Magee, J.M., Panchakshari, R.A., Rodig, S.J., Kepler, T.B., and

Alt, F.W. (2013). Microbial colonization influences early B-lineage development in the gut lamina propria. *Nature* *501*, 112–115.

Zhao, J.L., Rao, D.S., Boldin, M.P., Taganov, K.D., O'Connell, R.M., and Baltimore, D. (2011). NF-kappaB dysregulation in microRNA-146a-deficient mice drives the development of myeloid malignancies. *Proc. Natl. Acad. Sci. USA* *108*, 9184–9189.

Zhao, J.L., Rao, D.S., O'Connell, R.M., Garcia-Flores, Y., and Baltimore, D. (2013). MicroRNA-146a acts as a guardian of the quality and longevity of hematopoietic stem cells in mice. *Elife* *2*, e00537.